University of Bath

UNIVERSITY OF BATH

PHD

Iontophoresis in paediatric medicine: Non-invasive delivery and monitoring applications

Djabri, Asma

Award date:
2009

Awarding institution:
University of Bath

Link to publication

IONTOPHORESIS IN PAEDIATRIC MEDICINE:

NON-INVASIVE DRUG DELIVERY AND

MONITORING APPLICATIONS

ASMA DJABRI

A thesis submitted for the degree of Doctor of Philosophy

University of Bath
Department of Pharmacy and Pharmacology
June 2009

To my dear mother and father...

Table of contents

Acknowledgements

I am deeply grateful to my supervisors Prof. Richard H. Guy and Dr. M. Begoña Delgado-Charro for their guidance and support throughout my doctoral studies.

I would like to thank Prof. Adrian C. Williams and Dr. Stephen M. Husbands for accepting to evaluate my work.

I would like to thank Prof. Ian Wong, Dr. Joseph Standing, Dr. William van't Hoff, Dr. Penelope Brock, and Ms. Renate Tulloh for their collaboration in the iohexol *in vivo* project. I would also like to thank all the children who participated in the study and, of course, the nursing staff in the renal and chemotherapy wards, at Great Ormond Street Hospital for Children in London.

I am grateful to my colleagues and friends, past and present, for all of their support and friendship.

I would like to acknowledge the Algerian Government for partly sponsoring my doctoral studies.

Finally, but most importantly, I would like to thank my parents (***Souad*** and ***Aïssa***), my sisters (***Ikram***, ***Amina***, and ***Dhoha***), and my nephews and niece (***Rami***, ***Iskander***, and ***Melek***) for their unconditional love, patience, and inspiration. I wouldn't have made it without you all!

Abstract

This thesis investigated the possible use of transdermal iontophoresis in paediatric care, as an alternative strategy to the oral and intravenous routes. More specifically, the potential for non-invasive delivery of ranitidine, midazolam, and phenobarbital; and the clinical sampling of iohexol through the skin were examined.

The feasibility for monitoring kidney function was assessed *in vitro* and *in vivo* using the glomerular filtration rate (*GFR*) marker, iohexol. Sampling of iohexol *in vitro* was sensitive to the changes in its subdermal concentration, and pharmacokinetic parameters estimated from skin sampling agreed well with reference subdermal values. Similar observations were confirmed *in vivo* in a pilot study performed in four children undergoing routine iohexol *GFR* test. Iontophoresis was well tolerated in all subjects and the marker was successfully extracted through the skin. In 3 of 4 subjects, the elimination rate constant estimated from skin sampling data agreed well with blood sampling results. This study demonstrated the potential of transdermal iontophoresis as a non-invasive sampling approach which could significantly improve the quality-of-life of children.

Drug delivery by transdermal iontophoresis was examined *in vitro* for three commonly used paediatric medicaments: ranitidine, midazolam, and phenobarbital. Experiments used both intact and compromised pig skin to model the less resistant skin of premature babies. Iontophoretic delivery across intact skin was superior than passive delivery and optimised conditions were achieved by use of maximal molar fraction of the drug, higher current intensity, and appropriate vehicle pH. Pluronic® F-127 gels were suitable drug matrices for the iontophoretic delivery of ranitidine. Midazolam and phenobarbital transdermal delivery through partially compromised skin barriers was controlled by iontophoresis. Across highly compromised skin, however, passive diffusion increased drastically and iontophoretic control was lost. Overall, it was possible to deliver therapeutically meaningful fluxes of all three drugs with acceptable patch application area.

List of abbreviations

AUC	Area under the curve
BSA	Body surface area
C	Concentration
Cl	Clearance
ECV	Extracellular volume
F	Faraday's number
F-127	Pluronic® F-127 polymer
GFR	Glomerular filtration rate
HPLC	High performance liquid chromatography
I	Current intensity
IC	Ion chromatography
ISF	Interstitial fluid
J	Transport flux
K_e	Elimination rate constant
RAN	Ranitidine
T	Transference number
TEWL	Transepidermal water loss
V_d	Volume of distribution
z	Valence
Z	Transport efficiency

Introduction

A significant unmet need exists in paediatric medicine. Treatment therapy in this special population lacks age-appropriate formulations and suitable methods of drug administration and clinical sampling. This often results in failure of optimum therapy.

The subject of this thesis proposes an alternative non-invasive approach by which drugs and analytes can be delivered and sampled via the skin. The needle-free technique, known as "transdermal iontophoresis", makes use of an electrical current application which provides a driving force for compounds to move efficiently across the skin in a highly controlled and sustained manner [1-3]. This active transport of molecules is due to two phenomena. The first mechanism is "electromigration" and only concerns the transport of ionised species. It describes the direct result of interaction of the applied electrical field with the charged molecules [4]. This leads to the migration of the ions to the electrode of opposite polarity by moving into and through the skin. The efficiency of electromigration depends on the mobility, valence, and concentration of the ion of interest as well as the other ions present in the iontophoresis system. The second mechanism is "electroosmosis" and describes the movement of solutes along with the convective solvent flow, which is induced as a result of the skin's negative charge and therefore its permselectivity to cations over anions under the influence of current application [5]. The transport of neutral compounds during iontophoresis is mostly due to electroosmosis. The transport of cations is supplemented by electroosmosis as the latter phenomenon occurs in the same direction as the cation's electromigration across the skin. To distinguish drug delivery from clinical sampling, the term "reverse iontophoresis" is conventionally used to describe the extraction of analytes from the body.

1. Aims of the thesis

The objectives of this thesis are to evaluate the potential applications of transdermal iontophoresis as an alternative non-invasive route for drug administration and for clinical sampling in paediatric medicine. The validation of such approach is drug-specific and requires separate investigation for each individual therapeutic agent. For this reason, the aim of this thesis is more specifically focused on the feasibility to use transdermal iontophoresis as a non-invasive strategy for the delivery/sampling of four therapeutic agents, which were chosen from the list shown below.

2. List of candidates for possible iontophoretic applications

The therapeutic agents investigated in this thesis were selected from the following candidates: A) <u>Drug delivery:</u> tacrolimus (immunosuppressant), carbamazepine (for epilepsy, mood stabilisation, and neuralgia), phenobarbital (antiepileptic), midazolam (sedative), digoxin (for various heart conditions), ranitidine (for gastric acid reduction), furosemide (diuretic), and ondansetron (antiemetic). B) <u>Clinical sampling:</u> digoxin and tacrolimus (therapeutic drug monitoring necessary due to narrow therapeutic index), and iohexol (marker for kidney function).

These therapeutic agents are commonly used in paediatric medicine but the available dosage forms, at present, require significant improvement. The conventional routes of administration are by oral or intravenous delivery while clinical sampling is performed solely by intravenous means. Inherent disadvantages of the latter include the significant pain experienced during blood sampling, the potential risk of infection, and the technical difficulties associated with needle insertion. The same drawbacks, obviously, apply to drug delivery by the intravenous route. Even though oral delivery is the preferred route of administration, it is not appropriate in certain clinical conditions whereby, for example, the child is seriously ill, suffers from nausea/vomiting, is uncooperative, or in very young babies.

Paediatric oral delivery of the drugs mentioned earlier suffers from various pitfalls. The formulations of some drugs are only available as solid dosage forms (tacrolimus [6]) which is unsuitable for infants and young children due to inability of swallowing. Other medicaments are available in liquid forms but the conventional formulation can be too concentrated (e.g. phenobarbital [6]) for accurate and consistent dilutions to be made. Some liquid formulations are also alcohol-based (furosemide, phenobarbital, ranitidine [6]), a solvent usually avoided in paediatric treatments. Moreover, the unpalatability of some liquid formulations (midazolam [7]) may eventually lead to refusal of intake and failure to comply. Noncompliance may also arise with drugs of short half lives (midazolam, furosemide, ondansetron, ranitidine [8]) as they would have to be administered several times a day to maintain effective plasma concentrations. Many of the drugs listed above are also characterised by low and/or highly variable oral bioavailability (midazolam, ranitidine, digoxin, tacrolimus and carbamazepine [8-11]) both in children and adults. The continuous developmental changes in the child's digestive system also lead to highly unpredictable rates and extents of oral absorption and first-pass metabolism [12]. It follows that drugs with narrow therapeutic index such as digoxin and tacrolimus can have a detrimental effect on the child's health if slightly less or more of the drug is absorbed.

3. Selection criteria for suitable iontophoresis candidates

The therapeutic agents, investigated in this thesis for transdermal iontophoretic delivery and clinical sampling, were selected from the above list of candidates based on the following factors: Firstly, for drug delivery the smaller the dose required daily, the better possibility transdermal iontophoresis could deliver therapeutically meaningful levels of the drug. Conversely, for clinical sampling the higher the systemic concentration of the free (unbound) therapeutic agent in the body, the more likely there will be a successful extraction across the skin. Secondly, low molecular weight, charged, and hydrophilic molecule properties are the ideal physicochemical characteristics for efficient iontophoretic transport [13-16]. The

reasons being that: A) molecular weight is inversely proportional to the mobility of the compound which will directly affect its iontophoretic transport efficiency [16-18]. B) charged molecules are preferred over neutral compounds because transport rates achieved with electroosmosis are usually considered secondary to the effects electromigration usually exerts on the transport rates of relatively small charged permeants [5, 14]. While electromigration acts directly on the charged molecule providing a high driving force through the skin, the transport of neutral molecules is due to electroosmosis which is a stream of solvent flow created indirectly as a result of the skin's net negative charge. Cationic molecules are favoured over anionic compounds because, in addition to electromigration effect, the iontophoretic transport of the former is supplemented by electroosmosis, while the transport of the latter is against the stream of solvent flow [5, 14]. C) Several studies reported that iontophoresis of cationic lipophilic compounds attenuated or even reversed electroosmosis [19-21]. Lipophilic neutral solutes also exhibited lower electroosmotic transport compared to more hydrophilic compounds [22].

3.1   Selection for drug delivery applications

The following table provides details on the paediatric daily doses of the potential drug candidates along with their molecular weight, dissociation constant (pKa), lipophilicity (LogP), and aqueous solubility.

The daily doses required for tacrolimus and digoxin are very small but their physicochemical properties predict less suitability for iontophoretic delivery. The neutrality, high molecular weight, and water insolubility are all unfavourable characteristics for ideal iontophoresis candidates. In addition, the very high lipophilicity of tacrolimus is likely to affect its transport across the skin. The molecular weight of carbamazepine is significantly lower than the previous two drugs, however the required dose to achieve therapeutic systemic levels is very high for transdermal applications. This is in addition to carbamazepine being a neutral molecule with very low water solubility. Low solubility of furosemide is also an obstacle for transdermal applications in addition to the high daily doses required. Finally, the remaining drugs (midazolam, ondansetron, phenobarbital,

	Paediatric daily dose[1] (mg/kg)	Molecular weight[2]	pKa[3]	LogP[2]	Aqueous solubility[2]
Tacrolimus	0.03 – 0.1	804.0	Neutral	6.1	Practically insoluble
Digoxin	0.004 – 0.01	780.9	Neutral	1.3	Practically insoluble
Carbamazepine	10.6 – 31.7	236.3	Neutral	2.5	Very slightly soluble
Furosemide	8 – 20	330.8	4.7 (acid)	2.6	Practically insoluble
Midazolam	0.7 – 2.9	325.8	6.2 (base)	4.3	Sparingly soluble (salt): pH dependent
Ondansetron	0.5	293.4	7.4 (base)	2.1	Sparingly soluble (salt)
Phenobarbital	1.5 – 7.8	232.2	7.4 (acid)	1.5	Freely soluble (salt)
Ranitidine	0.7 – 6	314.4	2.3 (base) 8.2 (acid)	0.3	Freely soluble (salt)

[1] from references [6, 23]; [2] from reference [24]; [3] from reference [25].

and ranitidine) may all be potentially good candidates for transdermal delivery by iontophoresis.

3.2 Selection for clinical sampling applications

Three candidates for potential non-invasive sampling applications by reverse iontophoresis were examined. Digoxin and tacrolimus sampling for therapeutic drug monitoring purposes, and iohexol extraction for the estimation of glomerular filtration rate.

As already mentioned earlier, for an analyte to be efficiently extracted, its systemic "unbound" concentration must be sufficiently high for extracted samples to be analytically quantifiable. For tacrolimus, the trough concentration in whole

blood is 5 – 20 ng/ml, 99 % of which is bound to erythrocytes and plasma proteins [11]. It follows that the maximum unbound fraction of tacrolimus possibly available for extraction across the skin is < 0.2 ng/ml. As yet, the lowest quantitation limit reported in the literature is 0.1 ng/ml [11, 26], and given that the extraction efficiency of neutral molecules by iontophoresis does not usually exceed 20 µl/h.mA [3], tacrolimus sampling by reverse iontophoresis is not feasible. Similarly, the neutral drug digoxin does not appear to be, as yet, a suitable analyte that can be monitored non-invasively by reverse iontophoresis. This is due to its low systemic concentration (0.8 – 2 ng/ml) [6] and an analytical quantitation limit reported at only 0.25 ng/ml [26].

Iohexol is an exogenous non-ionic glomerular filtration rate marker. The dose administered to the patient is high (1.3 – 3.2 g) and distributes across the whole extracellular fluid. It does not bind to proteins or cells and it does not enter cells. The typical concentration of the marker 2 and 6 hours after administration of 3.2 g dose to children are reported at > 100 and 10 µg/ml, respectively [27]. It follows that with analytical quantitation limits reported as low as < 0.2 ng/ml [28], reverse iontophoresis of iohexol appears to have a potential application.

To sum up, based on balancing the properties preferred for transdermal iontophoresis candidates, three drugs were selected for investigation of possible delivery applications (ranitidine, midazolam, and phenobarbital) and one therapeutic agent was identified for clinical sampling application (iohexol).

4. Organisation of the thesis

The first chapter begins with an examination of the principals of conventional paediatric medicine. It then introduces the transdermal route as an alternative approach for drug delivery and clinical sampling. This is finally followed by a special focus on iontophoresis, the centre point of investigation of this thesis.

The second chapter presents the *in vitro* and *in vivo* examinations of reverse iontophoresis of iohexol as an alternative non-invasive technique to blood sampling, for the monitoring of kidney function.

The third, fourth, and fifth chapters investigated the *in vitro* feasibility of iontophoretic delivery of ranitidine, midazolam, and phenobarbital, respectively, through the skin at sufficiently high levels as to provide systemic therapeutic concentrations. Different conditions potentially affecting the iontophoretic delivery of these drugs were evaluated. Iontophoretic delivery of ranitidine was performed using both liquid (aqueous solution) and semi-solid (poloxamer gel) formulations. Transdermal delivery of midazolam and phenobarbital was examined using both intact and compromised skin to mimic the different skin barrier functions found in different groups of the paediatric population.

5. References

1. Delgado-Charro, M. B., and Guy, R. H., *Iontophoresis: Applications in drug delivery and non-invasive monitoring*, in *Transdermal drug delivery*, Guy, R. H., and Hadgraft, J., Editors. 2003, Marcel Dekker, Inc: New York. p. 199-225.

2. Kalia, Y. N., Naik, A., Garrison, J., and Guy, R. H., *Iontophoretic drug delivery.* Adv Drug Del Rev, 2004. **56**: p. 619-658.

3. Leboulanger, B., Guy, R. H., and Delgado-Charro, M. B., *Reverse iontophoresis for non-invasive transdermal monitoring.* Physiol Meas, 2004. **25**: p. R35-R50.

4. Phipps, J. B., and Gyory, J. R., *Transdermal ion migration.* Adv Drug Deliv Rev, 1992. **9**: p. 137-176.

5. Pikal, M. J., *The role of electroosmotic flow in transdermal iontophoresis.* Adv Drug Del Rev, 1992. **9**: p. 201-237.

6. *British national formulary for children 2008*. revised ed, ed. Martin, J. 2008, London: BMJ Group, RPS Publishing, and RCPCH Publications. 944 p.

7. Politis, G. D., *Preanesthetic sedation for pediatric patients lacking intravenous access*, in *Pediatric anesthesia handbook*, Yemen, T. A., Editor. 2002, McGraw-Hill, Health Professions Division: New York; London. p. 41-55.

8. Sweetman, S. C., *Martindale : The complete drug reference*. 34th ed. 2005, London: Pharmaceutical Press. 2756 p.

9. Payne, K., Mattheyse, F. J., Liebenberg, D., and Dawes, T., *The pharmacokinetics of midazolam in paediatric patients.* Eur J Clin Pharmacol, 1989. **37**: p. 267-272.

10. Blumer, J. L., Rothstein, F. C., Kaplan, B. S., Yamashita, T. S., Eshelman, F. N., Myers, C. M., and Reed, M. D., *Pharmacokinetic determination of ranitidine pharmacodynamics in pediatric ulcer disease.* J Pediatr, 1985. **107**: p. 301-306.

11.   Wallemacq, P. E., and Verbeeck, R. K., *Comparative clinical pharmacokinetics of tacrolimus in paediatric and adult patients* Clin Pharmacokin, 2001. **40**: p. 283-295.

12.   Kauffman, R. E., *Drug action and therapy in the infant and child*, in *Neonatal and pediatric pharmacology : Therapeutic principles in practice*, Yaffe, S. J., and Aranda, J. V., Editors. 2005, Lippincott Williams & Wilkins: Philadelphia; London. p. 20-31.

13.   Phipps, J. B., Scott, E. R., Gyory, J. R., and Padmanabhan, R. V., *Iontophoresis*, in *Encyclopedia of pharmaceutical technology*, Swarbrick, J., Editor. 2007, Informa Healthcare: New York; London. p. 2119-2132.

14.   Guy, R. H., Kalia, Y. N., Delgado-Charro, M. B., Merino, V., Lopez, A., and Marro, D., *Iontophoresis: Electrorepulsion and electroosmosis.* J Control Release, 2000. **64**: p. 129-132.

15.   Naik, A., Kalia, Y. N., and Guy, R. H., *Transdermal drug delivery: Overcoming the skin's barrier function.* Pharm Sci Tech Today, 2000. **3**: p. 318-326.

16.   Roberts, M. S., Lai, P. M., Cross, S. E., and Yoshida, N. H., *Solute structure as a determinant of iontophoretic transport*, in *Mechanisms of transdermal drug delivery*, Potts, R. O., and Guy, R. H., Editors. 1997, Marcel Dekker: New York. p. 291-349.

17.   Ruddy, S. B., and Hadzija, B. W., *Iontophoretic permeability of polyethylene glycols through hairless rat skin: Application of hydrodynamic theory for hindered transport through liquid-filled pores.* Drug Des Discov, 1992. **8**: p. 207-224.

18.   Yoshida, N. H., and Roberts, M. S., *Solute molecular-size and transdermal iontophoresis across excised human skin.* J Control Release, 1993. **25**: p. 177-195.

19.   Delgado-Charro, M. B., and Guy, R. H., *Characterization of convective solvent flow during iontophoresis.* Pharm Res, 1994. **11**: p. 929-935.

20.   Hoogstraate, A. J., Srinivasan, V., Sims, S. M., and Higuchi, W. I., *Iontophoretic enhancement of peptides: Behaviour of leuprolide versus model permeants.* J Control Release, 1994. **31**: p. 41-47.

21.   Hirvonen, J., and Guy, R. H., *Iontophoretic delivery across the skin: Electroosmosis and its modulation by drug substances.* Pharm Res, 1997. **14**: p. 1258-1263.

22.   Del Terzo, S., Behl, C. R., and Nash, R. A., *Iontophoretic transport of a homologous series of ionized and non ionized model compounds: Influence of hydrophobicity and mechanistic interpretation.* Pharm Res, 1989. **6**: p. 85-90

23.   Winter, M. E., *Carbamazepine: Drug monographs*, in *Basic clinical pharmacokinetics*. 2003, Lippincott Williams & Wilkins: London. p. 172-182.

24.   Moffat, A. C., Osselton, M. D., and Widdop, B., *Clarke's analysis of drugs and poisons : In pharmaceuticals, body fluids and postmortem material*. 3rd ed. 2004, London: Pharmaceutical Press.

25.   Brittain, H. G., *Profiles of drug substances, excipients and related methodology*. Vol. 33. 2007, London: Academic Press.

26.   Lunn, G., and Schmuff, N. R., *Hplc methods for pharmaceutical analysis*. 2000, New York ; Chichester: Wiley. 2327 p.

27.   Schwartz, G. J., Furth, S., Cole, S. R., Warady, B., and Munoz, A., *Glomerular filtration rate via plasma iohexol disappearance: Pilot study for chronic kidney disease in children.* Kidney Int, 2006. **69**: p. 2070-2077.

28.   Denis, M. C., Venne, K., Lesiege, D., Francoeur, M., Groleau, S., Guay, M., Cusson, J., and Furtos, A., *Development and evaluation of a liquid chromatography-mass spectrometry assay and its application for the assessment of renal function.* J Chromatogr A, 2008. **1189**: p. 410-416.

Chapter 1

The transdermal route in paediatrics

1. Paediatrics: a special category of medicine

Paediatric medicine is a discipline concerned with the clinical care of infants and children. The paediatric population is subdivided into age-related groups, starting from the neonate or newborn (birth – 1 month old), then the infant (1 – 12 months old), followed by the child (1 – 12 years old), and finally the adolescent (13 – 18 years old) [1]. Traditionally, drug therapy for children has been based on the principle that a child is just a "small" adult. This concept has been found to be therapeutically incorrect as a child is not only different from an adult by size and weight but also due to age-related physiological developments which lead to differences in the pharmacology of drugs and distinct drug efficacy, toxicity, and dosing regimen profiles [2-5]. The body of the paediatric subject is continuously developing from the most immature form at birth until it is equivalent to that of a young adult. The first year of life experiences the most rapid changes and development continues thereafter but at a slower pace [3]. Organs and systems whose development progressively changes during childhood include the gastrointestinal tract, the liver, the kidneys, and the body weight proportions contributed by the total body water (the sum of intracellular and extracellular water volume), body fat, and proteins [2-4]. All these features affect the drug disposition in the body (i.e. its pharmacokinetics: absorption, distribution, metabolism, and elimination) [3, 6, 7]. Although not as widely studied as the developmental changes affecting drug pharmacokinetics, age-dependent pharmacodynamic differences, either by alteration of the drug-receptor binding affinity or in the relation of the pharmacological effect exerted by the drug to its plasma concentration, have been reported for several drugs [8-11].

Unfortunately, the insufficiency or sometimes even the absence of clinical studies evaluating paediatric medicines leaves the physician in a dilemma as to what is the optimum dose to give; and with no guidance on the efficacy and toxicity they are forced to follow a "trial-and-error" approach whereby the licensed adult dosage regimen is scaled down according to the child's weight/size and response is monitored. A previous study evaluated the extent of using unlicensed and off-label

drugs in more than 600 children (Age: 4 days – 16 years) and found that over half of the prescriptions were outside the license of the medicine [12]. Another survey collected data from treatment courses prescribed to 70 neonates in the intensive care unit and found that more than 90 % of administered therapies were not approved (including both unlicensed and off-label use) [13].

2. Conventional routes of drug administration and clinical sampling

The principal routes of drug administration to paediatric patients are oral and intravenous. The former is the preferred route of administration as it is the least "interfering" to the quality of life of the patient [14]. In ideal paediatric practice, oral formulations are designed to be child-appropriate (e.g. solid and liquid based) to suit the swallowing ability and willingness of the child; and at various strengths to meet the different dosage requirements which vary according to the age and weight of the child. In reality, however, there is a significant lack of choice of available paediatric formulations. The "Make Medicines Child Size" initiative which was launched by the World Health Organisation at the end of 2007 highlights this crucial shortfall in paediatric practice and calls for the promotion of child-specific medicine.

Unlike adults, the formulation in which the drug is incorporated is crucial in paediatrics because it is the fundamental reason for successful oral delivery intake. Solid dosage forms such as tablets and capsules are inappropriate for neonates, infants, and young children. Even though it is usually accepted that children of school age are able to swallow solid dosage forms after some training [15, 16], the risk of accidental choking or aspiration should always be considered. Furthermore, many tablets are only available as fixed high strength doses originally designed for adults. To deliver age-appropriate doses for children, they are usually split to provide the smaller doses but this practice leads to highly variable doses even when a commercially available tablet cutter is used [17]. One study reported a difference of 50 – 150 % of the theoretical weight of the split portion of the tablet [18].

Liquid formulations are the most acceptable oral dosage forms for children but unfortunately they are not available for many essential paediatric drugs and clinicians often resort to crushing the tablets and dispersing fractions in a suitable vehicle (which can be water or even soft food) and probably other excipients to improve the solubility. Such practice is common and can lead to wide variability in the dose ingested, as well as stability, bioavailability, and safety issues [14, 19-21]. Commercial liquid formulations of bitter-tasting drugs are difficult, and often expensive, to mask the taste and smell of and will potentially lead to refusal of the child to consume the medication [22]. Stability of drugs present another limitation in liquid based formulations, especially in the case of diluted medicaments which are often executed because the available dose formulations are too concentrated for the child. Measurement of the required volume from a liquid formulation can also introduce inaccuracies in the dose delivered which may be detrimental to the patient's health especially with potent drugs with a narrow therapeutic index, or when given to very young babies.

The absorption of oral drugs can be highly variable and unpredictable due to the incomplete maturation of the child's gastrointestinal tract [3]. Examples of the developing physiological processes include gastric acidity and emptying time, intestinal surface area and motility, gastrointestinal enzymes and efflux transporters, biliary function, first-pass metabolism, and enterohepatic recirculation [2-4, 6, 7]. Furthermore, gastro-oesophageal reflux which is very common in babies up to the age of 1 year may result in regurgitation of the administered drug into the oesophagus and can therefore affect its absorption.

The intravenous route is employed when the clinical condition of the child does not allow for oral administration. Examples include seriously ill children, patients with nausea/vomiting, and uncooperative children. Very young babies are also administered drugs mainly by the intravenous route. In addition, certain drugs are either inactive or cause irritation when given orally and are therefore administered intravenously. The intravenous route is superior to oral delivery in that it by-passes losses due to incomplete absorption and first pass metabolism and results in 100 % bioavailability and a fast onset of action. However, the procedure

causes significant stress, pain and discomfort to the paediatric patient. In fact, needle insertion was found to be one of the most frightening hospital experiences that children recall [23, 24]. Additional pitfalls include the invasive nature of the intravenous route as well as the risk of causing infection and extravasation. These risks are even greater in children receiving multiple intravenous drug therapy, which is the case for most patients in the intensive care unit, who often have several intravenous access lines to avoid compatibility issues. Technical difficulties may, in addition, pose a challenge to the medical team whereby, for example, it may be very hard to find a suitable vein in a distressed child or a very young baby. Commercial intravenous formulations are often too concentrated and toxicity has been reported after slight over-administration of a small undiluted volume of the drug [25]. Hence, physicians resort to serial dilutions but these are commonly associated with calculation and measurement errors [26], in addition to the stability and sterility concerns of such extemporaneous preparations. Finally, formulation safety requirements must be taken into consideration including the pH, osmolality [27], and the type of solvents and excipients used [28, 29].

The intravenous route is the major sampling pathway for therapeutic drug monitoring and diagnostic testing in paediatric patients. As well as the disadvantages outlined above concerning distress to the child, risk of infection and technical difficulties, the volume of blood specimen to be sampled must be minimal. This is especially important in neonates who only have around 80 ml/kg circulating blood volume [30]. Blood sampling for this special group is also performed more frequently than any other paediatric subpopulation and anaemia in young infants is frequently reported as a result. This often leads to blood transfusions to compensate for the lost blood [31, 32] and adds additional risks associated with blood transfusions.

There is clearly a persistent unmet need for paediatric research and for tailored, age-appropriate dosage forms which provide optimum therapy; and the younger the age of the child the greater requirement for improvement. Optimum therapy not only includes achievement of accurate, predictable, and effective dosing and avoidance of adverse effects; but it also needs to address patient

acceptance (e.g. distress caused by injections, unpalatability of liquid oral formulations) and ability (e.g. swallowing solid oral dosage forms) which will ultimately lead to noncompliance issues. Children were described as "therapeutic orphans" back in 1968 [33] and although much has improved since then, paediatric medicine has still not realized the same achievements of "adult" medicine. Evidently, not only much improvement is needed within the oral and intravenous pathways but also other routes of administration/sampling should be explored. In this thesis, a "paediatric-friendly" yet potentially effective strategy to deliver and sample medicinal compounds by the transdermal route is considered.

3. The transdermal route: Alternative non-invasive drug delivery and clinical monitoring

Drug delivery and clinical sampling through the skin as an alternative route is very attractive in the paediatric population. First of all, it circumvents many of the difficulties faced with the oral and intravenous routes. It is easily accessed, minimally invasive, and painless as it does not involve the use of needles. Treatment using the transdermal route is therefore more likely to be acceptable for the paediatric patient. In addition, the transdermal route by-passes the first pass metabolism of oral delivery, the unpredictable oral absorption, as well as the unpalatability issue of liquid formulations. Transport rates can be controlled to deliver doses or sample analytes over extended periods of time. This makes transdermal delivery ideal for drugs used for chronic conditions (it is estimated that 1 in 5 children in the UK suffers from a chronic illness [34]) to provide steady levels of drug input and avoid the peak and trough effects observed with many oral products and with bolus intravenous injections; yet without the requirement for an intravenous infusion. Neonates will also benefit significantly from the transdermal route as they are often administered drugs by multiple and prolonged intravenous access. Sampling of drugs or clinical markers such as glucose by the transdermal route allows for frequent extraction points without the drawbacks of multiple blood

samples. This will allow for more accurate profiling of the levels of the analyte of interest minus the disadvantages and risks associated with intravenous sampling.

3.1 The skin

The skin is the largest organ in the body and is the interface between the internal body components and the external environment [35]. The characteristics of the skin in almost all of the paediatric sub-populations resemble adult skin [36, 37]. The exception is with premature babies born before 34 weeks gestation where the structure of the skin is not fully developed and the stratum corneum in particular is thinner than normal [36-39].

The structure of mature human skin is composed of 3 distinct layers (Figure 1): the subcutaneous tissue (also called hypodermis), the dermis, and the epidermis. Specialised structures including hair follicles, sebaceous glands, sweat glands (eccrine and apocrine), nerve endings and blood vessels are also present [35, 40].

The subcutaneous tissue is composed of a network of fat cells, fibroblasts and macrophages and is the innermost layer of the skin which connects to the dermis by collagen and elastin fibers. It serves as an insulator to the body by protecting it from heat and physical shock. In addition, the subcutaneous tissue carries the major neural and vascular systems for the dermis.

The dermis is composed of connective tissue which embeds several specialized structures. These include dermal adipose cells, hair follicles, sebaceous and sweat glands, lymphatic vessels and nerve endings. The dermis is also highly vascularised and the blood microcirculation is organised into two networks: the superficial vascular plexus spread just below the epidermis-dermis interface, and the deep plexus located at the junction of the dermis-subcutaneous tissue [41]. Through the vascular system, the dermis has an important role in the regulation of body temperature and the supply of oxygen and nutrients to the epidermis and dermis itself while also removing waste and toxins. Other important roles of the
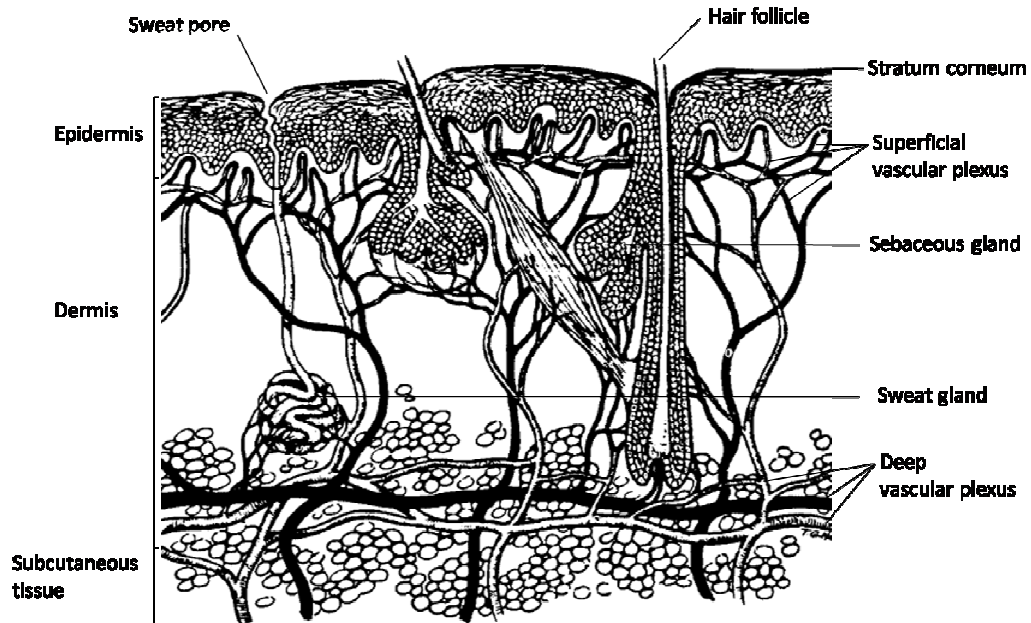
Figure 1: Illustration of the human skin structure (modified from [42])

dermis are the regulation of interstitial pressure, immunological response, and pain [35, 40, 43].

The final layer is the epidermis, an avascular structure with an average thickness of around 100 μm. It consists essentially of keratinocytes (90 – 95 %) in addition to melanocytes, Langerhans and Merkel cells [35, 40]. The epidermis is further subdivided into four distinct layers, which represent different stages of differentiated keratinocytes, starting from the stratum basale situated deepest at the interface with the dermis. The keratinocytes within this layer are the only cells that undergo division in the epidermis. Continuous differentiation of the keratinocytes originating from the stratum basale form the next three layers: the stratum spinosum, the stratum granulosum, and finally the stratum corneum, the outermost layer of the skin .

The keratinocytes in the stratum corneum layer are terminally differentiated nonviable cells and are referred to as corneocytes. The thickness of this compact layer is 10 – 20 μm and its arrangement has been likened to a brick-and-mortar organisation, with the corneocytes (brick) surrounded by a continuous matrix (mortar) of a mixture of specialized lipids which are organised as multiple bilayers.

This mixture mainly includes ceramides, cholesterol, and free fatty acids. Other lipids present in the "mortar" phase are di- and triglycerides, cholesterol sulphate, and sterol/wax esters.

The special architecture of the stratum corneum is responsible for the highly tortuous path to permeation and ensures excellent protective barrier function both inside-out, by controlling the exit of endogenous substances such as water loss, and outside-in barrier against the entrance of pathogens, chemicals, and radiation to the body. The stratum corneum is, therefore, a very effective barrier against the transdermal passive delivery and sampling of drugs and analytes [35, 40] and successful transport at therapeutically acceptable levels is limited to molecules with very specific properties [44].

As mentioned earlier, the structure of the skin in the premature neonate, born before 34 weeks gestation, is underdeveloped and is considerably different from that of the full-term neonate [36-39] in which case it exists as a fully functional barrier resembling intact adult skin [36, 37, 45]. Underdevelopment is observed in all layers of the skin structure (i.e. subcutaneous tissue, dermis and epidermis) [36, 38, 46] but probably the most important immaturity is in the epidermis layer and more critically the stratum corneum. The latter is strikingly thinner with altered lipid composition and structure [36-39, 47]. Nevertheless, the skin of premature infants will reach full maturity after 2 – 3 weeks of postnatal period [37] but very premature neonates may require up to 8 weeks for full development to be achieved [45]. The two major clinical hazardous consequences from an immature skin are the excessive water and heat losses from the body [48]. The stratum corneum is significantly more permeable and application of topical products (for example alcohols used as antiseptics [49]) may lead to significant systemic absorption and eventually life-threatening toxic effects. The increased permeability property could, however, be explored to the neonate's advantage by transdermal delivery or sampling of drugs and clinical analytes which may be otherwise considered unsuitable candidates to permeate through a fully developed skin barrier.

The following section provides examples of *in vivo* permeation studies and approved transdermal systems, some of which are applicable to paediatric subjects including the premature subgroup.

3.2   Passive transdermal systems:

The use of the transdermal route to therapeutically deliver and sample analytes into and from the body is significantly limited by the low permeability of the intact skin barrier and specifically the stratum corneum. Drugs applied on the skin permeate through by passive diffusion [50] and the permeability coefficient of the drug (K_p), which is formulation-dependent, is given by:

$$K_p = \frac{K \cdot D}{H}$$ Equation (1)

Where K is the drug's partition coefficient between the donor vehicle and the outer layer of the stratum corneum. H is the length of the diffusion path and D is the diffusivity of the drug within it. Drug permeation at steady state can be described by Fick's first law of diffusion, and the flux per unit area (J_{ss}) is defined in a simple form as [51]:

$$J_{ss} = K_p \times C$$ Equation (2)

Where C is concentration of the drug in the donor vehicle. According to the previous two relations, transdermal drug delivery by passive diffusion can be optimised by manipulation of K, D, and C.

Since the start of the transdermal patch developments in the 1970s, over ten transdermal passive drug systems reached approval and commercialization. These include the passive delivery of the first-approved transdermal drug: scopolamine for motion sickness, fentanyl for chronic pain management (approved for children > 2 years old), methyphenydate for attention deficit hyperactivity disorder (approved for children > 6 years old), buprenorphine for chronic pain relief, selegiline for depression, nitroglycerin for angina, clonidine for hypertension, nicotine for smoking cessation, oxybutynin for overactive bladder, rotigotine for Parkinson's

disease, testosterone for hormone replacement, and oestradiol and northisterone for hormone therapy and contraception [52, 53]. In addition to the transdermal patches, other drugs used for local effects include the anaesthetic lidocaine which is licensed for the dermal relief of pain associated with post-herpetic neuralgia in adults. It is also marketed as a cream (EMLA®, AstraZeneca PLC, London, UK) containing a eutectic mixture with prilocaine and is widely used in children > 1 year old to provide dermal anaesthesia prior to clinical procedures (e.g. venipuncture and intravenous catheter placement) [52, 54]. Most of the drugs mentioned above have common properties in that they are therapeutically very potent agents (i.e., daily doses < 10 mg) and possess certain physicochemical properties (e.g., MW < 500) which render them suitable for passive delivery [44].

There are no transdermal passive systems currently approved for premature neonates. A few *in vivo* studies investigated the passive permeation of the methylxanthines: theophylline and caffeine through the premature neonate skin and delivery at therapeutic levels was achieved [55-58]. These drugs are frequently used in the treatment of neonatal apnea, a very common condition in premature infants which requires several weeks of treatment [59]. In addition, therapeutic drug monitoring especially in the case of theophylline is important to avoid dangerous side effects (e.g. tachycardia) [59]. A previous study [60] attempted transdermal passive extraction of theophylline in premature babies and the rates of extracted drug were shown to correlate to the corresponding plasma concentrations measured by the conventional blood sampling method [60].

As stated above, for a compound to be suitable for transdermal passive delivery, it must meet strict characteristics. This poses a great limit to the range of therapeutic agents that can be delivered or sampled transdermally. In addition, a major pitfall with passive transdermal systems is the significant lag time for the permeation rates to provide a therapeutic systemic concentration. For example, for theophylline and caffeine permeation studies mentioned earlier, this was found to be 22 and 48 hours, respectively [56, 57].

The following sections introduce the concept of iontophoresis which is a physical enhancement method by which a wider spectrum of medicinal compounds can be delivered/sampled efficiently at significantly higher quantities by the transdermal route and at shorter lag times required to reach therapeutic systemic levels.

3.3 Active transdermal delivery systems: Iontophoresis

Transdermal iontophoresis is one of the many physical enhancement methods used to improve the delivery/sampling of medicinal compounds through the skin [44, 61]. The basic mechanisms of iontophoresis were recognised over 100 years ago but it was only in the past few decades that interest in drug delivery/sampling applications has been renewed. Iontophoresis has been used for both local delivery and systemic applications and a small number of approved products have reached the market [62, 63] as a result of extensive *in vitro* and *in vivo* studies [64-66]. The technique involves the application of a low electrical current ($\leq$ 0.5 mA/cm^2) across the skin to enhance the transdermal passage of molecules at levels significantly higher than passive transport and in a highly controlled and sustained manner [65, 67, 68]. The spectrum of compounds that could be delivered or sampled is considerably extended when iontophoresis is used, relative to passive diffusion, to include: macromolecules such as peptides, proteins, and nucleotides, and charged and/or hydrophilic compounds. The characteristics of such compounds make them the least ideal candidates for passive diffusion.

3.3.1 Description

A typical iontophoretic device (Figure 2) consists of two electrode compartments, anodal and cathodal. Each chamber, already filled with a current-conducting medium (e.g., solution or gel), is applied on a different site of the skin and a pair of electrodes is placed in direct contact with the formulations held in the compartments [65]. A small electrical current is then applied via a current source which is connected to the electrodes. This causes the following electrochemical reactions: oxidation at the anode electrode surface and reduction at the cathode
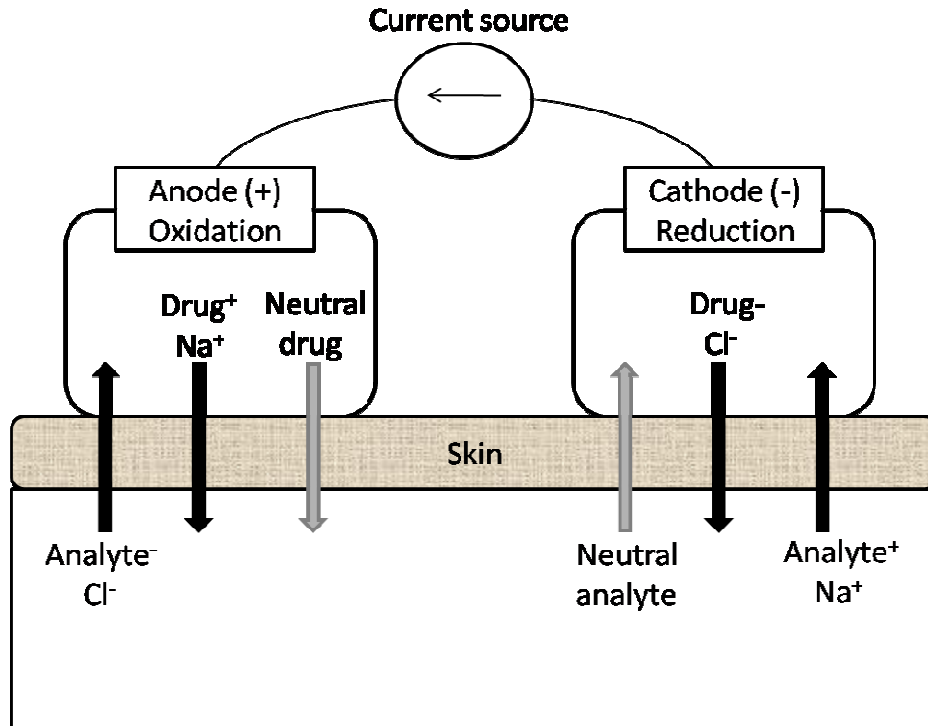
Figure 2: A schematic diagram illustrating a basic iontophoretic device. The mechanisms of iontophoretic transport across the skin are represented by: black arrows for electromigration and grey arrows for electroosmosis.

electrode interface. Electrodes made using silver/silver chloride are the most frequently used materials in iontophoresis owing to their reversibility, biocompatibility, and avoidance of formulation pH change during application (as opposed to other electrodes such as platinum) [69, 70].

The processes of oxidation and reduction of the Ag/AgCl electrodes will create an imbalance in the formulations which are separated by the skin. Equal consumption and release of chloride ions take place at the anode and cathode interface, respectively:

$$Anode: Ag + Cl^- \rightarrow AgCl + e^- \quad AND \quad Cathode: AgCl + e^- \rightarrow Ag + Cl^-$$

The imbalance created is restored by the movement of ions from the electrode chambers into the skin towards the electrode of opposite polarity and *vice versa* from beneath the skin into the electrode compartments [68]. That is, ions with a positive charge (cations) are repelled towards the cathode, and negatively

charged molecules (anions) migrate towards the anode. This is the principal concept for the direct effect of the applied electrical field on the transport of ions through the skin.

3.3.2 Transport mechanisms

There are three contributions to the total transport flux of a molecule (J_T) during iontophoresis [68]:

$$J_T = J_{EM} + J_{EO} + J_P \hspace{3cm} \text{Equation (3)}$$

P denotes passive diffusion of the molecule which occurs irrespective of electrical current application and is the result of the concentration gradient present at each side of the skin. Passive diffusion of the permeant may however increase during the course of iontophoresis due to increased permeability of the skin. Electromigration (*EM*) is the direct interaction of the applied current with charged species which results in the ion's migration to the electrode of opposite charge (Figure 2) [71]. Electroosmosis (*EO*) is due to the convective solvent flow induced as a result of the skin's negative charge [72].

Separation of the individual contribution of each of the above mentioned mechanisms is difficult. However, passive diffusion for charged and polar molecules across intact skin is usually negligible relative to the transport obtained with iontophoresis and it is generally assumed, and expected, that only electromigration and electroosmosis are the two dominant mechanisms during iontophoresis.

3.3.2.1 *Electromigration*

As mentioned earlier, ions (including the drug or analyte of interest) migrate towards the electrode chamber of opposite polarity in order to maintain eletroneutrality disturbed by the oxidation and reduction processes taking place at the anode and cathode, respectively, as a result of current flow. The rate at which each ion moves (i.e. electromigration flux, J_{EM}, mole/s) can be described by Faraday's law [71]:

$$J_{EM} = \frac{T \times I}{z \times F}$$

Equation (4)

Where I is the current intensity applied (amperes), F is Faraday's constant (coulombs/mole), z and T are, respectively, the numerical value of the valence and the transport number of the ion. As equation (4) outlines, the transport flux of the ion is directly influenced by the current intensity applied (controlled externally by the iontophoresis device) and by the transport number of the drug. The latter parameter describes the efficiency of the ion of interest as a charge "carrier" relative to the other ions (both co- and counter- ions) present in the iontophoresis system which also compete to carry a fraction of the charge. The conservation of charge principle implies that the total applied electrical current must equal the sum of individual currents carried by each of the ions present in the system. The transport number of the drug (T_d) depends on its own properties as well as those of competing ions [71]:

$$T_d = \frac{\mu_d \times c_d \times z_d}{\sum_i (\mu_i \times c_i \times z_i)}$$

Equation (5)

Where μ, c, and z are, respectively, the mobility, concentration, and absolute valence, within the skin, of either the drug (d) or any charge-carrying ion (i) in the iontophoresis system. For a binary cation delivery system, for example, the drug "d^+" competes with a co-ion "i^+" in the anode and a counter-ion "i^-" (typically chloride which represents the principal skin charge carrier ion that competes against the cations by migrating from the opposite side (subdermal) of the skin). The same is true for a binary anion delivery system where the negatively charged drug competes along with another anion present in the cathode donor formulation and also competes with counter-ions migrating from the subdermal side of skin (typically sodium ions).

Further development of equation (5) by Phipps and Gyory yielded the following expression for a binary cation system [71]:

$$T_{d+} = \frac{\dfrac{T^0_{d+}}{1-T^0_{d+}}}{\left(\dfrac{T^0_{d+}}{1-T^0_{d+}}\right)+BZ_+X_+\left(\dfrac{1}{1-T^0_{i+}}\right)+1}$$

Equation (6)

Where T^0_{d+} and T^0_{i+} are the transport numbers of the drug "d^+" and the co-ion "i^+" when present separately as the sole cation in the donor formulation (otherwise known as the single-ion condition) and, therefore, the only competition each cation is faced with is that from the counter-ion migrating from the opposite side of the skin. B is a proportionality constant which links the concentration ratio of the two cations within the skin to that in the donor formulation. Z_+ and X_+ are, respectively, the valence ratio (z_{i+}/z_{d+}) and the molar fraction ratio (x_{i+}/x_{d+}) of the two cations in the donor formulation ($x_{i+} + x_{d+} = 1$). The validity of this expression for several binary systems has been demonstrated by experimental data [71, 73]. However, prior knowledge of the factor B limits the usefulness of such application. A growing number of data have also revealed a simple direct linear trend between the transport number of some drugs and their molar fraction in the donor solution [73, 74].

Equation (5) also demonstrates that to achieve maximal transport for the drug, competition from the other ions (co- and counter- ions) must be minimised as much as possible. Competition from the endogenous counter-ions (principally chloride or sodium ions) is inevitable and cannot be modified. However, co-ions present in the donor formulation along with the drug can be minimised or sometimes even eliminated. The latter condition "single-ion", as predicted by Kasting and Keister [75], demonstrates that the transport number of the drug becomes independent of concentration and is only a function of the drug's diffusivity (D_d) within the membrane relative to that of the counter ion (D_i):

$$T^0_d = \frac{D_d}{D_d + D_i}$$

Equation (7)

Finally, a note is made about the transport number which is sometimes referred to as "transference" number. This is when iontophoretic transport fluxes

cannot be solely attributed to electromigration only (i.e., electroosmosis also contributes to the total flux observed) [76].

3.3.2.2 *Electroosmosis*

Electroosmosis is induced as a result of the skin's negative charge at physiological pH which makes the membrane more permselective to cations [77-79]. Hence, the electric current applied induces an electroosmotic convective solvent flow in the direction of cations migration (i.e., anode to cathode) [72, 77, 80]; and any dissolved solutes including neutral and charged molecules will be carried along with this stream of solvent. It follows that the iontophoretic transport of cations is supplemented by electroosmosis as it occurs in the same direction as their electromigration. Nevertheless, the contribution of electroosmosis to the iontophoretic transport of relatively low molecular weight cations is small and electromigration tends to dominate [81, 82]. However, for neutral species and high molecular weight cations, it is especially important as 1) neutral molecules experience no electromigration; and 2) electromigration of larger cations is small because of their low transport efficiency relative to the total system (i.e., low transport number).

The electroosmotic solvent flow (J_{vs}, volume.time^{-1}) has been quantified directly but this is not readily simple [79, 83-86]. Indirect measurements through so called "electroosmotic markers" have been used extensively in previous research studies. Examples of markers used in previous work are mannitol and acetaminophen [81, 87]. The electroosmotic flux of a solute ($J_{eo, solute}$) can be expressed as follows [83]:

$$J_{eo, \ solute} = J_{vs} \cdot C_{solute} \cdot (1 - \sigma_{solute}) = Z \cdot C_{solute}$$

Equation (8)

Where C_{solute} and σ_{solute} are, respectively, the solute concentration and its reflection coefficient at the membrane-solution interface [83, 88-90]. Z represents the iontophoretic transport efficiency of the solute through the skin; and is related

to the convective flow of the solvent (J_{vs}) as well as the reflection coefficient of the solute. The latter is a solute-membrane dependent index which reports on the level of reflection the permeant experiences, relative to the solvent, from the membrane as it is dragged through by the process of electroosmosis.

3.3.3 Drug delivery applications

A large number of studies have shown the ability of iontophoresis to deliver therapeutic doses of a wide variety of medicinal compounds. These include peptides and proteins [91, 92], oligonucleotides [93, 94], analgesics and local anaesthetics [95-106], anti-inflammatory drugs [107-117], anti-viral compounds [118-121], anti-Parkinson drugs [122-124], and anti-migraine agents [125-127].

There are currently three approved iontophoretic drug-prefilled delivery devices. The Macroduct® (approved for all ages including neonates) which locally delivers pilocarpine to diagnose cystic fibrosis (Figure 3), the LidoSite™ system (approved for children > 5 years old) which delivers lidocaine for local anaesthesia (Figure 4), and the Ionsys™ for the systemic delivery of fentanyl to relief post-operative pain (Figure 5).

Iontophoretic delivery of pilocarpine has been used extensively for several decades as a reliable test for the diagnosis of cystic fibrosis. The iontophoretic delivery of pilocarpine (5 minutes at 1.5 mA) induces sweat production which is

Figure 3: The Macroduct® iontophoretic system (Wescor Inc, Utah, USA) for diagnosis of cystic fibrosis [128].

Figure 4: The LidoSite[TM] iontophoretic system (Vyteris Inc, NJ, USA) for dermal anaesthesia [129].

then collected in the electrode compartments and quantified for chloride levels. High concentrations of chloride are indicative of cystic fibrosis [130].

LidoSite[TM] (Figure 4) was recently launched for use in subjects over 5 years old to minimise pain, by means of dermal anaesthesia, associated with invasive clinical procedures (e.g. venipuncture and intravenous catheter placement). This product is the culmination of considerable research which realised the special advantage of rapidly and more efficiently achieving dermal anaesthesia by lidocaine iontophoresis relative to passive permeation only. EMLA® eutectic cream is one popular example used to passively deliver lidocaine for dermal anaesthesia. While the use of this system requires 1 – 2 hours to reach desired effects and at only 3 – 5 mm depth [131, 132], iontophoresis of lidocaine was shown to have a much faster onset of action of ~ 10 minutes and a depth of anaesthesia reaching 6 – 10 mm [104, 105, 133-135]. In addition, comparative studies in children showed either superior or similar anaesthetic effect with lidocaine iontophoresis relative to EMLA cream [95, 106]. The systemic absorption of iontophoresed lidocaine was also found to be negligible despite repeated application [136] and the same study reported excellent tolerability of the application by the volunteers (Ages: 5 – 15
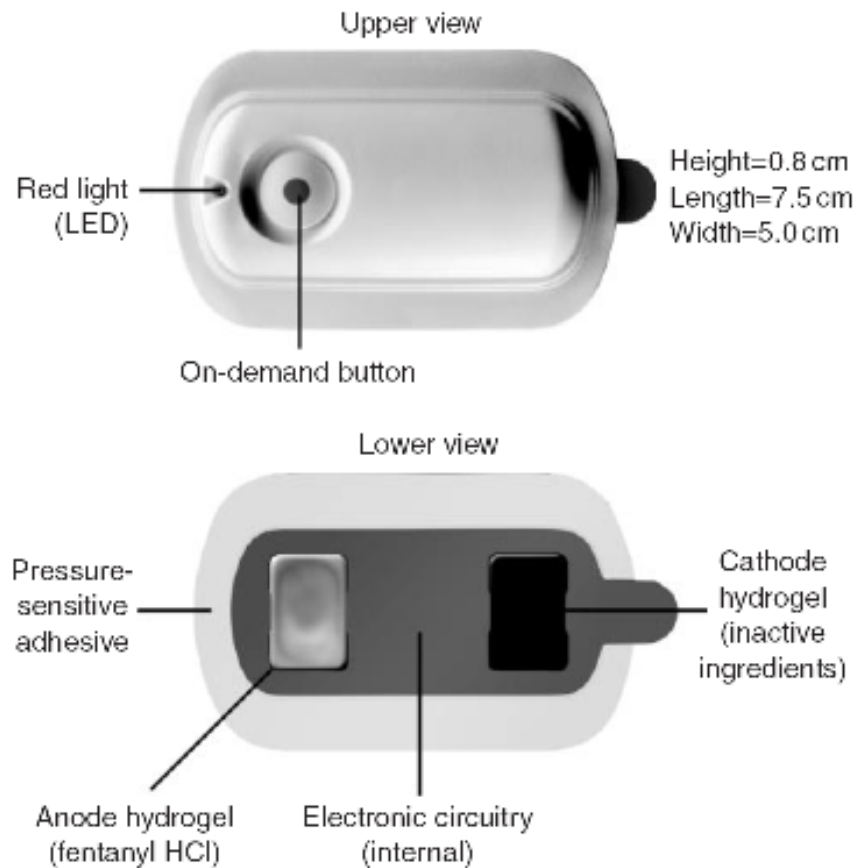
Figure 5: The Ionsys[TM] iontophoretic system (Janssen-Cilag Ltd) for acute pain control post-operation [137].

years). The efficacy, safety, and tolerability of lidocaine iontophoresis was further confirmed in a large randomized, controlled trial which involved 548 subjects, half of which were children (Ages: 5 – 17 years old) [138].

Also launched recently is the Ionsys[TM] transdermal iontophoretic device (Figure 5) for the systemic delivery of fentanyl to manage post-operative acute pain. In comparison with the passive fentanyl patch mentioned earlier (section 3.2) which is only approved for chronic pain management, the fast onset of action of the iontophoresis patch granted its application in acute pain management whereby a quick onset of analgesia is the ultimate goal for a successful therapy [137, 139]. The Ionsys[TM] system is programmed to deliver, on-demand, a dose of 40µg of fentanyl over a period of 10 minutes at 0.17 mA current. This is for a maximum number of 80 doses or a maximum duration of 24 hours, whichever is first. This dosage regimen was based on earlier *in vivo* studies which studied the systemic

concentrations of fentanyl resulting from different current intensities used [140, 141]. The effectiveness of Ionsys[TM] at post-operative pain control was reviewed relative to the conventional intravenous morphine patient-controlled analgesia (PCA) system and an equally effective analgesic effect was found [142] with the obvious yet crucial advantage of the non-invasiveness of the transdermal route.

3.4 Active transdermal systems for clinical sampling: Reverse iontophoresis

3.4.1 Definition

Owing to the symmetrical nature of iontophoresis, both transdermal delivery and sampling of molecules to/from the body are possible [143]. That is, the same applied current that promotes exogenous molecules to cross the skin and enter into the body, also drives analytes, present in the subdermal (interstitial) fluid, to move towards the external surface of the skin and be collected in a suitable collection device (Figure 2). The latter is referred to as "reverse iontophoresis" [67, 68]. The molecules extracted by reverse iontophoresis are originally present in the interstitial (subdermal) fluid that bathes the skin, which in turn is in direct communication with the blood, the main compartment for conventional sampling. The interstitial fluid can therefore serve as a good alternative sampling matrix for analytes.

Obviously, the transport mechanisms of reverse iontophoresis are exactly the same as iontophoresis (section 3.3.2). Cations and neutral analytes are therefore sampled at the cathodal side, while anions are assayed at the anodal side of the collection device.

3.4.2 Internal standard

In order to be able to correlate the reverse iontophoretic flux of the extracted analyte to its corresponding systemic concentration in the body, a calibration methodology must be employed whereby a proportionality factor is used to convert the extraction fluxes into "clinically meaningful" conventional numbers.

Moreover, due to potential inter- and intra-subject variations in the extraction efficiency of the analytes, a calibration concept using an "internal standard" was introduced [144, 145] and its extent of validity was tested *in vivo* for several analytes [146-148]. This approach takes advantage of the fact that: A) iontophoresis is non-selective and several analytes are simultaneously extracted to the appropriate electrode collection device; and B) amid these extracted analytes are some endogenous molecules which tend to be present in the body almost always at invariable concentrations (e.g., sodium and potassium). It follows that iontophoretic extraction of such molecules (J_{IS}), labelled as internal standards, is effectively constant when compared to the solute of interest whose extraction values (J_{solute}) depend on its respective systemic concentrations (C_{solute}). A proportionality factor (γ) can therefore be drawn relating the extraction fluxes of both analytes to their corresponding systemic concentrations:

$$\frac{J_{solute}}{J_{IS}} = \gamma \cdot \frac{C_{solute}}{C_{IS}} \qquad \text{Equation (9)}$$

If the proportionality factor and the systemic concentration of the internal standard (C_{IS}) are indeed constant in a wide subject population, equation (9) can be rewritten as:

$$\frac{J_{solute}}{J_{IS}} = \gamma^{\#} \cdot C_{solute} \qquad \text{Equation (10)}$$

Using equation (10), where $\gamma^{\#} = \gamma/C_{IS}$, the systemic concentration of the solute of interest can, indeed, be determined solely from the extraction flux data.

3.4.3   Clinical sampling applications

The effectiveness of using transdermal reverse iontophoresis as an alternative sampling technique demonstrated its usefulness in humans. Previous *in vivo* studies included lithium monitoring in bipolar patients [146], phenylalanine monitoring in phenylketonuria [149], urea sampling for the diagnosis and monitoring of chronic kidney disease [150], lactate [151], various amino-acids [152], and glucose sampling for diabetics [153, 154]. The latter application was further developed and led to the

Figure 6: The Glucowatch® Biographer (Johnson & Johnson, NJ, USA) [155].

commercialization of the first and only reverse iontophoresis-based device: the Glucowatch® Biographer (Figure 6) for adults and children over 7 years old [155, 156]. This device continuously monitors glucose levels, every 10 minutes, by sampling glucose up to 13 hours per day and provides, therefore, a superior amount of information concerning glucose levels over the traditional finger-prick technique (example in Figure 7). The Glucowatch® device, however, requires daily calibration with one blood sample to be able to confidently translate glucose extraction values to corresponding systemic glucose levels. Exploration of the internal standard concept could refine the current drawback of the device and may render the procedure totally non-invasive [147, 148, 157].
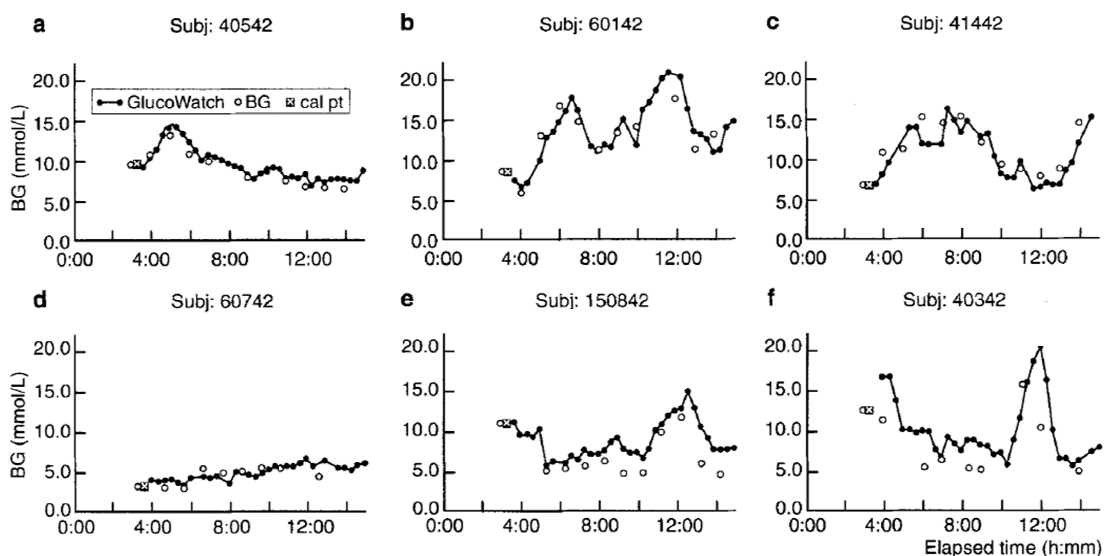

Figure 7: Representative data from six subjects comparing blood glucose levels (BG) with results from the Glucowatch® Biographer [158].

3.5   Pathways of transport

With the exception of some highly lipophilic molecules, the stratum corneum is the rate-limiting layer of the skin to the transport of most compounds. There are three pathways by which molecules move across intact stratum corneum: intercellular (or paracellular), intracellular (also called transcellular), and appendageal (also referred to as shunt) routes. The latter transport pathway exists due to the hair follicles and sweat ducts which offer low electrical resistance, natural "pores" at the surface of the skin. It has, therefore, been suggested that the shunt route plays an important pathway to iontophoretic transport [159] because the flow of current will follow the least resistant pathway provided by the shunt route. This has indeed been confirmed by several studies using different methods to identify the contribution of the principal pathway both in the case of ionised and neutral compounds.

Using a vibrating probe electrode to scan the surface of hairless mouse skin, the appendageal structures were found to carry most of the applied current [160]. Several subsequent studies [85, 161-164] used scanning electrochemical microscopy (SECM) to visualise the principal route of transport for both neutral and ionised molecules across either hairless mouse skin or human skin; and further confirmation of the localization of iontophoretic transport to appendageal pathways was found. These observations were subsequently re-enforced by another set of studies [165, 166] which employed a different technique to evaluate the shunt route contribution by means of using a skin sandwich. The latter comprised a piece of human stratum corneum placed on the top of a section of an epidermis from the same sample of human skin to effectively block the appendages of the lower stratum corneum. Iontophoretic transport of neutral and charged molecules was then tested and fluxes were compared to those obtained across human epidermis only and confirmed the importance of the appendageal route in iontophoresis.

Nevertheless, the intercellular pathway was also found to contribute as the dominant route for the iontophoretic transport of some compounds such as

mercuric ions [167]. The contribution of the intercellular and appendageal pathways during iontophoresis may well depend on the physicochemical properties of the permeant [168-170].

3.6 Tolerability and safety of transdermal iontophoretic applications

It must be acknowledged that when evaluating transdermal iontophoresis applications, the whole system should be considered. This includes all solutes and solvents used in the anode and cathode formulations (including the drug to be delivered) as well as the polymers used for example in the adhesive material necessary to affix the patch into the skin. All these components may themselves provoke skin irritation. Potential irritation or tissue trauma may result from the adhesive material and children are also usually scared of adhesive removal. This may subsequently lead to noncompliance. Further, the skin of premature neonates is especially prone to tissue trauma after adhesive removal because their skin is already compromised. There are, however, new technologies with both good adhesive properties and gentle effect on the skin when the patch is removed, ensuring less perturbation to the stratum corneum [171]. Finally, transdermal formulations for drug delivery usually contain high doses of the active ingredient. Accidental sucking, chewing, or sometimes ingestion of the transdermal patch by the child can potentially lead to fatal toxicities [172]. Strict guidelines for use and disposal of the patches are of paramount importance when the transdermal route is used in paediatric patients.

Iontophoresis is well supported, by clinical experience and various non-invasive bioengineering methods, as a safe procedure. The most frequent effects reported are tingling sensation during current application and erythema which tends to resolve quickly after current termination [173]. The tingling sensation is mostly felt at the beginning of iontophoresis and it can be minimised by "ramping" up the current slowly to the desired intensity over the first few minutes of iontophoresis. A general upper limit of 0.5 mA/cm^2 current density ensures minimal effects but incorrect use of the iontophoresis system may result in tissue irritation or even burning.

Several techniques were used *in vivo* to evaluate the acute effects of iontophoresis application on the barrier function of intact skin [174, 175]. These include non-invasive biophysical techniques such as transepidermal water loss (TEWL), attenuated total reflectance-fourier transform infrared (ATR-FTIR) spectroscopy, impedance spectroscopy (IS), and laser doppler flowmetry (LDF). TEWL, which as the name suggests measures the loss of water from the skin providing a very good indicator of the barrier integrity of the skin, was found to increase but this was attributed to enhanced hydration of the skin due to exposure to the applied formulation [176, 177]. ATR-FTIR records spectra of IR absorbance by the skin components and provides details on the ordering of the intercellular lipids of the stratum corneum as well as the level of hydration. From available data, iontophoresis does not seem to cause any significant effect apart from that associated with formulation exposure effect (in the absence of current) [176, 178]. Low-frequency IS, which measures the electrical resistance of the skin to the movements of ions through it, revealed a quick decrease in the skin's resistance during current application. This is obviously due to the fact that during iontophoresis, ions move across the skin at high levels which will result in reduction of the skin's electrical resistance. The recovery of skin impedance post-iontophoresis depends on the duration of current application as well as the density of the applied current [179]. LDF measures the cutaneous blood perfusion non-invasively. Local erythema observed post-iontophoresis is indicative of increased blood flow to the application area and this has indeed been confirmed by higher LDF measurements after iontophoresis application [176, 177].

3.7   *In vitro* transdermal permeation studies:

For obvious ethical, economic, and practical reasons, skin permeation studies are usually evaluated *in vitro* before *in vivo* investigations are deemed necessary or valid. The design of an *in vitro* experiment should, therefore, mimic *in vivo* conditions as close as possible. A typical *in vitro* setup for iontophoretic drug delivery involves the use of diffusion cells, a model skin membrane separating the diffusion cell compartments, mediums representing the drug formulation in the

donor chamber and a receptor phase placed in the subdermal compartment, and finally suitable electrodes and a power source. The types of diffusion cells used in this thesis are shown in Figure 8. The drug formulation to be delivered is placed either at the anode or cathode chamber depending on the drug's charge. Similarly, for reverse iontophoresis experiments, the analyte, present in the subdermal compartment, is sampled at either the anode or cathode chambers (or sometimes both) depending on the analyte's charge.
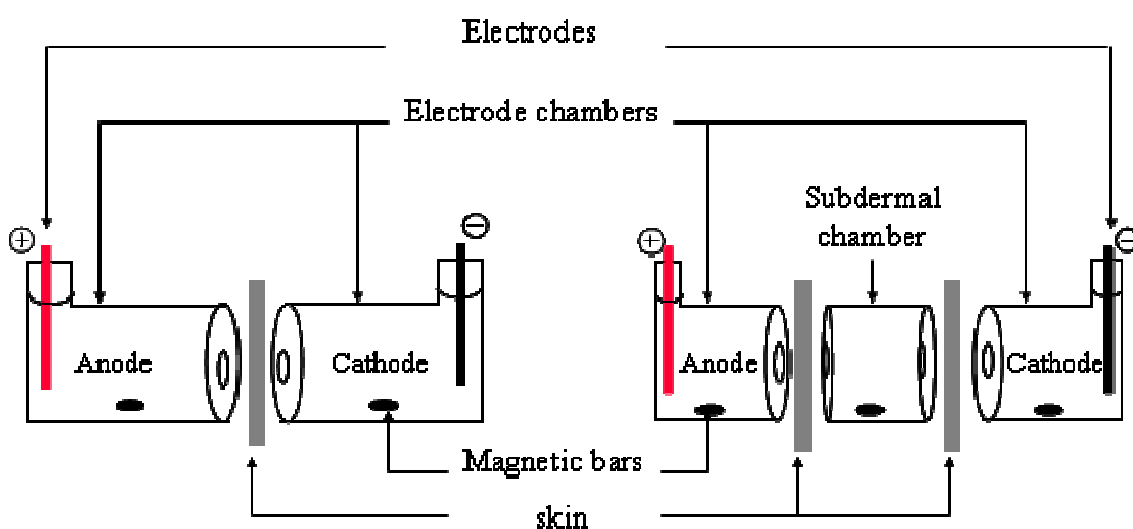
Figure 8: Schema of side-by-side diffusion cells, composed of either two compartments (left) or three compartments (right).

Pig skin was implemented for all permeation studies in this thesis because it is considered a suitable biological model to human skin. This is due to the considerable similarities observed in skin physiological properties (e.g. stratum corneum thickness), biophysical properties (e.g. TEWL and low-frequency IS), permselectivity (isoelectric point), and permeability properties to several compounds [78, 180-186].

Both intact and barrier compromised pig skin were used in this thesis. Intact pig skin represented the fully developed barrier function which is found in the majority of the paediatric population, and compromised pig skin represented the

underdeveloped skin barrier found in premature neonates. The rationale for using compromised pig skin as a model to premature skin is as follows:

Determination of the thickness of the stratum corneum is usually made by sequential tape-stripping of the skin and the level of barrier function removed is precisely guided by measurements of TEWL. In a previous study [183], the thickness of intact pig skin was found to be 11.8 ± 4.0 μm which was strikingly similar to that of human intact skin (10.9 ± 3.5 μm). By using the same concept of TEWL measurements, the skin of premature babies, whose barrier function is recognized to be compromised due to the incomplete development of the stratum corneum, was modelled *in vitro* by differentially-stripped, and therefore compromised, pig skin whereby the TEWL of the barrier function level mirrors that found for the skin of premature babies of different post-conceptional age [187]. Figure 9 shows the striking similarity when the TEWL measurements from the two barriers were superimposed. A subsequent study by the same group demonstrated that, by using the *in vitro* data obtained with differentially-stripped pig skin, the *in vivo* transdermal drug permeation behaviour could be predicted (at least comparatively) as a function of the post-conceptional age of the neonate [188].
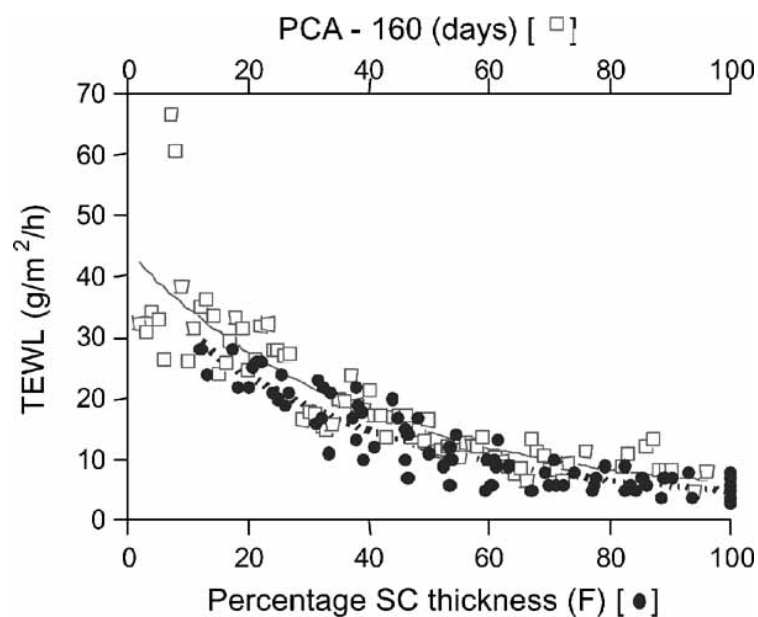

Figure 9: The transepidermal water loss parameter is used to link the barrier function properties of neonates (expressed empirically as days of the post-conceptional age minus 160) with compromised pig skin ([187])

4. References

1.   Sagraves, R., *Pediatric dosing and dosage forms*, in *Encyclopedia of pharmaceutical technology*, Swarbrick, J., Editor. 2007, Informa Healthcare: New York; London. p. 2629-2650.

2.   Blumer, J. L., and Reed, M. D., *Principles of neonatal pharmacology*, in *Neonatal and pediatric pharmacology : Therapeutic principles in practice*, Yaffe, S. J., and Aranda, J. V., Editors. 2005, Lippincott Williams & Wilkins: Philadelphia; London. p. 146-158.

3.   Kauffman, R. E., *Drug action and therapy in the infant and child*, in *Neonatal and pediatric pharmacology : Therapeutic principles in practice*, Yaffe, S. J., and Aranda, J. V., Editors. 2005, Lippincott Williams & Wilkins: Philadelphia; London. p. 20-31.

4.   Kearns, G. L., Abdel-Rahman, S. M., Alander, S. W., Blowey, D. L., Leeder, J. S., and Kauffman, R. E., *Developmental pharmacology - drug disposition, action, and therapy in infants and children.* N Eng J Med, 2003. **349**: p. 1157-1167.

5.   De Zwart, L. L., Haenen, H. E., Versantvoort, C. H., Wolterink, G., van Engelen, J. G., and Sips, A. J., *Role of biokinetics in risk assessment of drugs and chemicals in children.* Regul Toxicol Pharmacol, 2004. **39**: p. 282-309.

6.   Rane, A., *Drug metabolism and disposition in the infant and child*, in *Neonatal and pediatric pharmacology : Therapeutic principles in practice*, Yaffe, S. J., and Aranda, J. V., Editors. 2005, Lippincott Williams & Wilkins: Philadelphia; London. p. 32-43.

7.   Routledge, P. A., *Pharmacokinetics in children.* J Antimicrob Chemother, 1994. **34**: p. 19-24.

8.   Takahashi, H., Ishikawa, S., Nomoto, S., Nishigaki, Y., Ando, F., Kashima, T., Kimura, S., Kanamori, M., and Echizen, H., *Developmental changes in*

pharmacokinetics and pharmacodynamics of warfarin enantiomers in japanese children. Clin Pharmacol Ther, 2000. **68**: p. 541-555.

9.   Marshall, J. D., and Kearns, G. L., *Developmental pharmacodynamics of cyclosporine.* Clin Pharmacol Ther, 1999. **66**: p. 66-75.

10.   Marshall, J., Rodarte, A., Blumer, J., Khoo, K. C., Akbari, B., Kearns, G., and Netwo, P. P. R. U., *Pediatric pharmacodynamics of midazolam oral syrup.* J Clin Pharmacol, 2000. **40**: p. 578-589.

11.   De Wildt, S. N., Kearns, G. L., Sie, S. D., Hop, W. C. J., and Van den Anker, J. N., *Pharmacodynamics of intravenous and oral midazolam in preterm infants.* Clin Drug Invest, 2003. **23**: p. 27-38.

12.   Conroy, S., Choonara, I., Impicciatore, P., Mohn, A., Arnell, H., Rane, A. R., Knoeppel, C., Seyberth, H., Pandolfini, C., Raffaelli, M. P., Rocchi, F., Bonati, M., Jong, G., de Hoog, M., and Van den Anker, J., *Survey of unlicensed and off label drug use in paediatric wards in european countries.* Brit Med J, 2000. **320**: p. 79-82.

13.   Conroy, S., McIntyre, J., and Choonara, I., *Unlicensed and off label drug use in neonates.* Arch Dis Child, 1999. **80**: p. F142-F144.

14.   Tuleu, C., *Paediatric formulations in practice*, in *Paediatric drug handling*, Costello, I., Long, P. F., Wong, I. K., Tuleu, C., and Yeung, V., Editors. 2007, Pharmaceutical Press: London. p. 43-74.

15.   Nahata, M. C., *Drug formulations*, in *Neonatal and pediatric pharmacology : Therapeutic principles in practice*, Yaffe, S. J., and Aranda, J. V., Editors. 2005, Lippincott Williams & Wilkins: Philadelphia; London. p. 111-118.

16.   Schirm, E., Tobi, H., de Vries, T. W., Choonara, I., and De Jong-van den Berg, L. T. W., *Lack of appropriate formulations of medicines for children in the community.* Acta Paediatr, 2003. **92**: p. 1486-1489.

17.   Van Santen, E., Barends, D. M., and Frijlink, H. W., *Breaking of scored tablets: A review.* Eur J Pharm Biopharm, 2002. **53**: p. 139-145.

18.   Teng, J., Song, C. K., Williams, R. L., and Polli, J. E., *Lack of medication dose uniformity in commonly split tablets.* J Am Pharm Assoc (Wash), 2002. **42**: p. 195-199.

19.   Nahata, M. C., and Allen, L. V., Jr., *Extemporaneous drug formulations.* Clin Ther, 2008. **30**: p. 2112-2119.

20.   Pawar, S., and Kumar, A., *Issues in the formulation of drugs for oral use in children: Role of excipients.* Paediatr Drugs, 2002. **4**: p. 371-379.

21.   Standing, J. F., and Tuleu, C., *Paediatric formulations--getting to the heart of the problem.* Int J Pharm, 2005. **300**: p. 56-66.

22.   Mennella, J. A., and Beauchamp, G. K., *Optimizing oral medications for children.* Clin Ther, 2008. **30**: p. 2120-2132.

23.   Cummings, E. A., Reid, G. J., Finley, G. A., McGrath, P. J., and Ritchie, J. A., *Prevalence and source of pain in pediatric inpatients.* Pain, 1996. **68**: p. 25-31.

24.   McMurtry, C. M., *Needle and dread: Is it just a little poke? A call for implementation of evidence-based policies for the management of needle pain in clinical settings.* Paediatr Child Health, 2007. **12**: p. 101-102.

25.   Berman, W., Jr., Whitman, V., Marks, K. H., Friedman, Z., Maisels, M. J., and Musselman, J., *Inadvertent overadministration of digoxin to low-birth-weight infants.* J Pediatr, 1978. **92**: p. 1024-1025.

26.   Dyer, C., *Gmc clears doctors on accidental morphine overdose.* Brit Med J, 1999. **318**: p. 1167b-1167b.

27.   Glasgow, A. M., Boeckx, R. L., Miller, M. K., Macdonald, M. G., August, G. P., and Goodman, S. I., *Hyperosmolality in small infants due to propylene-glycol.* Pediatrics, 1983. **72**: p. 353-355.

28. Macdonald, M. G., Getson, P. R., Glasgow, A. M., Miller, M. K., Boeckx, R. L., and Johnson, E. L., *Propylene glycol increased incidence of seizures in low birth weight infants.* Pediatrics, 1987. **79**: p. 622-625.

29. Gershanik, J., Boecler, B., Ensley, H., McCloskey, S., and George, W., *The gasping syndrome and benzyl alcohol poisoning.* N Engl J Med, 1982. **307**: p. 1384-1388.

30. Koren, G., *Therapeutic drug monitoring principles in the neonate.* Clin Chem, 1997. **43**: p. 222-227.

31. Lin, J. C., Strauss, R. G., Kulhavy, J. C., Johnson, K. J., Zimmerman, M. B., Cress, G. A., Connolly, N. W., and Widness, J. A., *Phlebotomy overdraw in the neonatal intensive care nursery.* Pediatrics, 2000. **106**: p. E19.

32. Bishara, N., and Ohls, R. K., *Current controversies in the management of the anemia of prematurity.* Semin Perinatol, 2009. **33**: p. 29-34.

33. Shirkey, H., *Therapeutic orphans.* J Pediatr, 1968. **72**: p. 119-120.

34. Ernest, T. B., Elder, D. P., Martini, L. G., Roberts, M., and Ford, J. L., *Developing paediatric medicines: Identifying the needs and recognizing the challenges.* J Pharm Pharmacol, 2007. **59**: p. 1043-1055.

35. Walters, K. A., and Roberts, M. S., *The structure and function of the skin*, in *Dermatological and transdermal formulations*, Walters, K. A., Editor. 2002, Marcel Dekker: New York. p. 1-39.

36. Nonato, L. B., Kalia, Y. N., Naik, A., Lund, C. H., and Guy, R. H., *The development of skin barrier function in the neonate*, in *Topical absorption of dermatological products*, Bronaugh, R. L., and Maibach, H. I., Editors. 2002, Marcel Dekker: New York. p. 43-75.

37. Evans, N. J., and Rutter, N., *Development of the epidermis in the newborn.* Biol Neonate, 1986. **49**: p. 74-80.

38.   Rutter, N., *The immature skin.* Br Med Bull, 1988. **44**: p. 957-970.

39.   Barker, N., Hadgraft, J., and Rutter, N., *Skin permeability in the newborn.* J Invest Dermatol, 1987. **88**: p. 409-411.

40.   Williams, A., *Structure and function of human skin*, in *Transdermal and topical drug delivery from theory to clinical practice*. 2003, Pharmaceutical Press: London. p. 1-25.

41.   Braverman, I. M., *The cutaneous microcirculation.* J Invest Derm Symp P, 2000. **5**: p. 3-9.

42.   Yum, S. I., and Roe, J., *Capillary blood sampling for self-monitoring of blood glucose.* Diabetes Technol Ther, 1999. **1**: p. 29-37.

43.   Menon, G. K., *New insights into skin structure: Scratching the surface.* Adv Drug Del Rev, 2002. **54**: p. S3-S17.

44.   Naik, A., Kalia, Y. N., and Guy, R. H., *Transdermal drug delivery: Overcoming the skin's barrier function.* Pharm Sci Tech Today, 2000. **3**: p. 318-326.

45.   Kalia, Y. N., Nonato, L. B., Lund, C. H., and Guy, R. H., *Development of skin barrier function in premature infants.* J Invest Dermatol, 1998. **111**: p. 320-326.

46.   Rutter, N., *The dermis.* Semin Neonatol, 2000. **5**: p. 297-302.

47.   Lund, C., Kuller, J., Lane, A., Lott, J. W., and Raines, D. A., *Neonatal skin care: The scientific basis for practice.* J Obstet Gynecol Neonatal Nurs, 1999. **28**: p. 241-254.

48.   Rutter, N., *Clinical consequences of an immature barrier.* Semin Neonatol, 2000. **5**: p. 281-287.

49.   Harpin, V., and Rutter, N., *Percutaneous alcohol absorption and skin necrosis in a preterm infant.* Arch Dis Child, 1982. **57**: p. 477-479.

50.   Watkinson, A. C., and Brain, K. R., *Basic mathematical principles in skin permeation*, in *Dermatological and transdermal formulations*, Walters, K. A., Editor. 2002, Marcel Dekker: New York. p. 65-96.

51.   Barry, B. W., *Basic principles of diffusion through membranes*, in *Dermatological formulations : Percutaneous absorption*. 1983, Marcel Dekker: New York. p. 49-94.

52.   *U.S food and durg administration approved drug products*.   [access date 2009.   06/06];   Available   from: http://www.accessdata.fda.gov/scripts/cder/drugsatfda/index.cfm.

53.   *European medicines agency: Epars for authorised medicinal products for human   use*.   [access   date   2009.   06/06];   Available   from: http://www.emea.europa.eu/htms/human/epar/a.htm.

54.   *British national formulary for children 2008*. revised ed, ed. Martin, J. 2008, London: BMJ Group, RPS Publishing, and RCPCH Publications. 944 p.

55.   Micali, G., Bhatt, R. H., Distefano, G., Caltabiano, L., Cook, B., Fischer, J. H., Solomon, L. M., and West, D. P., *Evaluation of transdermal theophylline pharmacokinetics in neonates.* Pharmacotherapy, 1993. **13**: p. 386-390.

56.   Amato, M., Isenschmid, M., and Huppi, P., *Percutaneous caffeine application in the treatment of neonatal apnoea.* Eur J Pediatr, 1991. **150**: p. 592-594.

57.   Cartwright, R. G., Cartlidge, P. H., Rutter, N., Melia, C. D., and Davis, S. S., *Transdermal delivery of theophylline to premature infants using a hydrogel disc system.* Br J Clin Pharmacol, 1990. **29**: p. 533-539.

58.   Evans, N. J., Rutter, N., Hadgraft, J., and Parr, G., *Percutaneous administration of theophylline in the preterm infant.* J Pediatr, 1985. **107**: p. 307-311.

59.   Lopes, J. M., and Aranda, J. V., *Pharmacologic treatment of neonatal apnea*, in *Neonatal and pediatric pharmacology : Therapeutic principles in practice*, Yaffe, S.

J., and Aranda, J. V., Editors. 2005, Lippincott Williams & Wilkins: Philadelphia; London. p. 217-229.

60.   Murphy, M. G., Peck, C. C., Conner, D. P., Zamani, K., Merenstein, G. B., and Rodden, D., *Transcutaneous theophylline collection in preterm infants.* Clin Pharmacol Ther, 1990. **47**: p. 427-434.

61.   Brown, M. B., Martin, G. P., Jones, S. A., and Akomeah, F. K., *Dermal and transdermal drug delivery systems: Current and future prospects.* Drug Deliv, 2006. **13**: p. 175-187.

62.   Subramony, J. A., Sharma, A., and Phipps, J. B., *Microprocessor controlled transdermal drug delivery.* Int J Pharm, 2006. **317**: p. 1-6.

63.   Prausnitz, M. R., Mitragotri, S., and Langer, R., *Current status and future potential of transdermal drug delivery.* Nature Rev Drug Discov, 2004. **3**: p. 115-124.

64.   Delgado-Charro, M. B., and Guy, R. H., *Transdermal iontophoresis for controlled drug delivery and non-invasive monitoring.* Stp Pharma Sciences, 2001. **11**: p. 403-414.

65.   Kalia, Y. N., Naik, A., Garrison, J., and Guy, R. H., *Iontophoretic drug delivery.* Adv Drug Del Rev, 2004. **56**: p. 619-658.

66.   Delgado-Charro, M. B., *Recent advances on transdermal iontophoretic drug delivery and non-invasive sampling.* J Drug Deliv Sci Tec, 2009. **19**: p. 75-88.

67.   Leboulanger, B., Guy, R. H., and Delgado-Charro, M. B., *Reverse iontophoresis for non-invasive transdermal monitoring.* Physiol Meas, 2004. **25**: p. R35-R50.

68.   Delgado-Charro, M. B., and Guy, R. H., *Iontophoresis: Applications in drug delivery and non-invasive monitoring*, in *Transdermal drug delivery*, Guy, R. H., and Hadgraft, J., Editors. 2003, Marcel Dekker, Inc: New York. p. 199-225.

69.	Scott, E. R., Phipps, J. B., Gyory, J. R., and Padmanabhan, R. V., *Electrotransport systems for transdermal delivery: A practical implementation of iontophoresis*, in *Handbook of pharmaceutical controlled release technology*, Wise, D. L., Editor. 2000, Marcel Dekker: New York. p. 617-659.

70.	Cullander, C., Rao, G., and Guy, R. H., *Why silver/silver chloride? Criteria for iontophoresis electrodes*, in *Prediction of percutaneous penetration*, Brain, K. R., James, V. J., and Walters, K. A., Editors. 1993, STS Publishing. p. 381-390.

71.	Phipps, J. B., and Gyory, J. R., *Transdermal ion migration.* Adv Drug Del Rev, 1992. **9**: p. 137-176.

72.	Pikal, M. J., *The role of electroosmotic flow in transdermal iontophoresis.* Adv Drug Del Rev, 1992. **9**: p. 201-237.

73.	Mudry, B., Guy, R. H., and Delgado-Charro, M. B., *Prediction of iontophoretic transport across the skin.* J Control Release, 2006. **111**: p. 362-367.

74.	Marro, D., Kalia, Y. N., Delgado-Charro, M. B., and Guy, R. H., *Optimizing iontophoretic drug delivery: Identification and distribution of the charge-carrying species.* Pharm Res, 2001. **18**: p. 1709-1713.

75.	Kasting, G. B., and Keister, J. C., *Application of electrodiffusion theory for a homogeneous membrane to iontophoretic transport through skin.* J Control Release, 1989. **8**: p. 195-210.

76.	Helfferich, F. G., *Electrochemical properties*, in *Ion exchange*. 1962, McGraw-Hill: New York; London. p. 323-338.

77.	Burnette, R. R., and Ongpipattanakul, B., *Characterization of the permselective properties of excised human skin during iontophoresis.* J Pharm Sci, 1987. **76**: p. 765-773.

78.	Luzardo-Alvarez, A., Rodriguez-Fernandez, M., Blanco-Mendez, J., Guy, R. H., and Delgado-Charro, M. B., *Iontophoretic permselectivity of mammalian skin:*

Characterization of hairless mouse and porcine membrane models. Pharm Res, 1998. **15**: p. 984-987.

79.   Kim, A., Green, P. G., Rao, G., and Guy, R. H., *Convective solvent flow across the skin during iontophoresis.* Pharm Res, 1993. **10**: p. 1315-1320.

80.   Lakshminarayanaiah, N., *Transport phenomena in artificial membranes.* Chem Rev, 1965. **65**: p. 491-565.

81.   Marro, D., Kalia, Y. N., Delgado-Charro, M. B., and Guy, R. H., *Contributions of electromigration and electroosmosis to iontophoretic drug delivery.* Pharm Res, 2001. **18**: p. 1701-1708.

82.   Guy, R. H., Kalia, Y. N., Delgado-Charro, M. B., Merino, V., Lopez, A., and Marro, D., *Iontophoresis: Electrorepulsion and electroosmosis.* J Control Release, 2000. **64**: p. 129-132.

83.   Kedem, O., and Katchalsky, A., *Thermodynamic analysis of the permeability of biological membranes to non-electrolytes.* Biochim Biophys Acta, 1958. **27**: p. 229-246.

84.   Bath, B. D., Lee, R. D., White, H. S., and Scott, E. R., *Imaging molecular transport in porous membranes. Observation and analysis of electroosmotic flow in individual pores using the scanning electrochemical microscope.* Anal Chem, 1998. **70**: p. 1047-1058.

85.   Bath, B. D., Scott, E. R., Phipps, J. B., and White, H. S., *Scanning electrochemical microscopy of iontophoretic transport in hairless mouse skin. Analysis of the relative contributions of diffusion, migration, and electroosmosis to transport in hair follicles.* J Pharm Sci, 2000. **89**: p. 1537-1549.

86.   Pikal, M. J., and Shah, S., *Transport mechanisms in iontophoresis. Ii. Electroosmotic flow and transference number measurements for hairless mouse skin.* Pharm Res, 1990. **7**: p. 213-221.

87.   Abla, N., Naik, A., Guy, R. H., and Kalia, Y. N., *Effect of charge and molecular weight on transdermal peptide delivery by iontophoresis.* Pharm Res, 2005. **22**: p. 2069-2078.

88.   Pikal, M. J., *Penetration enhancement of peptide and protein drugs* in *Trends and future perspectives in peptide and protein drug delivery*, Lee, V. H. L., Hashida, M., and Mizushima, Y., Editors. 1995, Harwood Academic: Chur; Reading. p. 83-110.

89.   Yoshida, N. H., and Roberts, M. S., *Structure-transport relationships in transdermal iontophoresis.* Adv Drug Del Rev, 1992. **9**: p. 239-264.

90.   Kasting, G. B., *Theoretical models for iontophoretic delivery.* Adv Drug Del Rev, 1992. **9**: p. 177-199.

91.   Hirvonen, J., Kalia, Y. N., and Guy, R. H., *Transdermal delivery of peptides by iontophoresis.* Nat Biotechnol, 1996. **14**: p. 1710-1713.

92.   Green, P. G., *Iontophoretic delivery of peptide drugs.* J Control Release, 1996. **41**: p. 33-48.

93.   Van der Geest, R., Hueber, F., Szoka, F. C., Jr., and Guy, R. H., *Iontophoresis of bases, nucleosides, and nucleotides.* Pharm Res, 1996. **13**: p. 553-558.

94.   Brand, R. M., Wahl, A., and Iversen, P. L., *Effects of size and sequence on the iontophoretic delivery of oligonucleotides.* J Pharm Sci, 1998. **87**: p. 49-52.

95.   Galinkin, J. L., Rose, J. B., Harris, K., and Watcha, M. F., *Lidocaine iontophoresis versus eutectic mixture of local anesthetics (emla) for iv placement in children.* Anesth Analg, 2002. **94**: p. 1484-1488.

96.   Padmanabhan, R. V., Phipps, J. B., Lattin, G. A., and Sawchuk, R. J., *In vitro and in vivo evaluation of transdermal iontophoretic delivery of hydromorphone.* J Control Release, 1990. **11**: p. 123-135.

97.	Ashburn, M. A., Stephen, R. L., Ackerman, E., Petelenz, T. J., Hare, B., Pace, N. L., and Hofman, A. A., *Iontophoretic delivery of morphine for postoperative analgesia.* J Pain Symptom Manage, 1992. **7**: p. 27-33.

98.	Bose, S., Ravis, W. R., Lin, Y. J., Zhang, L., Hofmann, G. A., and Banga, A. K., *Electrically-assisted transdermal delivery of buprenorphine.* J Control Release, 2001. **73**: p. 197-203.

99.	Fang, J. Y., Sung, K. C., Wang, J. J., Chu, C. C., and Chen, K. T., *The effects of iontophoresis and electroporation on transdermal delivery of buprenorphine from solutions and hydrogels.* J Pharm Pharmacol, 2002. **54**: p. 1329-1337.

100.	Sung, K. C., Fang, J.-Y., and Yoa-Pu Hu, O., *Delivery of nalbuphine and its prodrugs across skin by passive diffusion and iontophoresis.* J Control Release, 2000. **67**: p. 1-8.

101.	Thysman, S., and Preat, V., *In vivo iontophoresis of fentanyl and sufentanil in rats: Pharmacokinetics and acute antinociceptive effects.* Anesth Analg, 1993. **77**: p. 61-66.

102.	Sinatra, R., *The fentanyl hcl patient-controlled transdermal system (pcts): An alternative to intravenous patient-controlled analgesia in the postoperative setting.* Clin Pharmacokinet, 2005. **44**: p. 1-6.

103.	Zeltzer, L., Regalado, M., Nichter, L. S., Barton, D., Jennings, S., and Pitt, L., *Iontophoresis versus subcutaneous injection: A comparison of two methods of local anesthesia delivery in children.* Pain, 1991. **44**: p. 73-78.

104.	Irsfeld, S., Klement, W., and Lipfert, P., *Dermal anaesthesia: Comparison of emla cream with iontophoretic local anaesthesia.* Br J Anaesth, 1993. **71**: p. 375-378.

105.	Russo, J., Jr., Lipman, A. G., Comstock, T. J., Page, B. C., and Stephen, R. L., *Lidocaine anesthesia: Comparison of iontophoresis, injection, and swabbing.* Am J Hosp Pharm, 1980. **37**: p. 843-847.

106. Squire, S. J., Kirchhoff, K. T., and Hissong, K., *Comparing two methods of topical anesthesia used before intravenous cannulation in pediatric patients.* J Pediatr Health Care, 2000. **14**: p. 68-72.

107. Sylvestre, J. P., Guy, R. H., and Delgado-Charro, M. B., *In vitro optimization of dexamethasone phosphate delivery by iontophoresis.* Phys Ther, 2008. **88**: p. 1177-1185.

108. Gay, C. L., Green, P. G., Guy, R. H., and Francoeur, M. L., *Iontophoretic delivery of piroxicam across the skin invitro.* J Control Release, 1992. **22**: p. 57-67.

109. Hui, X. Y., Anigbogu, A., Singh, P., Xiong, G., Poblete, N., Liu, P. C., and Maibach, H. I., *Pharmacokinetic and local tissue disposition of [c-14]sodium diclofenac following iontophoresis and systemic administration in rabbits.* J Pharm Sci, 2001. **90**: p. 1269-1276.

110. Curdy, C., Kalia, Y. N., Naik, A., and Guy, R. H., *Piroxicam delivery into human stratum corneum in vivo: Iontophoresis versus passive diffusion.* J Control Release, 2001. **76**: p. 73-79.

111. Tiwari, S. B., and Udupa, N., *Investigation into the potential of iontophoresis facilitated delivery of ketorolac.* Int J Pharm, 2003. **260**: p. 93-103.

112. Mathy, F. X., Lombry, C., Verbeeck, R. K., and Preat, V., *Study of the percutaneous penetration of flurbiprofen by cutaneous and subcutaneous microdialysis after iontophoretic delivery in rat.* J Pharm Sci, 2005. **94**: p. 144-152.

113. Singh, P., and Roberts, M. S., *Iontophoretic transdermal delivery of salicylic acid and lidocaine to local subcutaneous structures.* J Pharm Sci, 1993. **82**: p. 127-131.

114. Panus, P. C., Campbell, J., Kulkarni, S. B., Herrick, R. T., Ravis, W. R., and Banga, A. K., *Transdermal iontophoretic delivery of ketoprofen through human cadaver skin and in humans.* J Control Release, 1997. **44**: p. 113-121.

115.   Tashiro, Y., Kato, Y., Hayakawa, E., and Ito, K., *Iontophoretic transdermal delivery of ketoprofen: Effect of iontophoresis on drug transfer from skin to cutaneous blood.* Biol Pharm Bull, 2000. **23**: p. 1486-1490.

116.   Fang, J., Wang, R., Huang, Y., Wu, P. C., and Tsai, Y., *Passive and iontophoretic delivery of three diclofenac salts across various skin types.* Biol Pharm Bull, 2000. **23**: p. 1357-1362.

117.   Nirschl, R. P., Rodin, D. M., Ochiai, D. H., and Maartmann-Moe, C., *Iontophoretic administration of dexamethasone sodium phosphate for acute epicondylitis. A randomized, double-blinded, placebo-controlled study.* Am J Sports Med, 2003. **31**: p. 189-195.

118.   Oh, S. Y., Jeong, S. Y., Park, T. G., and Lee, J. H., *Enhanced transdermal delivery of azt (zidovudine) using iontophoresis and penetration enhancer.* J Control Release, 1998. **51**: p. 161-168.

119.   Volpato, N. M., Nicoli, S., Laureri, C., Colombo, P., and Santi, P., *In vitro acyclovir distribution in human skin layers after transdermal iontophoresis.* J Control Release, 1998. **50**: p. 291-296.

120.   Soroko, Y. T., Repking, M. C., Clemment, J. A., Mitchell, P. L., and Berg, R. L., *Treatment of plantar verrucae using 2% sodium salicylate iontophoresis.* Phys Ther, 2002. **82**: p. 1184-1191.

121.   Abla, N., Naik, A., Guy, R. H., and Kalia, Y. N., *Topical iontophoresis of valaciclovir hydrochloride improves cutaneous aciclovir delivery.* Pharm Res, 2006. **23**: p. 1842-1849.

122.   Luzardo-Alvarez, A., Delgado-Charro, M. B., and Blanco-Mendez, J., *Iontophoretic delivery of ropinirole hydrochloride: Effect of current density and vehicle formulation.* Pharm Res, 2001. **18**: p. 1714-1720.

123. Van der Geest, R., Danhof, M., and Bodde, H. E., *Iontophoretic delivery of apomorphine. 1: In vitro optimization and validation.* Pharm Res, 1997. **14**: p. 1798-1803.

124. van der Geest, R., van Laar, T., Gubbens-Stibbe, J. M., Bodde, H. E., and Danhof, M., *Iontophoretic delivery of apomorphine. 2: An in vivo study in patients with parkinson's disease.* Pharm Res, 1997. **14**: p. 1804-1810.

125. Femenia-Font, A., Balaguer-Fernandez, C., Merino, V., and Lopez-Castellano, A., *Iontophoretic transdermal delivery of sumatriptan: Effect of current density and ionic strength.* J Pharm Sci, 2005. **94**: p. 2183-2186.

126. Patel, S. R., Zhong, H., Sharma, A., and Kalia, Y. N., *In vitro and in vivo evaluation of the transdermal iontophoretic delivery of sumatriptan succinate.* Eur J Pharm Biopharm, 2007. **66**: p. 296-301.

127. Siegel, S. J., O'Neill, C., Dube, L. M., Kaldeway, P., Morris, R., Jackson, D., and Sebree, T., *A unique iontophoretic patch for optimal transdermal delivery of sumatriptan.* Pharm Res, 2007. **24**: p. 1919-1926.

128. *Macroduct sweat testing system description*. [access date 2009. 09/06]; Available from: http://www.wescor.com/biomedical/cysticfibrosis/macroduct.html#.

129. *Lidosite the first fda-approved pre-filled active anesthetic patch*. [access date 2009. 09/06]; Available from: http://www.vyteris.com/home/Our_Products/Lidosite.php.

130. Gibson, L. E., and Cooke, R. E., *A test for concentration of electrolytes in sweat in cystic fibrosis of the pancreas utilizing pilocarpine by iontophoresis.* Pediatrics, 1959. **23**: p. 545-549.

131. Lander, J., Hodgins, M., Nazarali, S., McTavish, J., Ouellette, J., and Friesen, E., *Determinants of success and failure of emla.* Pain, 1996. **64**: p. 89-97.

132.   Wahlgren, C. F., and Quiding, H., *Depth of cutaneous analgesia after application of a eutectic mixture of the local anesthetics lidocaine and prilocaine (emla cream).* J Am Acad Dermatol, 2000. **42**: p. 584-588.

133.   Wallace, M. S., Ridgeway, B., Jun, E., Schulteis, G., Rabussay, D., and Zhang, L., *Topical delivery of lidocaine in healthy volunteers by electroporation, electroincorporation, or iontophoresis: An evaluation of skin anesthesia.* Reg Anesth Pain Med, 2001. **26**: p. 229-238.

134.   Ashburn, M. A., Gauthier, M., Love, G., Basta, S., Gaylord, B., and Kessler, K., *Iontophoretic administration of 2% lidocaine hcl and 1:100,000 epinephrine in humans.* Clin J Pain, 1997. **13**: p. 22-26.

135.   Zempsky, W. T., Anand, K. J., Sullivan, K. M., Fraser, D., and Cucina, K., *Lidocaine iontophoresis for topical anesthesia before intravenous line placement in children.* J Pediatr, 1998. **132**: p. 1061-1063.

136.   Kearns, G. L., Heacook, J., Daly, S. J., Singh, H., Alander, S. W., and Qu, S., *Percutaneous lidocaine administration via a new iontophoresis system in children: Tolerability and absence of systemic bioavailability.* Pediatrics, 2003. **112**: p. 578-582.

137.   Power, I., *Fentanyl hcl iontophoretic transdermal system (its): Clinical application of iontophoretic technology in the management of acute postoperative pain.* Br J Anaesth, 2007. **98**: p. 4-11.

138.   Zempsky, W. T., Sullivan, J., Paulson, D. M., and Hoath, S. B., *Evaluation of a low-dose lidocaine iontophoresis system for topical anesthesia in adults and children: A randomized, controlled trial.* Clin Ther, 2004. **26**: p. 1110-1119.

139.   Sathyan, G., Phipps, B., and Gupta, S. K., *Passive absorption of fentanyl from the fentanyl hcl iontophoretic transdermal system.* Curr Med Res Opin, 2009. **25**: p. 363-366.

140. Gupta, S. K., Southam, M., Sathyan, G., and Klausner, M., *Effect of current density on pharmacokinetics following continuous or intermittent input from a fentanyl electrotransport system.* J Pharm Sci, 1998. **87**: p. 976-981.

141. Gupta, S. K., Bernstein, K. J., Noorduin, H., Van Peer, A., Sathyan, G., and Haak, R., *Fentanyl delivery from an electrotransport system: Delivery is a function of total current, not duration of current.* J Clin Pharmacol, 1998. **38**: p. 951-958.

142. Viscusi, E. R., Siccardi, M., Damaraju, C. V., Hewitt, D. J., and Kershaw, P., *The safety and efficacy of fentanyl iontophoretic transdermal system compared with morphine intravenous patient-controlled analgesia for postoperative pain management: An analysis of pooled data from three randomized, active-controlled clinical studies.* Anesth Analg, 2007. **105**: p. 1428-1436.

143. Glikfeld, P., Hinz, R. S., and Guy, R. H., *Noninvasive sampling of biological fluids by iontophoresis.* Pharm Res, 1989. **6**: p. 988-990.

144. Numajiri, S., Sugibayashi, K., and Morimoto, Y., *Non-invasive sampling of lactic acid ions by iontophoresis using chloride ion in the body as an internal standard.* J Pharm Biomed Anal, 1993. **11**: p. 903-909.

145. Delgado-Charro, M. B., and Guy, R. H., *Transdermal reverse iontophoresis of valproate: A noninvasive method for therapeutic drug monitoring.* Pharm Res, 2003. **20**: p. 1508-1513.

146. Leboulanger, B., Aubry, J. M., Bondolfi, G., Guy, R. H., and Delgado-Charro, M. B., *Lithium monitoring by reverse iontophoresis in vivo.* Clin Chem, 2004. **50**: p. 2091-2100.

147. Sieg, A., Guy, R. H., and Delgado-Charro, M. B., *Noninvasive glucose monitoring by reverse iontophoresis in vivo: Application of the internal standard concept.* Clin Chem, 2004. **50**: p. 1383-1390.

148.   Sieg, A., Guy, R. H., and Delgado-Charro, M. B., *Simultaneous extraction of urea and glucose by reverse iontophoresis in vivo.* Pharm Res, 2004. **21**: p. 1805-1810.

149.   Longo, N., Li, S. K., Yan, G., Kochambilli, R. P., Papangkorn, K., Berglund, D., Ghanem, A. H., Ashurst, C. L., Ernst, S. L., Pasquali, M., and Higuchi, W. I., *Noninvasive measurement of phenylalanine by iontophoretic extraction in patients with phenylketonuria.* J Inherit Metab Dis, 2007. **30**: p. 910-915.

150.   Wascotte, V., Rozet, E., Salvaterra, A., Hubert, P., Jadoul, M., Guy, R. H., and Preat, V., *Non-invasive diagnosis and monitoring of chronic kidney disease by reverse iontophoresis of urea in vivo.* Eur J Pharm Biopharm, 2008. **69**: p. 1077-1082.

151.   Nixon, S., Sieg, A., Delgado-Charro, M. B., and Guy, R. H., *Reverse iontophoresis of l-lactate: In vitro and in vivo studies.* J Pharm Sci, 2007. **96**: p. 3457-3465.

152.   Sieg, A., Jeanneret, F., Fathi, M., Hochstrasser, D., Rudaz, S., Veuthey, J. L., Guy, R. H., and Delgado-Charro, M. B., *Extraction of amino acids by reverse iontophoresis in vivo.* Eur J Pharm Biopharm, 2009. **72**: p. 226-231.

153.   Rao, G., Guy, R. H., Glikfeld, P., LaCourse, W. R., Leung, L., Tamada, J., Potts, R. O., and Azimi, N., *Reverse iontophoresis: Noninvasive glucose monitoring in vivo in humans.* Pharm Res, 1995. **12**: p. 1869-1873.

154.   Tamada, J. A., Bohannon, N. J. V., and Potts, R. O., *Measurement of glucose in diabetic subjects using noninvasive transdermal extraction.* Nat Med, 1995. **1**: p. 1198-1201.

155.   Potts, R. O., Tamada, J. A., and Tierney, M. J., *Glucose monitoring by reverse iontophoresis.* Diabetes Metab Res Rev, 2002. **18**: p. S49-S53.

156.   Tierney, M. J., Tamada, J. A., Potts, R. O., Jovanovic, L., and Garg, S., *Clinical evaluation of the glucowatch biographer: A continual, non-invasive glucose monitor for patients with diabetes.* Biosens Bioelectron, 2001. **16**: p. 621-629.

157.   Sieg, A., Guy, R. H., and Delgado-Charro, M. B. A., *Reverse iontophoresis for noninvasive glucose monitoring: The internal standard concept.* J Pharm Sci, 2003. **92**: p. 2295-2302.

158.   Tierney, M. J., Tamada, J. A., Potts, R. O., Eastman, R. C., Pitzer, K., Ackerman, N. R., and Fermi, S. J., *The glucowatch biographer: A frequent automatic and noninvasive glucose monitor.* Ann Med, 2000. **32**: p. 632-641.

159.   Cullander, C., *What are the pathways of iontophoretic current flow through mammalian skin.* Adv Drug Del Rev, 1992. **9**: p. 119-135.

160.   Cullander, C., and Guy, R. H., *Sites of iontophoretic current flow into the skin - identification and characterization with the vibrating probe electrode.* J Invest Dermatol, 1991. **97**: p. 55-64.

161.   Scott, E. R., Laplaza, A. I., White, H. S., and Phipps, J. B., *Transport of ionic species in skin: Contribution of pores to the overall skin conductance.* Pharm Res, 1993. **10**: p. 1699-1709.

162.   Scott, E. R., Phipps, J. B., and White, H. S., *Direct imaging of molecular transport through skin.* J Invest Dermatol, 1995. **104**: p. 142-145.

163.   Bath, B. D., White, H. S., and Scott, E. R., *Visualization and analysis of electroosmotic flow in hairless mouse skin.* Pharm Res, 2000. **17**: p. 471-475.

164.   Uitto, O. D., and White, H. S., *Electroosmotic pore transport in human skin.* Pharm Res, 2003. **20**: p. 646-652.

165.   Barry, B. W., *Drug delivery routes in skin: A novel approach.* Adv Drug Del Rev, 2002. **54** p. S31-S40.

166.   Essa, E. A., Bonner, M. C., and Barry, B. W., *Human skin sandwich for assessing shunt route penetration during passive and iontophoretic drug and liposome delivery.* J Pharm Pharmacol, 2002. **54**: p. 1481-1490.

167.   Monteiro-Riviere, N. A., Inman, A. O., and Riviere, J. E., *Identification of the pathway of iontophoretic drug delivery: Light and ultrastructural studies using mercuric chloride in pigs.* Pharm Res, 1994. **11**: p. 251-256.

168.   Turner, N. G., and Guy, R. H., *Iontophoretic transport pathways: Dependence on penetrant physicochemical properties.* J Pharm Sci, 1997. **86**: p. 1385-1389.

169.   Turner, N. G., Ferry, L., Price, M., Cullander, C., and Guy, R. H., *Iontophoresis of poly-l-lysines: The role of molecular weight?* Pharm Res, 1997. **14**: p. 1322-1331.

170.   Regnier, V., and Preat, V., *Localization of a fitc-labeled phosphorothioate oligodeoxynucleotide in the skin after topical delivery by iontophoresis and electroporation.* Pharm Res, 1998. **15**: p. 1596-1602.

171.   Adam, C., *Transdermal delivery: Exploring the properties of the gel-matrix technology.* Drug delivery technology, 2007. **7**: p. 36-41.

172.   Parekh, D., Miller, M. A., Borys, D., Patel, P. R., and Levsky, M. E., *Transdermal patch medication delivery systems and pediatric poisonings, 2002-2006.* Clin Pediatr, 2008. **47**: p. 659-663.

173.   Ledger, P. W., *Skin biological issues in electrically enhanced transdermal delivery.* Adv Drug Del Rev, 1992. **9**: p. 289-307.

174.   Curdy, C., Kalia, Y. N., and Guy, R. H., *Non-invasive assessment of the effects of iontophoresis on human skin in-vivo.* J Pharm Pharmacol, 2001. **53**: p. 769-777.

175.   Jadoul, A., Bouwstra, J., and Preat, V. V., *Effects of iontophoresis and electroporation on the stratum corneum. Review of the biophysical studies.* Adv Drug Del Rev, 1999. **35**: p. 89-105.

176.   Brand, R. M., Singh, P., AspeCarranza, E., Maibach, H. I., and Guy, R. H., *Acute effects of iontophoresis on human skin in vivo: Cutaneous blood flow and transepidermal water loss measurements.* Eur J Pharm Biopharm, 1997. **43**: p. 133-138.

177.   vanderGeest, R., Elshove, D. A. R., Danhof, M., Lavrijsen, A. P. M., and Bodde, H. E., *Non-invasive assessment of skin barrier integrity and skin irritation following iontophoretic current application in humans.* Journal of Controlled Release, 1996. **41**: p. 205-213.

178.   Thysman, S., Van Neste, D., and Preat, V., *Noninvasive investigation of human skin after in vivo iontophoresis.* Skin Pharmacol, 1995. **8**: p. 229-236.

179.   Oh, S. Y., and Guy, R. H., *Effects of iontophoresis on the electrical-properties of human skin in-vivo.* Int J Pharm, 1995. **124**: p. 137-142.

180.   Marro, D., Guy, R. H., and Delgado-Charro, M. B., *Characterization of the iontophoretic permselectivity properties of human and pig skin.* J Control Release, 2001. **70**: p. 213-217.

181.   Brain, K. R., Walters, K. A., and Watkinson, A. C., *Methods for studying percutaneous absorption*, in *Dermatological and transdermal formulations*, Walters, K. A., Editor. 2002, Marcel Dekker: New York. p. 216-293.

182.   Dick, I. P., and Scott, R. C., *Pig ear skin as an in-vitro model for human skin permeability.* J Pharm Pharmacol, 1992. **44**: p. 640-645.

183.   Sekkat, N., Kalia, Y. N., and Guy, R. H., *Biophysical study of porcine ear skin in vitro and its comparison to human skin in vivo.* J Pharm Sci, 2002. **91**: p. 2376-2381.

184.   Schmook, F. P., Meingassner, J. G., and Billich, A., *Comparison of human skin or epidermis models with human and animal skin in in-vitro percutaneous absorption.* Int J Pharm, 2001. **215**: p. 51-56.

185.   Bartek, M. J., LaBudde, J. A., and Maibach, H. I., *Skin permeability in vivo: Comparison in rat, rabbit, pig and man.* J Invest Dermatol, 1972. **58**: p. 114-123.

186.   Simon, G. A., and Maibach, H. I., *The pig as an experimental animal model of percutaneous permeation in man: Qualitative and quantitative observations - an overview.* Skin Pharmacol Appl, 2000. **13**: p. 229-234.

187.   Sekkat, N., Kalia, Y. N., and Guy, R. H., *Development of an in vitro model for premature neonatal skin: Biophysical characterization using transepidermal water loss.* J Pharm Sci, 2004. **93**: p. 2936-2940.

188.   Sekkat, N., Kalia, Y. N., and Guy, R. H., *Porcine ear skin as a model for the assessment of transdermal drug delivery to premature neonates.* Pharm Res, 2004. **21**: p. 1390-1397.

Chapter 2

Non-invasive monitoring of kidney function: *in vitro* and *in vivo* sampling of iohexol by transdermal reverse iontophoresis

Chapter summary

The objective of this study was to assess the feasibility of transdermal reverse iontophoresis, as an alternative approach to blood sampling, for monitoring kidney function using iohexol as the *GFR* marker.

First, *in vitro* experiments were performed using abdominal pig skin. Correlation between iohexol subdermal concentrations and the corresponding skin extraction fluxes was evaluated. Then, to reduce the time required for iohexol skin sampling to achieve steady extraction, a 3 hour pre-treatment of the skin with direct current was introduced. Finally, simulations of iohexol subdermal concentration decay over time, representing different pharmacokinetic profiles, were performed. Transdermal extraction fluxes were measured to evaluate whether the changes in the subdermal concentration of the marker were followed and whether kinetic parameters determined from the two sets of data were correlated. After a delay, extraction fluxes of iohexol tracked the corresponding subdermal concentrations well. The 3 hour pre-treatment period was modestly effective in reducing the time for extraction fluxes to reach steady levels. The simulated pharmacokinetic parameters of iohexol were estimated reliably and precisely from the iontophoretic extraction data. Overall, these *in vitro* results demonstrated encouraging potential for *in vivo* applications. Such was the focus of the subsequent investigation.

An *in vivo* study was performed in four children, undergoing a routine iohexol *GFR* test. The test involved an intravenous bolus dose of iohexol, followed by blood samples taken approximately 3 and 4 hours later to determine the marker's clearance and hence *GFR*. Iontophoresis was performed simultaneously for 5.5 hours, extraction samples were collected at approximately 2.5, 3.5, 4.5, and 5.5 hours post-injection, and were analysed for iohexol. Iontophoresis was well-tolerated and all participants completed the study. Iontophoresis caused mild erythema and slight tingling and itching sensations. Iohexol was successfully extracted by reverse iontophoresis and was quantified together with sodium and

potassium. After the first 2 hours of current application, the iohexol extraction rates tracked the decreases in iohexol's blood concentration during the elimination phase. In three of the four subjects, elimination rate constants determined from reverse iontophoresis agreed well with the blood sampling data. The *GFR* values estimated using both sampling approaches highlight the potential of reverse iontophoresis as an alternative sampling approach in the iohexol *GFR* test. In summary, the results obtained provide *in vivo* proof-of-concept and a larger study is now justified for further optimisation and validation. Such non-invasive alternative sampling approach would significantly improve the quality-of-life of children undergoing evaluation of their renal function.

1. Introduction

Monitoring glomerular filtration rate (*GFR*), as a sensitive indicator of kidney function, is an integral part of clinical medicine. It is used for diagnosing and monitoring the progression of disease, evaluation of treatment efficacy, and achievement of optimum therapy whilst avoiding over- or under- dosing (e.g., in chemotherapy). *GFR* is determined indirectly through measurement of the clearance of "filtration markers". Ideally, these markers are non-toxic substances which are exclusively and completely cleared by the glomerulus, are neither bound to blood cells or proteins, metabolised, nor renally reabsorbed. It is for the aforementioned reasons that the measured clearance of an ideal filtration marker is equivalent to the patient's *GFR*.

Rapid advances in the medical field necessitated ongoing efforts to improve *GFR* quantification. Investigations started back in 1928 when the concept of marker clearance, as a measure of kidney function, was introduced [1]. Since then, several markers have been proposed for *GFR* measurements [2]; but with limitations: creatinine, for example, can give an inaccurate estimation of *GFR* as its levels in the blood are affected by nutrition, diet, and muscle mass (age and gender dependent) [3]. Tubular secretion, which can be erratically variable, also plays a role in its clearance and this makes creatinine less than an ideal renal marker [3, 4]. Although traditionally regarded as the gold-standard for *GFR* estimation, inulin needs to be continuously administered by injection, and collection of timed urine samples is required to obtain the correct *GFR* value. These limitations make the use of inulin unpopular especially in children [2, 5, 6]. Radio-labelled markers (e.g., ^{51}Chromium-labelled edetic acid, Cr-EDTA) have also been used but are impractical owing to the expensive cost, the special requirements a hospital needs for the handling, storage, and disposal of radioactive compounds, the relatively large blood samples required (5ml), and the obvious concern for using radioactivity [3, 7].
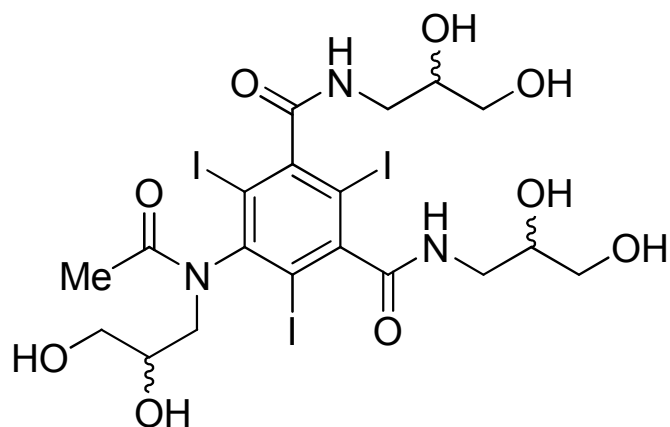
Figure 1: Chemical structure of iohexol (M.W. 821.14, LogP -3.05).

Over the past twenty years, a new filtration marker, iohexol (Figure 1), has been increasingly used [3, 8-10] because of its established safety record [11], cost effectiveness [7, 8], reliability, accuracy [12], and its non-radioactive nature. It is claimed by many to be the new "gold standard" for *GFR* measurement [3, 5, 8, 13] and is used in both adults and children. Other clinical uses of iohexol are as a non-ionic monomeric contrast agent for various radiography imaging procedures [14]. Iohexol does not enter cells and does not bind to proteins or blood cells [7]. Iohexol is not metabolised and, after intravenous administration, it is eliminated unchanged almost exclusively by the glomerulus [6, 7, 15, 16]. Iohexol distributes into a volume equal to the extracellular fluid (plasma + interstitial fluid) volume (*ECV*) [7, 15-19] and for this reason, it has been suggested as a useful tracer of this body compartment [17, 20, 21].

The iohexol *GFR* test involves a single intravenous bolus administration of the marker. Then, at specific time intervals post-administration, blood samples are drawn from the patient, analysed for iohexol, and the results are used to calculate the clearance of iohexol which reports directly on the *GFR* of the patient. The iohexol plasma profile [plasma concentration (*C_p*) *versus* time (*t*)] is best described by a two-compartment bi-exponential model (Figure 2) [6, 12, 14]. The first-order distribution reflects the equilibration process between the intravascular extracellular (representing the plasma) and the extravascular extracellular (representing the interstitial fluid) compartments which is achieved after about 2 –
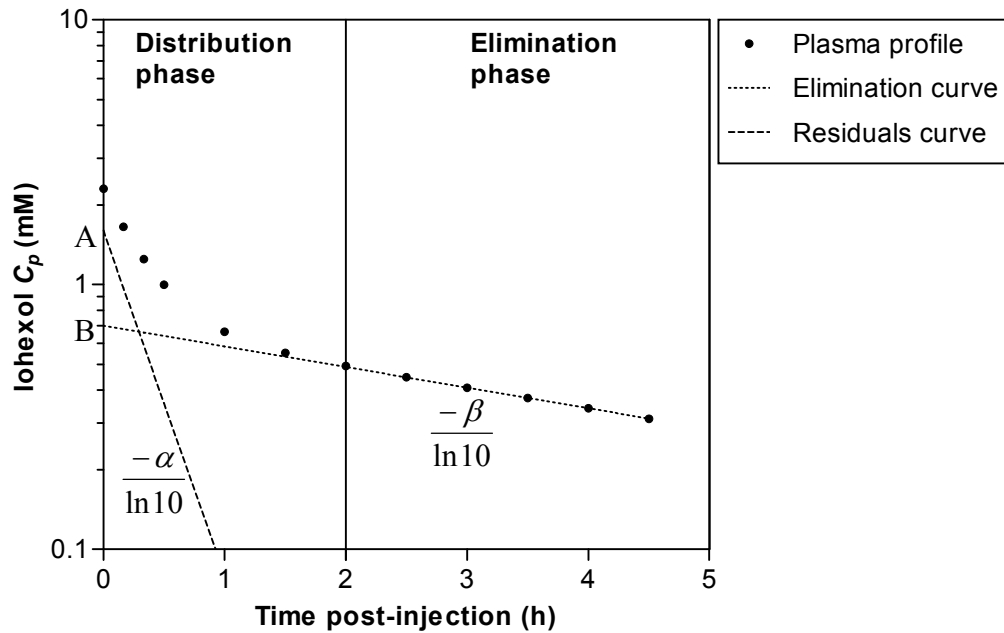
Figure 2: Illustrative example of iohexol plasma concentration (C_p) *versus* time (t) profile. Plasma concentrations may be described by a two-exponential, two-compartment model of the form: $C_p = A\ e^{-\alpha t} + B\ e^{-\beta t}$

3 hours post-iohexol administration [7, 16, 22]. Once the distribution of iohexol reaches equilibrium, its plasma disappearance profile follows a first-order decline over time governed, only, by the elimination process.

GFR is equal to the clearance of iohexol (*Cl*) and is usually expressed normalised to a body index. Body surface area (BSA) is the most commonly used index and the reference BSA is 1.73 m^2 (representing the normal BSA of an average adult).

The clearance of iohexol is calculated as follows:

$$Cl = \frac{Dose}{AUC_0^\infty} = \frac{Dose}{\frac{A}{\alpha} + \frac{B}{\beta}}$$
Equation (1)

Where *Dose* is the amount of iohexol administered to the patient and AUC_0^∞ is the area under the concentration *versus* time profile from *t = 0* to *t = ∞*. B and *β* respectively denote the Y-intercept and slope of the elimination curve (Figure 2). *A* and *α* are, respectively, the Y-intercept and slope of the residual curve which

reflects the distribution process only and is attained from iohexol concentration profile by means of deconvolution.

Accurate determination of iohexol's clearance using the two compartment model (Equation 1) necessitates numerous blood samples taken during the distribution and elimination phases. For both practical and ethical reasons, this approach has proved unpopular, especially in the paediatric population. As a result, simplified models have been introduced whereby only the elimination phase of iohexol is considered [23]. Thus, an assumption of a first-order one-compartment model can be made (Equation 2) and fewer sampling points, made after equilibrium in iohexol distribution is accomplished, are therefore required.

$$C_p = B \cdot e^{-\beta \cdot t} \cong C_0 \cdot e^{-K_e \cdot t} \qquad \text{Equation (2)}$$

Where C_0 is assumed to be the plasma concentration at $t = 0$, K_e is the elimination rate constant (equivalent to β in Equation 1). The clearance of iohexol using this simplified model is calculated as follows:

$$Cl = K_e \cdot V_d = \left(\frac{Dose}{\frac{C_0}{K_e}} \right) = \left(\frac{Dose}{\frac{B}{\beta}} \right) \qquad \text{Equation (3)}$$

Where V_d is the volume of distribution of iohexol. To account for errors arising from this simplification (compare Equations 1 and 3), correction factors are used to avoid overestimation of *GFR* [6, 7, 23-25].

Even though the use of the simplified mono-compartment approach in the iohexol *GFR* test improves the practicability of the procedure with less sampling points required, some disadvantages remain. At least 2 blood samples are still essential to provide necessary data about the elimination phase. Blood sampling is invasive and may cause infection. In addition, patients (particularly children) may experience significant pain and distress. Needle insertion, in fact, is one of the most frightening experiences that children remember from a stay in the hospital [26, 27]. Technical difficulties when sampling (such as finding a suitable vein in a distressed

child) pose a significant issue to the medical team. Finally, the less frequent sampling carries the risk of estimation errors limiting, therefore, the precision of *GFR* determination [6, 28]. It follows that the need for a less invasive, but still accurate, alternative technique for iohexol sampling is, thus, greatly desirable. In particular, the paediatric population would benefit immensely from such alternative sampling tools in the iohexol *GFR* test.

The principal objective addressed in this study was to assess the feasibility of transdermal reverse iontophoresis as an alternative non-invasive sampling tool for iohexol. The study is divided into two parts:

First, an *in vitro* investigation was performed to provide a preliminary proof-of-concept for subsequent *in vivo* evaluation. Correlation between iohexol subdermal concentrations, representative of typical, clinical plasma levels usually observed in patients, and the corresponding iontophoretic extraction fluxes was assessed. Then, an iontophoretic pre-treatment period was introduced prior to iohexol sampling to attempt to reduce the time required to achieve steady extraction rates. Finally, iohexol transdermal extraction fluxes were followed to evaluate the correlation to the subdermal concentration of the marker whose disappearance was simulated with different first-order pharmacokinetic models.

Second, a pilot study verified that iohexol could, indeed, be extracted *in vivo* by transdermal iontophoresis, and then considered whether the extraction fluxes were sensitive to the decline of the marker's blood concentration. This would allow the elimination rate constant (K_e) and *GFR* of each subject to be estimated from the skin sampling data and comparison with the corresponding parameters calculated from blood sampling. Finally, the local effect of iontophoresis on the skin and participant feedback were evaluated.

2. In vitro study

A. Materials and methods

A.1 Chemicals

Iohexol (98% pure), acetaminophen (≥99%), silver wire (99.99%), and silver chloride (99.999%) were purchased from Sigma Aldrich (Gillingham, UK). Tris base (α, α, α-Tris-(hydroxymethyl)-methylamine), sodium chloride, and potassium chloride were from Acros (Geel, Belgium). Hydrochloric acid (37 %w/w), methanol, and trifluoroacetic acid were obtained from Fisher Scientific (Loughborough, UK). All reagents were at least analytical grade and deionised water (resistivity ≥ 18.2 MΩ.cm, Barnsted Nanopure Diamond^{TM}, Dubuque, IA) was used for the preparation of all solutions.

A.2 Skin

Fresh pig skin was obtained from a local slaughterhouse, cleaned under cold running water, and stored in a refrigerator until the following day. Abdominal skin was dermatomed (Zimmer™ Electric Dermatome, Dover, Ohio; nominal thickness 750 µm), cut into pieces of appropriate size, wrapped individually in Parafilm™, and then kept in a freezer (-20 °C) until use. Immediately prior to the permeation experiment, the skin was thawed at room temperature for 30 minutes and visible hairs were carefully cut with scissors. The skin was then mounted directly onto the diffusion cells.

A.3 Iontophoresis

Anodal iontophoretic transport studies were performed using Ag/AgCl electrodes connected to a power supply (KEPCO 1000M, Flushing, NY, USA) which delivered direct, constant current. Electrode and subdermal solutions were magnetically stirred for the duration of the experiment (Multipoint-6 stirrer,

Thermo Scientific Variomag, Cole-Parmer, London, UK). The number of replicates was 4 – 12.

Fixed-subdermal concentration extraction: Experiments were performed using side-by-side two-compartment diffusion cells (skin transport area = 0.71 cm^2, volume 3 ml). Abdominal skin was sandwiched between the chambers, with the stratum corneum facing the cathode compartment. Prior to iontophoresis, the skin was hydrated for 30 minutes in the presence of 25 mM Tris buffer solution in both compartments (no iohexol). The subdermal (anode) solution also contained 133 mM NaCl and 4 mM KCl to mimic physiological conditions. The final pH of both solutions was adjusted to 7.4 with HCl.

The correlation of iohexol iontophoretic extraction with its subdermal concentration was investigated. After the 30-minute hydration period, the cathode compartment was emptied and refilled with fresh buffer. The anode solution was replaced with one of 5 concentrations ranging from 0.15 to 2.44 mM, reflecting the clinical range found in *GFR* measurements. The current (0.36 mA) was applied for 6 hours. Every hour, the current was stopped, 1 ml from the cathode solution was withdrawn for analysis and replaced by the same volume of fresh buffer solution. A passive diffusion control was also performed using the highest concentration of iohexol (2.44 mM).

Subsequently, the effect of a 3 hour iontophoretic pre-treatment of the skin on iohexol extraction was examined. In this case, post-30 minute hydration, but before the introduction of iohexol into the subdermal (anode) compartment, the skin was exposed to a constant current of 0.36 mA for 3 hours. Acetaminophen (7.5 mM) was also present in the anode solution, allowing electroosmotic flow to be monitored. After the pre-treatment period, the anode solution was replaced and 2.44 mM iohexol was added along with 7.5 mM acetaminophen in Tris buffer (25 mM Tris, 133 mM NaCl, 4 mM KCl; pH 7.4). The current was then re-applied for a further 6 hours. Sampling for iohexol and acetaminophen from the cathode compartment was performed hourly. A passive diffusion control was also

performed in a separate experiment using skin which had been exposed to a 3 hour constant current pre-treatment (0.36 mA) in the absence of iohexol.

Pharmacokinetic simulations: Side-by-side three compartment diffusion cells were used (skin transport area = 1.02 cm^2). Anode and cathode electrode chambers (volume 1.9 ml) were each separated from a central compartment (volume 3.75 ml) by a piece of excised pig skin oriented so that the stratum corneum was facing towards the electrode chambers. The electrode chambers contained 25 mM Tris (pH 7.4) in the cathode, and 90 mM NaCl (necessary for electrochemical reactions) in 25 mM Tris buffer (pH 7.4) in the anode compartment. Using a syringe pump (Genie 8, Kent Scientific Corporation, Torrington CT, USA), the subdermal compartment was continuously infused with Tris buffer solution (25 mM Tris, 133 mM NaCl, 4 mM KCl, pH 7.4) at specific flow rates (Table 1). This allowed the progressive clearance of iohexol from the subdermal compartment. Two sets of experiments were performed:

First, after hydration of the skin for 30 minutes (no iohexol), the solutions were refreshed and 0.31 mM iohexol was introduced into the subdermal compartment. At this point, the syringe pump continuously infused the subdermal compartment at 1.5 ml/h rate (i.e., simulation of a mono-exponential decay of iohexol); and a 0.5 mA constant current was applied for 6 hours. Every 30 minutes, the current was stopped and the entire cathodal solution was replaced with fresh buffer. Samples (10 µl) were also collected from the subdermal compartment at the mid-point of each iontophoretic sampling period.

The second set of experiments pre-exposed the skin to 3 hours of constant current (0.5 mA) in the absence of iohexol. After the pre-treatment period, all solutions were refreshed and iohexol (at 1.22 or 6.04 mM) was introduced into the subdermal compartment. Constant, direct current (0.5 mA) was applied for 6 hours. At the same time, the syringe pump was used to continuously clear iohexol from the subdermal compartment. Samples were collected from both the subdermal and cathodal compartment as before. A summary of the experimental conditions is in Table 1.

Table 1: Experimental conditions used in the pharmacokinetic simulation studies.

Skin condition	Initial subdermal [iohexol] (mM)	Pump flow rate (ml/h)
Untreated	0.31	1.5
Pre-treated with 0.5 mA current (3 h) in the absence of iohexol	1.22	1.0
	6.04	First 3 hours: 3.0 Thereafter: 1.0

A.4   Sample analysis

Iohexol and acetaminophen were quantified simultaneously by high performance liquid chromatography with UV detection (254 nm). The method was modified from a previous publication [29] and used an HPLC system (Dionex, Sunnyvale, CA) comprising a P680 pump with ASI-100 autosampler, TCC-100 thermostated column compartment, PDA-100 diode array detector, and an Acclaim 120, C18 (150 x 4.6 mm, 5 µm) reversed-phase column (Dionex, UK) thermostated at 60°C. The mobile phase, 13.5 mM TFA (pH 2.2):MeOH (95:5 v/v), was pumped through the system at 1 ml/min. The validation parameters are found in Appendix (1A).

A.5   Data analysis and statistics

Data analysis and regressions were performed using Graph Pad Prism V.5.00 (Graph Pad Software Inc., CA, USA). Unless otherwise stated, data are represented as the mean ± standard deviation (SD). Extraction fluxes were calculated as the amounts transported per unit time. Statistical significance was set at $p < 0.05$. The slopes of the linear regressions of extraction fluxes *versus* subdermal concentrations were compared by ANCOVA test. Fluxes at different times were compared by repeated-measures ANOVA followed by Tuckey's post-test. Two-way repeated-measures ANOVA followed by Bonferroni post-test was used to compare the experiments evaluating the effect of skin pre-treatment on extraction fluxes. The same test was also used for comparison of iontophoretic extraction efficiencies of iohexol and acetaminophen.

The results from each iontophoresis cell, used for the pharmacokinetic simulations of subdermal concentration and extraction flux *versus* time profiles, were individually fitted with the corresponding regression equation. AUC_0^t was calculated by the trapezoidal rule (Graph Pad Prism) and AUC_0^∞ was determined from the last measured concentration divided by the elimination rate constant. Statistical comparison of the kinetic parameters obtained from the subdermal concentration and iontophoretic extraction data were performed with two-tailed Mann-Whitney test.

B. Results and discussion

B.1 Fixed-subdermal concentration extraction

Iohexol is a hydrophilic (LogP = -3.05), polar, neutral compound. The mechanisms contributing to its extraction flux during transdermal iontophoresis are passive diffusion and electroosmosis. Therefore, iontophoretic extraction towards the cathode was selected as the most efficient method for iohexol sampling. This is because at physiological pH, the net charge on the skin is negative and electroosmosis proceeds in the direction of anode to cathode [30].

Passive extraction of iohexol was negligible when compared to iontophoresis. Its flux only reached 0.06 ± 0.04 nmol/h over 6 hours when 2.44 mM of iohexol was present in the subdermal compartment. In contrast, iontophoretic extraction fluxes were nearly 80 times higher. Moreover, even when a smaller subdermal concentration (0.15 mM, i.e., one-sixteenth of that used in the passive diffusion experiment) was iontophoresed, an extraction flux of 0.31 ± 0.08 nmol/h was observed. Clearly, therefore, iontophoresis offers a much more efficient sampling technique than passive diffusion.

The first objective was to demonstrate a linear correlation between iohexol subdermal concentrations, chosen to represent the clinical range typically observed in patients, and the corresponding iontophoretic extraction fluxes. Figure 3 reveals that this was indeed the case and such proportionality improves with time of iontophoresis (e.g., r^2 0.88 at 6 h). These findings are in line with previous studies reported for other neutral compounds (e.g., glucose, mannitol, phenylalanine, phenytoin, and urea) [31-35]. The slopes of this linear relationship (Z, µl/h) after different times of iontophoresis are in Table 2, and represent the iontophoretic extraction efficiency of iohexol. The values increased with time up to 4 hours after which the pooled, average Z was 1.81 ± 0.13 µl/h (Mean ± SE).
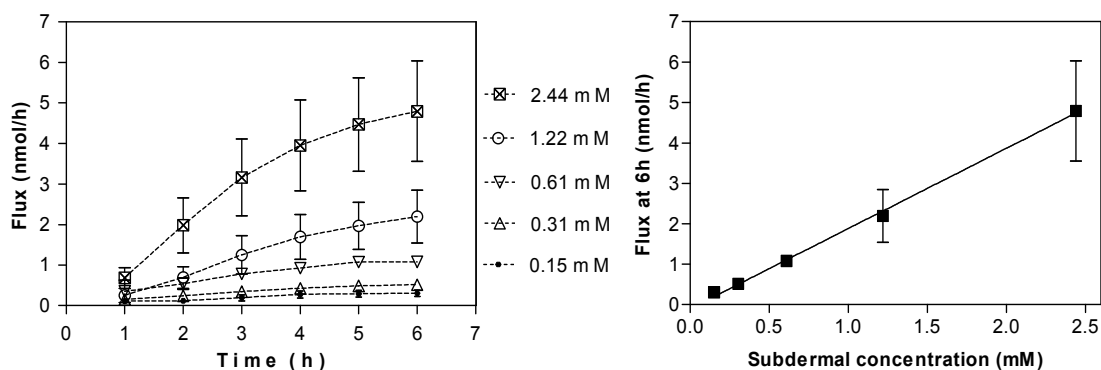
Figure 3: Reverse iontophoretic extraction fluxes of iohexol as a function of time and subdermal iohexol concentration. Data are represented as the mean ± SD of 4 - 7 replicates.

The delay for reaching constant levels of extraction is due to the time needed for the electroosmotic solvent flow to establish a steady stream across the skin but may also be solute-specific. When iohexol molecules are dragged along with the electroosmotic solvent flow across the skin, a fraction, relative to the solvent, may be reflected by the membrane and steady extraction of iohexol is therefore slowed down. It is worth noting, though, that this lag time may be artificially long *in vitro* because the skin membranes used in these experiments had a nominal thickness of 750 µm and therefore a longer diffusion path for iohexol than what would be otherwise present *in vivo*.

Table 2: Linear regressions of iohexol iontophoretic extraction flux (J_t, nmol/h) as a function of its subdermal concentration (C_t, mM) at different times of iontophoresis [$J_t = Z \cdot C_t +$ Y-intercept*]. Z values are expressed as the best-fit slope values ± standard error of the regression (SE).

Time (h)	1	2	3	4	5	6
Z (µl/h)	0.23 ± 0.04	0.80 ± 0.08	1.29 ± 0.11	1.62 ± 0.13	1.84 ± 0.13	1.99 ± 0.14
r^2	0.52	0.78	0.83	0.86	0.88	0.88

* The Y-intercept was always ≤ 0.10 nmol/h.

B.2   Effect of iontophoretic pre-treatment of the skin on iohexol transport

The second objective was to examine whether the time required to reach a stable efficiency of extraction could be shortened. The relevance of such a goal to a clinical application is clear. A three hour iontophoresis (0.36 mA) pre-treatment was introduced before addition of iohexol into the subdermal compartment. Three hours was chosen because: 1) in the previous set of experiments (section B.1), the fluxes stabilised after at least 3 hours of iontophoresis application, and 2) when iohexol is administered to patients as a renal marker, its distribution phase takes 2 – 3 hours to be accomplished. Data from this phase are not used in the calculation of *GFR* (with the simplified approach), and therefore a 2 – 3 hour "window" exists that might be used to stabilise the transdermal extraction flux of iohexol.

The pre-treatment slightly increased the total extraction flux of iohexol (Figure 4) and values measured at 2 through 5 hours were significantly higher than without pre-treatment ($p < 0.001$ (2 h) and $p < 0.05$ (5 h)). However, there was no statistical difference at 6 hours. A small increase ($p < 0.001$) in the passive diffusion,
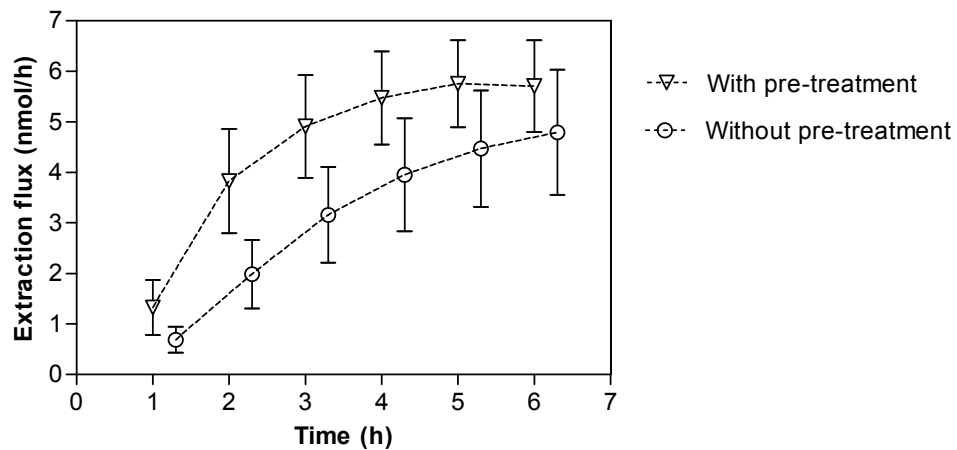

Figure 4: Effects of a 3 hour iontophoresis pre-treatment (0.36mA) on iohexol extraction fluxes. The initial subdermal concentration of iohexol was 2.44 mM. Data representing "Without pre-treatment" are slightly nudged to the right for clarity. Data are presented as mean ± SD of 7 – 12 replicates.
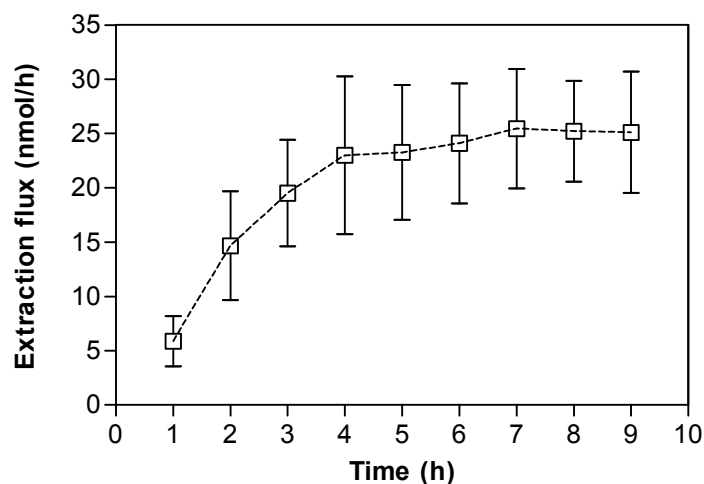
Figure 5: Iontophoretic extraction fluxes (mean ± SD, *n* = 6) of acetaminophen as a function of time. Fluxes approach constant values from 4 hours. Electroosmosis is the sole contributor to acetaminophen's transport across the skin, the passive diffusion of which was negligible (data not shown).

from J_{6h} = 0.06 ± 0.04 to 0.24 ± 0.04 nmol/h was found when the skin was pre-iontophoresed but the resulting contribution remained negligible compared to the electrotransport.

The pre-treatment shortened the time required to reach stable extraction fluxes of iohexol by about 1 hour. Acetaminophen (pKa 9.5) is uncharged at pH 7.4 and was used to track electroosmosis throughout the pre-treatment experiment. Figure 5 shows that steady extraction of this marker is achieved within 4 hours of current application. However, even after skin pre-treatment, iohexol required 3 hours to reach steady extraction, although the electroosmotic solvent flow is already established across the skin at the time of iohexol addition to the subdermal compartment.

The extraction efficiency of iohexol and acetaminophen through untreated skin differed significantly (Table 3). For example, after 6 hours of iontophoresis Z = 1.96 ± 0.51 µl/h for iohexol and 3.21 ± 0.74 µl/h for acetaminophen. The values are, however, less than 2.5 fold different despite the much larger molecular weight of iohexol (821.14 Da) compared to acetaminophen (151.17 Da). A better correlation is perhaps found in the molecular size differences. The Stokes radius of iohexol is

Table 3: Extraction efficiencies of iohexol and acetaminophen after different times of iontophoresis. Data are represented as the mean ± SD of 6 – 7 replicates.

Time (h)	$Z_{iohexol}$ (µl/h)	$Z_{acetaminophen}$ (µl/h)	Significant difference*
1	0.28 ± 0.11	0.78 ± 0.31	No
2	0.81 ± 0.28	1.96 ± 0.67	$p < 0.01$
3	1.30 ± 0.39	2.60 ± 0.66	$p < 0.001$
4	1.62 ± 0.46	3.07 ± 0.97	$p < 0.001$
5	1.83 ± 0.47	3.10 ± 0.83	$p < 0.001$
6	1.96 ± 0.51	3.21 ± 0.74	$p < 0.01$

* Two-way repeated-measures ANOVA followed by Bonferroni post-test.

reported to be 1.1 nm [36] whereas that of acetaminophen is 0.36 nm [37]; a factor of 3 difference. Previous studies demonstrated a dependence of the magnitude of electrotransport efficiency on the molecular size of the solute [38, 39]. One example [38] examined the transport efficiencies of 26 polyethylene glycols (neutral molecules) of various molecular weights (282 – 1382 Da, corresponding to Stokes radii of 0.38 – 0.81 nm). The mean transport efficiencies, which were measured across full thickness hairless rat skin under the application of 1 mA (0.5 mA/cm^2) direct constant current for 14 hours, were found to decrease from 10.1 µl/h.mA for the smallest molecule to 0.23 µl/h.mA for the bulkiest. It is interesting to note that the extraction efficiency of iohexol [Z_{6h} = 5.46 ± 1.41 µl/h.mA] was twice higher than the iontophoretic efficiencies of two polyethylene glycols of similar molecular weights (810 and 854 Da; Stokes radii 0.62 and 0.64 nm) which measured at 2.8 and 2.64 µl/h.mA. This is although the previous study used rat skin which is known to be more permeable than pig skin.

B.3   Pharmacokinetic simulations

When used in *GFR* tests, iohexol is given as an intravenous bolus injection and its concentration in the body then decreases over time. The previous experiments established the linear proportionality between iohexol's subdermal concentration and its corresponding extraction flux under "static conditions", in which the subdermal concentration of iohexol was held constant throughout the experiment. The next objective was to further examine this linear dependency when the subdermal concentrations of iohexol were gradually cleared by simulated first-order elimination. Pharmacokinetic parameters estimated from the subdermal concentration data were compared to those deduced from the iontophoretic extraction results.

Two experiments were performed in which the subdermal concentration of iohexol was progressively decreased to simulate a first-order elimination process. The first experiment involved no iontophoretic pre-treatment and was characterized by an "injected bolus" of 1144 nmoles of iohexol in a volume of distribution of 3.75 ml (the volume of the subdermal compartment), with a clearance of 1.5 ml/h (the syringe-pump flow rate). The second involved a 3 hour pre-treatment period at 0.5 mA (after which all compartments were refreshed with new solutions), an iohexol dose of 4575 nmoles directly "injected" into the subdermal chamber (volume again 3.75 ml), with a clearance of 1 ml/h.

The concentration in the subdermal compartment (C_t) decays according to the standard first order kinetic equation:

$$C_t = C_0 \cdot e^{-K_e \cdot t}$$

Equation (4)

Where C_0 is the subdermal concentration at time (t) = 0, and K_e is the first order elimination constant. It is also true that:

$$C_0 = Dose/V_d$$

Equation (5)

Where *Dose* is the amount of iohexol introduced into the subdermal compartment of volume (V_d) at $t = 0$, and,

$$K_e = Cl/V_d$$

<div align="right">Equation (6)</div>

Where *Cl* is the clearance. A model-independent estimate of the clearance may also be derived from:

$$Cl_{ind} = Dose/AUC_0^\infty$$

<div align="right">Equation (7)</div>

Where AUC_0^∞ is the area under the concentration *versus* time profile from $t = 0$ to $t = \infty$.

The iontophoretic extraction flux (J_t) as a function of time is expected to be proportional to C_t, that is:

$$J_t = Z \cdot C_t = Z \cdot C_0 \cdot e^{-K_e \cdot t}$$

<div align="right">Equation (8)</div>

Where *Z* is a proportionality constant, previously referred to as the iontophoretic extraction efficiency of iohexol.

From the linear decay of LnC_t and LnJ_t as a function of time (Figure 6), values of K_e were deduced from both the measured subdermal concentrations and the
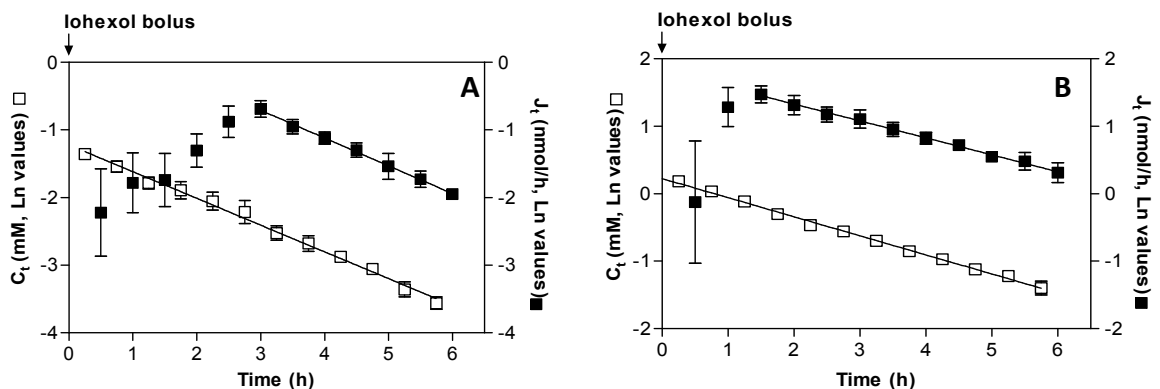

Figure 6: Mono-exponential decay simulations. Iohexol subdermal concentrations (C_t, open squares) and iontophoretic extraction fluxes (J_t, filled squares) as a function of time. (A) without iontophoretic pre-treatment, (B) following a 3 hour iontophoretic pre-treatment. Data are represented as the mean ± SD of 4 − 5 replicates.

Table 4: Pharmacokinetic parameters derived from the simulated first-order elimination model of iohexol subdermal concentration (C_t) and the corresponding extraction fluxes (J_t).

		r^2 $\geq$	K_e [a] (h^{-1})	C_0 [b] (mM)	V_d [c] (ml)	Cl [d] (ml/h)	Cl_{ind} [e] (ml/h)
No pre-treatment	C_t	0.98	0.38 ± 0.05	0.29 ± 0.02	4.02 ± 0.28	1.51 ± 0.14	1.53 ± 0.1
	J_t	0.94	0.41 ± 0.03	0.36 ± 0.08	3.26 ± 0.63	1.34 ± 0.17	1.31 ± 0.2
With Pre-treatment	C_t	0.99	0.28 ± 0.01	1.23 ± 0.05	3.71 ± 0.16	1.04 ± 0.05	1.04 ± 0.06
	J_t	0.90	0.25 ± 0.05	1.21 ± 0.18	3.89 ± 0.63	0.96 ± 0.05	0.96 ± 0.05

[a] Determined from the slope of the linear regression. [b] Determined from the intercept of the linear regression. [c] Calculated from: $V_d = Dose/C_0$. [d] Calculated from: $Cl = K_e . V_d$. [e] Model independent clearance: $Cl_{ind} = Dose/AUC_0^\infty$.

iontophoretic extraction fluxes. The results in Table 4 show a remarkably good agreement between the two determinations, both when the iontophoresis pre-treatment was used or not.

Extrapolation of the linear data of the plots in Figure 6 to t = 0 yields intercepts equal to C_0 and ZC_0, respectively, for the subdermal concentration and iontophoretic extraction results. The former yields results (0.29 ± 0.02 mM and 1.23 ± 0.05 mM for no pre-treatment and with pre-treatment, respectively) which are very close to the actual values given by equation (5): 0.305 mM and 1.22 mM.

From the results in Figure 6, and application of equation (8), it is possible to estimate Z for the experiments without and with iontophoretic pre-treatment: 4.8 ± 0.5 µl/h and 5.3 ± 0.4 µl/h, respectively. With these values, and the extrapolated intercepts of the linear LnJ_t data to t = 0, C_0 can be found from the reverse iontophoresis results. Table 4 shows that the agreement between these results and the actual values is rather good.

With the derived C_0 and K_e, from the subdermal concentration and reverse iontophoretic flux results, together with the known iohexol doses delivered to the subdermal compartment at t = 0, permits V_d, Cl, and the model-independent clearance to be derived using equations (5), (6), and (7) (Table 4). Once again, good agreement between the derived values is observed in addition to the consistency with the "ideal" values (V_d = 3.75 ml, Cl = 1.5 ml/h and V_d = 3.75 ml, Cl = 1 ml/h for without and with iontophoresis pre-treatment, respectively). Similar correlations were also found in a previous *in vitro* study which investigated reverse iontophoresis as an alternative non-invasive sampling procedure to lithium monitoring [40].

After confirmation of the good correlation of the iontophoretic extraction fluxes of iohexol with its subdermal concentrations cleared by first-order elimination kinetics, the next experiment investigated whether an abrupt change in the elimination rate of iohexol from the subdermal compartment would be as well tracked and reflected in the iontophoretic extraction fluxes. The study started after a 3 hour iontophoretic pre-treatment of the skin. Then, all compartments were refreshed with new solutions and the subdermal chamber now contained 6.04 mM iohexol. The syringe pump was programmed to perfuse the subdermal compartment at a constant rate of 3 ml/h for the first 3 hours. At the end of 3 hours, the infusion rate was abruptly changed to 1 ml/h for the remaining 3 hours. Hence, the concentration of iohexol in the subdermal compartment (C_t) decayed according to the following equation:

$$C_t = D \cdot e^{-\delta \cdot t}$$ Equation (9)

Where $D = A$ and $\delta = \alpha$ at times [t = 0 – 3 hours], and $D = B$ and $\delta = \beta$ at times [t = 3 – 6 hours]. As in the previous section, the iontophoretic extraction flux (J_t) deduced as a function of time is expected to follow:

$$J_t = Z \cdot D \cdot e^{-\delta \cdot t}$$ Equation (10)

Consistent with the previous results, the linear data for the decay of LnC_t and
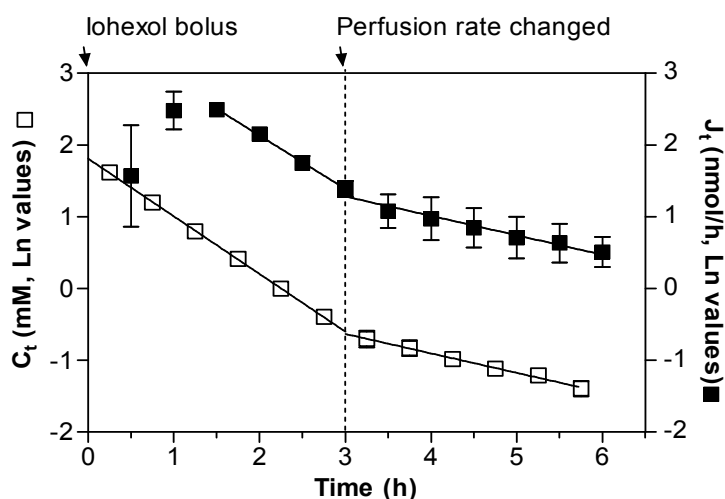
Figure 7: Simulated bi-phasic decay of iohexol. Iohexol subdermal concentrations (C_t, open squares) and iontophoretic extraction fluxes (J_t, filled squares), expressed semi-logarithmically, as a function of time. Data are represented as the mean ± SD of 4 – 5 replicates.

LnJ_t as a function of time (Figure 7) showed excellent correlation of the extraction fluxes to the changes in iohexol's concentration in the subdermal compartment. Once again, determination of D and δ from the two phases of the experiment (i.e., [A, α] and [B, β]) demonstrated remarkable similarities between the subdermal concentration and corresponding iontophoretic extraction data (Table 5).

Overall, experiments in this part of study simulated first-order disappearance of iohexol from the subdermal compartment. Concomitant measurements of the iontophoretic extraction fluxes confirmed its sensitivity to track the concentration change and the kinetic parameters deduced from both data were very similar.

Table 5: Kinetic parameters derived from the simulated non-compartmental model for iohexol subdermal concentration (C_t) and the corresponding extraction fluxes (J_t). See equations (9) and (10) in the text for definitions.

	r^2 ≥	A (mM)	$α$ (h^{-1})	B (mM)	$β$ (h^{-1})
C_t	0.99	6.12 ± 0.16	0.80 ± 0.01	0.53 ± 0.07	0.27 ± 0.03
J_t	0.97	6.18 ± 0.68	0.74 ± 0.02	0.55 ± 0.10	0.23 ± 0.04

3. In vivo study

A. Materials and methods

A.1 Chemicals

Iohexol (98% pure) was purchased from Sigma Aldrich (Gillingham, UK). Sodium chloride, potassium chloride, and methanesulfonic acid (99%) were obtained from Acros (Geel, Belgium). Acetonitrile was provided by Fisher Scientific (Loughborough, UK). All reagents were at least analytical grade and deionised water (resistivity ≥ 18.2 MΩ.cm, Barnsted Nanopure Diamond^{TM}, Dubuque, IA) was used for the preparation of all solutions.

A.2 Subjects

Four children, undergoing a routine iohexol *GFR* test at Great Ormond Street Hospital for Children (GOSH), participated in the study (Ages: 9.1, 13, 7.4, and 12 years old; 1 female and 3 males). Approval was granted from the Institute of Child Health/ Great Ormond Street Hospital Research Ethics Committee, and prior written consent and assent from the parent and child, respectively, were obtained before beginning the study (see Appendix 2 for forms). Participants did not have any skin condition, such as eczema, irritated or damaged skin.

A.3 Iohexol sampling by the routine intravenous method and the alternative technique, transdermal reverse iontophoresis

The routine *GFR* test involved the bolus intravenous administration of 2 ml of Omnipaque 300 (Nycomed Amersham plc, Bucks., UK), equivalent to 1294 mg iohexol. Subsequently, two 1 ml blood samples were taken from the subject at approximately 3 and 4 hours post-injection. The samples were analysed for iohexol by the GOSH clinical chemistry laboratory. Transdermal reverse iontophoresis was carried out in parallel on the non-dominant arm of the participant. The arm was

first cleaned with an alcohol wipe and then allowed to dry. Constant, direct current (Figure 8) was delivered from a "Phoresor® II auto" device (PM850, Iomed, Salt Lake city, Utah, USA) to the electrode patches (Iogel small, Iomed, Salt Lake city, Utah, USA) affixed to the subject's skin. The anode was a dispersive pad (active area 22.6 cm^2) incorporating a silver/silver chloride electrode in karaya gel. The cathode (active area 7.2 cm^2) was a silver chloride electrode integrated into a dried gel which was hydrated with 1.3 ml of ultrapure water. The Phoresor® precisely delivered 0.5 mA (0.07 mA/cm^2 at the cathode sampling site) of current (except for participant number 3 for whom the applied current was 0.3 mA) for 5 hours, beginning 0.5 hours after the intravenous dose of iohexol. Both patches were refreshed after 2 and 4 hours of current passage, and the cathodal patch was additionally replaced at 3 hours (see schematic below). When the patches were exchanged, the current was interrupted briefly.

Photographs of the participants' arms were taken before and after iontophoresis to investigate the effect of current passage on the skin. Participants also completed a short questionnaire just after the start of iontophoresis and towards the end of the experiment. The questionnaire used the Wong-Baker faces pain scale [41] to indicate the level of sensation experienced during iontophoresis. Subjects were also asked whether transdermal iontophoresis was preferred over blood sampling.

	Skin sampling (i.e., patch replacement)		

Start of iontophoresis

0h　　1h　　2h　　3h　　4h　　5h　　6h

Intravenous administration of iohexol

	Blood sampling	
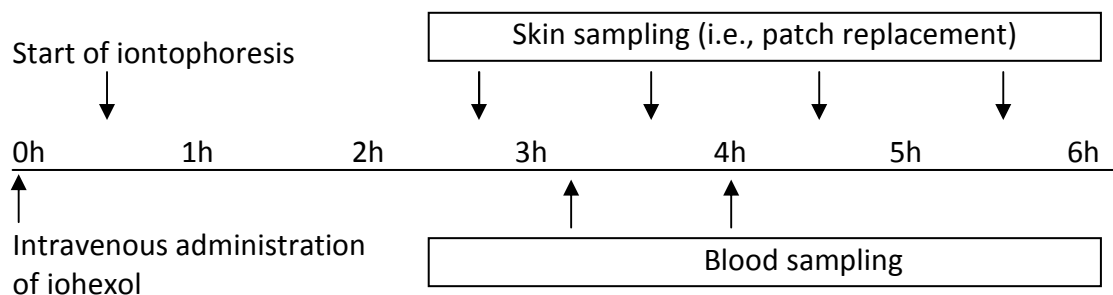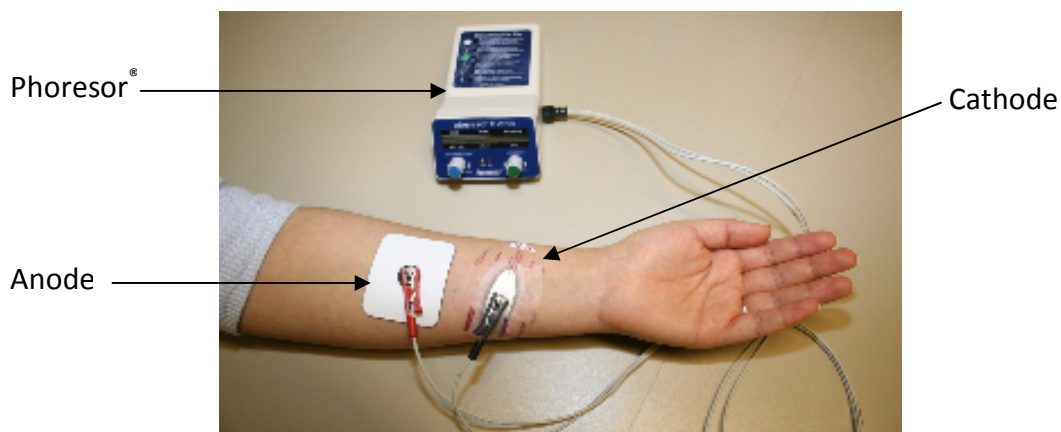
Figure 8: Experimental setup for transdermal reverse iontophoresis.

A.4 Sample analysis

The cathodal patches were immersed in 7 ml of water and shaken at 240 rpm (HS260 Basic, IKA, Sigma Aldrich, Gillingham, UK) for 24 hours to extract the reverse-iontophoretically transported compounds. The extracts were filtered by centrifugation (45 minutes at 7500 RCF) using Amicon® ultrafiltration tubes (MWCO 5 kDa, Millipore, Watford, UK).

Iohexol was quantified by high performance liquid chromatography. The method used a Shimadzu HPLC system (LC-2010A HT, Kyoto, Japan) comprising an autosampler, a UV diode array detector set at 254 nm wavelength, and a HiQ-Sil^{TM} C18 (250 x 4.6 mm, 5 µm) reversed-phase column (Jasco, UK) thermostated at 40°C. The mobile phase, water:acetonitrile (70:30, %v/v), was pumped through the system at 1 ml/min flow rate. The effective run for each injected sample (20 µl) was 7 minutes and a wash step (water:acetonitrile, 20:80, %v/v) for 38 minutes followed by a 10 minute column re-equilibration with the initial mobile phase was implemented after each run.

Sodium and potassium in the extracts were analysed by ion chromatography with suppressed conductivity detection. The method was modified from a previous publication [42] and used an IC system (Dionex, Sunnyvale, CA) comprising a GP-50 gradient pump, an AS-50 autosampler and thermal compartment, and an ED-50 electrochemical detector. The mobile phase, 20 mM methanesulfonic acid, was

pumped at 1 ml/min through a Dionex IonPac^{TM} CS12A (250 x 4 mm) column thermostated at 30 °C and connected to a Dionex CSRS Ultra II suppressor (4 mm) set at a current of 80 mA.

The validation parameters of the analytical methods are in Appendix (1B).

A.5 Calculations and statistical analysis

Data analysis and regression were performed using Graph Pad Prism V.5.00 (Graph Pad Software Inc., CA, USA). The slope and intercept of regression lines were expressed as the best-fit value ± standard error of the regression (SE). Statistical comparisons of extraction fluxes of sodium and potassium at different times of iontophoresis were determined using repeated-measures ANOVA test. The level of significance was set at $p < 0.05$. The blood concentrations of iohexol were plotted at the exact times of blood sampling; whereas the transdermal extraction fluxes were plotted at the midpoint of the respective extraction interval. As the sampling times of blood measurements did not coincide with the sampling times of reverse iontophoresis, the corresponding plasma concentrations, when correlated to iontophoretic extraction fluxes, were adjusted by interpolation.

A.5.1 Calculation of iohexol's elimination rate constant (K_e)

From blood sampling

To obtain an estimate of the *GFR* from the measured iohexol concentrations (C_{p,t_1} and C_{p,t_2}) in the blood samples withdrawn from the subject at approximately 3 (t_1) and 4 (t_2) hours post-injection, a first order mono-compartment model was assumed, where the distribution phase was ignored, so that:

$$C_{p,t_1} = C_0 \cdot e^{-K_e \cdot t_1} \quad \text{(Eq. 11)} \; ; \quad C_{p,t_2} = C_0 \cdot e^{-K_e \cdot t_2} \quad \text{(Eq. 12)}$$

Where C_0 is assumed to be iohexol's blood concentration at $t = 0$ and K_e is the elimination rate constant of the marker. Taking logarithms of equations (11) and (12) and subtracting one from the other allows K_e to be found:

$$\ln\left(C_{p,t_1}/C_{p,t_2}\right) = K_e \cdot (t_2 - t_1)$$ (Equation 13)

From skin sampling

The reverse iontophoretic extraction fluxes of iohexol (J_{ioh}) were similarly assumed to decay with first-order kinetics and were anticipated to follow the changes in the marker's blood levels (this is after distribution of iohexol has reached equilibrium across the extracellular fluid, i.e., 2 – 3 hours post-injection):

$$J_{ioh} = Z \cdot C_p = Z \cdot C_0 \cdot e^{-K_e \cdot t}$$ Equation (14)

And a semi-logarithmic plot of *LnJ*$_{ioh}$ versus time therefore yields a straight line, the slope of which is - K_e:

$$\ln J_{ioh} = \ln(Z \cdot C_0) - K_e \cdot t$$ Equation (15)

K_e was also estimated after calibration of iohexol's iontophoretic extraction flux (J_{ioh}) with that of a potential internal standard candidate (J_{IS}, either sodium or potassium), simultaneously extracted with iohexol:

$$\ln(J_{ioh}/J_{IS}) = \ln Z' \cdot C_p = \ln(Z' \cdot C_0) - K_e \cdot t$$ Equation (16)

Where $Z' = Z \cdot J_{IS}$ and J_{IS} is expected to be constant owing to the constant systemic concentration of the internal standard.

A.5.2 Calculation of iohexol's clearance (Cl) and *GFR*

Once the elimination rate constant is known, iohexol clearance (Cl) can be estimated assuming a value for its volume of distribution (V_d, see below for methods of determination), and corrected according to the Brøchner-Mortensen formula [6, 7, 23-25]. The subject's *GFR*, indexed to body surface area (BSA), is equivalent to the corrected clearance of iohexol (Cl_{corr}) normalised to 1.73 m^2 (the body surface area of an average adult):

$$GFR = Cl_{corr} \times \left[\frac{1.73}{BSA_{patient}}\right]$$ Equation (17)

$$= [(0.990778 \times Cl) - (0.001218 \times Cl^2)] \times \left[\frac{1.73}{BSA_{patient}}\right]$$

Where $Cl = K_e \cdot V_d$. The volume of distribution was calculated using one of the following methods:

Slope-only methods

The volume of distribution of iohexol is equal to the extracellular volume (*ECV*) [7, 15-19], except for oedematous patients, premature babies and in other particular disease states. Two approaches can be used to estimate V_d:

1) *"Theoretical approach":* The *ECV* of an average adult (*BSA* 1.73 m^2) is approximately 13.5 L (approximately 20% of body weight) and *GFR* is conventionally indexed to a reference *BSA* of an average adult. It follows that 13.5 L could be used directly as iohexol's V_d already normalised to a *BSA* of an average adult [43, 44]. It should be noted though that children up to a certain age have an *ECV* that tends to be much higher than that of adults (>20% of body weight) [45].

2) *"Empirical approach":* Formulae, which link experimentally determined V_d of iohexol to the height and/or weight of the patient, have been derived for different population groups (male, female, adults, and children) [46-48]. The formulae selected here (equation 18) is based on findings from 100 infants and children with an average age of 6 ± 1 years (range: 2 days - 14 years) [47]. The empirical relationship was made after determination of iohexol's V_d from the marker's concentrations determined from two blood samples taken at 3 and 4 hours post-bolus injection of iohexol.

$$V_d(ml) = 231 \cdot Weight\ (kg) + 1215$$ Equation (18)

Slope-intercept method

$$V_d = \frac{Dose}{C_0}$$

<div align="right">Equation (19)</div>

Where *Dose* is the amount of iohexol administered to the subject and C_0 is estimated from blood sampling data by re-arrangement of equations 11 and 12, so that:

$$\ln C_0 = \frac{\ln C_{p,t_1} + \ln C_{p,t_2} + K_e \cdot (t_1 + t_2)}{2}$$

<div align="right">Equation (20)</div>

C_0 may also be estimated from iohexol's reverse iontophoretic extraction data using the extrapolated intercepts of the linear LnJ_t or $Ln(J_{ioh}/J_{IS})$ data to $t = 0$ (based on equations 14 and 16, respectively). However, this requires prior knowledge of the Z and Z' values, respectively.

B. Results and discussion

This study examined the potential use of reverse iontophoresis as a non-invasive sampling tool for iohexol and was compared to the reference blood sampling method currently adopted in clinical practice.

Iohexol was successfully extracted by transdermal iontophoresis. The blood concentrations of the marker and its iontophoretic extraction fluxes are presented semi-logarithmically in Figure 9 as a function of time post-injection. All extraction fluxes correspond to a current intensity of 0.5 mA except in subject 3 for whom the applied current was lowered to 0.3 mA as from the 5th minute post-current initiation.
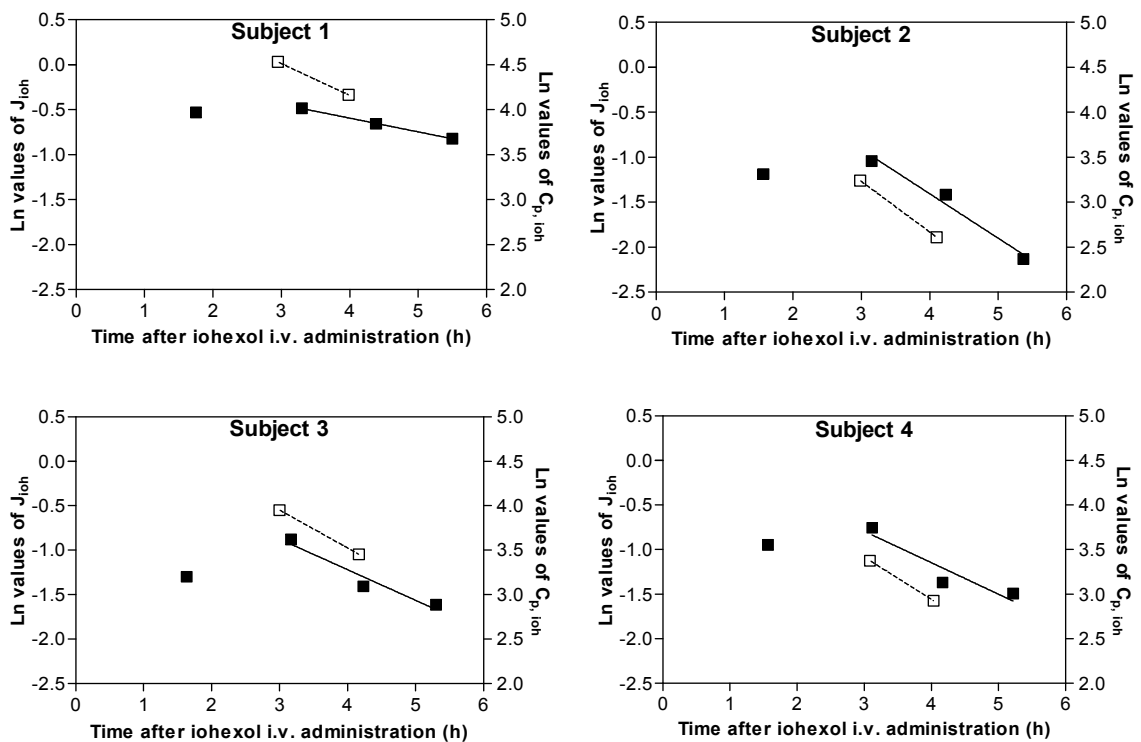
Figure 9: Iohexol transdermal iontophoretic extraction fluxes (J_{ioh}, µg/h, filled squares) and its blood concentrations ($C_{p,ioh}$, µg/ml, open squares) as a function of time post-injection. The blood concentrations of iohexol are plotted at the exact times of blood sampling; whereas the transdermal extraction fluxes are plotted at the midpoint of the respective extraction interval. The regression lines are also shown for both sampling techniques. Current applied was 0.5 mA in all subjects except participant 3 for whom it was 0.3 mA.

Sodium and potassium were evaluated as possible internal standard candidates, for the calibration of iohexol's extraction fluxes. These ions are usually present in the body at reasonably constant values; 125-145 mM for sodium and 3.4-4.7 mM for potassium. Both cations are extracted with iohexol to the cathode. Figure 10 shows the measured extraction fluxes in the *in vivo* experiments. Sodium extraction rates (expressed as mean ± SD) measured in the first interval (361 ± 22 µg/h.mA) were significantly lower than the subsequent values (544 ± 123 µg/h.mA); while potassium fluxes showed no statistical difference at any of the sampling intervals (mean value: 206 ± 38 µg/h.mA). Extraction rates of sodium and potassium were more or less in agreement with previous *in vivo* studies [49, 50]. High variability was, however, observed with coefficients of variation (*CV*) of 23 % and 19% for sodium and potassium, respectively. It is not entirely clear as to why such high variability was observed considering that the systemic levels of these cations should be constant. In addition, the high mobility together with the high systemic concentration of sodium relative to the other competing ions imply that the iontophoretic extraction rates of sodium should be insensitive to variations in its systemic concentration; and on the contrary to the present study, previous *in vivo* research in adults showed a *CV* of less than 10 % [49, 50]. Potassium, however, demonstrated high variation [50] and it was suggested by the authors that iontophoresis interferes with the concentration gradient of potassium, which exists
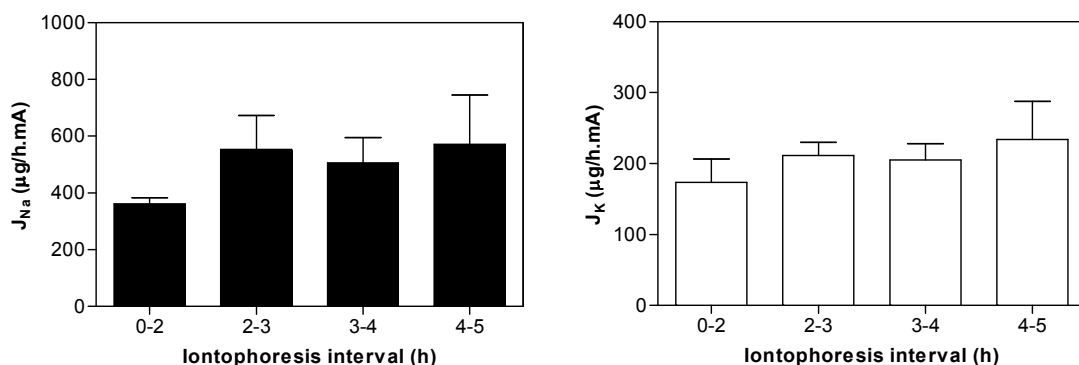

Figure 10: Iontophoretic extraction fluxes of sodium and potassium (J_{Na} and J_{K}, expressed as mean ± SD) at each sampling interval. Extraction fluxes of sodium measured in the first interval are statistically different from the subsequent values. Differences in extraction fluxes of potassium showed no statistical significance.

naturally in the epidermis [51], and as a result, the skin's continuous attempts to restore the concentration gradient might have been the underlying cause for the variability of data observed.

It is worth noting that measurement errors were potentially present in the design of this study because the patches employed are originally developed for drug delivery rather than as collection devices for extracted analytes. The cathode compartment, where iohexol, sodium, and potassium were sampled, is composed of gel polymers. Upon removal of the cathodal patch, some gel adherent to the skin was left on the application site and not all of the reverse iontophoretically extracted analytes were recovered in the patch.

B.1 Elimination rate constant of iohexol

First of all, data presented in Figure 9 show that, after a period of ≤ 2 hours of current application starting 0.5 hour post-intravenous injection of the marker, iohexol extraction fluxes (expressed semi-logarithmically) decreased linearly with time ($r^2 \geq 0.87$). This is in line with the expected exponential decline in iohexol concentration present in the subdermal (interstitial) fluid, from which the marker is reverse iontophoretically extracted from.

Secondly, following a bolus injection of iohexol, 2 − 3 hours are required for the marker to distribute fully across its volume, known to be the extracellular fluid volume (plasma + ISF). During this time, the concentration of iohexol in ISF increases from zero, and the concentration in plasma decreases from the highest concentration, at time = 0. At the point of equilibrium (i.e. 2 − 3 hours), there is no net movement of iohexol between the two compartments (plasma and ISF) and the average concentration of iohexol in ISF is reported to be closely similar to that in the plasma [3, 6, 52, 53]. Thereafter, due to the continuous first-order elimination of plasma iohexol by glomerular filtration, the concentration of iohexol in ISF is expected to 'track' the concentration in the plasma but be, at any time point, somewhat greater by a proportion that would depend on the *GFR*.

The preceding information in the earlier two paragraphs lead to the following hypothesis: transdermal iontophoretic sampling of iohexol, once steady iontophoretic extraction was achieved, was sensitive to the first order elimination of iohexol, after distribution of the administered dose reached equilibrium. Hence, the elimination rate constant of iohexol (K_e) for each subject was calculated according to equation (13) for the reference method, blood sampling, and equation (15) for the non-invasive alternative method, skin sampling. The results shown in Table 6 indicate that, except for the first subject, K_e values determined from reverse iontophoresis agree well with the blood sampling data. It has to be acknowledged that the reference method used in this study relied on two blood samples only in the estimation of the elimination rate constant. It follows that in the event of a measurement error in one of the data points, K_e could be significantly altered and precision of the "true" reference measurements is limited.

Table 6 also shows K_e values, determined according to equation (16), of iohexol's iontophoretic extraction flux data calibrated with those of potential internal standard candidates (either sodium or potassium). Although the number of subjects is too small for any distinct conclusions to be made, estimation of K_e after

Table 6: Elimination rate constants (h^{-1}, expressed as absolute values (blood sampling) or best-fit estimate ± SE (skin sampling)) according to equations (13), (15) and (16). Numbers in brackets represent the ratios of the elimination rate constants estimated from the reference blood sampling and skin sampling.

Subject / Technique	1	2	3	4
Blood sampling	0.35	0.56	0.43	0.48
Skin sampling	0.15 ± 0.003 (2.33)	0.49 ± 0.08 (1.14)	0.35 ± 0.09 (1.23)	0.35 ± 0.14 (1.37)
Skin sampling: Normalised with Na$^+$	0.18 ± 0.09 (1.94)	0.51 ± 0.07 (1.10)	0.42 ± 0.06 (1.02)	0.27 ± 0.16 (1.78)
Skin sampling: Normalised with K$^+$	0.19 ± 0.03 (1.84)	0.47 ± 0.1 (1.19)	0.52 ± 0.07 (0.83)	0.33 ± 0.18 (1.46)

internal standard normalisation may offer slightly more precision to the iontophoretic extraction method. Inaccuracies arising from experimental errors will be apparent in the extraction fluxes of the internal standards because their fluxes are anticipated to be constant, and normalisation of iohexol's extraction fluxes may, therefore, minimise measurement errors. Such suppositions require further validation in a larger study.

In general, K_e estimated by skin sampling were consistently lower than those calculated from blood sampling. The significance of such differences cannot be appropriately tested owing to the small number of subjects recruited in the study. When interpreting iontophoretic extraction data, it must always be remembered that sampling is from the interstitial fluid and not from the blood. For example, it was found that the response of extraction fluxes of glucose to increased blood concentration is delayed due to a physiological lag which exists in glucose levels in the interstitial fluid compared to blood concentrations at the same time [49, 54, 55]. For iohexol, the rate at which the marker is cleared from the plasma, after distribution reached equilibrium, should be reflected by the same rate of change in iohexol levels in the interstitial fluid regardless of whether the concentrations of iohexol in the interstitial fluid are different from those in the blood.

B.2 Estimation of *GFR* from the two sampling approaches

GFR is best estimated with multiple blood samples whereby a complete profiling of iohexol's plasma disappearance over time provides an accurate estimation of the marker's clearance. In practice, however, multiple sampling procedures are unattractive to both patients (and especially children) and the medical staff. It is for this reason that simplified models have been introduced where a single-compartment assumption is made and only the elimination phase of iohexol's plasma concentration profile is considered. As a result, the number of blood samples is reduced to 2 – 4 samples. Some research groups even suggest that only 1 blood sample may be sufficient. The reference, blood sampling, method in this study relied upon 2 blood samples taken approximately 3 and 4 hours after iohexol intravenous administration. *GFR* was determined from both skin and blood

sampling data using the slope-only and slope-intercept methods and the results are presented in Figure 11. Except for subject 1, estimation of *GFR* using the slope-only methods produced similar measurements between skin and blood sampling techniques. Obviously, the same differences observed in K_e values were translated proportionally into differences in iohexol's clearance and hence to differences in *GFR*. Similarly, the drawback noted above concerning the reference method which used two blood samples only in the determination of K_e and hence *GFR* is not without risk of measurement errors.
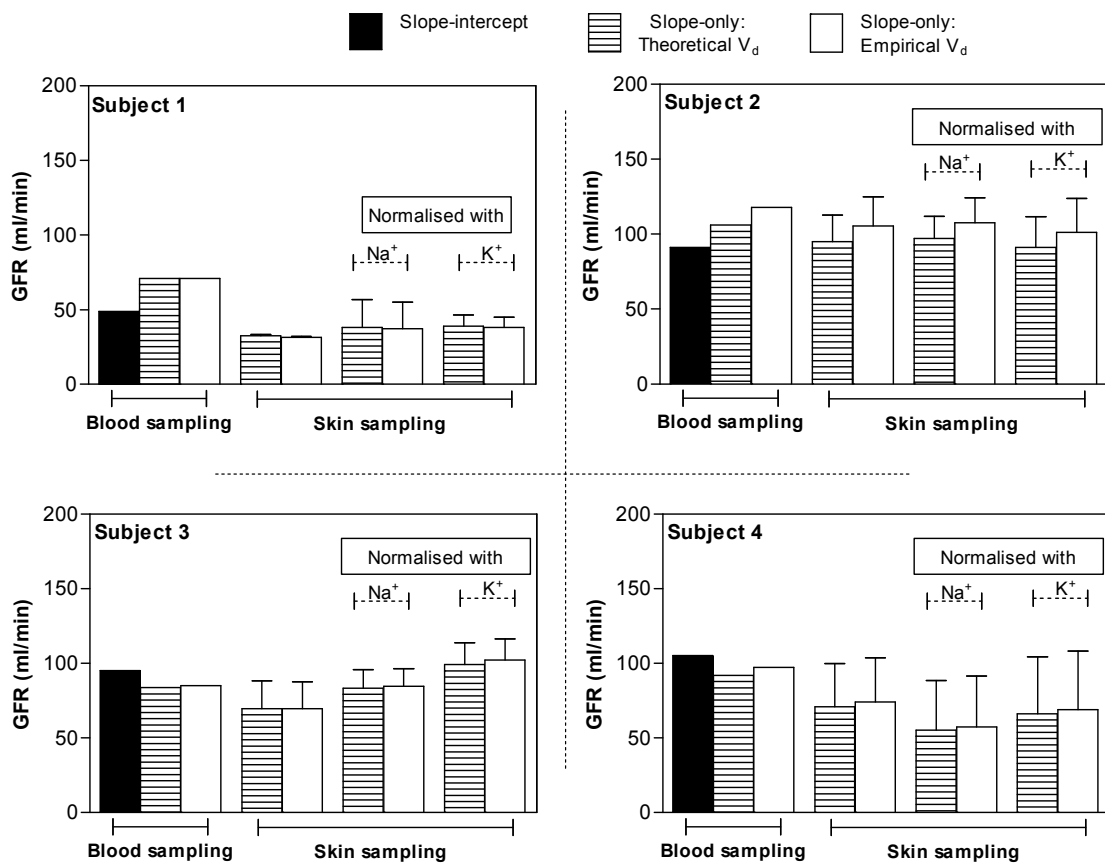
Figure 11: Calculated *GFR* values from blood and skin sampling data using the slope-only methods after determination of the volume of distribution (V_d) either theoretically or empirically. *GFR* is also calculated from blood sampling using the slope-intercept method. 3 sets of data from Skin sampling were used: A) iohexol extraction fluxes, B) iohexol fluxes normalised with sodium fluxes, and C) iohexol fluxes normalised with potassium fluxes.

Finally, it is worth acknowledging that the current practice of how *GFR* is represented has been questioned and a more ideal representation of glomerular filtration was proposed to be *GFR* indexed to the body fluid it regulates; that is ECV, rather than *GFR* normalised to BSA (which already carries its own pitfalls in children) [23, 46, 56, 57]. This alternative parameter (*GFR/ECV*) describes the *GFR* per unit *ECF* volume and closely approximates to K_e. This approach is advantageous because *GFR* is dependent on *ECV*. So, in the event of *ECV* becoming abnormal due to an independent factor (e.g., hypovolaemia) other than a kidney filtration problem, *GFR* will change to correct *ECV*. However, this change is not because of a renal deterioration but rather due to the kidneys adjusting the filtration rate to accommodate for the *ECV* changes.

B.3 Relation between iohexol's systemic concentrations and iontophoretic extraction fluxes

Iohexol is a neutral molecule and its iontophoretic extraction flux is, therefore, due to electroosmosis. The extraction flux is also expected to be linearly proportional to its blood concentration as discussed previously. To assess the relationship between iohexol's iontophoretic extraction fluxes (J_{ioh}) with corresponding blood concentrations (C_p), both direct correlation (i.e. $J_{ioh} = Z \cdot C_p$) and the use of internal standard calibration concept ($J_{ioh}/J_{IS} = Z' \cdot C_p$) were evaluated. First, data in Figure 9 were rearranged to represent extraction fluxes, after 3 and 4 hours of current passage, as a function of corresponding blood concentrations of the marker (Figure 12A). The *Z* values from each subject's data are shown in Table 7A along with a common *Z* constant representing the slope of the linear regression of data from all subjects. A reasonable correlation (r^2 0.69) was found between blood concentrations and extraction fluxes with a common *Z* constant of 11.6 ± 3.2 µl/h.mA. The Y-intercept (i.e. when $C_{p, ioh}$ = 0) of the regression line (0.46 ± 0.14 µg/h.mA) is probably indicative of the fact that iohexol's concentration in the subdermal (interstitial) fluid, from which the marker is reverse iontophoretically extracted from, is higher than the respective concentration in the plasma at any time point post-distribution equilibrium.
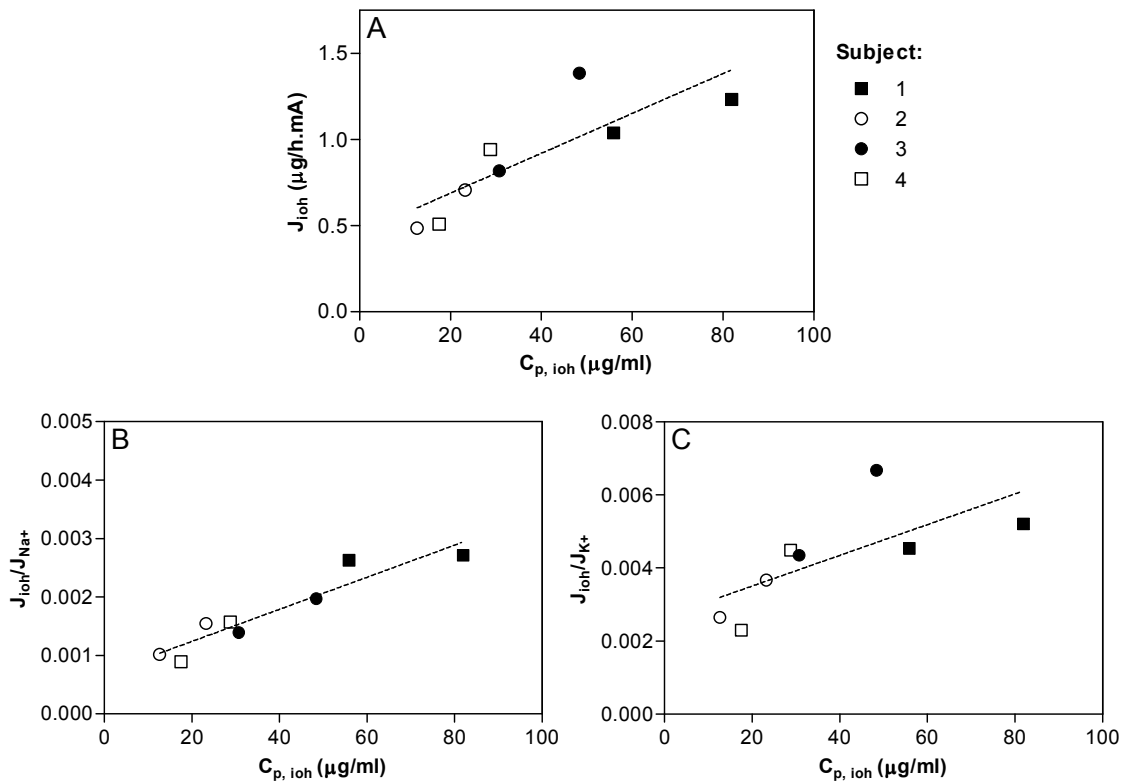
Figure 12: A) Iohexol extraction fluxes (J_{ioh}), **B)** The ratio of iohexol and sodium extraction fluxes (J_{ioh}/J_{Na}), and **B)** The ratio of iohexol and potassium extraction fluxes (J_{ioh}/J_K), as a function of corresponding iohexol blood concentrations ($C_{p,\ ioh}$). Iohexol blood concentrations used in the regressions were corrected for the respective times of the middle of each iontophoretic period.

From the limited data this study provides, it can be generally observed that individual Z measurements varied considerably between the four subjects (range 7.5 − 19.2 µl/h.mA) (Table 7A). However, extraction efficiencies were less variable within each subject; and values obtained from subjects 2 to 4, as opposed to subject 1, were relatively similar. The extraction efficiency of iohexol between participants may be different as in the case for glucose whose *in vivo* extraction exhibited both inter- and intra-subject variability [49, 58]. It may, on the other hand, follow the same pattern as urea (another neutral molecule) which demonstrated a relatively constant extraction efficiency in different human volunteers [58, 59]. Both glucose and urea are endogenous molecules and both have abundant reservoirs present in the skin [60, 61]. It was suggested that the variability in glucose extraction efficiency was attributed to the complex biochemical and metabolic processes

Table 7: Calculated values of *Z* and *Z'* parameters from (A) extraction fluxes of iohexol (J_{ioh}), (B) the ratio of iohexol and sodium extraction fluxes (J_{ioh}/J_{Na}), and (C) the ratio of iohexol and potassium extraction fluxes (J_{ioh}/J_K), as a function of corresponding blood concentrations of iohexol (C_p).

	Time point (h)	Subject 1	Subject 2	Subject 3	Subject 4	All subjects
(A): Z (µl/h.mA)	3	7.5	15.2	14.3	16.3	11.6 ± 3.2* (r^2 0.69)
J_{ioh} = Z . C_p	4	9.3	19.2	13.3	14.5	
(B): Z'_{Na} (µl/g)	3	33.1	66.5	40.7	54.5	27.4 ± 4* (r^2 0.89)
J_{ioh}/J_{Na} = Z'_{Na} . C_p	4	47.1	80.7	45.3	51.1	
(C): Z'_K (µl/g)	3	63.5	157.6	137.9	155.9	42.1 ± 17.6* (r^2 0.49)
J_{ioh}/J_K = Z'_K . C_p	4	81.2	209.6	141.5	131.2	

* Represent the slope of the pooled regression ± SE

involving glucose which happen on and within the skin and hence disturb the constancy of glucose extraction efficiency. Iohexol may be classed as an "inert" molecule; it is not metabolised, it does not bind to proteins or tissue nor enter cells, it distribute throughout the ECF volume, and finally it is excreted, by glomerular filtration, unchanged almost completely in 24 hours (i.e., no accumulation). It may be postulated, therefore, that iohexol extraction efficiency may behave more like urea than glucose. Another molecule which showed excellent constant extraction efficiency, after depletion of the skin reservoir caused by chronic use, is lithium [50]. It is, however, a positively-charged drug with a significantly smaller molecular weight and the mechanism of transport during reverse iontophoresis is mainly by electromigration rather than electroosmosis. To sum up, it is clear that in order to establish a firm association between extraction fluxes and blood concentrations of iohexol, a more rigorous validation study, with a higher number of subjects and more sampling points with shorter intervals, is necessary.

Calibration of iohexol extraction fluxes with sodium as a potential internal standard (Figure 12B) resulted in a good correlation (r^2 0.89) between extraction ratio data (J_{ioh}/J_{Na}) from all subjects and blood concentrations (common *Z'* value =

27.4 ± 4 µl/g, Table 7B) but individual Z' values were scattered between 31.1 and 80.7 µl/g. Calibration with potassium produced a lower overall correlation (r^2 0.49, Figure 12C) and a common *Z'* value of 42.1 ± 17.6 µl/g (range 63.5 − 209.6 µl/g, Table 7C). The use of sodium as an internal standard for lithium resulted in better linear correlation and allowed more precise prediction of serum concentration of lithium [50]. The same concept did not prove valid when sodium was tested as an internal standard for glucose calibration [49] and it was suggested that a better internal standard would be one that is transported by the same mechanism as glucose (i.e., electroosmosis) during reverse iontophoresis. This idea was subsequently tested using urea as a neutral internal standard [58]. Urea performed relatively well as a potential internal standard for glucose but the variability of glucose extraction due to other factors other than extraction efficiency limited the usefulness of such approach.

B.4   Local effects on the skin and participant feedback

The procedures used in the study were well tolerated and all four participants completed the trial. Only subject 3 was uncomfortable with the original current settings (0.5 mA) and the intensity was, hence, lowered to 0.3 mA as from the 5th minute post-current initiation. Mild erythema at the patch application skin sites was noticed in all subjects and was more pronounced at the cathodal site (Figure 13). The adhesive material of the cathodal patch caused mild irritation to the skin of subject number 2 with a few small red spots.

Sensation was evaluated by the universal Wong-Baker pain scale questionnaire; with 0 representing no pain and 5 demonstrating worst pain. Sensation was most felt at the beginning of the study (Pain scale ranged from 0 − 2) and diminished completely for most participants by the end of the study (Pain scale ranged from 0 − 1). The causes for the pain were from the adhesives contained in the patches and also from the tingling or itching sensation that iontophoresis tends to provoke. 3 out of 4 subjects reported more tingling/itching sensations below the anodal pad. This may be owing to the larger surface area of the anodal pad when compared to the cathodal patch (22.6 *versus* 7.2 cm^2) and therefore, as suggested

previously [62], more nociceptors (pain receptors below the skin) may have been stimulated as a result of electrical current application. Similar observations of erythema and tingling or itching sensations were reported in the literature [50, 62, 63].

All participants preferred skin sampling by iontophoresis over blood sampling. Feedback from participants and their parents included suggestions to significantly improve on the iontophoresis system to a more compact, all-in-one fully-portable device. The frequent removal of the patches was also disliked by the children due to the discomfort caused by the adhesive sides of the patches. The size of the patches was also not appropriate for the paediatric population and changes to the design would need to be addressed in future clinical studies.

Subject 1:

Before

After
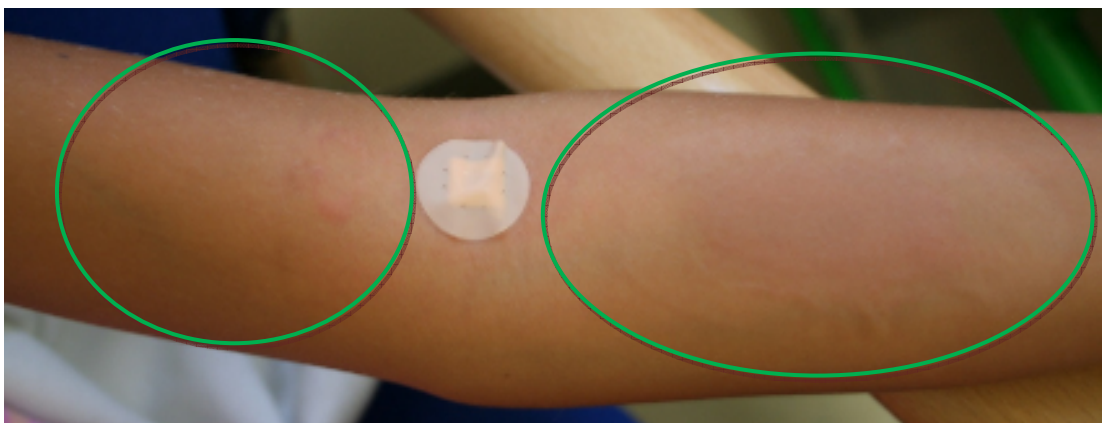
Subject 2

Before
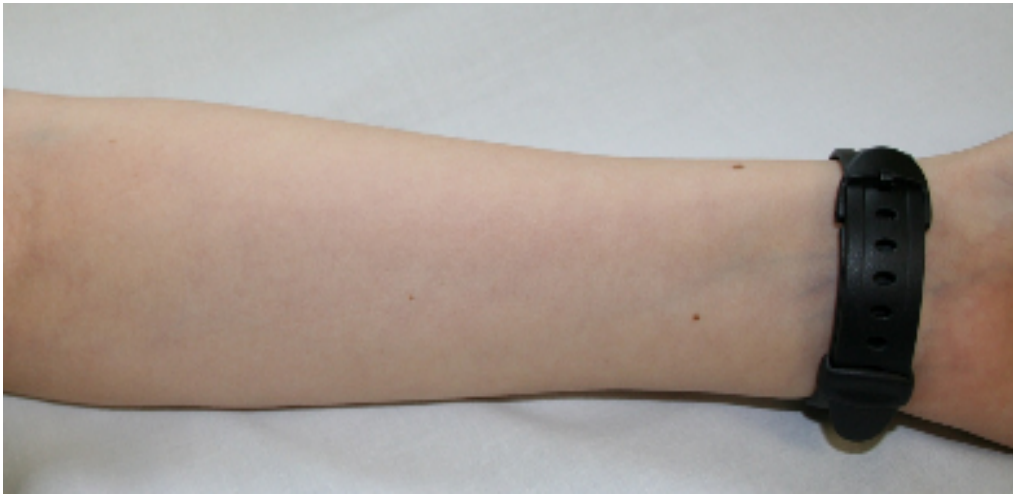
After
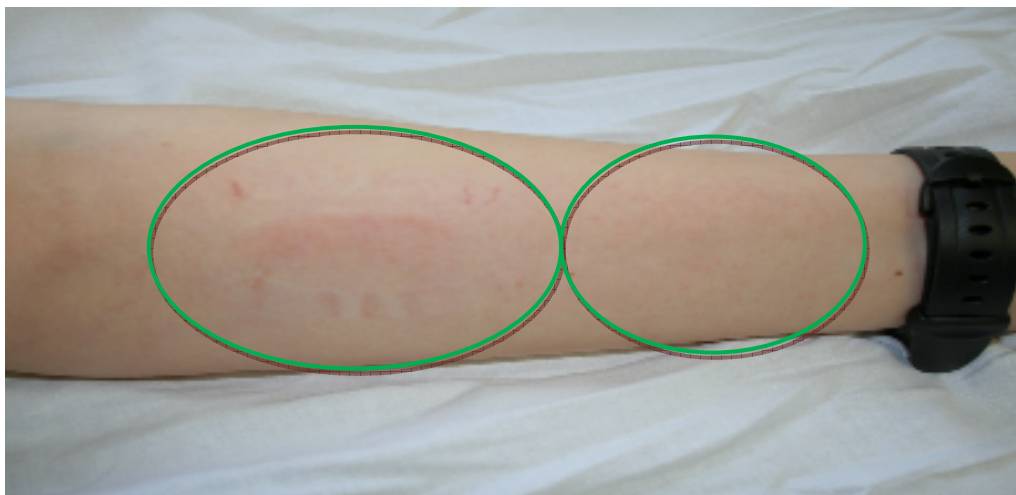
Subject 3

Before

After
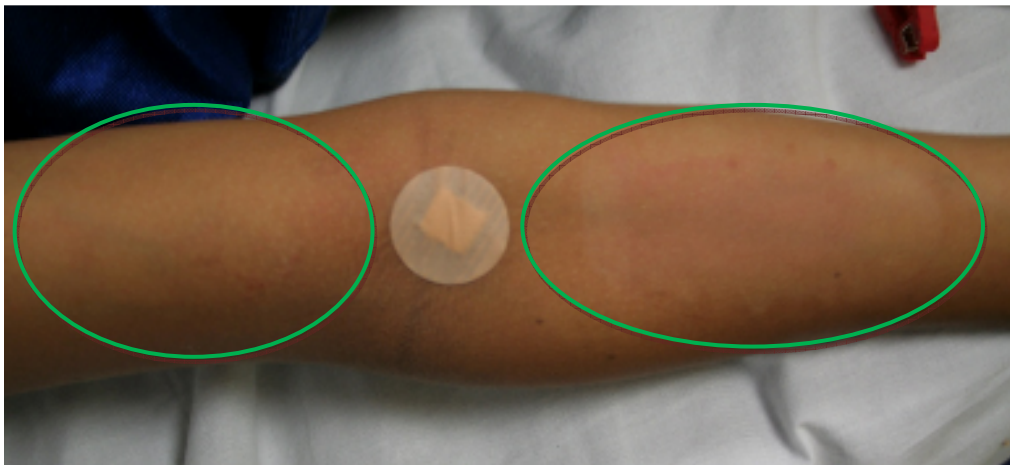
Subject 4

Before
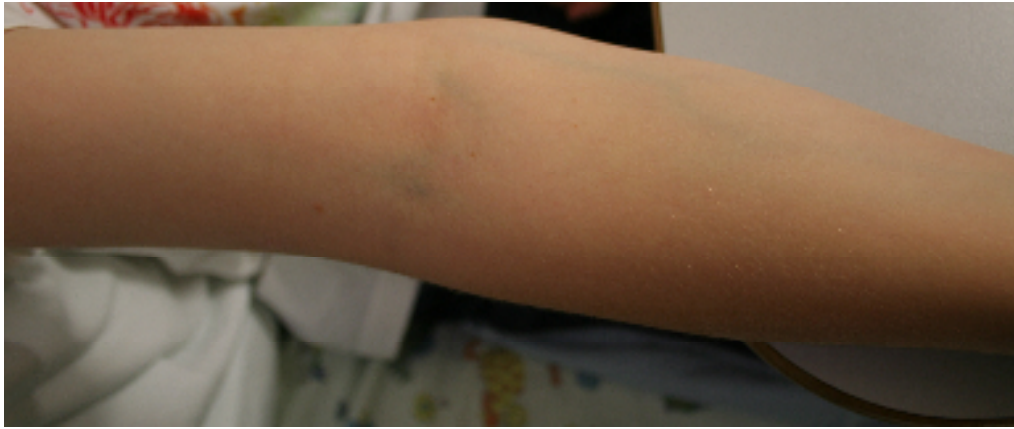
After

Figure 13: Local effects of the iontophoresis system on the skin for each subject. Each participant's arm was photographed before and immediately after the study.

4. Chapter conclusions

The overall *in vitro* results presented here demonstrated the feasibility of using transdermal reverse iontophoresis as a non-invasive sampling alternative for iohexol. After a period of lag time, iohexol extraction was linearly proportional to its subdermal concentration. Skin pre-treatment with 3 hours current passage only shortened the time taken to reach stable extraction by 1 hour. Reverse iontophoresis allowed the estimation of iohexol's pharmacokinetic parameters which were remarkably similar to those calculated using the subdermal concentration data. Hence, the potential for *GFR* determination non-invasively is a real possibility. These findings clearly warranted for an *in vivo* investigation which was subsequently performed as a proof-of-concept study and, indeed, demonstrated that iohexol sampling by transdermal reverse iontophoresis was possible. In general, estimation of the elimination rate constant of the marker, which reported directly on glomerular filtration, was similar between the reference blood sampling technique and the alternative skin sampling. Prediction of *GFR* by iontophoresis is, therefore, potentially possible and a larger study is warranted to further validate the non-invasive sampling concept proposed in the present study.

5. References

1.	Moller, E., McIntosh, J. F., and Van Slyke, D. D., *Studies of urea excretion. 2: Relationship between urine volume and the rate of urea excretion by normal adults.* J Clin Invest, 1928. **6**: p. 427-465.

2.	Schwartz, G. J., and Furth, S. L., *Glomerular filtration rate measurement and estimation in chronic kidney disease.* Pediatr Nephrol, 2007. **22**: p. 1839-1848.

3.	Frennby, B., and Gunnar, S., *Contrast media as markers of gfr.* Eur Radiol, 2002. **12**: p. 475-484.

4.	Shemesh, O., Golbetz, H., Kriss, J. P., and Myers, B. D., *Limitations of creatinine as a filtration marker in glomerulopathic patients.* Kidney Int, 1985. **28**: p. 830-838.

5.	Brandstrom, E., Grzegorczyk, A., Jacobsson, L., Friberg, P., Lindahl, A., and Aurell, M., *Gfr measurement with iohexol and 51cr-edta. A comparison of the two favoured gfr markers in europe.* Nephrol Dial Transplant, 1998. **13**: p. 1176-1182.

6.	Schwartz, G. J., Furth, S., Cole, S. R., Warady, B., and Munoz, A., *Glomerular filtration rate via plasma iohexol disappearance: Pilot study for chronic kidney disease in children.* Kidney Int, 2006. **69**: p. 2070-2077.

7.	Krutzen, E., Back, S. E., Nilsson-Ehle, I., and Nilsson-Ehle, P., *Plasma clearance of a new contrast agent, iohexol: A method for the assessment of glomerular filtration rate.* J Lab Clin Med, 1984. **104**: p. 955-961.

8.	Nilsson-Ehle, P., *Iohexol clearance for the determination of glomerular filtration rate: 15 years´ experience in clinical practice.* J Int Fed Clin Chem, 2001. **13**: p. 1-5.

9.	O'Reilly, P. H., Brooman, P. J., Martin, P. J., Pollard, A. J., Farah, N. B., and Mason, G. C., *Accuracy and reproducibility of a new contrast clearance method for the determination of glomerular filtration rate.* Br Med J, 1986. **293**: p. 234-236.

10.   Work, D. F., and Schwartz, G. J., *Estimating and measuring glomerular filtration rate in children.* Curr Opin Nephrol Hypertens, 2008. **17**: p. 320-325.

11.   Andrew, E., *Assessment of the safety of contrast media*, in *Textbook of contrast media*, Dawson, P., Cosgrove, D. O., and Grainger, R. G., Editors. 1999, Isis Medical Media: Oxford. p. 47 - 60.

12.   Gaspari, F., Perico, N., Ruggenenti, P., Mosconi, L., Amuchastegui, C. S., Guerini, E., Daina, E., and Remuzzi, G., *Plasma-clearance of nonradioactive iohexol as a measure of glomerular-filtration rate.* J Am Soc Nephrol, 1995. **6**: p. 257-263.

13.   Brown, S. C. W., and O'reilly, P. H., *Iohexol clearance for the determination of glomerular-filtration rate in clinical-practice - evidence for a new gold standard.* J Urology, 1991. **146**: p. 675-679.

14.   Bourin, M., Jolliet, P., and Ballereau, F., *An overview of the clinical pharmacokinetics of x-ray contrast media.* Clin Pharmacokinet, 1997. **32**: p. 180-193.

15.   Edelson J, S. D., Palace G. , *Pharmacokinetics of iohexol, a new nonionic radiocontrast agent, in humans.* Journal of Pharmaceutical Sciences, 1984. **73**: p. 993-995.

16.   Olsson, B., Aulie, A., Sveen, K., and Andrew, E., *Human pharmacokinetics of iohexol. A new nonionic contrast medium.* Invest Radiol, 1983. **18**: p. 177-182.

17.   Zdolsek, J. H., Lisander, B., and Hahn, R. G., *Measuring the size of the extracellular fluid space using bromide, iohexol, and sodium dilution.* Anesth Analg, 2005. **101**: p. 1770-1777.

18.   Rahn, K. H., Heidenreich, S., and Bruckner, D., *How to assess glomerular function and damage in humans.* J Hypertens, 1999. **17**: p. 309-317.

19.   Hartwig, P., Mutzel, W., and Taenzer, V., *Pharmacokinetics of iohexol, iopamidol, iopromide, and iosimide compared with meglumine diatrizoate.* Fortschr Geb Rontgenstrahlen Nuklearmed Erganzungsbd, 1989. **128**: p. 220-223.

20.   Zdolsek, H. J., Lisander, B., Jones, A. W., and Sjoberg, F., *Albumin supplementation during the first week after a burn does not mobilise tissue oedema in humans.* Intens Care Med, 2001. **27**: p. 844-852.

21.   Johnsson, E., Attman, P. O., Samuelsson, O., and Haraldsson, B., *Improved clearance of iohexol with longer haemodialysis despite similar kt/v for urea.* Nephrol Dial Transplant, 1999. **14**: p. 2407-2412.

22.   Stake, G., Monn, E., Rootwelt, K., and Monclair, T., *The clearance of iohexol as a measure of the glomerular filtration rate in children with chronic renal failure.* Scand J Clin Lab Inv, 1991. **51**: p. 729-734.

23.   Peters, A., *The kinetic basis of glomerular filtration rate measurement and new concepts of indexation to body size.* Eur J Nucl Med Mol I, 2004. **31**: p. 137-149.

24.   Brochner-Mortensen, J., *A simple method for the determination of glomerular filtration rate.* Scand J Clin Lab Invest, 1972. **30**: p. 271-274.

25.   Brochner-Mortensen, J., Haahr, J., and Christoffersen, J., *A simple method for accurate assessment of the glomerular filtration rate in children.* Scand J Clin Lab Invest, 1974. **33**: p. 140-143.

26.   Cummings, E. A., Reid, G. J., Finley, G. A., McGrath, P. J., and Ritchie, J. A., *Prevalence and source of pain in pediatric inpatients.* Pain, 1996. **68**: p. 25-31.

27.   McMurtry, C. M., *Needle and dread: Is it just a little poke? A call for implementation of evidence-based policies for the management of needle pain in clinical settings.* Paediatr Child Health, 2007. **12**: p. 101-102.

28.   Sterner, G., Frennby, B., Mansson, S., Nyman, U., Van Westen, D., and Almen, T., *Determining 'true' glomerular filtration rate in healthy adults using infusion of inulin and comparing it with values obtained using other clearance techniques or prediction equations.* Scand J Urol Nephrol, 2008. **42**: p. 278-285.

29.   Farthing, D., Sica, D. A., Fakhry, I., Larus, T., Ghosh, S., Farthing, C., Vranian, M., and Gehr, T., *Simple hplc-uv method for determination of iohexol, iothalamate,*

p-aminohippuric acid and n-acetyl-p-aminohippuric acid in human plasma and urine with erpf, gfr and erpf/gfr ratio determination using colorimetric analysis. J Chromatogr B, 2005. **826**: p. 267-272.

30.   Burnette, R. R., and Ongpipattanakul, B., *Characterization of the permselective properties of excised human skin during iontophoresis.* J Pharm Sci, 1987. **76**: p. 765-773.

31.   Sieg, A., Guy, R. H., and Delgado-Charro, M. B. A., *Reverse iontophoresis for noninvasive glucose monitoring: The internal standard concept.* J Pharm Sci, 2003. **92**: p. 2295-2302.

32.   Wascotte, V., Delgado-Charro, M., Rozet, E., Wallemacq, P., Hubert, P., Guy, R., and Préat, V., *Monitoring of urea and potassium by reverse iontophoresis in vitro.* Pharm Res, 2007.

33.   Rao, G., Glikfeld, P., and Guy, R. H., *Reverse iontophoresis - development of a noninvasive approach for glucose monitoring.* Pharm Res, 1993. **10**: p. 1751-1755.

34.   Merino, V., Lopez, A., Hochstrasser, D., and Guy, R. H., *Noninvasive sampling of phenylalanine by reverse iontophoresis.* J Control Release, 1999. **61**: p. 65-69.

35.   Leboulanger, B., Guy, R. H., and Delgado-Charro, M. B., *Non-invasive monitoring of phenytoin by reverse iontophoresis.* Eur J Pharm Sci, 2004. **22**: p. 427-433.

36.   Sontum, P. C., Christiansen, C., Kasparkova, V., and Skotland, T., *Evidence against molecular aggregates in concentrated solutions of x-ray contrast media.* Int J Pharm, 1998. **169**: p. 203-212.

37.   Falk, B., Garramone, S., and Shivkumar, S., *Diffusion coefficient of paracetamol in a chitosan hydrogel.* Mater Lett, 2004. **58**: p. 3261-3265.

38.   Ruddy, S. B., and Hadzija, B. W., *Iontophoretic permeability of polyethylene glycols through hairless rat skin: Application of hydrodynamic theory for hindered transport through liquid-filled pores.* Drug Des Discov, 1992. **8**: p. 207-224.

39.   Yoshida, N. H., and Roberts, M. S., *Solute molecular-size and transdermal iontophoresis across excised human skin.* J Control Release, 1993. **25**: p. 177-195.

40.   Leboulanger, B., Fathi, M., Guy, R. H., and Delgado-Charro, M. B., *Reverse iontophoresis as a noninvasive tool for lithium monitoring and pharmacokinetic profiling.* Pharm Res, 2004. **21**: p. 1214-1222.

41.   Wong, D. L., and Baker, C. M., *Pain in children: Comparison of assessment scales.* Pediatr Nurs, 1988. **14**: p. 9-17.

42.   Sylvestre, J. P., Guy, R. H., and Delgado-Charro, M. B., *In vitro optimization of dexamethasone phosphate delivery by iontophoresis.* Phys Ther, 2008. **88**: p. 1177-1185.

43.   Peters, A. M., Henderson, B. L., and Lui, D., *Comparison between terminal slope rate constant and "Slope/intercept" As measures of glomerular filtration rate using the single-compartment simplification.* Eur J Nucl Med, 2001. **28**: p. 320-326.

44.   Bird, N. J., Peters, C., Michell, A. R., and Peters, A. M., *Comparison between slope-intercept and slope-only techniques for measuring glomerular filtration rate: Use of two independent markers and an independent arbiter.* Nucl Med Commun, 2007. **28**: p. 711-718.

45.   Flynn, M. A., Hanna, F. M., and Lutz, R. N., *Estimation of body water compartments of preschool children. I. Normal children.* Am J Clin Nutr, 1967. **20**: p. 1125-1128.

46.   Bird, N. J., Henderson, B. L., Lui, D., Ballinger, J. R., and Peters, A. M., *Indexing glomerular filtration rate to suit children.* J Nucl Med, 2003. **44**: p. 1037-1043.

47.   Stake, G., and Monclair, T., *A single plasma sample method for estimation of the glomerular filtration rate in infants and children using iohexol, 1: Establishment of a body weight-related formula for the distribution volume of iohexol.* Scand J Clin Lab Invest, 1991. **51**: p. 335-342.

48.   Gaspari, F., Guerini, E., Perico, N., Mosconi, L., Ruggenenti, P., and Remuzzi, G., *Glomerular filtration rate determined from a single plasma sample after intravenous iohexol injection: Is it reliable?* J Am Soc Nephrol, 1996. **7**: p. 2689-2693.

49.   Sieg, A., Guy, R. H., and Delgado-Charro, M. B., *Noninvasive glucose monitoring by reverse iontophoresis in vivo: Application of the internal standard concept.* Clin Chem, 2004. **50**: p. 1383-1390.

50.   Leboulanger, B., Aubry, J. M., Bondolfi, G., Guy, R. H., and Delgado-Charro, M. B., *Lithium monitoring by reverse iontophoresis in vivo.* Clin Chem, 2004. **50**: p. 2091-2100.

51.   Denda, M., Hosoi, J., and Asida, Y., *Visual imaging of ion distribution in human epidermis.* Biochem Biophys Res Commun, 2000. **272**: p. 134-137.

52.   Tauber, U., Mutzel, W., and Schulze, P. E., *Whole body autoradiographic distribution studies on nonionic x-ray contrast agents in pregnant rats.* Fortschr Geb Rontgenstrahlen Nuklearmed Erganzungsbd, 1989. **128**: p. 215-219.

53.   Dawson, P., *Pharmacokinetics of water-soluble iodinated x-ray contrast agent*, in *Textbook of contrast media*, Dawson, P., Cosgrove, D. O., and Grainger, R. G., Editors. 1999, Isis Medical Media: Oxford. p. 61 - 74.

54.   Aussedat, B., Dupire-Angel, M., Gifford, R., Klein, J. C., Wilson, G. S., and Reach, G., *Interstitial glucose concentration and glycemia: Implications for continuous subcutaneous glucose monitoring.* Am J Physiol Endocrinol Metab, 2000. **278**: p. E716-728.

55.   Kulcu, E., Tamada, J. A., Reach, G., Potts, R. O., and Lesho, M. J., *Physiological differences between interstitial glucose and blood glucose measured in human subjects.* Diabetes Care, 2003. **26**: p. 2405-2409.

56.   Peters, A. M., Henderson, B. L., and Lui, D., *Indexed glomerular filtration rate as a function of age and body size.* Clin Sci, 2000. **98**: p. 439-444.

57.   Peters, A. M., *Expressing glomerular filtration rate in terms of extracellular fluid volume.* Nephrol Dial Transplant, 1992. **7**: p. 205-210.

58.   Sieg, A., Guy, R. H., and Delgado-Charro, M. B., *Simultaneous extraction of urea and glucose by reverse iontophoresis in vivo.* Pharm Res, 2004. **21**: p. 1805-1810.

59.   Wascotte, V., Rozet, E., Salvaterra, A., Hubert, P., Jadoul, M., Guy, R. H., and Preat, V., *Non-invasive diagnosis and monitoring of chronic kidney disease by reverse iontophoresis of urea in vivo.* Eur J Pharm Biopharm, 2008. **69**: p. 1077-1082.

60.   Wascotte, V., Caspers, P., de Sterke, J., Jadoul, M., Guy, R. H., and Preat, V., *Assessment of the "Skin reservoir" Of urea by confocal raman microspectroscopy and reverse iontophoresis in vivo.* Pharm Res, 2007. **24**: p. 1897-1901.

61.   Sieg, A., Guy, R. H., and Delgado-Charro, M. B., *Noninvasive and minimally invasive methods for transdermal glucose monitoring.* Diabetes Technol Ther, 2005. **7**: p. 174-197.

62.   Rao, G., Guy, R. H., Glikfeld, P., LaCourse, W. R., Leung, L., Tamada, J., Potts, R. O., and Azimi, N., *Reverse iontophoresis: Noninvasive glucose monitoring in vivo in humans.* Pharm Res, 1995. **12**: p. 1869-1873.

63.   Ledger, P. W., *Skin biological issues in electrically enhanced transdermal delivery.* Adv Drug Del Rev, 1992. **9**: p. 289-307.

Chapter 3

Transdermal iontophoretic delivery of Ranitidine: An opportunity in paediatric drug therapy

Chapter summary

The objective of this study was to examine whether transdermal iontophoresis might be useful for the delivery of ranitidine hydrochloride to children. Constant, direct current, anodal iontophoresis of ranitidine was performed *in vitro* across dermatomed pig skin. First, the effect of donor vehicle, current intensity, and drug concentration were examined using aqueous solutions. It was found that drug delivery was higher at pH 7 (donor vehicle: 5 mM Tris) than pH 5.6 (donor vehicle: water). In the presence of low levels of competing background electrolyte (5 mM Tris), ranitidine delivery increased linearly with applied current but was independent of the donor drug concentration. The second part of the study evaluated the use of two Pluronic® F-127 gels as potential vehicles for the delivery of ranitidine. The gel formulations were characterised by apparent viscosity, conductivity and passive permeation measurements. Iontophoretic delivery of ranitidine was only slightly affected when delivered from the gel formulations relative to aqueous solutions; and 30 %w/w F-127 gel was more viscous than 20 %w/w formulation. It was found that paediatric therapeutic doses of ranitidine (neonates: 0.09 - 0.17 µmol/kg.h; 1 month − 12 years: 0.36 − 0.71 µmol/kg.h) could be easily achieved by transdermal iontophoresis with acceptable patch sizes (0.2 − 1.5 cm^2/kg).

1. Introduction

Ranitidine is used extensively in paediatric medicine especially in intensive care. It is prescribed in a variety of clinical indications where gastric acid reduction is necessary [1]. This includes gastro-oesophageal reflux disease, benign gastric and duodenal ulcerations, prophylaxis of acid aspiration prior to surgery, and treatment as well as prophylaxis from stress-induced gastrointestinal ulcers and consequent haemorrhage. Routes of administration include oral and intravenous delivery. Ranitidine's oral bioavailability is highly variable between paediatric subjects especially in the neonates (40 – 80 %) [2-4]. This is due to incomplete absorption of the drug from the gastro-intestinal tract as well as first-pass metabolism. The need for frequent dosing (2 - 4 times a day), due to the short half life of ranitidine (2 – 3 hours [3, 5]), and the bitter taste of the oral solution reduce child compliance. In addition, some formulations contain up to 8 % alcohol and no oral preparation is licensed for use in children under 3 years of age; parenteral delivery is only licensed for children over 6 months old [1] and has inherent pitfalls such as pain and distress, invasiveness, risk of infection, and technical difficulties.

The transdermal route can provide an alternative approach for the delivery of ranitidine. The relatively non-invasive nature of this administration method renders the application particularly attractive in paediatric medicine. Iontophoresis is an interesting option because it is possible to control delivery rates over extended periods of time. Ranitidine hydrochloride (Figure 1) is a good candidate for iontophoresis and target rates for therapeutic delivery are as follows: neonates, 0.09 - 0.17 µmol/kg.h; 1 month – 12 years: 0.36 – 0.71 µmol/kg.h). These values are equivalent to the recommended intravenous infusion rates currently used in clinical care [1]. Ranitidine has a molecular weight of 314.4 Da (free base), free water solubility and the logP (octanol/water) is reported at 0.3 [6]. Ranitidine has two basic groups with pKa values of 2.3 and 8.2 [7] and is thus present predominantly as a monovalent cation at pH values between 4 and 7. Anodal delivery of ranitidine in this pH range is therefore expected to be largely due to electromigration with electroosmosis also anticipated but making a smaller contribution.
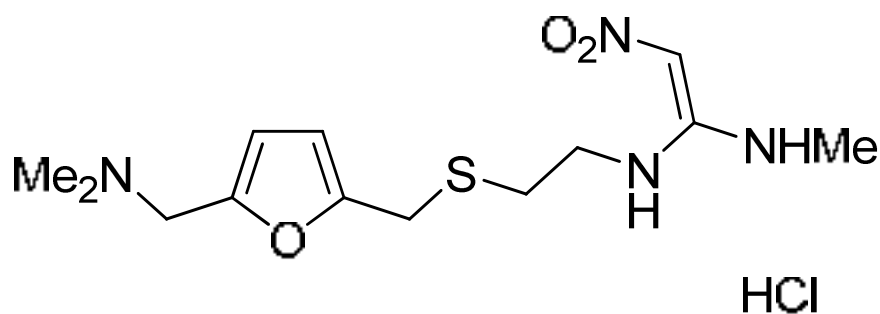
Figure 1: Chemical structure of ranitidine hydrochloride (M.W. 350.9, LogP 0.3, pKa 2.3 and 8.2).

In vitro investigations of transdermal iontophoresis, as a potential administration route for a specific drug, are performed mostly using solution-based vehicles because of easy preparation and manipulation. However, transdermal systems for clinical usage are typically semi-solid preparations. It is, therefore, important to test the *in vitro* delivery of the drug of interest from such preparations and mimic the *in vivo* situation as closely as possible. Semi-solid formulations often incorporate polymeric structures and hydrogels represent a specific example. These are attractive because while they provide the rigidity needed to firmly hold the application to the skin and prevent leakage, the presence of a high water content also provides a suitable conductive medium for iontophoresis.

Pluronic F-127, a surface active gel-forming agent, has been used frequently in percutaneous applications [8, 9]. It is composed of triblocks of polyoxyethylene-polyoxypropylene copolymers at a ratio of 70% ethylene oxide (hydrophilic) and 30% propylene oxide (hydrophobic), and with an average molecular weight between 9840 and 14600 Da [8, 10]. F-127 forms a gel by entanglement and packing of the micelles [10, 11]. The higher the concentration of the polymer or the higher the temperature, the greater the entanglement and the more rigid the gel becomes. F-127 hydrogels are favoured vehicles in transdermal iontophoresis for the following reasons: 1) The non-ionic nature of the surfactant avoids competition with the drug to carry the applied current. It also reduces potential interaction between the polymer and the drug molecules. Charged polymers have been shown

to carry electrical current to a certain extent and it was also suggested that they may bind to the ionised drug [12-15]. 2) F-127 is safe as evident in its widespread use in various pharmaceutical preparations intended for different routes of administration [8]. 3) The thermo-reversible properties of the polymer make its use as a transdermal carrier attractive. At 15 – 30 %w/w concentrations in water, F-127 exists in liquid state at low temperature (≤ 5 °C) but forms a semi-solid gel at higher temperatures (> 15 °C). These unique rheological properties offer the advantage of easy fabrication and straightforward incorporation of the electrodes. They also provide firm application on the skin contours preventing leakage from the transdermal system.

The purpose of this *in vitro* study was to investigate transdermal iontophoresis for the delivery of ranitidine to paediatric patients. The rate of input when ranitidine is administered as a continuous intravenous infusion was used as a guide to the target transdermal flux needed to achieve effective therapeutic levels. *In vitro* experiments were conducted to examine the effects of donor vehicle, drug concentration, and current intensity on the iontophoretic delivery of ranitidine from aqueous solutions. The most appropriate conditions were then adopted in gelled formulations and their performance as potential delivery systems for ranitidine was evaluated.

2. Materials and methods

2.1 Chemicals

Ranitidine hydrochloride (RAN), silver wire (99.99%), silver chloride (99.999%), and Pluronic® F-127 were purchased from Sigma Aldrich (Gillingham, UK). Tris base (α, α, α-Tris-(hydroxymethyl)-methylamine) and sodium chloride were obtained from Acros (Geel, Belgium). Acetonitrile, hydrochloric acid, glacial acetic acid, and triethylamine were provided by Fisher Scientific (Loughborough, UK). All reagents were at least analytical grade and deionised water (resistivity ≥ 18.2 MΩ.cm, Barnsted Nanopure Diamond^{TM}, Dubuque, IA) was used for the preparation of all solutions.

2.2 Skin

Fresh pig skin was obtained from a local slaughterhouse, cleaned under cold running water, and stored in a refrigerator until the following day. Abdominal skin was dermatomed (Zimmer™ Electric Dermatome, Dover, Ohio. Nominal thickness 750 µm), cut into pieces of appropriate size, wrapped individually in Parafilm™, and then kept in a freezer (-20 °C) until use. Immediately prior to the permeation experiment, the skin was thawed at room temperature for 30 minutes and visible hairs were carefully cut with scissors. The skin was then mounted directly onto the diffusion cells.

2.3 Iontophoresis

Side-by-side two-compartment diffusion cells (active transport area = 0.78 cm^2, volume = 3 ml) were utilised in all experiments. The skin was mounted between the two chambers with the epidermal side oriented towards the anode compartment. The receptor chamber always held 154 mM sodium chloride solution (unbuffered, pH ~ 6) and was magnetically stirred (Multipoint-6 stirrer, Thermo Scientific Variomag, Cole-Parmer, London, UK) at 400 rpm throughout the experiment. Anodal, direct, constant current was delivered using Ag/AgCl

electrodes and a power supply (KEPCO 1000M, Flushing, NY, USA). Hourly samples (0.5 ml) of the receptor phase were withdrawn for analysis and replaced with fresh solution. Separate passive diffusion controls (no current) were also performed.

2.3.1 Ranitidine delivery from aqueous solutions

Prior to the start of the transport study, the skin was left for 30 minutes in contact with the donor vehicle without drug, and 154 mM sodium chloride in the receptor chamber. Both compartments were then emptied and refilled with a donor solution containing ranitidine and fresh receptor solution. Experiments examined donor vehicle, drug concentration, and current intensity effects on the iontophoretic delivery of ranitidine. Specific conditions are described in Table 1.

2.3.2 Ranitidine delivery from gel formulations

Two gel formulations were prepared according to the "cold method" [16]. Solutions containing 150 mM ranitidine in 5 mM Tris (pH 7) were cooled to 3 – 5 °C under continuous gentle agitation. F-127 (at 20 and 30 %w/w) was then incorporated slowly into the solutions and resulting formulations were left stirring for 2 days to achieve complete homogeneity.

Table 1: Types of experiments performed to characterise ranitidine transdermal delivery from aqueous solutions.

	Donor vehicle	RAN conc. (mM)	pH	Current intensity (mA)	n**
Donor vehicle effect	Water	25	5.6 (unbuffered)	0.3	5
	5 mM Tris		7*		5
Current effect	5 mM Tris	50	7*	0.1	5
				0.2	4
				0.3	5
Concentration effect	5 mM Tris	25	7*	0.3	5
		50			5
		150			5
Passive diffusion	5 mM Tris	150	7*	0	3

* pH adjusted to 7 with 1 M HCl. ** number of replicates

For the permeation experiments, 3.3 grams of each formulation was introduced into the donor compartment and constant current (0.3 mA) was delivered for 6 hours. The voltage of each iontophoresis system was monitored regularly using a voltmeter (DM-51 digital multimeter, ECG®, Taiwan). All experiments were conducted in a laboratory with controlled temperature: 22.2 ± 0.9 °C, and both compartments were covered with Parafilm to avoid water evaporation. Number of replicates were 5 (iontophoresis) and 3 (passive diffusion controls).

2.4 Viscosity measurements

The apparent viscosities of the gel formulations were determined using a Bohlin rheometer (Malvern, UK) equipped with a cone-plate system. The angle of the cone was 4° and the diameter of the plate was 40 mm. Three specific shear rates were tested (0.1, 1, or 10 s^{-1}) under a gap size set at 150 mm. Readings were performed at 22.1 ± 0.2 °C and gels were allowed to equilibrate on the plate for 5 minutes before the measurements started. The viscosities of control formulations (without ranitidine) were also verified and all measurements were performed in triplicate.

2.5 Conductivity measurements

The conductivities of the gel formulations were measured using a conductimeter (T-120, Metrohm, Herisau, Switzerland, cell reference = 0.85) at 22 °C. These were compared to the conductivity of ranitidine in aqueous solution. Measurements were performed in triplicate.

2.6 Sample analysis

Quantification of ranitidine was performed by high performance liquid chromatography with UV detection (315 nm). The method was modified from a previous publication [17] and used a Jasco HPLC system comprising a PU-980 pump with an AS-1595 autosampler, a UV-975 UV-VIS detector, and a HiQ-Sil^{TM} C18 (250 x 4.6 mm, 5μm) reversed-phase column (Jasco, UK) thermostated at 25 °C. The

mobile phase (pH 3.8) consisted of a mixture of water, acetonitrile, acetic acid, and triethylamine (85:15:1.5:0.2, respectively in volume), and was pumped through the system at 1 ml/min. The validation parameters are found in Appendix (1C).

2.7 Data analysis and statistics

Data analysis and regressions were performed using Graph Pad Prism V.5.00 (Graph Pad Software Inc., CA, USA). Unless otherwise stated, data are represented as the mean ± standard deviation (SD). Transport fluxes were calculated as the amounts delivered per unit time. Comparisons made between different sets of data were assessed by either two-tailed unpaired t-test (for 2 groups) or one-way ANOVA (for > 2 groups) which was followed by Tukey's post-test. Comparison of ranitidine transdermal delivery from gel formulations relative to aqueous solution was made with two-way ANOVA followed by Bonferroni post-test. Statistical significance was set at $p < 0.05$.

The transference number (T) of ranitidine was computed from Faraday's law [18]:

$$T = \frac{J \times z \times F}{I} \qquad \text{Equation (1)}$$

Where J is the drug flux observed at 6 h, I is the current intensity applied, F is Faraday's constant, and z is the numerical value of the valence of the drug ion (= 1).

3. Results and discussion

3.1 Ranitidine delivery from aqueous solutions

The donor concentrations of ranitidine hydrochloride (25 – 150 mM) provided sufficient chloride ions for the Ag/AgCl electrochemistry at the anode. The passive diffusion flux of ranitidine from the highest donor concentration used (150 mM) was only 0.1 ± 0.04 nmol/h after 6 hours and was negligible relative to that achieved with iontophoresis.

3.1.1 Effect of donor vehicle

The first iontophoresis experiment used a donor solution containing only ranitidine hydrochloride (25 mM) in water. The pH of this unbuffered solution was around 5.6 and was low enough to ensure complete ionisation of the more basic group of ranitidine (pKa 8.2). Ranitidine was the only cation present in the donor compartment therefore resulting in the maximal iontophoretic transport possible. The flux reached 0.61 ± 0.08 μmol/h after 6 hours of current passage (Figure 2), corresponding to a transference number, calculated with equation (1), of 5.47 ± 0.67 %. The next donor vehicle examined contained 5 mM Tris buffer and the final
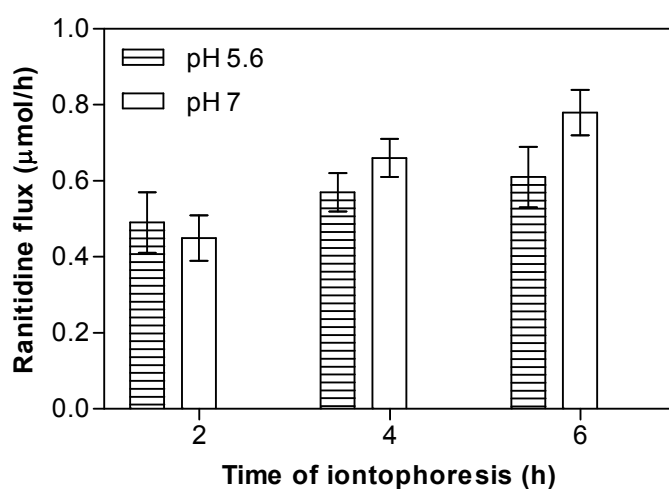
Figure 2: Ranitidine iontophoretic transport from 25 mM drug solutions of pH 5.6 (in water) and 7 (in 5 mM Tris buffer). Current applied was 0.3 mA. Data represent the mean ± SD.

pH was adjusted to 7 with HCl. Initially, the iontophoretic transport fluxes were similar to those at pH 5.6. However, from the fourth hour of iontophoresis, a significantly higher flux at pH 7 ($p < 0.05$) was found attainting 0.78 ± 0.07 μmol/h after 6 hours of current passage (Figure 2). This corresponds to a transference number of 6.95 ± 0.58 %. It follows that even though the addition of Tris introduced co-ion competition with ranitidine (4.6 mM Tris is positively charged at pH 7, pKa 8.1), the higher pH of the donor solution also increased the magnitude of both electroosmosis and electromigration. The isoelectric point of porcine skin has been reported to be approximately 4.4 [19]; above this pH, the net charge of the skin is negative. The skin is therefore more permselective to cations [18-20]. Similar findings have been previously observed for other cations. Sieg *et al.* [21] found a significant increase in the iontophoretic flux of sodium when the pH was raised from 6.3 to 7.4 (8 ± 0.3 *versus* 10.7 ± 0.7 μmol/h.cm^2). However, a further increase to pH 8.5 did not produce any difference from values obtained at pH 7.4. Wearley *et al.* [22] tested the delivery of verapamil (MW 454.6, pKa 8.9) under pulsed direct current using donor solutions containing 105 mM verapamil in acetate buffer (pH 4-6). Again, the permeation rates of this fully ionised cation were enhanced as the pH of the donor solution was increased. Another example is sumatriptan (MW 295.5, pKa 9.6), the iontophoretic transport of which was significantly higher when the donor pH was raised from 5 to 7 [23].

3.1.2 Effect of current intensity

This part of study aimed: 1) to confirm that iontophoresis provides a controllable dosing system, and 2) to check that small current intensities can deliver therapeutic levels of ranitidine. While it is accepted that a current density of up to 0.5 mA/cm^2 is usually tolerable by humans, delivering target doses with smaller currents is very desirable in children (especially neonates) to minimise discomfort. Three intensities were examined: 0.1, 0.2, and 0.3 mA, (0.13, 0.26, and 0.39 mA/cm^2) for a fixed drug donor concentration (50 mM). As expected and in agreement with Faraday's law (equation 1), an excellent linear correlation (r^2 0.97, $p < 0.0001$) was found (Figure 3) between current intensity and ranitidine's permeation across the skin. Similar examples of this well-established relation are
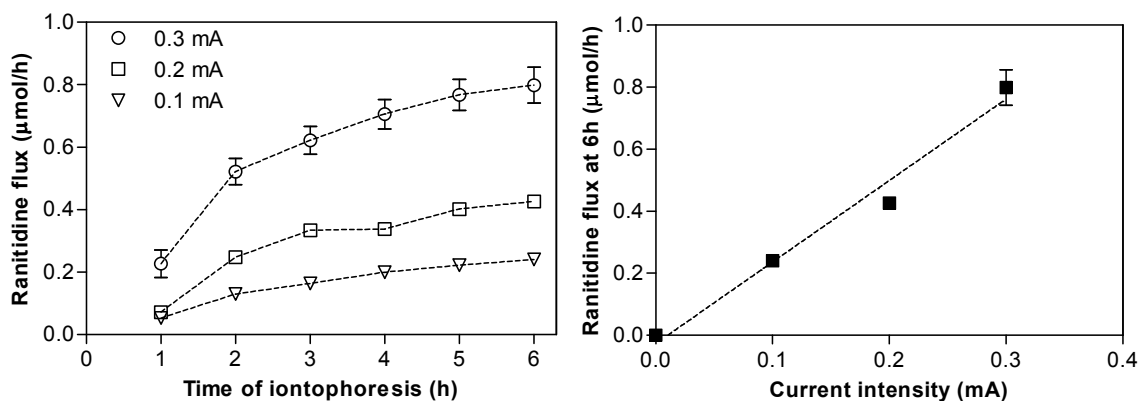
Figure 3: Delivery fluxes of ranitidine (mean ± SD) as a function of time of iontophoresis (left) and current intensity (right). Ranitidine was delivered from a 50 mM donor solution (5 mM Tris, pH 7).

found in previous publications [24-27]. The slope of the line in the right-hand panel of Figure 3 corresponds to a transference number of 7.05 ± 0.33 % (± SE); a value very similar to that previously obtained with 25 mM ranitidine in 5 mM Tris (pH 7) (6.95 ± 0.58 %, section 3.1.1). This observation is explained in the next section.

At the lowest current (i.e., 0.13 mA/cm^2), the delivery rate was 0.31 ± 0.02 μmol/h.cm^2. The recommended intravenous infusion doses of ranitidine are: neonates, 0.09 - 0.17 μmol/kg.h, and older than 1 month, 0.36 – 0.71 μmol/kg.h [1]. It follows that iontophoresis using 0.13 mA/cm^2 can deliver therapeutically effective levels of ranitidine with a patch application area (anode + cathode) ranging from only 0.6 – 1.1 cm^2/kg for neonates and 2.3 – 4.6 cm^2/kg for the older group. Obviously the use of higher current densities would significantly reduce the patch size needed to deliver the same therapeutic levels of ranitidine. Indeed, using 0.39 mA/cm^2 current density, areas of only 0.2 – 1.4 cm^2/kg would be required, a very acceptable range for transdermal delivery. Figure 4 illustrates the iontophoretic patch areas required for different groups of paediatric subjects as a function of current density applied.
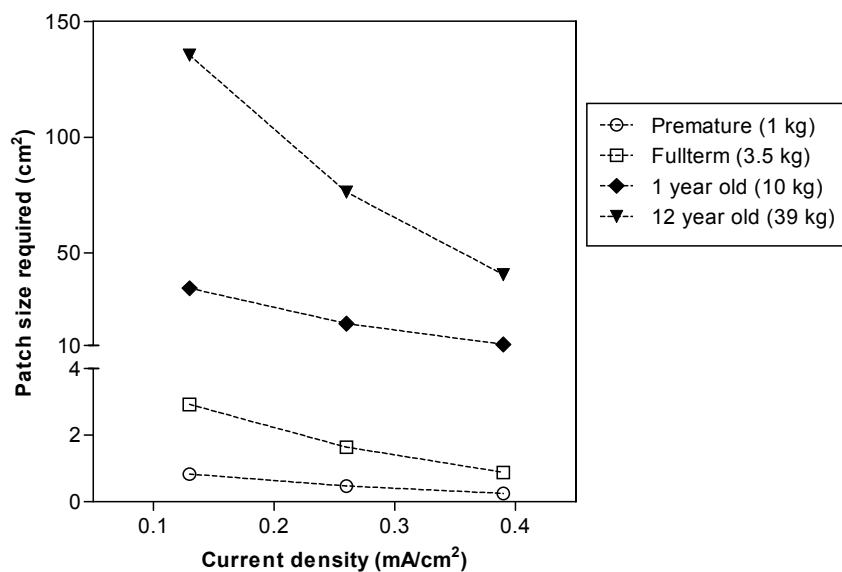
Figure 4: Estimated patch areas (anode + cathode) required to achieve therapeutic input rates of ranitidine by iontophoresis, as a function of current density applied. 4 age groups are used to illustrate the range of areas necessary in the paediatric population.

3.1.3   Effect of drug concentration

Figure 5 shows that the delivery rates achieved using three different drug concentrations (25, 50, and 150 mM) in the donor solution were not significantly different, ranging from 0.90 ± 0.10 to 0.78 ± 0.07 µmol/h. This is due to the fact that the molar fraction of ranitidine, relative to the only other competing co-ion (i.e., Tris) did not differ appreciably in the three conditions (0.84, 0.91, and 0.97 for 25, 50, and 150 mM drug concentrations, respectively).

3.2   Ranitidine delivery from gel formulations

The optimum conditions established using solution-based donor vehicles were then used to develop a gel formulation based on Pluronic F-127 (at 20 or 30 %w/w). Ranitidine was delivered from a 150 mM drug concentration in 5 mM Tris buffer (pH 7) and at 0.3 mA current intensity. The highest concentration of the drug was chosen to mitigate against any possible effects of gelation of the vehicle on the release of ranitidine.
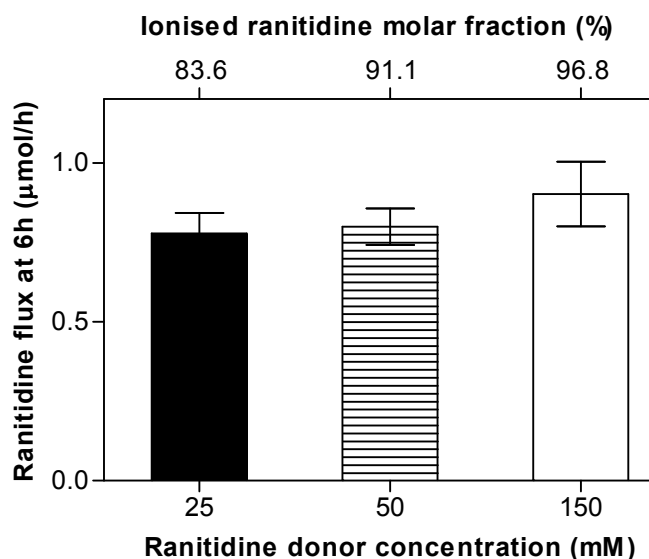
Figure 5: Ranitidine transport fluxes (6 h) as a function its donor concentration and molar fraction. Data are represented as the mean ± SD.

3.2.1 Apparent viscosity measurements

Figure 6 depicts the apparent viscosity of each gel formulation measured at 22 °C using a cone and plate rheometer. A relatively high gap size was used to avoid possible collapse of the micelle structures present in the gel formulations. As is evident in the Figure, the presence of ranitidine did not affect the apparent viscosity of the gel formulations implying that the drug did not interfere with either the micellisation or the entanglement and packing of the F-127 polymer.

Both drug-loaded gel formulations were semi-solid at 22 °C but their viscosities differed significantly. For example, when the applied shear rate was 0.1 s^{-1}, the apparent viscosity of the gel containing 20 %w/w F-127 was 863 ± 67 Pa.s; whereas for the same shear rate, the apparent viscosity of 30 %w/w F-127 gel was 5139 ± 302 Pa.s. Incorporation of 20 % F-127 formed a "soft" gel structure while 30 % produced a more rigid semi-solid consistency which is more appropriate in transdermal applications. The flow curves of the gel formulations conformed to the Ostwald-De Waele power law [28-30]: $$\eta = K \times \gamma^{n-1}$$ Equation (2)

Where η is the apparent viscosity, K is the flow consistency index, n is the power-law index, and γ is the applied shear rate. As the table in Figure 6 shows, n
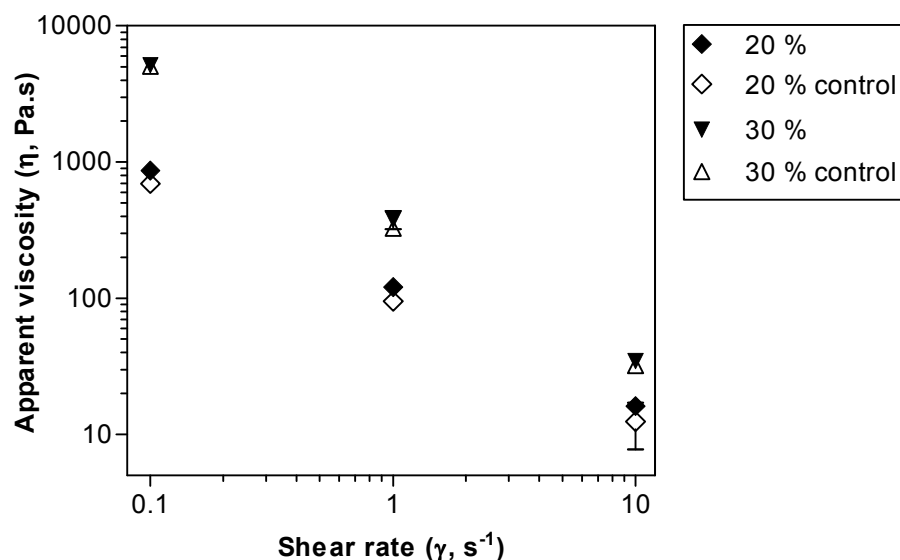
| Formulation: F-127 %w/w	r^2	K	n
20	0.999 (0.975)	119 ± 1 (91 ± 5)	0.14 ± 0.01 (0.11 ± 0.03)
30	0.998 (0.997)	405 ± 8 (375 ± 8)	-0.07 ± 0.01 (-0.1 ± 0.01)

Figure 6: Flow curves of the apparent viscosities of the gels measured at different shear rates and parameters derived from data regression using the power law relation: $\eta = K \times \gamma^{n-1}$. ($\eta$ is the apparent viscosity measured at a particular shear rate (γ). K is the flow consistency index and n is the power-law index). Values between brackets in the table indicate the control formulations (i.e., no drug).

index values of all formulations were below 1 and are indicative of pseudoplastic behaviour. The gels are shear-thinning fluids because an inverse relationship is found between the applied shear rate and the apparent viscosity. Even at high shear rates, the apparent viscosity of the gel formulations remained in the linear region of the power law. This is indicative of the stable structure of the gel formulations under the shear rates applied because the micelles which form the basis of the internal network of the gel were not perturbed.

3.2.1 Conductivity measurements

The conductivities of the donor formulations were 7.9 ± 0.1, 4.3 ± 0.03, and
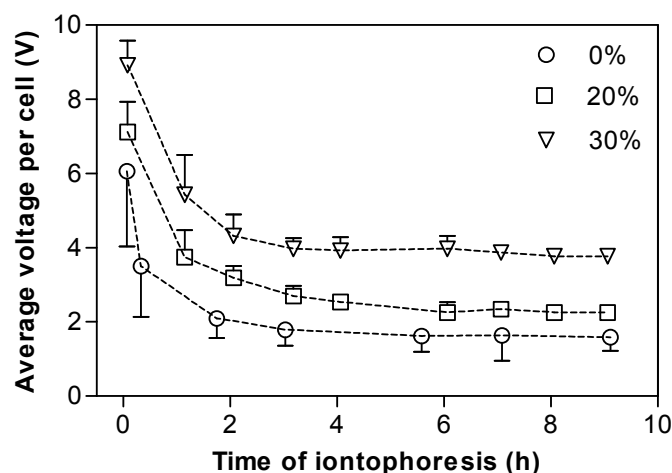
Figure 7: Average voltage measurements as a function of time of current application (0.3 mA). Data shown represent the mean ± SD.

2.9 ± 0.02 mSi/cm) for 0, 20, and 30 %w/w F-127 gels respectively. All values differed significantly (*p < 0.0001*). The viscosity of the formulation affected its conductivity indirectly as follows [31-33]: 1) the diffusivity of each ion present in the formulation is inversely dependent on the viscosity of the formulation (Stokes-Einstein relation); 2) the conductivity of the formulation is proportional to the ions' mobility; and 3) the diffusivity of the ion is directly related to its mobility (Einstein relation).

3.2.2 Voltage measurements

The voltage of each diffusion cell was monitored throughout the iontophoresis experiment (0.3 mA) because the resistance of the system as a conductive medium was expected to be higher with the gel formulations. The sources of resistance include the electrodes used, the donor and receptor vehicles, and the skin that separates both vehicles. Figure 7 describes the average voltage per cell as a function of time of iontophoresis. The voltage started at high levels for all formulations and decreased gradually until it levelled off to apparent steady values. The reduction in the voltage from the initially high values are due to the skin becoming more conductive as ions from both the donor and receptor vehicles enter and move across the skin. In agreement with the conductivity results, Figure 7 also shows that the voltage increased with higher F-127 concentration in the donor
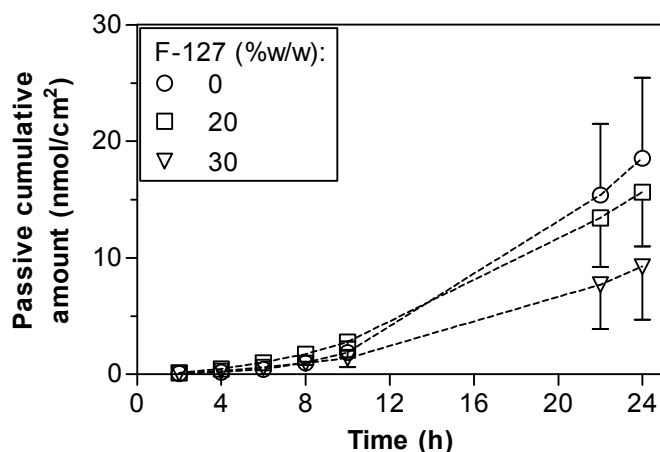
Figure 8: The passive diffusion of ranitidine both from gel formulations and liquid solution. Data are expressed as the mean ± SD.

formulation due to the higher resistance of the donor vehicle to conduct the applied current. Nevertheless, the voltage associated with 30 % gel was still acceptable and using such gel produced an efficient conductive medium for iontophoretic application.

3.2.3   Permeation studies

Figure 8 shows the passive diffusion profiles of ranitidine from donor formulations containing 0 (control), 20 and 30 %w/w of the gelling agent F-127. After 24 hours, cumulative amounts of 18.6 ± 6.9, 15.6 ± 4.7, and 9.2 ± 4.6 nmol/cm^2 of drug permeated through the skin, respectively. As suggested by previous investigators, the lower permeation rates accompanied by increasing the concentration of the gelling agent are attributed to lower release rates from the gel formulations [34-39]. Reduced release characteristics through the matrix of the gel may be because of a change in the thermodynamic activity of ranitidine in the donor formulation (higher solubility) and/or the resistance of the gel formulation to the diffusion of ranitidine through it (by either a longer diffusion path, or the higher formulation viscosity which leads to lower diffusivity of the drug (Stokes–Einstein relation [32, 33]), or both factors together). Figure 9 presents the iontophoretic delivery rates of ranitidine from the F-127 gels. The transport rates at 6 hours were 0.90 ± 0.10 (0 % F-127), 0.95 ± 0.10 (20 % F-127), and 0.75 ± 0.07 μmole/h (30 % F-127). Two-way ANOVA tests revealed that delivery fluxes (measured as of the 4th
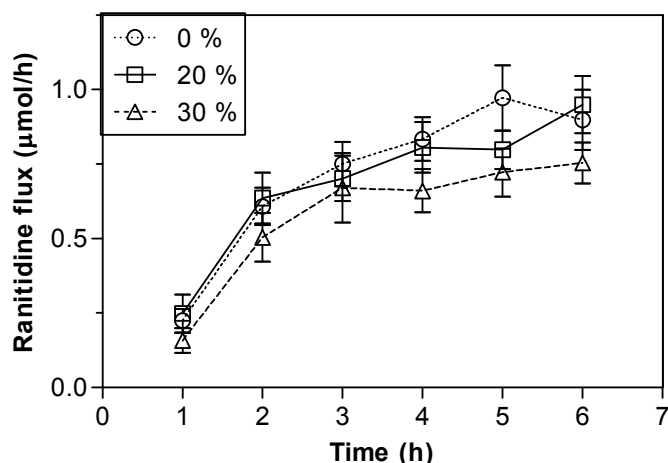
Figure 9: Iontophoretic delivery fluxes of ranitidine from donor formulations containing 0, 20, and 30 %w/w F-127. Data are represented as the mean ± SD.

hour of current passage) from 30 % F-127 donor formulation were statistically lower than the other two formulations. Nevertheless, the use of 30 % gel formulation as iontophoresis vehicle for ranitidine delivery only reduced fluxes by about 20 %. The corresponding transference numbers of ranitidine using 0, 20 and 30 %w/w F-127 donor formulations are 8.05 ± 0.91, 8.48 ± 0.87, and 6.73 ± 0.63 %, respectively. Using the flux rates achieved with the gel formulations and assuming a one-to-one *in vitro:in vivo* correlation, patch areas required to achieve therapeutic input levels of ranitidine are estimated in Table 2. In summary, the use of F-127 gel formulations in the iontophoretic delivery of ranitidine did indeed deliver therapeutically meaningful fluxes with acceptable patch application areas.

Table 2: The patch sizes (anode + cathode) required to achieve target systemic levels of ranitidine in different groups of the paediatric population.

	Target input rate (μmol/h.kg)[1]	*In vitro* transdermal rates achieved[2] (μmol/h.cm^2)	Total area of patch required (cm^2/kg)
Neonate	0.09 – 0.17	Solution: 1.16 ± 0.13	0.1 – 0.3
			0.1 – 0.3
			0.2 – 0.4
		Gel 20%: 1.22 ± 0.13	
> 1 month – 12 years	0.36 – 0.71		0.6 – 1.2
			0.6 – 1.2
		Gel 30%: 0.97 ± 0.09	0.7 – 1.5

[1]: = intravenous infusion rate. [2]: fluxes correspond to 6 hour measurement of iontophoresis (0.39 mA/cm^2), using 150 mM drug solution (pH 7).

4. Chapter conclusions

Transdermal iontophoresis of ranitidine enhanced its delivery significantly relative to passive diffusion. The manipulation of different parameters allowed the selection of the best conditions under which ranitidine's iontophoretic delivery achieved target doses with both solution and gel formulations. In particular, the gel formulation composed of 30 %w/w F-127 polymer showed good potential as a semi-solid matrix for the iontophoretic delivery of ranitidine. This is owing to its good viscosity, acceptable electrical conductivity and iontophoretic efficiency. Assuming a one-to-one *in vitro-in vivo* correlation and delivering a current of 0.39 mA/cm^2 through a 30 % gel containing 150 mM ranitidine, therapeutic levels of ranitidine in children up to the age of 12 years can be achieved with a total patch system of 0.2 – 1.5 cm^2/kg dimensions; a very acceptable range indeed.

5. References

1.   *British national formulary for children 2008*. revised ed, ed. Martin, J. 2008, London: BMJ Group, RPS Publishing, and RCPCH Publications. 944 p.

2.   Garg, D. C., Weidler, D. J., and Eshelman, F. N., *Ranitidine bioavailability and kinetics in normal male subjects.* Clin Pharmacol Ther, 1983. **33**: p. 445-452.

3.   Blumer, J. L., Rothstein, F. C., Kaplan, B. S., Yamashita, T. S., Eshelman, F. N., Myers, C. M., and Reed, M. D., *Pharmacokinetic determination of ranitidine pharmacodynamics in pediatric ulcer disease.* J Pediatr, 1985. **107**: p. 301-306.

4.   Vanhecken, A. M., Tjandramaga, T. B., Mullie, A., Verbesselt, R., and Deschepper, P. J., *Ranitidine - single dose pharmacokinetics and absolute bioavailability in man.* Brit J Clin Pharmaco, 1982. **14**: p. 195-200.

5.   Lugo, R. A., Harrison, A. M., Cash, J., Sweeley, J., and Vernon, D. D., *Pharmacokinetics and pharmacodynamics of ranitidine in critically ill children.* Crit Care Med, 2001. **29**: p. 759-764.

6.   Moffat, A. C., Osselton, M. D., and Widdop, B., *Clarke's analysis of drugs and poisons : In pharmaceuticals, body fluids and postmortem material*. 3rd ed. 2004, London: Pharmaceutical Press.

7.   Brittain, H. G., *Profiles of drug substances, excipients and related methodology*. Vol. 33. 2007, London: Academic Press.

8.   Collett, J. H., *Monographs: Poloxamer*, in *Handbook of pharmaceutical excipients*, Rowe, R. C., Sheskey, P. J., and Owen, S. C., Editors. 2006, Pharmaceutical Press ; American Pharmacists Association: London. p. 535.

9.   Escobar-Chavez, J. J., Lopez-Cervantes, M., Naik, A., Kalia, Y. N., Quintanar-Guerrero, D., and Ganem-Quintanar, A., *Applications of thermo-reversible pluronic f-127 gels in pharmaceutical formulations.* J Pharm Pharm Sci, 2006. **9**: p. 339-358.

10.   Booth, C., and Attwood, D., *Effects of block architecture and composition on the association properties of poly(oxyalkylene) copolymers in aqueous solution.* Macromol Rapid Comm, 2000. **21**: p. 501-527.

11.   Cabana, A., AitKadi, A., and Juhasz, J., *Study of the gelation process of polyethylene oxide(a) polypropylene oxide(b) polyethylene oxide(a) copolymer (poloxamer 407) aqueous solutions.* J Colloid Interf Sci, 1997. **190**: p. 307-312.

12.   Taveira, S. F., Nomizo, A., and Lopez, R. F., *Effect of the iontophoresis of a chitosan gel on doxorubicin skin penetration and cytotoxicity.* J Control Release, 2009. **134**: p. 35-40.

13.   Fang, J. Y., Sung, K. C., Wang, J. J., Chu, C. C., and Chen, K. T., *The effects of iontophoresis and electroporation on transdermal delivery of buprenorphine from solutions and hydrogels.* J Pharm Pharmacol, 2002. **54**: p. 1329-1337.

14.   Al-Khalili, M., Meidan, V. M., and Michniak, B. B., *Iontophoretic transdermal delivery of buspirone hydrochloride in hairless mouse skin.* AAPS PharmSci, 2003. **5**: p. E14.

15.   Gupta, S. K., Kumar, S., Bolton, S., Behl, C. R., and Malick, A. W., *Effect of chemical enhancers and conducting gels on iontophoretic transdermal delivery of cromolyn sodium.* J Control Release, 1994. **31**: p. 229-236.

16.   Schmolka, I. R., *Artificial skin. I. Preparation and properties of pluronic f-127 gels for treatment of burns.* J Biomed Mater Res, 1972. **6**: p. 571-582.

17.   Oo, C. Y., Kuhn, R. J., Desai, N., and Mcnamara, P. J., *Active-transport of cimetidine into human-milk.* Clin Pharmacol Ther, 1995. **58**: p. 548-555.

18.   Phipps, J. B., and Gyory, J. R., *Transdermal ion migration.* Adv Drug Del Rev, 1992. **9**: p. 137-176.

19.   Marro, D., Guy, R. H., and Delgado-Charro, M. B., *Characterization of the iontophoretic permselectivity properties of human and pig skin.* J Control Release, 2001. **70**: p. 213-217.

20.   Santi, P., and Guy, R. H., *Reverse iontophoresis - parameters determining electroosmotic flow .1. Ph and ionic strength.* J Control Release, 1996. **38**: p. 159-165.

21.   Sieg, A., Guy, R. H., and Delgado-Charro, M. B., *Electroosmosis in transdermal iontophoresis: Implications for noninvasive and calibration-free glucose monitoring.* Biophys J, 2004. **87**: p. 3344-3350.

22.   Wearley, L., Jue-Chen, L., and Chien, Y. W., *Iontophoresis-facilitated transdermal delivery of verapamil 1. In vitro evaluation and mechanistic studies.* J Control Release, 1989. **8**: p. 237-250.

23.   Patel, S. R., Zhong, H., Sharma, A., and Kalia, Y. N., *In vitro and in vivo evaluation of the transdermal iontophoretic delivery of sumatriptan succinate.* Eur J Pharm Biopharm, 2007. **66**: p. 296-301.

24.   Green, P., Shroot, B., Bernard, F., Pilgrim, W. R., and Guy, R. H., *In vitro and in vivo iontophoresis of a tripeptide across nude rat skin.* J Control Release, 1992. **20**: p. 209-217.

25.   Padmanabhan, R. V., Phipps, J. B., Lattin, G. A., and Sawchuk, R. J., *In vitro and in vivo evaluation of transdermal iontophoretic delivery of hydromorphone.* J Control Release, 1990. **11**: p. 123-135.

26.   Van der Geest, R., Danhof, M., and Bodde, H. E., *Iontophoretic delivery of apomorphine. 1: In vitro optimization and validation.* Pharm Res, 1997. **14**: p. 1798-1803.

27.   Singh, P., Boniello, S., Liu, P., and Dinh, S., *Transdermal iontophoretic delivery of methylphenidate hcl in vitro.* Int J Pharm, 1999. **178**: p. 121-128.

28.   Macosko, C. W., *Rheology : Principles, measurements, and applications*. 1994, Cambridge: VCH. 550 p.

29.   Malkin, A., *Rheology fundamentals*. 1994, Ontario: ChemTec. 324 p.

30.	Goodwin, J. W., and Hughes, R. W., *Rheology for chemists : An introduction.* 2nd ed. 2008, Cambridge: RSC Publishing. 264 p.

31.	Bard, A. J., and Faulkner, L. R., *Potentials and thermodynamics of cells*, in *Electrochemical methods : Fundamentals and applications*, Bard, A. J., and Faulkner, L. R., Editors. 2001, John Wiley: New York ; Chichester. p. 44-86.

32.	Atkins, P. W., *Molecules in motion: Ion transport and molecular diffusion*, in *Physical chemistry*, Atkins, P. W., Editor. 1978, Oxford University Press: Oxford. p. 819-848.

33.	Attwood, D., and Florence, A. T., *Physical pharmacy.* 2008, London: Pharmaceutical press. 182.

34.	Gilbert, J. C., Hadgraft, J., Bye, A., and Brookes, L. G., *Drug release from pluronic f-127 gels.* Int J Pharm, 1986. **32**: p. 223-228.

35.	Stamatialis, D. F., Rolevink, H. H., and Koops, G. H., *Transdermal timolol delivery from a pluronic gel.* J Control Release, 2006. **116**: p. e53-55.

36.	Su, H.-L., and Miller, S. C., *In vitro release of nicotinic acid alkyl esters from poloxamer vehicles.* Int J Pharm, 1990. **66**: p. 213-221.

37.	Khalil, E., Schaefer, U. F., and Sallam, A., *Release characteristics of diclofenac diethylamine from emulgels containing pluronic f127.* J Drug Deliv Sci Tec, 2006. **16**: p. 381-387.

38.	Kotwal, V., Bhise, K., and Thube, R., *Enhancement of iontophoretic transport of diphenhydramine hydrochloride thermosensitive gel by optimization of ph, polymer concentration, electrode design, and pulse rate.* AAPS PharmSciTech, 2007. **8**: p. E120.

39.	Shin, S. C., Cho, C. W., and Choi, H. K., *Permeation of piroxicam from the poloxamer gels.* Drug Dev Ind Pharm, 1999. **25**: p. 273-278.

Chapter 4

In vitro transdermal delivery of Midazolam hydrochloride by iontophoresis

Chapter summary

The purpose of this study was to assess whether transdermal iontophoretic delivery of midazolam may provide a useful treatment strategy for paediatric patients. Experiments were performed *in vitro* using intact pig skin as well as barriers from which the stratum corneum had been stripped to different extents to model the less resistant skin of premature babies. The impact of current intensity, midazolam concentration, ion composition and pH of the drug formulation were examined. Drug delivery was increased by increasing the current, by higher pH, and by maximising the mole fraction of midazolam in the driving electrode formulation. Compromisation of the barrier to 50 % of its normal function led to an approximately 60-fold increase in the passive permeation of midazolam; complete removal of the stratum corneum resulted in a further 20-fold enhancement. In contrast, with iontophoresis, the current controlled transport through the half-compromised skin; across a fully impaired barrier, however, iontophoretic control was undermined by the very high passive contribution. Overall, it was possible to control midazolam delivery in most situations, and iontophoresis could deliver a therapeutically meaningful flux. Further work to explore these observations is warranted.

1. Introduction

Midazolam, a short acting benzodiazepine, is used in paediatric medicine as a sedative for operations, premedication and in intensive care where continuous sedation is an integral part of patient care [1]. It is especially used in infants and (in particular) premature neonates. Depending on the individual case, midazolam is delivered either by the oral, rectal, buccal, nasal, or intravenous (either as bolus or continuous infusion) route.

When given orally, midazolam undergoes extensive first pass metabolism resulting in low bioavailability of 15 – 30 % [2]. Its half life is short (2 hours, but longer in neonates [3]) and frequent dosing, as a result, is necessary to sustain therapeutic efficacy. The bitter taste of the oral solution is also problematic. Of course, oral delivery to infants and children in intensive care is often inappropriate, and the same can be said of the buccal route. Intravenous delivery is currently the most commonly used administration method, despite being associated with the risk of infection and pain. More specific problems include precipitation of midazolam at pH > 5, and incompatibility with both parenteral nutrition and drugs such as ranitidine and furosemide [4-7]. These issues are not infrequent and necessitate a separate intravenous line for midazolam, a far from ideal situation in infants and children for whom their small size renders multiple i.v access lines more difficult and invasive. Children in intensive care and neonates are often continuously infused with midazolam to provide continuous and stable sedative effects, and again there are complications related to compliance and scarring at the injection site. Rectal or nasal administration have been proposed as alternatives to intravenous delivery, but the former has been linked to low and inconsistent absorption rates [2, 8], while the latter is not recommended due to irritation of the nasal mucosa resulting in an intense burning sensation [1, 9].

Transdermal iontophoresis may offer an advantageous, alternative route for the delivery of midazolam. To be successful, transdermal iontophoresis must deliver target dosing rates achieved by intravenous administration. Typical intravenous

regimens recommended for continuous sedation in paediatric intensive care are as follows: 1) premature neonates of gestational age less than 32 weeks, 30 μg/kg/h; 2) neonates of more than 32 weeks gestational age to infants up to 6 months, 60 μg/kg/h; 3) Older than 6 months, a loading dose of 30 – 300 μg/kg as a slow intravenous injection, followed by continuous infusion of 30 – 120 μg/kg/h.

The skin barrier of neonates whose gestational age is more than 34 weeks resembles adult skin [10]. Premature neonates of less than 34 weeks gestation, are, however, characterized by an underdeveloped skin barrier with incomplete formation of stratum corneum structure [11, 12]. The level of barrier impairment depends on the post-conceptional age of the neonate (i.e., the sum of the gestation age at birth and the post-natal age), and has been evaluated using measurements of transepidermal water loss (TEWL) [13-16]. A reduced barrier function is associated with an elevated TEWL value. As the developing skin barrier matures, TEWL decreases accordingly until a fully functional barrier is established. The immature barrier of premature neonates often causes some critical issues such as thermoregulation control, and increased permeability characteristics in comparison with intact skin which may augment the risks of toxicity to chemicals. It could, however, be used in favour to the transdermal delivery of drugs and this potential has indeed been explored *in vivo*, for example, in the delivery of theophylline and caffeine [17, 18].

To study transdermal permeation of potential drugs in the paediatric population, a range of skin membranes, the barrier functions of which mirror those of premature neonates and older ages, need to be investigated. For obvious ethical reasons, excised skin from humans and especially children are rarely available. Pig skin is often used, as an alternative to human skin, to assess transdermal permeation of drugs [19-21]. In addition, it has been demonstrated that pig skin, from which the stratum corneum has been differentially tape-stripped to provide different degrees of compromised barriers, can be used as an *in vitro* model to the premature neonatal skin at different levels of skin maturation (i.e., different gestational age) [22].

The objective of this study was to investigate *in vitro* the feasibility of delivery of midazolam by transdermal iontophoresis. First, intact pig skin was used to consider the variables determining the iontophoretic delivery of midazolam. Second, transdermal delivery of the drug was tested through pig skin from which the stratum corneum had been stripped to different extents so as to model the less resistant skin of premature babies.

2. Materials and methods

2.1 Chemicals

Midazolam hydrochloride was obtained from Apin Chemicals (Oxford, UK), silver wire (99.99%), silver chloride (99.999%), and sodium hydroxide pellets were purchased from Sigma Aldrich (Gillingham, UK). Sodium chloride, citric acid monohydrate, trisodium citrate dehydrate, disodium hydrogen phosphate, potassium dihydrogen phosphate, and phosphoric acid (85 %) were obtained from Acros (Geel, Belgium). Acetonitrile and hydrochloric acid were provided by Fisher Scientific (Loughborough, UK). All reagents were at least analytical grade and deionised water (resistivity ≥ 18.2 MΩ.cm, Barnsted Nanopure Diamond™, Dubuque, IA) was used for the preparation of all solutions.

2.2 Skin

Fresh pig skin was obtained from a local slaughterhouse, cleaned under cold running water, and stored in a refrigerator until the following day. Dorsal skin was dermatomed (Zimmer™ Electric Dermatome, Dover, Ohio; nominal thickness 750 µm), cut into pieces of appropriate size, wrapped individually in Parafilm™, and then kept in a freezer (-20 °C) until use. Prior to the permeation experiment, the skin was thawed at room temperature for 30 minutes and visible hairs were carefully cut with scissors. The skin was either used as is or was tape-stripped to create two impaired barriers: half compromised (40 – 60 %) and fully compromised (100 %).

The tape-stripping procedure was as follows: First, a 10 x 10 cm^2 area of skin was divided into 3 pieces. The first piece represented the intact skin barrier and an initial, baseline reading of TEWL was measured using an evaporimeter (AquaFlux AF-102, Biox Systems Ltd., London, UK). TEWL was recorded once the reading had stabilised (maximum duration set at 3 minutes) and the average reading was 9.0 ± 1.7 g/m^2.h. The second piece of skin was repeatedly stripped with adhesive tape (2 x 2 cm^2, Scotch Book Tape, 3M, St. Paul, MN) to progressively remove the stratum

corneum and produce 100 % barrier impairment. A 1.5 x 1.5 cm^2 template was affixed onto the skin before the stripping procedure to ensure the removal of stratum corneum from the same skin location. Periodic measurement of TEWL allowed the degree of barrier impairment to be quantified and 100 % derangement was deemed to have been achieved when TEWL did not increase further. Between 17 and 25 tapes were needed to produce a fully compromised skin with a mean TEWL of 153 ± 11 g/m^2.h. Finally, the third piece of skin was also sequentially stripped until TEWL reached 40 − 60 % of that of the fully perturbed barrier. Between 13 and 16 tapes produced a half-compromised barrier with a mean TEWL of 76 ± 8 g/m^2.h.

2.3 Iontophoresis

Amber side-by-side two-compartment diffusion cells (active transport area = 0.71 cm^2, volume = 3 ml) were utilised in all experiments. The skin was mounted between the two chambers with the epidermal side oriented towards the anode compartment. The receptor chamber always held 154 mM sodium chloride solution (unbuffered, pH ~ 6). For 30 minutes prior to the start of the transport study, the skin was left in contact with the donor vehicle without drug, and 154 mM sodium chloride in the receptor chamber. Both compartments were then emptied and refilled with a donor solution containing midazolam and fresh receptor solution. Both compartments were magnetically stirred (Multipoint-6 stirrer, Thermo Scientific Variomag, Cole-Parmer, London, UK) at 400 rpm throughout the experiment. A direct constant current was delivered from a power supply (KEPCO 1000M, Flushing, NY, USA) using Ag/AgCl electrodes. Hourly samples (1 ml) of the receptor phase were withdrawn for analysis and replaced with fresh solution. Separate passive diffusion controls (no current) were also performed. The experiments performed are summarised in Table 1.

To investigate possible drug accumulation in the skin, the donor and receptor solutions were replaced with fresh drug-free solutions at the end of iontophoresis and the release of midazolam into the receptor phase was then followed over the next 15 hours.

Table 1: Experimental conditions performed to characterise midazolam transdermal delivery.

	Donor vehicle		Midazolam conc. (mM)	pH**	Current intensity (mA)	Replicates
pH effect	10 mM citrate* + 30 mM NaCl		7.5	3	0.36	4
				3.5		3
				4		4
				4.5		4
Current effect	10 mM Citrate* + 30 mM NaCl		7.5	3.5	0.1	3
					0.2	3
					0.36	3
Co-ion competition	Water		15.9	3.6	0.36	5
	10 mM citrate* + NaCl either:	0 mM	15	3.5		6
		30				9
		90				5
Concentration effect	10 mM Citrate* + 30 mM NaCl		1	3.5	0.36	3
			7.5			3
			15			9
Skin barrier effect: Passive diffusion and iontophoresis	10 mM Citrate* + 30 mM NaCl		15	3.5	Passive: - Iontophoresis: 0.36	Passive: 3 Iontophoresis: 5-9

* The citrate buffer comprised 7.4 mM citric acid monohydrate and 2.6 mM trisodium citrate dehydrate. ** Final pH of the drug solution in citrate buffer was always 3.5 except in pH effect experiments where it was adjusted to 3 with HCl; and to 4 and 4.5 with NaOH. pH change at the end of all permeation experiments did not exceed ± 0.1 in citrate buffer vehicles and ± 0.2 in water vehicle.

2.4   Sample analysis

Quantification of midazolam was performed by high performance liquid chromatography with UV detection (220 nm). The method used a Jasco HPLC system comprising a PU-980 pump with an AS-1595 autosampler, a UV-975 UV-VIS detector, and an Acclaim 120, C18 (150 x 4.6 mm, 5µm) reversed-phase column (Dionex, UK) which was thermostated at 25 °C. The mobile phase consisted of 50 mM phosphate buffer (pH 2 with phosphoric acid) and acetonitrile (70 : 30) and was pumped through the system at 1 ml/min. The validation parameters are found in Appendix (1D).

2.5   Data analysis and statistics

Data analysis and regressions were performed using Graph Pad Prism V.5.00 (Graph Pad Software Inc., CA, USA). Unless otherwise stated, data are represented as the mean ± standard deviation (SD). Transport fluxes were calculated as the amounts delivered per unit time. Comparisons made between different sets of data were assessed by either two-tailed unpaired t-test (for 2 groups) or one-way ANOVA (for > 2 groups) followed by Tukey's post-test. Statistical significance was set at *p < 0.05*.

The transference number (T) of midazolam was computed according to Faraday's law [23]:

$$T = \frac{J \times z \times F}{I} \qquad\qquad \text{Equation (1)}$$

Where *J* is the drug flux observed at 6 h of iontophoresis, *I* is the current intensity applied, *F* is Faraday's constant, and *z* is the numerical value of the valence of the drug ion.

3. Results and discussion

The passive flux of midazolam hydrochloride (applied as a 15 mM solution at pH 3.5) through intact pig skin was 0.06 ± 0.01 nmol/h.cm^2 at 21 h. This flux value is substantially smaller than a previously reported value of 12.9 nmol/h.cm^2 [24]. The latter result was obtained when radio-labelled midazolam maleate (11.3 mM in water, unbuffered) was applied to hairless mouse skin, a model which is known to be more permeable than the human counterpart [25, 26] and more susceptible to the effects of a low pH vehicle.

As shown below, iontophoresis through intact skin was significantly higher than passive diffusion, the contribution of which to the observed fluxes could be neglected.

3.1 pH effect

Midazolam is a weak base with pKa value of 6.15 [27] and a molecular weight of 325.8. It is lipophilic (LogP 4.33, [28]) and has very low aqueous solubility at pH values higher than 5. The solubility is considerably higher at acidic pH where midazolam is ionised [29]. Hence, experiments were performed at pH values of 3, 3.5, 4, and 4.5. Donor solutions (containing 7.5 mM midazolam) at pH 4.5 were slightly cloudy but no precipitation was observed for the duration of the experiment. Figure 1 depicts transport fluxes of midazolam as a function of pH when 0.36 mA current was passed for 6 hours. Drug delivery increased with increasing pH. Despite the lower solubility of midazolam at pH 4.5, the highest transport ($p < 0.05$) was observed in this case (J_{6h} = 17.7 ± 3.2 nmol/h); at pH 3, in contrast, the flux was only 6.0 ± 3.0 nmol/h. At intermediate pHs, drug flux fell between these two extremes. The effect of pH on midazolam transport can be described as follows:
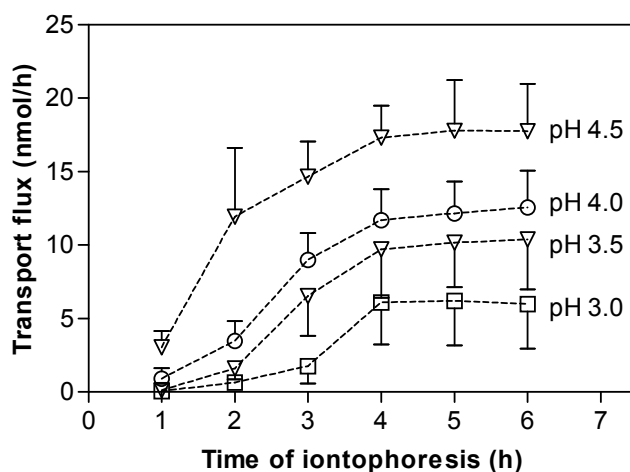
Figure 1: Midazolam iontophoretic transport (mean ± SD) as a function of donor solution pH. Midazolam was delivered from 7.5 mM drug solution under 0.36 mA current.

1) Lowering the donor pH leads to a rise in the presence of hydronium ions in the drug formulation (0.03 mM at pH 4.5, increasing to 1 mM at pH 3). As a result, there is more co-ion competition against midazolam owing to the fact that hydronium ions are much more efficient as charge carriers due to their high mobility properties. Acyclovir, 5-OH-DPAT, and 5-Aminolevulinic acid are example drugs whose anodal iontophoretic transport was studied at low pH values with similar observations about the effect of hydronium ion competition [30-32].

2) Lowering the donor pH results in less net negative charge (or even charge reversal) on the skin affecting both electroosmosis and electromigration of the cation [23, 33, 34]. Electroosmosis in particular is severely affected at low pH values. Pig skin was demonstrated to have an isoelectric point of ~ 4.4 [34]. This means that at this pH, the skin had a net charge of zero and is neither permselective to cations nor anions. Above this pH, the skin is negatively charged, permselective to cations, and, under iontophoresis, electroosmosis takes place in the direction of anode-to-cathode; further boosting the anodal transport of midazolam. When pH values are below the isoelectric point, reversal of the skin net charge occurs, leading to preferential passage of anions, which in turn results in induction of electroosmosis at the opposite direction to midazolam transport (cathode-to-anode). Midazolam anodal delivery is therefore retarded as the pH is progressively lowered. Similar observations were noted for other cations such as
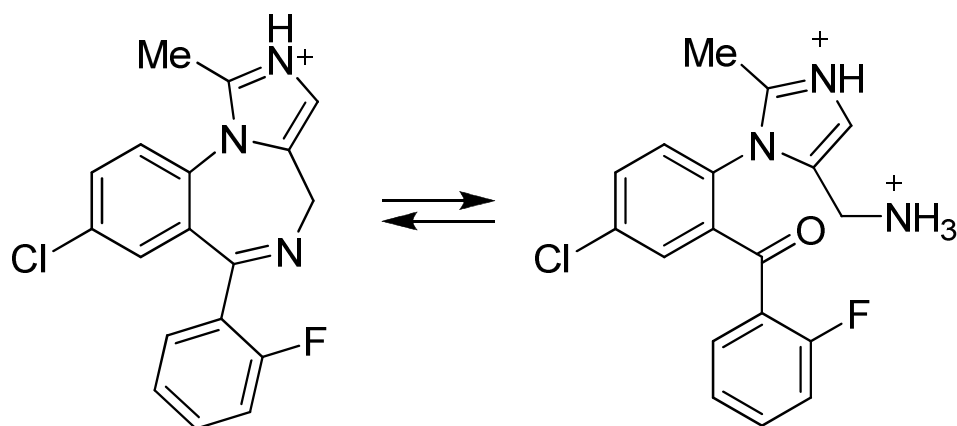
Figure 2: Midazolam exists in a pH-dependent equilibrium with an open-ring structure in acidic conditions.

the dopamine agonists: apomorphine, 5-OH-DPAT, and rotigotine [30, 35, 36], whose anodal delivery was tested using donor solutions of pH values 3 – 6.

3) In acidic conditions, midazolam exists in a pH-dependent equilibrium with a double charged ring-opened structure [29, 37] (Figure 2). Previous work which quantified the percentage of the open-ring structure of midazolam as a function of solution pH [29, 37, 38] is summarised in Figure 3. It is therefore estimated that ~ 19, 9, 4, ad 2 % of midazolam ions are present as divalent cations at pH: 3, 3.5, 4, and 4.5, respectively. These are only estimates from available literature and may not reflect exact percentages in this study because different buffers were used. Divalent midazolam cations may behave differently from the monovalent ions and so is their iontophoretic transport efficiency. Even though equation (1) expects that an increase in drug valence results in lower electrotransport as fewer molecules are needed to carry the same quantity of charge, the transference number of the drug is also altered with valence as reported in a previous study where divalent peptides were found to be more efficient at carrying charge than monovalent peptides of similar molecular weight [39]. Nonetheless, even though a fifth of midazolam may have been present as divalent cations at pH 3, the fact that the skin was also positively charged at pH 3 and the higher presence of competing hydronium ions undermined any noticeable effect of the drug's double charge on the total transport.
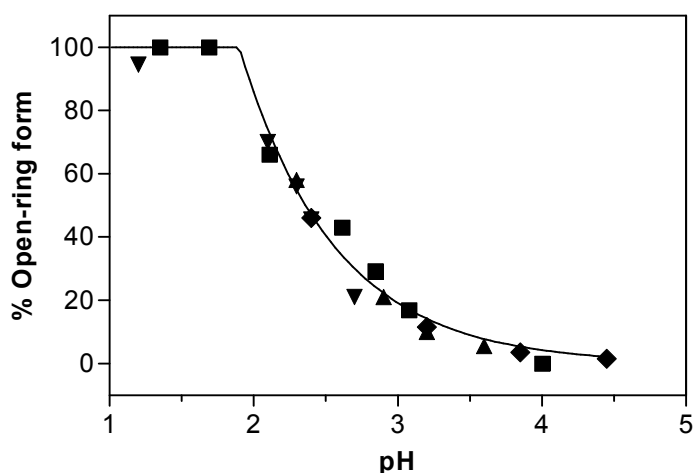
Figure 3: A summary of published work [29, 37, 38] which quantified the percentage of the open-ring structure of midazolam as a function of solution pH. Different symbols summarise different techniques used.

To sum up, midazolam transport from pH 4.5 donor solution was significantly more effective than at lower pH values. However, solutions made at this pH (7.5 mM midazolam) were cloudy and may have been near saturation levels. Hence, to ensure complete solubility, pH 3.5 was chosen for the subsequent experiments as it allowed usage of higher concentrations of the drug.

Faraday's law (equation 1) dictates that the iontophoretic transport of an ion is a function of both the current intensity applied and the transference number. These factors are the subject of the next sections. The total fluxes observed during midazolam iontophoresis were assumed to be attributed to its electromigration only. This is because: 1) as mentioned above, passive diffusion was found to be negligible, and 2) contribution from electroosmosis was also neglected because, at pH 3.5, any effect of electroosmosis would be in the direction of the cathode-to-anode which is opposite to midazolam's anodal delivery.

3.2 Current effect

As expected, increasing the current intensity led to proportional enhancement of midazolam iontophoretic fluxes (Figure 4), in agreement with Faraday's law (equation 1). These results reaffirm the major role of current intensity

in controlling iontophoretic delivery and similar findings have been reported previously for many compounds [40-45]. The gradient of the line in the right-hand panel of Figure 4 equals the drug's transference number: 0.22 ± 0.03 % (± SE, $p <$ 0.0001, r^2 0.88). Midazolam's transference number is approximately 30-fold smaller than that of ranitidine (chapter 3). While both cations have similar molecular weight (325.8 *versus* 314.4 Da), midazolam is much more lipophilic (LogP 4.3 *versus* 0.3). The significant difference in the drug molar fraction in the donor solution (midazolam: 15.8 %, ranitidine: 91.1 %) and the effect of pH (3.5 for midazolam and 7 for ranitidine) discussed above account for the much superior transport efficiency of ranitidine over midazolam.
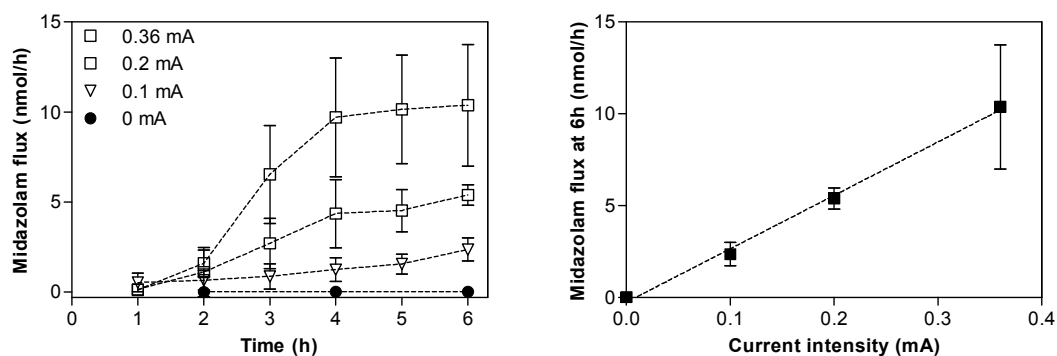
Figure 4: Delivery fluxes of Midazolam (mean ± SD) as a function of time (left) and current intensity (right). Midazolam was delivered from a 7.5 mM donor solution in the presence of 37.8 mM sodium ions (pH 3.5).

3.3   Mole fraction effect

It has been shown previously that the molar fraction of the drug in the donor solution, as opposed to its concentration, determines the transport efficiency of the drug [23, 46-48]. This was demonstrated in the previous chapter for ranitidine. However, for very lipophilic cations, this relationship sometimes does not hold (e.g., ropinirole, LogP 3.3, [49]).

Midazolam iontophoretic delivery was measured from constant pH, donor solutions, as a function of 1) competing co-ion concentration (drug concentration is
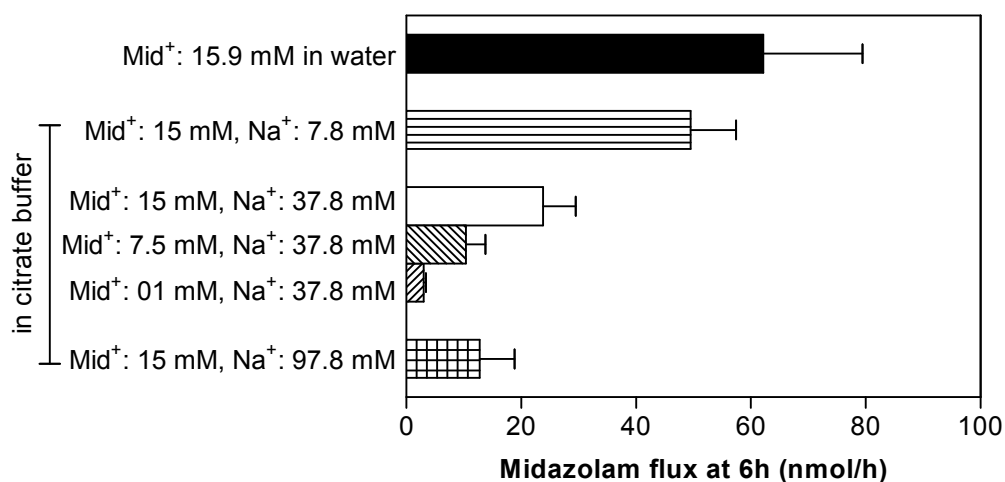
Figure 5: Midazolam transport from different donor vehicles. Flux values (mean ± SD) at the 6th hour of iontophoresis (0.36 mA). Drug concentration was 15.9 mM in water (pH 3.6) and 1 - 15 mM in citrate buffer (pH 3.5) containing 7.8 – 97.8 mM Na^+.

fixed), and 2) drug concentration (co-ion concentration is fixed). Figure 5 compares midazolam delivery from the different donor solutions. As expected, the most efficient delivery of midazolam was from water (J_{6h} = 62.2 ± 17.3 nmol/h), where midazolam competes only with hydronium ions. Introduction of extraneous sodium ions in the donor solution buffer decreased midazolam transport as did lowering the concentration of the drug. Figure 6 plots the drug transference number, calculated using equation (1), as a function of its molar fraction. A simple linear regression of the data yielded a straight line of a slope equal to $(1.34 ± 0.09)*10^{-2}$ (r^2 0.86, *p < 0.0001*) and an intercept indistinguishable from zero. The co-ions which competed with midazolam were sodium and hydronium ions; the latter were taken into account because at pH 3.5, their concentration reached 0.3 mM. The aqueous mobility of hydronium ions is 36.25 x 10^{-4} cm^2/s.V [50], 7 times superior to that of sodium (5.19 x 10^{-4} cm^2/s.V) and much higher, of course, than midazolam. It should be acknowledged, however, that combining the concentrations of the competing co-ions without consideration of the high mobility differences may introduce an artefact to the relation observed with the corresponding drug transference number.
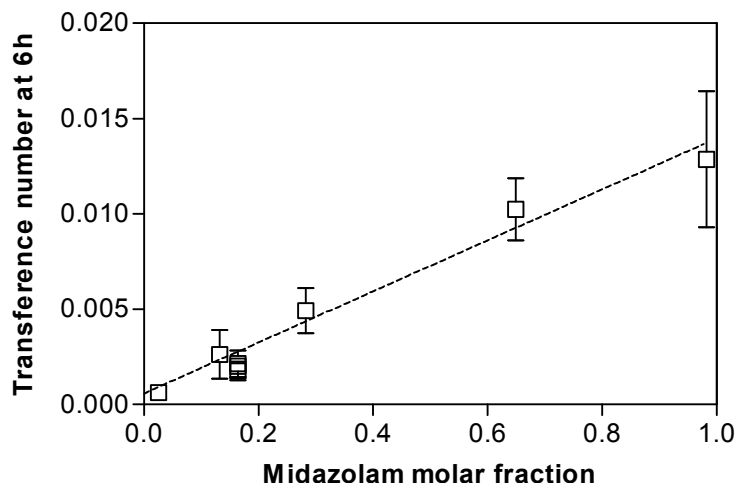
Figure 6: Transference numbers of midazolam (mean ± SD), measured using flux values at 6 hours of iontophoresis, as a function of the drug's molar fraction. A simple linear regression (broken line) is used to fit the data points. See text for more details.

3.4 Permeation across compromised skin

Pig skin was progressively stripped to provide either fully or half compromised barrier function. Figure 7 compares passive and iontophoretic delivery fluxes of midazolam through barrier impaired skin relative to intact skin. As expected, passive diffusion increased dramatically with barrier derangement. While midazolam flux through intact skin was only 0.03 ± 0.01 nmol/h after 6 hours, stratum corneum removal impaired the barrier function of the skin which became much more permeable; drug fluxes of 1.9 ± 0.3 and 32.5 ± 8.4 nmol/h were measured for half- and fully-compromised skin barriers, respectively. This accounts for more than 1000-fold enhancement when the stratum corneum was completely ablated.

The same experiments performed for passive diffusion were repeated but now with application of a constant electrical current of 0.36 mA intensity. As depicted in Figure 7, delivery of midazolam through half impaired skin barrier did not differ from intact skin (J_{6h}: 27.1 ± 13.8 *versus* 23.8 ± 5.7 nmol/h); indicating that
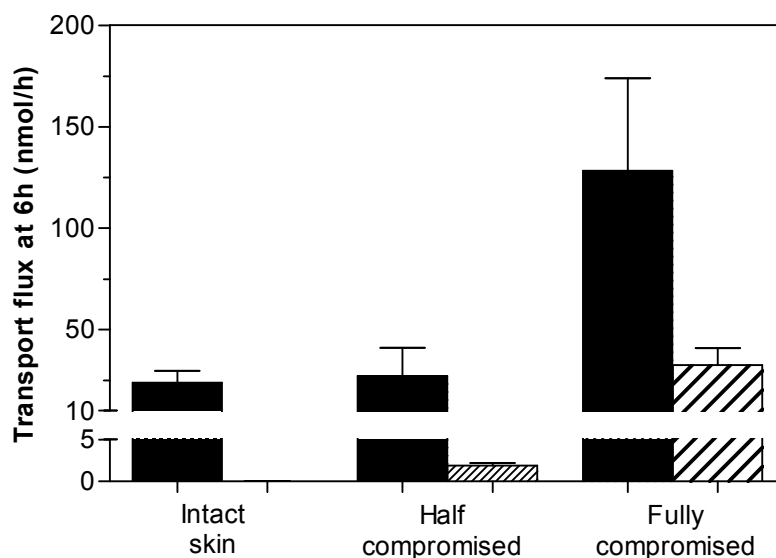
Figure 7: Passive (shaded bars) and Iontophoretic (filled bars) transport fluxes (mean ± SD) of midazolam delivered from 15 mM drug solution (pH 3.5) through intact, half-compromised, and fully impaired barrier function.

the applied current continued to control the rates of midazolam delivery through a skin barrier whose function was impaired by up to 50 %. However, across a fully compromised barrier, a fivefold increase in total flux, J_{6h} = 128.3 ± 45.7 nmol/h, was observed. This suggests that the magnitude and contribution of the three transport mechanisms (i.e. passive, electroosmosis, and electromigration) to the total fluxes observed have changed.

Previous studies on several compounds showed that while electroosmosis generally becomes absent at complete barrier compromisation, electromigration either remained constant or reduced with perturbed skin barrier [51-56]. In addition, passive diffusion was always found to increase significantly with stratum corneum removal. For example, the iontophoretic transport of the positively charged nalbufine pivalate from a pH 4 donor solution doubled across fully impaired hairless mouse skin barrier (138.6 ± 28.8 *versus* 79.2 ± 25.5 nmol/h.cm^2) [51]. This effect is, however, accounted for by the enhancement of passive diffusion which increased from 7.2 ± 1.9 to 70.6 ± 4.0 nmol/h.cm^2.

For midazolam, the progressive removal of the stratum corneum led to passive diffusion playing an increasingly more important transport mechanism in

the total delivery observed under current application. In the complete absence of barrier function, iontophoretic control was undermined by the very high enhanced passive permeation of midazolam. It is worth noting that because of the lipophilic nature of midazolam (LogP 4.3), high amounts of the drug may have accumulated in the epidermal layers including the stratum corneum and may not have partitioned into the subsequent layers of the skin and eventually into the receptor solution. It follows that the removal of the stratum corneum resulted in significantly higher passive permeation especially under iontophoresis where the concentration gradient of midazolam within the skin is probably higher than that in the absence of electrical current. As additional information, Table 2 shows the amounts passively released from the skin during 15 hours after termination of the current. These amounts were accordingly significantly higher as the stratum corneum barrier was progressively compromised.

Table 2: Comparison between the cumulative amount of midazolam transported by iontophoresis after 6 hours 0.36 mA current, with the amounts subsequently released from the skin 15 hours post current termination. Data shown (nmol, mean ± SD) correspond to intact and compromised skin with 15 mM drug concentration.

Skin type	Intact	Half compromised	Fully compromised
Cumulative amount permeated at 6 hour	101 ± 28	91 ± 57	485 ± 192
Amount released 15 hours after current cessation	33 ± 6	104 ± 11	276 ± 42

Figure 8 plots the transport fluxes, observed after passive diffusion and iontophoresis of midazolam, as a function of the TEWL measurements of the respective skin barriers. Similar to previous findings [18, 56, 57], an excellent relationship was observed with midazolam passive diffusion and the TEWL of the skin (r^2 0.99). With iontophoresis, even though the data were more scattered, an empirical fit with the respective TEWL values produced a good relation (r^2 0.80).
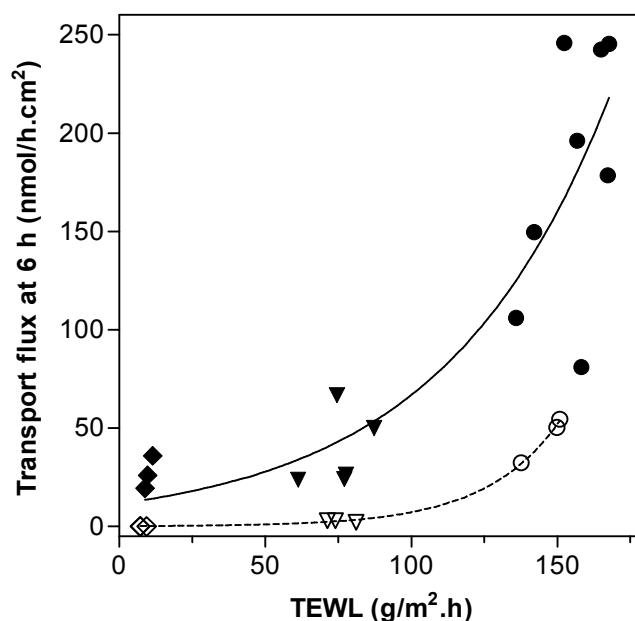
Figure 8: Relationship between the 6 hour transport fluxes of midazolam and TEWL values. Open symbols and discontinuous line refer to passive diffusion data and its empirical fit. Filled bars and continuous line correspond to iontophoresis data and its empirical fit. Each level of skin barrier is represented by a certain type of symbol. Intact, half- and fully-compromised skin barrier are respectively symbolized by star, triangle, and circle bars. Equations corresponding to the empirical fits are: Passive diffusion (n = 9, r^2 0.99 : J_{6h} = 0.14 . $e^{0.04 \cdot TEWL}$), iontophoresis (n = 16, r^2 0.80 : J_{6h} = 11.64 . $e^{0.02 \cdot TEWL}$)

3.5 Feasibility of midazolam transdermal delivery

Transdermal delivery of midazolam would offer a potential advantage to the paediatric population and this is especially significant in premature babies. This special group of patients is frequently critically ill, and multiple drug therapies are often prescribed and administered predominantly by the intravenous route.

Assuming a one-to-one *in vitro:in vivo* correlation, patch sizes required to achieve therapeutic levels will differ depending on the age of the paediatric patient. Premature neonates with significantly immature skin barrier function only require a ~ 1 cm^2/kg patch (anode + cathode) to deliver therapeutic doses of midazolam by iontophoresis. However, application of a 2 cm^2/kg passive patch of midazolam will also deliver the same amount as the 1cm^2/kg iontophoresis patch. Nevertheless, due the continuously developing skin barrier of the premature baby which reaches

fully maturity by 2 – 3 weeks postnatal age [10] (but may extend to 8 weeks in the very premature [14]), the passive diffusion of midazolam will dramatically decrease over the first few weeks and therefore the advantage of using iontophoresis instead is obvious.

Premature neonates (< 32 weeks gestational age) whose skin barrier is up to 50 % impaired would require iontophoretic patches of ~ 2 cm^2/kg to provide similar levels as typical intravenous infusion rates of midazolam (~ 0.08 µmol/h.kg). For neonates of more than 32 weeks gestational age to babies of up to 6 months old, the required size increases to ~ 4 cm^2/kg due to the higher intravenous infusion rates used in this age group (~ 0.17 µmol/h.kg). Older children up to 12 years of age would require areas of ~ 2 – 8 cm^2/kg corresponding to a recommended infusion dosing of ~ 0.08 – 0.33 µmol/h.kg.

Overall, the iontophoretic delivery of midazolam can achieve therapeutic levels and further optimisation of the delivery conditions is possible. In this study, the highest transdermal flux of midazolam through intact skin, that is 0.09 ± 0.02 µmol/h.cm^2, was achieved when the donor solution contained 15.9 mM midazolam in water (pH 3.6). The delivery rates can be improved further by increasing the pH of the drug solution. As demonstrated earlier, increasing the pH from 3.5 to 4.5 enhanced the flux by twofold; but was also associated with decreased drug solubility. This can, however, be circumvented by incorporation of solubilising agents such as the use of cyclodextrins. This potential was reported in a previous publication [58], whereby the solubility of midazolam at higher pH values was greatly enhanced upon addition of 10 % of either a negatively charged or a neutral cyclodextrin. Midazolam solubility at pH 5 was ~ 15 and 6 mM, respectively. Addition of 0.1 % hydroxypropyl methylcellulose to the negatively charged cyclodextrin further increased the solubility to ~ 30 mM.

4. Chapter conclusions

This study demonstrated that midazolam transdermal iontophoresis across intact pig skin increased with pH, current intensity, and molar fraction. Permeation through stripped pig skin was also tested to simulate different barrier levels found in premature neonates. Passive diffusion was enhanced dramatically with barrier derangement but iontophoresis only increased noticeably in the complete absence of the stratum corneum. Midazolam transdermal delivery can achieve therapeutically meaningful fluxes and future work is warranted to further optimise these findings.

5. References

1. *British national formulary for children 2008*. revised ed, ed. Martin, J. 2008, London: BMJ Group, RPS Publishing, and RCPCH Publications. 944 p.

2. Payne, K., Mattheyse, F. J., Liebenberg, D., and Dawes, T., *The pharmacokinetics of midazolam in paediatric patients.* Eur J Clin Pharmacol, 1989. **37**: p. 267-272.

3. Jacqz-Aigrain, E., Wood, C., and Robieux, I., *Pharmacokinetics of midazolam in critically ill neonates.* Eur J Clin Pharmacol, 1990. **39**: p. 191-192.

4. Trissel, L. A., Gilbert, D. L., Martinez, J. F., Baker, M. B., Walter, W. V., and Mirtallo, J. M., *Compatibility of parenteral nutrient solutions with selected drugs during simulated y-site administration.* Am J Health-Syst Ph, 1997. **54**: p. 1295-1300.

5. Forman, J. K., and Souney, P. F., *Visual compatibility of midazolam hydrochloride with common preoperative injectable medications.* Am J Hosp Pharm, 1987. **44**: p. 2298-2299.

6. Chiu, M. F., and Schwartz, M. L., *Visual compatibility of injectable drugs used in the intensive care unit.* Am J Health-Syst Ph, 1997. **54**: p. 64-65.

7. Swart, E. L., Mooren, R. A. G., and Vanloenen, A. C., *Compatibility of midazolam hydrochloride and lorazepam with selected drugs during simulated y-site administration.* Am J Health-Syst Ph, 1995. **52**: p. 2020-2022.

8. Malinovsky, J. M., Lejus, C., Servin, F., Lepage, J. Y., Le Normand, Y., Testa, S., Cozian, A., and Pinaud, M., *Plasma concentrations of midazolam after i.V., nasal or rectal administration in children.* Br J Anaesth, 1993. **70**: p. 617-620.

9. Lugo, R. A., Fishbein, M., Nahata, M. C., and Lininger, B., *Complication of intranasal midazolam.* Pediatrics, 1993. **92**: p. 638.

10. Evans, N. J., and Rutter, N., *Development of the epidermis in the newborn.* Biol Neonate, 1986. **49**: p. 74-80.

11.   Barker, N., Hadgraft, J., and Rutter, N., *Skin permeability in the newborn.* J Invest Dermatol, 1987. **88**: p. 409-411.

12.   Nonato, L. B., Kalia, Y. N., Naik, A., Lund, C. H., and Guy, R. H., *The development of skin barrier function in the neonate*, in *Topical absorption of dermatological products*, Bronaugh, R. L., and Maibach, H. I., Editors. 2002, Marcel Dekker: New York. p. 43-75.

13.   Rutter, N., and Hull, D., *Water loss from the skin of term and preterm babies.* Arch Dis Child, 1979. **54**: p. 858-868.

14.   Kalia, Y. N., Nonato, L. B., Lund, C. H., and Guy, R. H., *Development of skin barrier function in premature infants.* J Invest Dermatol, 1998. **111**: p. 320-326.

15.   Rutter, N., *The immature skin.* Br Med Bull, 1988. **44**: p. 957-970.

16.   Agren, J., Sjors, G., and Sedin, G., *Transepidermal water loss in infants born at 24 and 25 weeks of gestation.* Acta Paediatr, 1998. **87**: p. 1185-1190.

17.   Amato, M., Isenschmid, M., and Huppi, P., *Percutaneous caffeine application in the treatment of neonatal apnoea.* Eur J Pediatr, 1991. **150**: p. 592-594.

18.   Cartwright, R. G., Cartlidge, P. H., Rutter, N., Melia, C. D., and Davis, S. S., *Transdermal delivery of theophylline to premature infants using a hydrogel disc system.* Br J Clin Pharmacol, 1990. **29**: p. 533-539.

19.   Sekkat, N., and Guy, R. H., *Biological models to study skin permeation*, in *Pharmacokinetic optimization in drug research*, Testa, B., Van de Waterbeemd, H., Folkers, G., and Guy, R. H., Editors. 2001, Wiley: Zurich. p. 101-117.

20.   Sekkat, N., Kalia, Y. N., and Guy, R. H., *Biophysical study of porcine ear skin in vitro and its comparison to human skin in vivo.* J Pharm Sci, 2002. **91**: p. 2376-2381.

21.   Dick, I. P., and Scott, R. C., *Pig ear skin as an in-vitro model for human skin permeability.* J Pharm Pharmacol, 1992. **44**: p. 640-645.

22.   Sekkat, N., Kalia, Y. N., and Guy, R. H., *Development of an in vitro model for premature neonatal skin: Biophysical characterization using transepidermal water loss.* J Pharm Sci, 2004. **93**: p. 2936-2940.

23.   Phipps, J. B., and Gyory, J. R., *Transdermal ion migration.* Adv Drug Del Rev, 1992. **9**: p. 137-176.

24.   Touitou, E., *Transdermal delivery of anxiolytics - invitro skin permeation of midazolam maleate and diazepam.* Int J Pharm, 1986. **33**: p. 37-43.

25.   Bond, J. R., and Barry, B. W., *Hairless mouse skin is limited as a model for assessing the effects of penetration enhancers in human-skin.* J Invest Dermatol, 1988. **90**: p. 810-813.

26.   Bond, J. R., and Barry, B. W., *Limitations of hairless mouse skin as a model for invitro permeation studies through human-skin - hydration damage.* J Invest Dermatol, 1988. **90**: p. 486-489.

27.   Brittain, H. G., *Profiles of drug substances, excipients and related methodology*. Vol. 33. 2007, London: Academic Press.

28.   Moffat, A. C., Osselton, M. D., and Widdop, B., *Clarke's analysis of drugs and poisons : In pharmaceuticals, body fluids and postmortem material*. 3rd ed. 2004, London: Pharmaceutical Press.

29.   Andersin, R., *Solubility and acid-base behaviour of midazolam in media of different ph, studied by ultraviolet spectrophotometry with multicomponent software.* J Pharm Biomed Anal, 1991. **9**: p. 451-455.

30.   Nugroho, A. K., Li, L., Dijkstra, D., Wikstrom, H., Danhof, M., and Bouwstra, J. A., *Transdermal iontophoresis of the dopamine agonist 5-oh-dpat in human skin in vitro.* J Control Release, 2005. **103**: p. 393-403.

31.   Padula, C., Sartori, F., Marra, F., and Santi, P., *The influence of iontophoresis on acyclovir transport and accumulation in rabbit ear skin.* Pharm Res, 2005. **22**: p. 1519-1524.

32.   Lopez, R. F. V., Bentley, M. V. r. L. B., Delgado-Charro, M. B. a., and Guy, R. H., *Iontophoretic delivery of 5-aminolevulinic acid (ala): Effect of ph.* Pharm Res, 2001. **18**: p. 311-315.

33.   Santi, P., and Guy, R. H., *Reverse iontophoresis - parameters determining electroosmotic flow .1. Ph and ionic strength.* J Control Release, 1996. **38**: p. 159-165.

34.   Marro, D., Guy, R. H., and Delgado-Charro, M. B., *Characterization of the iontophoretic permselectivity properties of human and pig skin.* J Control Release, 2001. **70**: p. 213-217.

35.   Li, G. L., Danhof, M., and Bouwstra, J. A., *Iontophoretic delivery of apomorphine in vitro: Physicochemic considerations.* Pharm Res, 2001. **18**: p. 1509-1513.

36.   Nugroho, A. K., Li, G. L., Danhof, M., and Bouwstra, J. A., *Transdermal iontophoresis of rotigotine across human stratum corneum in vitro: Influence of ph and nacl concentration.* Pharm Res, 2004. **21**: p. 844-850.

37.   Bhattacharyya, P. K., and Grant, A., *Simultaneous determinations of a monofluorinated imidazo[1,5-a][1,4]benzodiazepine and the corresponding benzophenone as a function of ph and in aqueous formulations by f-19 nuclear magnetic-resonance spectrometry.* Anal Chim Acta, 1982. **142**: p. 249-257.

38.   Gerecke, M., *Chemical-structure and properties of midazolam compared with other benzodiazepines.* Brit J Clin Pharmaco, 1983. **16**: p. S11-S16.

39.   Abla, N., Naik, A., Guy, R. H., and Kalia, Y. N., *Effect of charge and molecular weight on transdermal peptide delivery by iontophoresis.* Pharm Res, 2005. **22**: p. 2069-2078.

40.   Schuetz, Y. B., Naik, A., Guy, R. H., Vuaridel, E., and Kalia, Y. N., *Transdermal iontophoretic delivery of triptorelin in vitro.* J Pharm Sci, 2005. **94**: p. 2175-2182.

41.   Chu, D. L., Chiou, H. J., and Wang, D. P., *Characterization of transdermal delivery of nefopam hydrochloride under iontophoresis.* Drug Dev Ind Pharm, 1994. **20**: p. 2775-2785.

42.   Green, P., Shroot, B., Bernard, F., Pilgrim, W. R., and Guy, R. H., *In vitro and in vivo iontophoresis of a tripeptide across nude rat skin.* J Control Release, 1992. **20**: p. 209-217.

43.   Padmanabhan, R. V., Phipps, J. B., Lattin, G. A., and Sawchuk, R. J., *In vitro and in vivo evaluation of transdermal iontophoretic delivery of hydromorphone.* J Control Release, 1990. **11**: p. 123-135.

44.   Van der Geest, R., Danhof, M., and Bodde, H. E., *Iontophoretic delivery of apomorphine. 1: In vitro optimization and validation.* Pharm Res, 1997. **14**: p. 1798-1803.

45.   Singh, P., Boniello, S., Liu, P., and Dinh, S., *Transdermal iontophoretic delivery of methylphenidate hcl in vitro.* Int J Pharm, 1999. **178**: p. 121-128.

46.   Mudry, B., Guy, R. H., and Delgado-Charro, M. B., *Prediction of iontophoretic transport across the skin.* J Control Release, 2006. **111**: p. 362-367.

47.   Marro, D., Kalia, Y. N., Delgado-Charro, M. B., and Guy, R. H., *Optimizing iontophoretic drug delivery: Identification and distribution of the charge-carrying species.* Pharm Res, 2001. **18**: p. 1709-1713.

48.   Mudry, B., Guy, R. H., and Delgado-Charro, M. B., *Transport numbers in transdermal iontophoresis.* Biophys J, 2006. **90**: p. 2822-2830.

49.   Luzardo-Alvarez, A., Delgado-Charro, M. B., and Blanco-Mendez, J., *Iontophoretic delivery of ropinirole hydrochloride: Effect of current density and vehicle formulation.* Pharm Res, 2001. **18**: p. 1714-1720.

50.   Bard, A. J., and Faulkner, L. R., *Electrochemical methods : Fundamentals and applications*. 2nd ed. 2001, New York ; Chichester: John Wiley. 833 p.

51.   Sung, K. C., Fang, J.-Y., and Yoa-Pu Hu, O., *Delivery of nalbuphine and its prodrugs across skin by passive diffusion and iontophoresis.* J Control Release, 2000. **67**: p. 1-8.

52.   Fang, J. Y., Sung, K. C., Wang, J. J., Chu, C. C., and Chen, K. T., *The effects of iontophoresis and electroporation on transdermal delivery of buprenorphine from solutions and hydrogels.* J Pharm Pharmacol, 2002. **54**: p. 1329-1337.

53.   Hirsch, A. C., Upasani, R. S., and Banga, A. K., *Factorial design approach to evaluate interactions between electrically assisted enhancement and skin stripping for delivery of tacrine.* J Control Release, 2005. **103**: p. 113-121.

54.   Abla, N., Naik, A., Guy, R. H., and Kalia, Y. N., *Contributions of electromigration and electroosmosis to peptide iontophoresis across intact and impaired skin.* J Control Release, 2005. **108**: p. 319-330.

55.   Sekkat, N., Naik, A., Kalia, Y. N., Glikfeld, P., and Guy, R. H., *Reverse iontophoretic monitoring in premature neonates: Feasibility and potential.* J Control Release, 2002. **81**: p. 83-89.

56.   Sekkat, N., Kalia, Y. N., and Guy, R. H., *Porcine ear skin as a model for the assessment of transdermal drug delivery to premature neonates.* Pharm Res, 2004. **21**: p. 1390-1397.

57.   Levin, J., and Maibach, H., *The correlation between transepidermal water loss and percutaneous absorption: An overview.* J Control Release, 2005. **103**: p. 291-299.

58.   Loftsson, T., Gudmundsdottir, H., Sigurjonsdottir, J. F., Sigurdsson, H. H., Sigfusson, S. D., Masson, M., and Stefansson, E., *Cyclodextrin solubilization of benzodiazepines: Formulation of midazolam nasal spray.* Int J Pharm, 2001. **212**: p. 29-40.

Chapter 5

Transdermal iontophoretic delivery of phenobarbital sodium: an *in vitro* study

Chapter summary

The objective of this investigation was to evaluate the potential use of phenobarbital transdermal delivery in paediatric care. *In vitro* experiments were performed using intact and tape-stripped pig skin to model the less resistant skin of premature babies. Cathodal iontophoretic delivery of phenobarbital was superior compared to anodal transport and optimised delivery conditions were achieved by reduction of competing co-ion presence in the drug formulation. Phenobarbital transport across intact or partially compromised skin was controlled by iontophoresis which was more efficient relative to passive diffusion. Across highly compromised skin, however, passive diffusion increased drastically and iontophoretic control was lost. Overall findings demonstrate the feasibility of phenobarbital transdermal delivery for paediatric patients.

1. Introduction

Phenobarbital (Figure 1) is a barbiturate drug used in the treatment of different forms of epilepsy. It is the most widely used antiepileptic drug in the world and is frequently prescribed as a first-line choice to control neonatal seizures [1-3]. Due to developmental changes in children, the pharmacokinetics of phenobarbital are highly variable in this population group; and doses are, therefore, titrated according to the individual's response for adequate seizure control. For optimum response, target therapeutic plasma concentrations are set between 60 − 180 nmol/ml. Such wide window is the result of different responses of individuals. The lower value is usually satisfactory but other factors such as drug tolerance and seizure type may require higher concentrations. The elimination half-life of phenobarbital in children is 30 − 75 hours but it is considerably prolonged in neonates (100 − 200 hours) [2, 4, 5]. Phenobarbital distribution volume decreases with age with 0.9 − 1 L/kg reported for neonates (including premature) and infants of up to 4 months. For older children, the volume of distribution decreases to 0.45 − 0.7 L/kg [4]. The average clearance of phenobarbital in neonates is about 4.3 ml/h.kg whereas for older children (up to 12 years), a mean value of approximately 8 ml/h.kg is observed [6, 7].

Even though the long half-life permits once daily administration of phenobarbital, adverse effects associated with peak concentrations usually necessitate administration of multiple smaller doses instead. Tablets are unsuitable
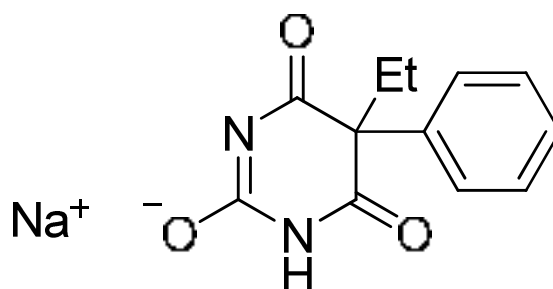
Figure 1: Chemical structure of phenobarbital sodium (M.W. 254.2, LogP 1.5, pKa 7.4).

for neonates and young children and the only other approved oral alternative is an elixir formulation which contains 38 % alcohol [8]. Regular administration of the elixir may potentially cause alcohol toxicity, especially to neonates [9]. Intravenous injections must be delivered slowly over 20 minutes otherwise shock, hypotension, and apnoea occur [1, 3, 5]. The only commercially available parenteral formulation of phenobarbital is also very concentrated (200 mg/ml) making accurate dilutions to suitable doses difficult for young infants and children. In addition, injections may cause extravasation due to the high pH (10 – 11) as well as the high osmolality of the injected solution [3].

Transdermal delivery of phenobarbital by passive diffusion has been previously suggested as an alternative route of administration [10]. Phenobarbital delivery was investigated (from an 8.6 mM drug dissolved in 100 % ethanol) across human epidermis excised from adults (45 ± 15 years), premature (29 – 35 weeks gestation age), and full-term neonates (37 – 40 weeks gestation age). While drug fluxes through full-term neonatal skin resembled that across adult skin (0.5 ± 0.1 nmol/h.cm^2), phenobarbital permeated at higher rates through premature skin and fluxes were inversely related to the gestational age of the neonate (Figure 2). The average flux was found to be around 1.8 ± 0.6 nmol/h.cm^2 and, assuming one-to-one *in vitro:in vivo* correlation, a 25 cm^2 transdermal patch was suggested by the authors to be suitable for a 1 kg premature baby to reach a target systemic concentration of about 14 nmol/ml. Two notes should be made about these findings: First, practical issues such as the use of ethanol as the solvent and a 25 cm^2/kg patch are clinically unacceptable for neonates because: 1) ethanol toxicity has been reported from percutaneous absorption of alcoholic cleaning products [11]; and 2) the body surface area of a 1 kg premature neonate is roughly 100 cm^2 [1], i.e., 4 times the suggested patch area without consideration of areas which are not suitable for patch application (e.g., head). The second point worth acknowledging was that the systemic concentration implied (14 nmol/ml) was lower than the recommended target for paediatric patients which is reported to be 60 – 180 nmol/ml [8]. It is also of importance to note that the skin samples tested from the premature group were from neonates born at 29 – 35 weeks of gestation.
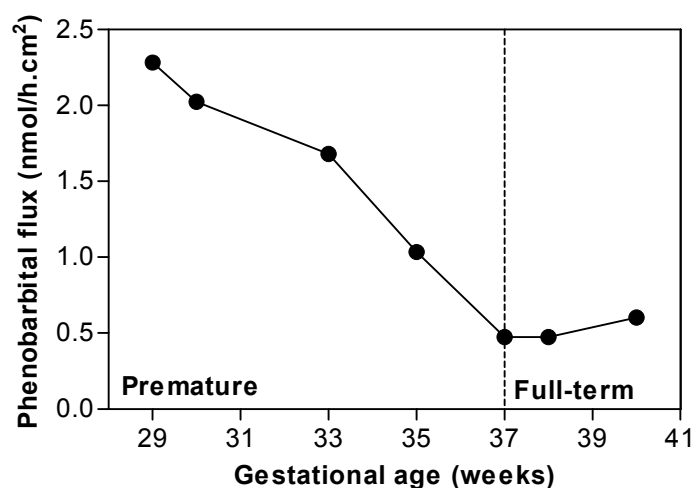
Figure 2: Phenobarbital delivery fluxes through human epidermis skin samples excised from premature and full-term neonates. Re-drawn from [10].

The latter range does not provide a complete representation of this age group because premature neonates born at a gestation age as low as 23 weeks survive (although the rate of survival is lower with lower gestation age). Overall, conditions at which this early study were run were not optimum and passive diffusion of phenobarbital is possibly not an efficient way to deliver the drug by the transdermal route.

The present study suggests an alternative and, perhaps, a better approach to the delivery of phenobarbital across both intact and premature skin. Using iontophoresis as a physical enhancement method, improved delivery of the drug is expected and smaller patch sizes should be needed to attain the target systemic levels. The sodium salt of the drug has increased aqueous solubility avoiding the need for the use of co-solvents such as ethanol. Barrier functions of intact and damaged (premature) skin were modelled *in vitro* using pig skin, whose stratum-corneum was differentially tape-stripped to provide a compromised barrier at different levels [12].

2. Materials and methods

2.1 Chemicals

Phenobarbital sodium, silver wire (99.99%), silver chloride (99.999%), sodium hydroxide pellets, and NaOH 50% solution (ion chromatography eluent grade) were purchased from Sigma Aldrich (Gillingham, UK). Potassium dihydrogen phosphate, 4-(2-hydroxyethyl)-1-piperazineethanesulfonic acid (HEPES) and sodium chloride were obtained from Acros (Geel, Belgium). Acetonitrile and hydrochloric acid were provided by Fisher Scientific (Loughborough, UK). All reagents were at least analytical grade and deionised water (resistivity ≥ 18.2 MΩ.cm, Barnsted Nanopure Diamond^{TM}, Dubuque, IA) was used for the preparation of all solutions.

2.2 Skin

Fresh pig skin was obtained from a local slaughterhouse, cleaned under cold running water, and stored in a refrigerator until the following day. Abdominal skin was dermatomed (Zimmer™ Electric Dermatome, Dover, Ohio; nominal thickness 750 μm),), cut into pieces of appropriate size, wrapped individually in Parafilm™, and then kept in a freezer (-20 °C) until use. Prior to the permeation experiment, the skin was thawed at room temperature for 30 minutes and visible hairs were carefully cut with scissors. The skin was either used as is or was tape-stripped, as described in chapter 4, to create different degrees of compromised skin. Three levels of barrier function impairment were studied: 20 – 40 % (Intermediate "less" barrier), 60 – 80 % (Intermediate "plus" barrier), and 100 % (fully compromised barrier). Between 13 and 23 tapes were needed to produce a fully compromised barrier.

2.3 Iontophoresis

Side-by-side two-compartment diffusion cells (active transport area = 0.78 cm^2, volume = 3.3 ml) were utilised in all experiments. The skin was mounted between the two chambers with the epidermal side oriented towards the cathode compartment. The receptor chamber always held 154 mM sodium chloride solution

(unbuffered, pH ~ 6). For 30 minutes prior to the start of the transport study, the skin was left in contact with the donor vehicle without drug, and 154 mM sodium chloride in the receptor chamber. Both compartments were then emptied and refilled with a donor solution containing phenobarbital and fresh receptor solution. Both compartments were magnetically stirred (Multipoint-6 stirrer, Thermo Scientific Variomag, Cole-Parmer, London, UK) at 300 rpm throughout the experiment. A direct constant current of 0.4 mA (0.5 mA/cm^2) was delivered from and a power supply (KEPCO 1000M, Flushing, NY, USA) using Ag/AgCl electrodes. Hourly samples (0.5 ml) of the receptor phase were withdrawn for analysis and replaced with fresh solution. Experiments which compared phenobarbital iontophoretic delivery through different skin barriers were additionally examined for passive permeation post-current termination. Separate passive diffusion controls (no current) through both intact and compromised skin were also performed. The experiments performed are summarised in Table 1.

Another set of investigations studied the effect of iontophoresis on the passive permeability of intact skin to phenobarbital. Prior to the permeation study and in the absence of phenobarbital (i.e. donor compartment contained water, pH 8.5, and receptor compartment contained unbuffered 154 mM NaCl), a 0.4 mA current was applied through the skin for 5 hours. At this point, the current was terminated and both compartments were then emptied and refilled with a donor solution containing phenobarbital and fresh receptor solution. Passive diffusion was then followed over 24 hours. To account for skin hydration effect, the same experiment was repeated but there was no electrical current in the 5 hour pre-treatment step.

2.4   Sample analysis

Quantification of phenobarbital was performed by high performance liquid chromatography with UV detection (215 nm). The method was modified from a previous publication [13] and used a Jasco HPLC system comprising a PU-980 pump with an AS-1595 autosampler, a UV-975 UV-VIS detector, and an Acclaim 120, C18 (150 x 4.6 mm, 5μm) reversed-phase column (Dionex, UK) which was thermostated

Table 1: Summary of experimental conditions performed to characterise phenobarbital transdermal delivery through intact and barrier impaired pig skin.

Skin barrier	Donor vehicle	Drug (mM)	Experiment settings and duration	n [a]
Intact	Water (pH 8.5 adjusted with HCl)	50	(1) Cathodal iontophoresis (5h), then passive diffusion [b] (5h)	3
			Passive diffusion (24h) [c]	3 – 4
	50 mM NaCl (pH 7.4 adjusted with HCl)	15	(2) Cathodal iontophoresis (5h)	4
			Anodal iontophoresis (5h)	4
			Passive diffusion (24h)	6
	Water (pH 7.4 adjusted with HCl)	15	(3) Cathodal iontophoresis (5h)	6
			(4) Cathodal iontophoresis (5h). Donor solution exchanged hourly [d]	5
	10 mM HEPES (pH 7.4)	15	(5) Cathodal iontophoresis (5h). Donor solution exchanged hourly [d]	5
Impaired: 20 – 40 % 60 – 80 % 100 %	Water (pH 8.5 adjusted with HCl)	50	Cathodal iontophoresis (5h), then passive diffusion [b] (5h)	4 5 3
			Passive diffusion (24h)	3 4 3

[a]: Number of replicates, [b]: Passive diffusion post-iontophoresis with the drug solution left in the donor chamber, [c]: Three passive diffusion experiments were performed. The skin was either used immediately in the permeation study or was subjected to a 5 hour pre-treatment step prior to the start of phenobarbital permeation experiment. The pre-treatment step was either with iontophoresis at 0.4 mA intensity or a hydration period with water in the donor chamber and 154 mM NaCl in the receptor compartment. [d]: The donor solution was exchanged hourly to minimise chloride ions released as a result of electrode electrochemical reactions.

at 30 °C. The mobile phase, pumped at 1 ml/min, consisted of phosphate buffer (0.067 M KH_2PO_4) and acetonitrile (70 : 30) and the pH was adjusted to 6 with NaOH.

Chloride was analysed by ion chromatography with suppressed conductivity detection. The method [14] used an IC system (Dionex, Sunnyvale, CA) comprising a GP-50 gradient pump, an AS-50 autosampler and thermal compartment, and an ED-50 electrochemical detector. The mobile phase, 35 mM NaOH, was pumped

isocratically (1ml/min flow rate) through a Dionex IonPac[TM] AS16 (250 x 4 mm) column thermostated at 30°C and connected to a Dionex ASRS Ultra II suppressor (4 mm) which was set at a current of 90 mA.

The validation parameters of phenobarbital and chloride analytical methods are found in Appendix (1E).

2.5   Data analysis and statistics

Data analysis and regressions were performed using Graph Pad Prism V.5.00 (Graph Pad Software Inc., CA, USA). Unless otherwise stated, data are represented as the mean ± standard deviation (SD). Transport fluxes were calculated as the amounts delivered per unit time. Comparisons made between different sets of data were assessed by either two-tailed unpaired t-test (for 2 groups) or one-way ANOVA (for > 2 groups) followed by Tukey's post-test. Fluxes at different times were compared by repeated-measures ANOVA followed by Tuckey's post-test. Statistical significance was set at $p < 0.05$.

The transference number (T) of phenobarbital was computed according to Faraday's law [15]:

$$T = \frac{J \times z \times F}{I}$$
Equation (1)

Where J is the drug flux observed, I is the current intensity applied, F is Faraday's constant, and z is the numerical value of the valence of the drug ion (= 1).

3. Results and discussion

3.1 Permeation across intact skin

3.1.1 Passive diffusion

The passive diffusion of phenobarbital across the skin was determined from a 50 mM aqueous solution of the sodium salt of the drug. Three permeation studies were performed using 1) untreated skin, 2) skin pre-treated with 0.4 mA current for 5 hours (phenobarbital absent), and 3) skin pre-hydrated for 5 hours (no phenobarbital). The third experiment served as a control for the second. Figure 3 shows the cumulative amount of drug permeated as a function of time. The cumulative amounts transported over 24 hours post-drug application were: 92 ± 34, 415 ± 125, and 222 ± 36 nmol/cm^2 for untreated, pre-iontophoresed, and pre-hydrated skin, respectively. Passive diffusion across pre-iontophoresed skin was significantly higher than through untreated ($p < 0.01$) and pre-hydrated ($p < 0.05$) skin. Increased permeability of skin previously exposed to direct current was reported previously [16].
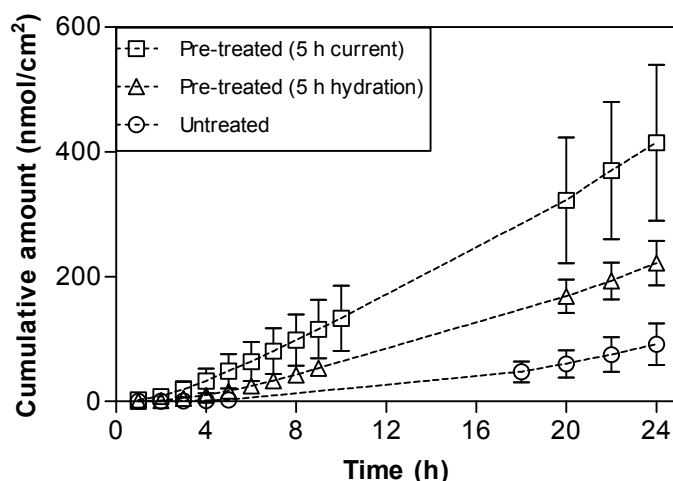
Figure 3: Passive diffusion of phenobarbital through untreated and pre-treated intact pig skin. Pre-treatment was either with 5 hours direct current at 0.4 mA intensity or 5 hours hydration. Phenobarbital was not present in the pre-treatment periods. Data are represented as the mean ± SD.

3.1.2 Iontophoretic delivery

The first iontophoresis study employed a simple drug donor of 50 mM sodium phenobarbital dissolved in water. The pH of this solution was 9.6 and was considered too alkaline for skin application. The pH was therefore reduced to 8.5 by the addition of HCl rendering phenobarbital ~ 93 % in the ionised form. Cathodal iontophoresis resulted in drug delivery which was nearly 400-fold higher than passive diffusion (Figure 4). After only 1 hour of current application, the phenobarbital flux was 222 ± 94 nmol/h, increasing to 387 ± 57 nmol/h by 3 hours; at the end of the experiment (5 h), the flux was 341 ± 65 nmol/h. It follows that iontophoretic fluxes reached relatively constant levels quickly after the start of iontophoresis suggesting the rapid achievement of stable phenobarbital delivery rates.
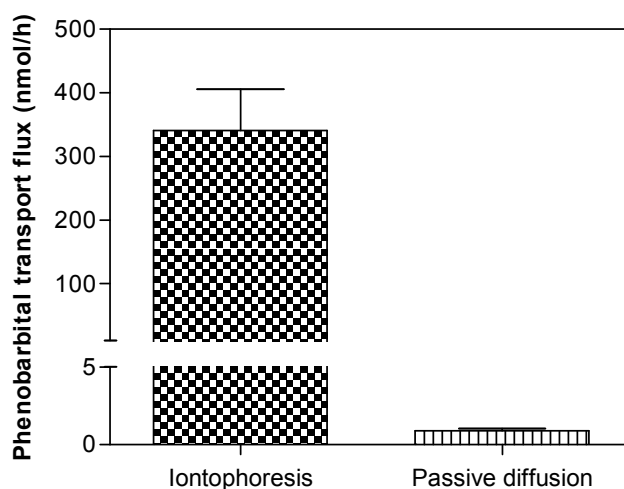
Figure 4: Passive and iontophoretic transport fluxes at 5 hours (mean ± SD) when phenobarbital was delivered from 50 mM drug solution in water (pH 8.5. 92.6 % of the drug is negatively charged).

3.1.3 Anodal *versus* cathodal delivery

A second set of iontophoresis experiments was performed with a donor pH of 7.4. The solubility of phenobarbital decreased at this pH and a lower drug concentration was used (15 mM). Both anodal and cathodal delivery were

investigated because at pH 7.4, phenobarbital (pKa 7.4) existed as equal concentrations of the negatively charged ions and the neutral form of the drug. This means that phenobarbital can be delivered by both electroosmosis (with anodal iontophoresis) and electromigration (with cathodal iontophoresis). A 50 mM NaCl solution was used as the donor vehicle to sustain the Ag/AgCl electrochemistry during anodal delivery. As shown in Figure 5, cathodal iontophoresis was much more efficient at transporting phenobarbital than anodal iontophoresis. When the contribution of passive diffusion was accounted for, the corrected cathodal and anodal fluxes at 5 hours were 42 ± 13 and 7.1 ± 3.8 nmol/h, respectively. This is, of course, because electromigration is a much more efficient transport mechanism than electroosmosis, as it has been previously observed. Merino *et al.* tested the anodal and cathodal delivery of the weak acid 5-fluorouracil (pKa 8) at various pH values [17]. The authors reported that at pH 8.5 (75 % of the drug was negatively charged) cathodal was much higher than anodal delivery. Moreover, even at pH 7.4 whereby only 25 % of the drug was negatively charged, rates of the drug delivered from either the anode or the cathode were of equal magnitude. Similarly, electromigration of phenytoin at pH 7.4, where only 11 % of the drug was negatively charged, resulted in similar transport rates as electroosmosis of the remaining 89 % present as the uncharged drug [18].
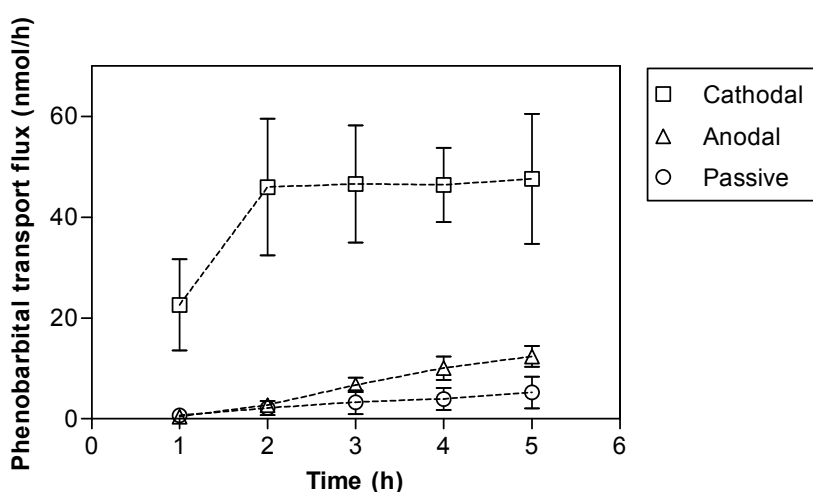
Figure 5: Passive diffusion, anodal, and cathodal iontophoresis of phenobarbital when delivered from 15 mM drug solution which also contained 50 mM NaCl. The final pH of the donor solution was 7.4. All data points represent the mean ± SD.

3.1.4   Co-ion competition

The cathodal delivery of phenobarbital was next optimised by minimising competition from the anions present in the donor solution. First, the background electrolyte in the donor solution (i.e. 50 mM NaCl) was removed. The second experiment, in addition to removal of NaCl, attempted to reduce the accumulation of the chloride ions which are gradually released from the cathode as a result of continuous reduction of the silver chloride under current flow. Accumulation was restricted by hourly replacement of the donor solution. The third experiment used 10 mM HEPES as a buffer for the donor solution instead of the unbuffered water. The buffer capacity when 15 mM phenobarbital sodium was added was sufficient that there was no need to adjust the pH to 7.4 with HCl which, in the preceding experiments, led to the introduction of chloride ions at a concentration of approximately 6 mM. Again, to avoid the build up of chloride ions released from the electrode, the donor solution was exchanged hourly. It is estimated that chloride ions, released each hour from the electrodes at 0.4 mA current, resulted in a concentration of 4.5 mM. Figure 6 sketches the evolution of chloride concentration in the donor formulation as a function of time of current application. Estimated values of chloride were similar to those measured experimentally by ion chromatography.
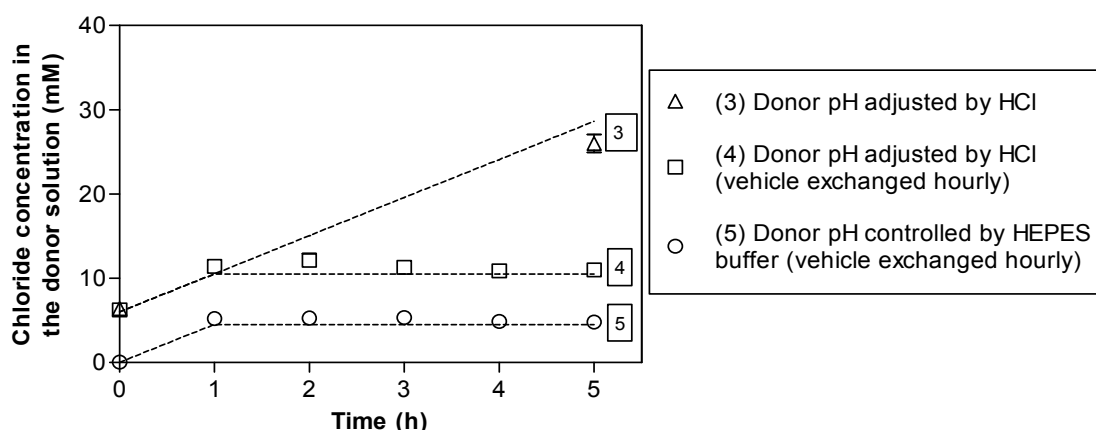
Figure 6: Estimated donor solution content of chloride ions (dashed lines) and corresponding experimental measurements by ion chromatography (represented by the symbols, mean ± SD). Estimated concentrations assumed that the chloride ions remained in the donor formulation. Conditions tested refer to experiments number 3, 4, and 5 in Table 1.

Phenobarbital delivery using the three improved experiments are compared to the un-optimised condition in Figure 7. In agreement with previous findings, the more co-ion competition present, the lower drug transport. The dependence of phenobarbital transference number (calculated using equation 1) to its molar fraction in the donor system is shown in Figure 8. As expected, a linear relation was observed with a slope equal to 0.033 ± 0.002 (r^2 0.79, $p < 0.0001$) and an intercept of 0.002 ± 0.001. From this relation, one can predict the maximal flux, which is obtained when the molar fraction of the drug is 100 %, to be 554 ± 30 nmol/h (equivalent to a transference number of 0.037 ± 0.002). As acknowledged in the previous chapter concerning the significantly different mobilities of hydronium and sodium ions, the mobility of HEPES anions is expected to be much smaller than chloride ions; and therefore adding the molar concentrations of the competing co-ions without consideration of significant mobility differences may introduce an artefact to the relation observed with the corresponding drug transference number.
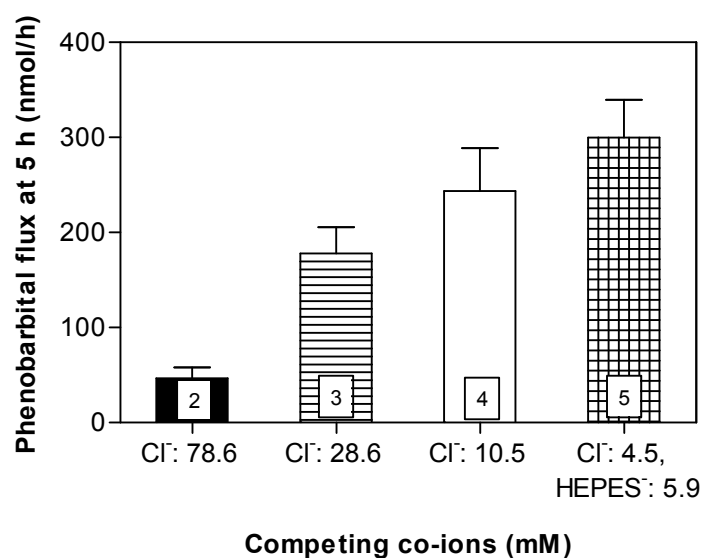
Figure 7: Phenobarbital transport from different donor vehicles (pH 7.4) which contained various amounts of competing co-ions (See experiments 2-5 in Table 1). The flux values (mean ± SD) represent the 5th hour of iontophoresis (0.4 mA). Drug concentration was 15 mM, half of which was negatively charged.
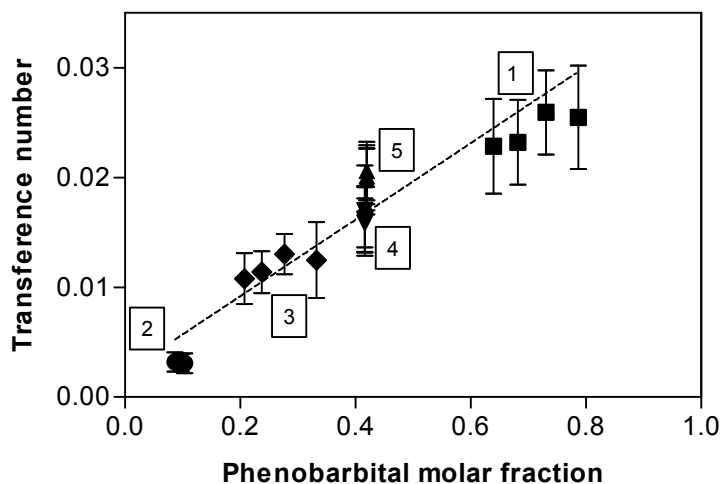
Figure 8: Transference numbers of phenobarbital (T, mean ± SD) as a function of its molar fraction (x). The latter parameter was calculated from the estimated molar concentrations of phenobarbital, HEPES, and chloride species. The sources for chloride ions included NaCl (used as background electrolyte), HCl (used to adjust the donor solution pH), and the electrode electrochemical reaction. Data expressed by the same symbol and number represent the same experimental conditions which are outlined in Table 1. The dashed line shows the linear regression of all data points. The corresponding equation for the best-fit linear regression is: $[T = 0.002(\pm0.001) + 0.035(\pm0.002)x]$ (r^2 = 0.79).

3.2 Permeation across compromised skin

The objective of this part of study was to examine the permeation of phenobarbital across barrier compromised skin. Three impaired levels of barrier function were evaluated against intact skin for passive as well as iontophoretic delivery of phenobarbital. The average TEWL measurement ($g/m^2.h$) for the different skin barriers was as follows: 11 ± 1, 44 ± 10, 114 ± 20, and 158 ± 25, respectively for intact, intermediate "less"(20 – 40 %), intermediate "plus" (60 – 80 %), and fully compromised skin. The TEWL values were significantly higher than what Sekkat *et al.* reported in the study which validated the usefulness of serially stripped pig skin as a model for the developing premature skin [12], and also a following study which applied this principal in the transdermal permeation of phenobarbital, caffeine, and lidocaine [13]. The discrepancies are by a factor of two for intact skin TEWL and a factor of four for fully compromised skin and are probably due to the different TEWL measurement devices employed in each study. While this study used a closed-chamber evaporimeter (AquaFlux AF102, Biox), the

previous work was performed with an open-chamber instrument (EP1, Servomed). The manufacturers of Aquaflux state that although closed and open chamber evaporimeters correlate well, the actual TEWL readings measured by each instrument disagree due to calibration differences used by different manufacturers. They estimate TEWL values from Aquaflux to be twice higher than an open-chamber device [19, 20]. These claims are well supported by publications highlighting disagreements of readings of TEWL probes from different manufacturers as well as from within the same manufactured model [21-23]. It is also worth noting that the discrepancies observed between the range of TEWL measurements and previously reported values may also be down to the fixed number of tapes (20 tapes) employed in the earlier studies which were deemed sufficient for removal of most of the stratum corneum. External factors such as the pressure applied when the tape is affixed to and removed from the skin can influence the amount of stratum corneum removed [24] and hence the TEWL readings.

The passive diffusion results are in Figure 9A. Permeation of phenobarbital increased dramatically as the stratum corneum was progressively removed. Flux after 5 hours diffusion through intact skin was only 0.9 ± 0.2 nmol/h but increased to 810 ± 251 nmol/h for fully compromised skin. Barriers with intermediate impairment levels were between the two extreme limits mentioned above. When only 20 – 40 % of the barrier efficiency was compromised, more phenobarbital permeated the skin and fluxes reached 31 ± 12 nmol/h. Skin with 60 – 80 % barrier deficiency was significantly less resistant to the permeation of phenobarbital and flux values of 561 ± 179 nmol/h were achieved after 5 hours passive diffusion.

A previous study [13] showed similar permeation rates of phenobarbital across intact full-thickness pig ear skin when delivered from a saturated solution of the unionised drug (4.3 mM, pH 5). Permeation through fully compromised skin was around 30 times higher than intact skin. In the present study, however, an enhancement factor of more than 900 fold was observed. Phenobarbital concentration used here was 50 mM of the salt form of the drug and most of it was ionised (only 3.7 mM was neutral).
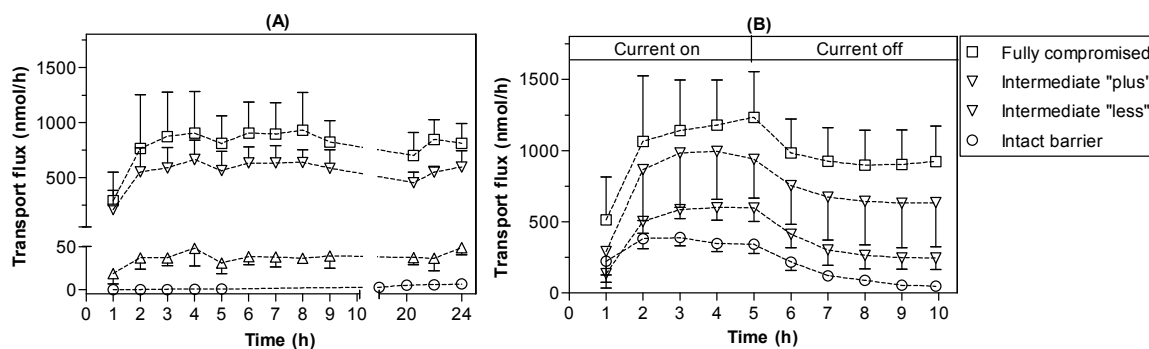
Figure 9: Passive (A) and Iontophoretic (B) transport fluxes (mean ± SD) of phenobarbital delivered from 50 mM drug solution through intact and compromised skin barriers. Graph (B) also include the passive diffusion of phenobarbital post-current termination.

Another study on a different drug showed similar permeation behaviour of 5-fluorouracil (LogP -1.0) when delivered from a pH 8.5 vehicle [25]. The drug (23 mM), 75 % of which was present as negatively charged ions, possessed small permeation through intact full thickness nude mouse skin (amount permeated after 6 hours was < 0.03 $\mu mol/cm^2$). When stratum-corneum stripped skin was used, however, significantly enhanced levels were observed and approximately 17 $\mu mol/cm^2$ permeated the skin after 6 hour diffusion (> 550 fold difference).

Iontophoretic delivery of phenobarbital through compromised skin barriers was next studied. Figure 9B depicts the flux rates during 5 hours iontophoresis (0.4 mA) followed by 5 hours diffusion in the absence of current application. Table 2 presents the fluxes during the last hour of the permeation studies. It was found that the total fluxes observed during iontophoresis increased with the level of skin impairment. There was a 3.6 fold enhancement, relative to intact skin, when the stratum corneum was completely removed. If the contribution of passive diffusion post-phenobarbital iontophoresis is accounted for in the total fluxes observed during iontophoresis, electrotransport fluxes are statistically indistinguishable between all skin barriers tested. It follows that while iontophoretic fluxes may have remained constant regardless of the skin barrier, passive diffusion increased remarkably with highly compromised skin and this undermined iontophoretic contribution and control over the overall transport.

Table 2: Transport fluxes of phenobarbital (in µmol/h, mean ± SD), through different barrier-impaired skin, measured after 5 hours of (1) iontophoresis, and (2) passive diffusion post-iontophoresis. The corrected fluxes (3) were calculated by subtracting (2) from (1).

Skin barrier	Iontophoresis[1]	Passive post-iontophoresis[2]	Corrected flux[3]
Intact	0.34 ± 0.06	0.05 ± 0.01	0.30 ± 0.07
Intermediate "less"	0.60 ± 0.09	0.24 ± 0.08	0.35 ± 0.08
Intermediate "plus"	0.94 ± 0.27	0.63 ± 0.31	0.31 ± 0.09
Fully compromised	1.23 ± 0.32	0.92 ± 0.25	0.31 ± 0.08

Finally, a summary of both passive and iontophoretic transport rates as a function of TEWL is shown in Figure 10. Similar to previous studies [13, 26, 27], the TEWL measurements, depicting the level of skin barrier function, were found to relate well to the passive diffusion of phenobarbital (r^2 0.85, $p < 0.0001$). Iontophoretic fluxes also showed good dependence to the respective TEWL readings of the skin barriers (r^2 0.82, $p < 0.0001$).

3.3 Feasibility of phenobarbital transdermal delivery

Maintenance of an effective systemic level of the anticonvulsant ensures successful seizure control. For phenobarbital, the target steady state concentration ranges between 60 – 180 nmol/ml depending on the response of the individual patient. Assuming one-to-one *in vitro*:*in vivo* correlation, the transdermal delivery of phenobarbital to neonates (including premature and full-term) is feasible. Permeation only by passive diffusion can be used for premature neonates with significantly immature skin (see Table 3 *A* and *B*). However, as the skin barrier of the neonate matures, iontophoresis is more effective at delivering desirable rates of phenobarbital with smaller patches than simply by passive diffusion (Table 3 *C*
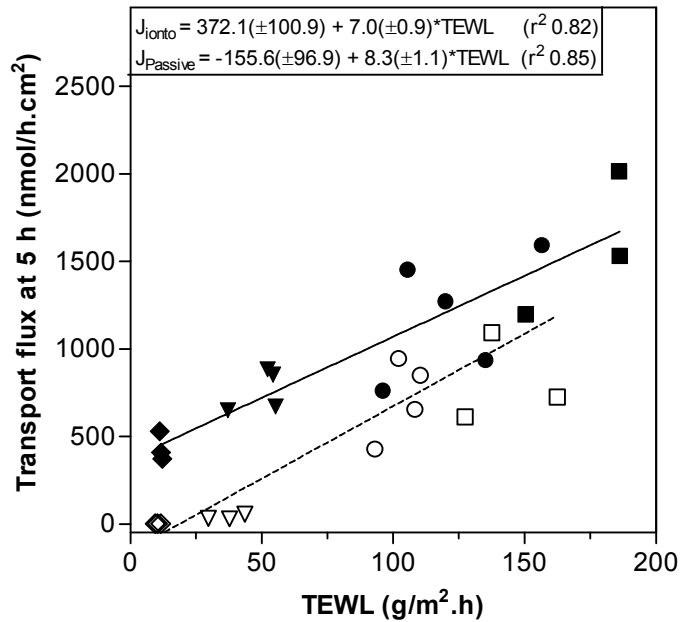
Figure 10: Relationship between the 5 hour transport fluxes of phenobarbital and TEWL values. Open symbols and discontinuous line refer to passive diffusion data and its linear regression. Filled bars and continuous line correspond to iontophoresis data and its linear regression. Intact, Intermediate "less" (20–40 %), intermediate "plus" (60–80 %) and fully compromised skin barrier are respectively symbolized by star, triangle, circle, and square bars.

and *D*). Due to the unpredictability of the precise degree of barrier immaturity of the premature neonate, it may be necessary for safety purposes to use transdermal patches with rate-limiting membranes to deliver phenobarbital. In this way, the maximum permeation rate is controlled by the patch and potential toxicity is avoided.

Iontophoresis can also be used to deliver therapeutic amounts of phenobarbital to infants over 1 month old to young children (Table 3 *E*). Older children, however, may not benefit from phenobarbital transdermal delivery because the requisite patch area becomes too large especially for those who require systemic concentrations at the higher end of the therapeutic window for phenobarbital. It is noteworthy to consider that the thickness of the skin used in this study (750 μm) meant a longer diffusion pathway for phenobarbital by the presence of a possible extra "barrier", the dermis, to the permeation of phenobarbital through the skin. Iontophoretic delivery of R-apomorphine (M.W.

267.3, LogP 2.3) [28] and 5-OH-DPAT (M.W. 247.4, LogP 2.2) [29] was found to decrease when transported across dermatomed human skin (200 – 300 μm) compared to its delivery through human stratum corneum. It is therefore possible that transport fluxes could be higher *in vivo* whereby the presence of blood vessels throughout the dermis which are in close proximity to the epidermal surface [30] may provide quicker and probably higher uptake of the drug into the systemic circulation. This study showed that steady fluxes of phenobarbital through pig skin are achieved in less than 2 hours. It is therefore anticipated that *in vivo*, a stable input rate of phenobarbital will be achieved quickly.

Table 3: The patch sizes required to achieve target systemic levels of phenobarbital in different groups of the paediatric population. Calculations assume a one-to-one *in vitro:in vivo* correlation

		Target input rate (μmol/h.kg)[1]	*In vitro* transdermal rates achieved[2] (μmol/h.cm^2)	Total area of patch required (cm^2/kg)
Neonate	Premature skin[3]	0.26 (but can be up to 0.77)	A) Fully compromised: Ionto: 1.5 ± 0.4 Passive: 1.1 ± 0.4	0.4 (1.1)[4] 0.2 (0.7)[5]
			B) Intermediate "plus": Ionto: 1.2 ± 0.4 Passive: 0.8 ± 0.2	0.4 (1.3)[4] 0.3 (1.0)[5]
			C) Intermediate "less": Ionto: 0.7 ± 0.1 Passive: 0.05 ± 0.02	0.7 (2.1)[4] 5.3 (15.8)[5]
	Intact skin		D) Ionto: 0.5 ± 0.1 Passive: negligible	1.1 (3.3)[4]
> 1 month – 12 years		0.5 – 1.4	E) Ionto: 0.5 ± 0.1 Passive: negligible	2.1 (6.2)[4]

[1]: calculated by multiplying the clearance by target steady state systemic concentration. [2]: fluxes are the average values of 2 – 5 hours of either iontophoresis (0.5 mA/cm^2) or passive diffusion, using 50 mM drug solution (pH 8.5). [3]: represented by data obtained with stratum corneum-stripped pig skin. [4]: area includes anode + cathode patches. [5]: represents one passive patch.

4. Chapter conclusions

This study demonstrated that cathodal iontophoresis of phenobarbital through intact skin is more efficient than anodal iontophoresis and passive diffusion. Competition from anions present in the donor formulation must be minimised to realise maximal effects of phenobarbital delivery. Premature babies with significantly compromised barrier function may benefit equally from passive patches due to their highly permeable skin. Paediatric patients with a more established skin barrier will however benefit significantly from the use iontophoresis to deliver therapeutic levels of phenobarbital.

5. References

1.   Avery, G. B., MacDonald, M. G., Seshia, M. M. K., and Mullett, M. D., *Avery's neonatology : Pathophysiology & management of the newborn*. 6th ed. 2005, Philadelphia: Lippincott Williams & Wilkins. 1748 p.

2.   Yaffe, S. J., and Aranda, J. V., *Neonatal and pediatric pharmacology : Therapeutic principles in practice*. 3rd ed. 2005, Philadelphia; London: Lippincott Williams & Wilkins. 938 p.

3.   Hey, E., *Neonatal formulary 5 : Drugs use in pregnancy and the first year of life*. 5th ed. 2007, Oxford: Blackwell. 309 p.

4.   Pellock, J. M., Dodson, W. E., and Bourgeois, B. F. D., *Pediatric epilepsy : Diagnosis and therapy*. 2nd ed. 2001, New York: Demos. 666 p.

5.   Sweetman, S. C., *Martindale : The complete drug reference*. 34th ed. 2005, London: Pharmaceutical Press. 2756 p.

6.   Touw, D. J., Graafland, O., Cranendonk, A., Vermeulen, R. J., and van Weissenbruch, M. M., *Clinical pharmacokinetics of phenobarbital in neonates.* Eur J Pharm Sci, 2000. **12**: p. 111-116.

7.   Bauer, L. A., *Applied clinical pharmacokinetics*. 2nd ed. 2008, New York; London: McGraw-Hill Medical. 826 p.

8.   *British national formulary for children 2008*. revised ed, ed. Martin, J. 2008, London: BMJ Group, RPS Publishing, and RCPCH Publications. 944 p.

9.   Colquhoun-Flannery, W., and Wheeler, R., *Treating neonatal jaundice with phenobarbitone - the inadvertent administration of significant doses of ethyl-alcohol.* Arch Dis Child, 1992. **67**: p. 152-152.

10.   Bonina, F. P., Montenegro, L., Micali, G., West, D. P., Palicharla, P., and Koch, R. L., *In-vitro percutaneous-absorption evaluation of phenobarbital through hairless mouse, adult and premature human skin.* Int J Pharm, 1993. **98**: p. 93-99.

11.   Harpin, V., and Rutter, N., *Percutaneous alcohol absorption and skin necrosis in a preterm infant.* Arch Dis Child, 1982. **57**: p. 477-479.

12.   Sekkat, N., Kalia, Y. N., and Guy, R. H., *Development of an in vitro model for premature neonatal skin: Biophysical characterization using transepidermal water loss.* J Pharm Sci, 2004. **93**: p. 2936-2940.

13.   Sekkat, N., Kalia, Y. N., and Guy, R. H., *Porcine ear skin as a model for the assessment of transdermal drug delivery to premature neonates.* Pharm Res, 2004. **21**: p. 1390-1397.

14.   Sylvestre, J. P., Diaz-Marin, C., Delgado-Charro, M. B., and Guy, R. H., *Iontophoresis of dexamethasone phosphate: Competition with chloride ions.* J Control Release, 2008. **131**: p. 41-46.

15.   Phipps, J. B., and Gyory, J. R., *Transdermal ion migration.* Adv Drug Del Rev, 1992. **9**: p. 137-176.

16.   Green, P., Shroot, B., Bernard, F., Pilgrim, W. R., and Guy, R. H., *In vitro and in vivo iontophoresis of a tripeptide across nude rat skin.* J Control Release, 1992. **20**: p. 209-217.

17.   Merino, V., Lopez, A., Kalia, Y. N., and Guy, R. H., *Electrorepulsion versus electroosmosis: Effect of ph on the iontophoretic flux of 5-fluorouracil.* Pharm Res, 1999. **16**: p. 758-761.

18.   Leboulanger, B., Guy, R. H., and Delgado-Charro, M. B., *Non-invasive monitoring of phenytoin by reverse iontophoresis.* Eur J Pharm Sci, 2004. **22**: p. 427-433.

19.   Packham, H., Gee, R., Stevens, M., Chilcott, R., Dalton, C., Stevens, A., and Weston, N. *Traceable calibration for tewl: Does it make a difference in practice?* US-Regional ISBS meeting,Orlando, FL. 2004 [access date 2009. 10/05]; Available from: http://www.biox.biz/Library/Conference/ConfContribDetails06.htm.

20.   Imhof, R. E. *How do aquaflux tewl measurements compare with conventional open-chamber measurements?*   [access date 2009. 10/05]; Available from: http://www.biox.biz/Support/FAQAnswer01.htm.

21.   Imhof, R. E., De Jesus, M. E., Xiao, P., Ciortea, L. I., and Berg, E. P., *Closed-chamber transepidermal water loss measurement: Microclimate, calibration and performance.* Int J Cosmet Sci, 2009. **31**: p. 97-118.

22.   Pinnagoda, J., Tupker, R. A., Coenraads, P. J., and Nater, J. P., *Comparability and reproducibility of the results of water loss measurements: A study of 4 evaporimeters.* Contact Dermatitis, 1989. **20**: p. 241-246.

23.   Fluhr, J. W., Feingold, K. R., and Elias, P. M., *Transepidermal water loss reflects permeability barrier status: Validation in human and rodent in vivo and ex vivo models.* Exp Dermatol, 2006. **15**: p. 483-492.

24.   Escobar-Chavez, J. J., Merino-Sanjuan, V., Lopez-Cervantes, M., Urban-Morlan, Z., Pinon-Segundo, E., Quintanar-Guerrero, D., and Ganem-Quintanar, A., *The tape-stripping technique as a method for drug quantification in skin.* J Pharm Pharm Sci, 2008. **11**: p. 104-130.

25.   Fang, J. Y., Hung, C. F., Fang, Y. P., and Chan, T. F., *Transdermal iontophoresis of 5-fluorouracil combined with electroporation and laser treatment.* Int J Pharm, 2004. **270**: p. 241-249.

26.   Cartwright, R. G., Cartlidge, P. H., Rutter, N., Melia, C. D., and Davis, S. S., *Transdermal delivery of theophylline to premature infants using a hydrogel disc system.* Br J Clin Pharmacol, 1990. **29**: p. 533-539.

27.   Levin, J., and Maibach, H., *The correlation between transepidermal water loss and percutaneous absorption: An overview.* J Control Release, 2005. **103**: p. 291-299.

28.   Van der Geest, R., Danhof, M., and Bodde, H. E., *Iontophoretic delivery of apomorphine. 1: In vitro optimization and validation.* Pharm Res, 1997. **14**: p. 1798-1803.

29.   Nugroho, A. K., Li, L., Dijkstra, D., Wikstrom, H., Danhof, M., and Bouwstra, J. A., *Transdermal iontophoresis of the dopamine agonist 5-oh-dpat in human skin in vitro.* J Control Release, 2005. **103**: p. 393-403.

30.   Braverman, I. M., *The cutaneous microcirculation.* J Invest Derm Symp P, 2000. **5**: p. 3-9.

Conclusion and perspectives

In this thesis, the use of transdermal iontophoresis in paediatric medicine was evaluated as an alternative to the oral and intravenous routes. More specifically, the feasibility of delivering three commonly used paediatric drugs, ranitidine, midazolam and phenobarbital, at therapeutic systemic levels were evaluated *in vitro*; and the potential for the clinical sampling of a renal marker, iohexol, through the skin was examined both *in vitro* and *in vivo* to evaluate the use of transdermal reverse iontophoresis as an alternative non-invasive method to blood sampling.

1. Drug delivery by transdermal iontophoresis

Ranitidine, midazolam, and phenobarbital transdermal delivery was investigated *in vitro* using dermatomed pig skin. The passive delivery of all drug candidates through intact skin was negligible relative to iontophoretic delivery. Findings from ranitidine and midazolam iontophoretic transport studies confirm the direct control current intensity has on the delivery rates of drugs. This allows for easy manipulation of the dose to be delivered. Data from the three drugs confirm the importance of drug molar fraction and pH of the driving electrode formulation. The former is optimised by maximising drug concentration and minimising co-ion presence. The latter improves delivery of cations by setting a pH value which ensures maximal ionisation of the drug, minimal competition from hydronium ions, and finally a higher net negative charge of the skin to ensure higher electroosmotic and electromigration fluxes. With respect to phenobarbital, delivery of the negatively charged drug ions by electromigration was superior than delivery of the neutral form at equivalent concentration. Hence, even though half of phenobarbital molecules are neutral at pH 7, iontophoretic transport by electromigration (cathodal) is more efficient than electroosmosis (anodal). Confirmed with ranitidine

transport findings, pluronic gels show to be suitable drug matrices for iontophoretic delivery applications.

Transdermal delivery of midazolam and phenobarbital was evaluated using both intact pig skin as well as barriers from which the stratum corneum had been stripped to different extents to model the less resistant skin of premature babies. Drug delivery through partially compromised skin barriers (up to 50 % barrier function impairment) was controlled by iontophoresis. Across highly compromised barrier, however, iontophoretic control was undermined by the very high passive contribution. Both passive and iontophoretic transport of midazolam and phenobarbital across different barrier functions showed good relation with the transepidermal water loss readings of the different skin barriers.

With assumption of one-to-one *in vitro:in vivo* correlation, therapeutic systemic doses can be achieved by transdermal iontophoresis using patch sizes of A) 0.2 – 1.5 cm^2/kg for ranitidine, B) 1 – 4 cm^2/kg (babies up to 6 months old) and 2 – 8 cm^2/kg (6 months old up to 12 years) for midazolam, and C) 0.4 – 3.3 cm^2/kg (neonates) and 2.1 – 6.2 cm^2/kg (infants to 12 years) for phenobarbital.

Overall, the *in vitro* iontophoretic delivery of ranitidine, midazolam, and phenobarbital show that iontophoresis could deliver therapeutically meaningful fluxes of the drugs. Further *in vitro* and *in vivo* work to explore these observations is now warranted. It is also recommended that due to the unpredictability of the precise degree of barrier immaturity in premature babies, it may be necessary for safety reasons to use rate-limiting membranes to control the maximum amounts of the drug that could transfer from the driving electrode formulation into the baby's skin. Finally, the solubility of midazolam at higher pH values requires further improvement. Not only this is beneficial for avoidance of skin irritation due to low pH, but also the iontophoretic delivery fluxes of the drug can be significantly increased at higher pH values. The use of cyclodextrins as solubilising agents is an attractive option as the solubility of midazolam has already been shown to increase with incorporation of cyclodextrin.

2. Clinical sampling by transdermal reverse iontophoresis

Iohexol is an exogenous kidney marker whose clearance is equivalent to the glomerular filtration rate (*GFR*). Blood samples withdrawn from the patient following a bolus injection of the marker are analysed for iohexol and the clearance is calculated from the plasma concentration data. In this thesis, the feasibility of using transdermal reverse iontophoresis, as an alternative to blood withdrawal, for sampling iohexol non-invasively was assessed both *in vitro* and *in vivo*.

Iohexol extraction fluxes *in vitro* correlated highly, after a period of lag time, to the subdermal concentrations of the marker. The lag time was modestly reduced by 1 hour following skin pre-treatment with 3 hours current application. Extraction data also permitted the prediction of the pharmacokinetic parameters of the simulated iohexol's subdermal concentration decay model. Most importantly was the estimation of the elimination rate constant which was remarkably similar to that calculated from the subdermal concentration data. Such high sensitivity of reverse iontophoresis to track instantaneous changes of the subdermal iohexol prompted the next step of performing an *in vivo* proof-of-concept study. Four children undergoing routine iohexol *GFR* test were recruited and reverse iontophoresis was performed simultaneously to the routine test. In agreement with *in vitro* findings, after a period of lag time, iohexol extraction fluxes tracked the changes in blood concentrations of the marker. Moreover, with the exception of one subject, estimation of the elimination rate constant from both sampling methodologies (blood *versus* skin) showed good agreement. These positive initial results warrant further exploration and validation in a larger study. Estimation of *GFR* by transdermal reverse iontophoresis will offer a great advantage over the current method (blood sampling). This was evidently apparent when feedback from all participants revealed their preference to having "skin sampling" over blood sampling. Points requiring improvement in future studies include optimisation of the iontophoresis collection compartments. In this study, a commercially available patch set originally designed for single-use drug delivery applications was used. The patch size, vehicle composition, and adhesive properties were all not optimised for

reverse iontophoretic application and for paediatric use. Alternative collection devices are therefore recommended with smaller areas, appropriate vehicle composition, and gentle-adhesive properties.

The development of a compact, fully portable all-in-one iontophoresis device for iohexol sampling is the ultimate product desired for use in children. For this to be made possible, further validation studies are needed coupled with significant improvement on the design of such "sampling kit".

Appendices

Appendix 1.

Analytical methods validation

parameters

Analysis of all compounds was performed with either high performance liquid chromatography (HPLC) with UV detection (iohexol, acetaminophen, ranitidine, midazolam, and phenobarbital) or ion chromatography (sodium and potassium). All validation parameters were obtained from a minimum number of replicate of 3. Specificity was always tested to exclude any peak interference from other compounds present in the permeation system (including the formulations used and possible molecules released from the skin). A minimum of 5 levels of standards spanning the linearity range was always used to obtain the calibration curves. Analysis of solutions from each skin permeation experiment involved running the full range of standards twice: at the beginning and at the end of each run.

A. Chapter 2, in vitro study: iohexol and acetaminophen

Iohexol

Linearity range (µg/ml)	0.1 – 250 (r > 0.99)		0.01 – 100 (r > 0.99)	
Injection volume (µl)	100		200	
Retention time (min)	6.4		6.3	
Accuracy (%)	50 µg/ml	102.2	50 µg/ml	101.7
	5 µg/ml	101.2	5 µg/ml	101.4
	0.5 µg/ml	98.9	0.5 µg/ml	101.5
Precision (Coefficient of variance)	50 µg/ml	0.61	50 µg/ml	0.08
	5 µg/ml	0.97	5 µg/ml	0.37
	0.5 µg/ml	0.79	0.5 µg/ml	0.30
Limit of quantitation (µg/ml)	0.1 (Accuracy: 101.4 %) (Precision: 1.02)		0.01 (Accuracy: 103.1 %) (Precision: 2.24)	

Acetaminophen

Linearity range (µg/ml)	0.025 – 100 (r > 0.99)	
Injection volume (µl)	100	
Retention time (min)	7.4	
Accuracy (%)	50 µg/ml	102.2
	5 µg/ml	101.9
	0.5 µg/ml	101.5
Precision (Coefficient of variance)	50 µg/ml	0.08
	5 µg/ml	0.28
	0.5 µg/ml	0.17
Limit of quantitation (µg/ml)	0.03 (Accuracy: 103.5 %) (Precision: 0.81)	

B. Chapter 2, in vivo study: iohexol, sodium, and potassium

Iohexol

Linearity range (µg/ml)	0.005 – 10 (r > 0.99)	
Injection volume (µl)	20	
Retention time (min)	5	
Accuracy (%)	10 µg/ml	100.6
	1 µg/ml	98.9
	0.1 µg/ml	104.03
Precision (Coefficient of variance)	10 µg/ml	0.09
	1 µg/ml	1.15
	0.1 µg/ml	3.57
Limit of quantitation (µg/ml)	0.005 (Accuracy: 122.6 %) (Precision: 14.11)	

Sodium and potassium

	Sodium		Potassium	
Linearity range (mM)	0.5 – 10 (r > 0.99)		0.05 – 10 (r > 0.99)	
Injection volume (µl)	5		5	
Retention time (min)	4.1		5.7	
Accuracy (%)	10 mM	99.3	10 mM	99.9
	5 mM	101.3	1 mM	102.2
	1 mM	108.7	0.1 mM	83.2
Precision (Coefficient of variance)	10 mM	2.23	10 mM	2.54
	5 mM	2.11	1 mM	6.18
	1 mM	2.78	0.1 mM	14.79
Limit of quantitation (mM)	0.5 (Accuracy: 112.9 %) (Precision: 9.83)		0.05 (Accuracy: 86.0 %) (Precision: 8.16)	

C. Chapter 3: ranitidine

Linearity range (µg/ml)	0.1 – 500 (r > 0.99)	
Injection volume (µl)	5	
Retention time (min)	2.5	
Accuracy (%)	500 µg/ml	100.1
	50 µg/ml	96.68
	5 µg/ml	99.76
Precision (Coefficient of variance)	500 µg/ml	0.54
	50 µg/ml	0.88
	5 µg/ml	1.90
Limit of quantitation (µg/ml)	0.1 (Accuracy: 104.1 %) (Precision: 2.56)	

D. Chapter 4: midazolam

Linearity range (µg/ml)	0.025 – 50 (r > 0.99)	
Injection volume (µl)	50	
Retention time (min)	6	
Accuracy (%)	25 µg/ml	100.7
	1 µg/ml	100.1
	0.025 µg/ml	98.8
Precision (Coefficient of variance)	25 µg/ml	0.32
	1 µg/ml	0.57
	0.025 µg/ml	0.92
Limit of quantitation (µg/ml)	0.025 (Accuracy: 98.8 %) (Precision: 0.92)	

E. Chapter 5: phenobarbital and chloride

Phenobarbital

Linearity range (µg/ml)	0.1 – 50 (r > 0.99)	
Injection volume (µl)	50	
Retention time (min)	6.4	
Accuracy (%)	50 µg/ml	101.3
	5 µg/ml	99.4
	0.5 µg/ml	101.7
Precision (Coefficient of variance)	50 µg/ml	0.47
	5 µg/ml	0.13
	0.5 µg/ml	0.45
Limit of quantitation (µg/ml)	0.1 (Accuracy: 97.2 %) (Precision: 2.20)	

Chloride

Linearity range (mM)	0.1 – 100 (r > 0.99)	
Injection volume (µl)	5	
Retention time (min)	4.1	
Accuracy (%)	100 mM	99.7
	10 mM	98.8
	1 mM	98.6
Precision (Coefficient of variance)	100 mM	1.51
	10 mM	1.96
	1 mM	8.26
Limit of quantitation (mM)	0.1 (Accuracy: 108.1 %) (Precision: 11.93)	

Appendix 2.

Ethics documents for the *in vivo*

iohexol study (Chapter 2)

Project proposal:

Assessment of kidney function: Non-invasive transdermal iontophoresis as an alternative to blood sampling in the iohexol GFR test

Investigators:

Dr. William van't Hoff (Principal Investigator)
Consultant Paediatric Nephrologist
Great Ormond Street Hospital
London WC1N 3JH
vanthw@gosh.nhs.uk

Dr. Penelope Brock
Consultant Paediatric Oncologist
Great Ormond Street Hospital
London WC1N 3JH

Ms. Renate Tulloh
Nurse Practitioner, Neuro-Oncology
Great Ormond Street Hospital
London WC1N 3JH

Ms. Asma Djabri
PhD Research Student
Dept of Pharmacy and Pharmacology
University of Bath

Prof. Richard H. Guy (Chief Investigator)
Head of Department, Professor of Pharmaceutical Sciences
Dept of Pharmacy and Pharmacology
University of Bath

Prof. Ian Wong
Professor of Paediatric Medicines Research
Director of Centre for Paediatric Pharmacy Research
School of Pharmacy
London

Dr. M. Begoña Delgado-Charro
Lecturer in Pharmaceutics
Dept of Pharmacy and Pharmacology
University of Bath

1. Background

Measurement of Glomerular filtration rate (GFR) is used as the best indicator of kidney function. GFR is measured using markers which are ideally completely cleared by the kidneys. There has always been ongoing research to improve GFR measurement and several markers have been used for this purpose [1]; with major limitations: creatinine, can give inaccurate estimation of GFR as its levels in the blood are affected by nutrition, diet, and muscle mass. Although traditionally regarded as the gold-standard for GFR estimation; inulin needs to be continuously administered by injection, and collection of timed urine samples is required in order to obtain correct GFR value. These make the use of inulin unpopular especially in children. Chromium EDTA, a radio-labelled marker, has been in use in Great Ormond Street Hospital for over 30 years. However, it proved to be impractical due to the expensive cost, the special requirements a hospital needs for the handling, storage, and disposal of such special radiation compounds, as well as the relatively large blood samples required (5ml).

Over the past twenty years, a new filtration marker, iohexol, has been increasingly gaining widespread use; and since July 2007, iohexol has replaced Chromium EDTA in Great Ormond Street Hospital (GOSH). This is due to its established safety record, cost effectiveness, reliability, accurateness, and being non-radioactive. It is claimed by many to be the "new" gold standard for GFR measurement. At GOSH, iohexol is administered as an intravenous bolus injection. Then, two to three blood samples, taken 3, 4 and 6 hours post-administration, are drawn from the patient to measure iohexol blood concentration which will give information on how well the kidneys are clearing iohexol [2]. So, the measured clearance of iohexol reports directly on the GFR and kidney function. However, the need for blood samples to correctly estimate iohexol clearance makes the procedure associated with various disadvantages; namely pain and discomfort to the patient; invasiveness, and risk of infection. Technical difficulties are also a major downside for blood sampling. All these limitations are even more significant in certain patient populations such as children. The less frequent sampling also makes GFR estimation less precise.

Thus, the need for less invasive, but still accurate, sampling techniques of iohexol, that lack the disadvantages of blood sampling, is highly desirable.

One possibility is transdermal "iontophoresis", whereby the application of a small electrical current across the skin is used to facilitate the active transport of molecules present in the subdermal fluid (the fluid that bathes the cell layers below the outer layer of the skin) from inside the body into the surface of the skin at levels much higher than those of their passive transport [3]. The subdermal fluid is in direct communication with blood and can therefore serve as a good alternative sampling matrix.

We are interested in performing our study in children because of the sensitivity that many children have about blood sampling. A non-invasive technique might be particularly appealing to them.

Figure 1. Example of an iontophoretic system: Phoresor® II auto device (power supply) connected to Iogel® small patches (IOMED, Salt Lake city, Utah, USA). Each pair of patches is composed of a karaya gel dispersive pad (the square pad) and a hydratable gel-sponge patch (the oval patch).

Transdermal iontophoresis has been used in our laboratory (Pharmacy department, University of Bath) for many years and in previous human studies, we have demonstrated the usefulness of this technique for glucose sampling [4, 5],

lithium monitoring in bipolar patients [6], urea sampling for the diagnosis and monitoring of chronic kidney disease [7], lactate [8] and various amino-acids [9].

The Glucowatch[®] Biographer (approved for both adults and children in the USA) [10] is an iontophoretic device used to continuously monitor glucose levels in diabetics by sampling glucose over 12 hours per day and therefore providing a superior amount of information, regarding glucose levels, over the traditional finger-prick technique.

Iontophoresis is a safe technique and several devices are approved and available commercially for both drug delivery and monitoring, e.g. Phoresor[®] II auto (figure 1) for various iontophoresis applications, LidoSite[TM] system which delivers lidocaine for induction of local anaesthesia, Ionsys[TM] for delivery of fentanyl to relief post-operative pain, Macroduct[®] (approved for neonates, children and adults and used routinely in Great Ormond Street Hospital) for delivery of pilocarpine to diagnose cystic fibrosis, and, as mentioned above, the Glucowatch[®] Biographer approved for glucose monitoring.

The iontophoretic system is typically composed of an external power-supply that passes current through two patches (Anode and cathode) (figure 1). The square pad represents the anode patch and is composed of a silver/silver chloride electrode incorporated in a karaya gel dispersive pad. The oval-shaped patch represents the cathode and is composed of a silver chloride electrode integrated in a hydratable gel-sponge patch. The dry gel in the oval patch is wetted with water before it is attached to the skin.

Our *in vitro* studies performed with pig skin (a good model for human skin) show excellent correlation between Iohexol iontophoretic sampling levels with the corresponding subdermal concentrations. Two different simulated models (mono- and bi-exponential) of iohexol elimination have been tested and confirmed that, after a period of 2.5 hours lag time needed for the conditioning of the skin, transdermal sampling of iohexol by iontophoresis followed closely its subdermal concentration (figure 2).
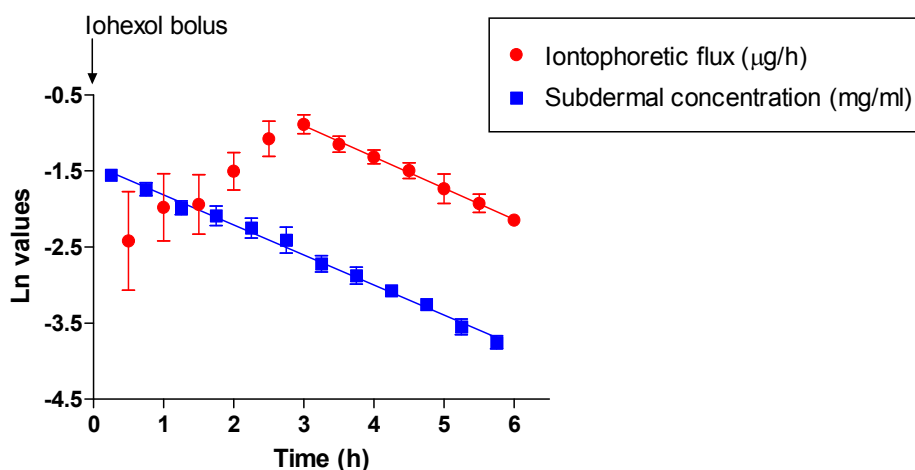
Figure 2. Iohexol subdermal concentration (mg/ml) and iontophoretic sampling flux (μg/h) as a function of time (Mean ± SD)

In clinical practice, estimation of GFR is made possible by the calculated pharmacokinetic parameters of iohexol, which depict a guide to how the body handles iohexol. The most important pharmacokinetic parameters used for GFR estimation are: Elimination rate constant of iohexol (K_e), calculated from the slope of iohexol log concentration-time profile and iohexol initial concentration at time 0 (C_0), measured by back-extrapolating the log values of iohexol concentration-time profile. From these two parameters, the volume of distribution of iohexol (V_d) and therefore its clearance (Cl) are calculated following these equations:

$$V_d = \text{Administered dose of iohexol}/C_0$$

$$Cl = K_e \cdot V_d$$

GFR of the patient is then estimated from the corrected iohexol clearance. This correction is made to account for some errors arising from the less frequent blood samples which are not sufficient for a complete profiling of iohexol concentration over time.

Our *in vitro* experiments show that pharmacokinetic parameters estimated from iohexol subdermal concentration data correlated well to those calculated from the transdermal iontophoresis sampling data (table 1). Similar correlations were also found in a previous *in vitro* study with lithium [11].

Table 1. Iohexol pharmacokinetic parameters estimated from its subdermal concentration data and iontophoretic sampling data (K_e: elimination rate constant; C_0: subdermal concentration of iohexol at time 0; V_d: volume of distribution, Cl: clearance)

Parameter / Data source	$r^2 \geq$	K_e (h^{-1})	C_0 (mg/ml)	V_d (ml)	Cl (ml/h)
Subdermal	0.98	0.37 ± 0.01	0.29 ± 0.02	4.02 ± 0.28	1.51 ± 0.14
Iontophoresis	0.94	0.41 ± 0.03	0.36 ± 0.08	3.26 ± 0.63	1.34 ± 0.17

2. Objectives

The principal objective of this study is to assess the feasibility of using transdermal iontophoresis, as an alternative approach to blood sampling, for the clinical monitoring of kidney function, using iohexol as the filtration marker.

Data obtained from iohexol skin sampling, using iontophoresis, will be used to evaluate its association to that of the blood sampling approach. Pharmacokinetic parameters of Iohexol, estimated from both sampling techniques will then be compared to confirm if there is correlation.

3. Protocol

We plan to recruit 12 children undergoing routine iohexol GFR test (see section 5 for calculation of sample size). At GOSH, approximately 1000 children have a routine GFR test each year. We intend to carry out transdermal iontophoresis in parallel to the routine GFR test to compare values obtained from both sampling procedures. Usually, the routine GFR test takes between 4 and 6 hours. Participation in the study is for around 6 to 6.5 hours and will take place in the same ward and at the same time as the participant's routine GFR test.

The iontophoresis device

The study will be carried out using an approved (CE mark) current device, the "Phoresor® II auto" (Model: PM850, Iomed, Salt Lake city, Utah, USA. Figure 1), already in the market for more than 10 years and used for iontophoresis in hospitals and health clinics for both adults and children. The device has safety features, which will automatically activate upon, for example, an increase in the resistance of the current circuit above a pre-set limit. The device is also fully controllable manually and the current could be stopped at any time should, for example, the volunteer decides to withdraw from the study for any reason. Prior to use in the Trust, the device will be checked for electrical safety by the Department of Biomedical Engineering at Great Ormond Street Hospital.

The Phoresor® II device is a small, light and portable machine. A strap-worn pouch, to carry the device, will be used to make participation in this study more comfortable.

The device will be cleansed thoroughly with alcoholic wipes before and after each study.

Experimental protocol:

1)   A minimum of 24 hours (for inpatients) or 2 weeks (for outpatients) is given to potential participants and their parents to read the participant information sheets and decide on whether they would like to take part in the study. They are encouraged to ask any questions and full explanation of all steps involved is provided to them. The participant as well as the parent will be requested to inform us if the child suffers from any skin condition, such as eczema, or has irritated or damaged skin. Informed consent from the parent and child (as appropriate to age and understanding) will be taken.

2)   Upon participant and parent positive consent, a special code number instead of the participant's name is used throughout the study to make participation completely confidential. The consent form is the only document which includes both the participant name as well as the allocated code number. All

consent forms will be stored in a locked cabinet and only the local collaborators will have access to it.

3) During the 12 hours before the study's commencement, the participant is required not to apply any cosmetic products, such as creams, onto the arm used in the study.

4) Iontophoresis is performed on the non-dominant arm of the participant. The arm is first cleansed with a routine alcohol wipe and then allowed to dry naturally.

5) The iontophoresis system is composed of the Phoresor® II device and two electrode patches (a square dispersive pad and an oval gel-sponge patch). After hydration of the oval patch with 1.5 ml sterile water for injection, the square pad and the hydrated oval patch are affixed onto the arm of the participant. The Phoresor® II device is then connected to the electrodes and is set to precisely deliver 0.8 mA of constant direct current (~0.1 mA/cm^2).

6) In total, current is passed for 5 hours starting 0.5 hours after the volunteer receives their routine intravenous dose of iohexol. Both patches are replaced with new ones after 2 and 4 hours of current passage. The oval patch is additionally replaced at 3 hours (see illustration below). So, a total of 7 patches are used. Each time we do a patch exchange, we stop the current briefly.

7) The used patches are stored in coded containers in a secured laboratory for up to 6 months for analysis.

8) When analysis is performed, each oval patch is extracted with water and then analysed for iohexol. Other normal body substances such as salts (e.g. sodium) and sugars may also be measured but no foreign substances such as drugs will be looked at.
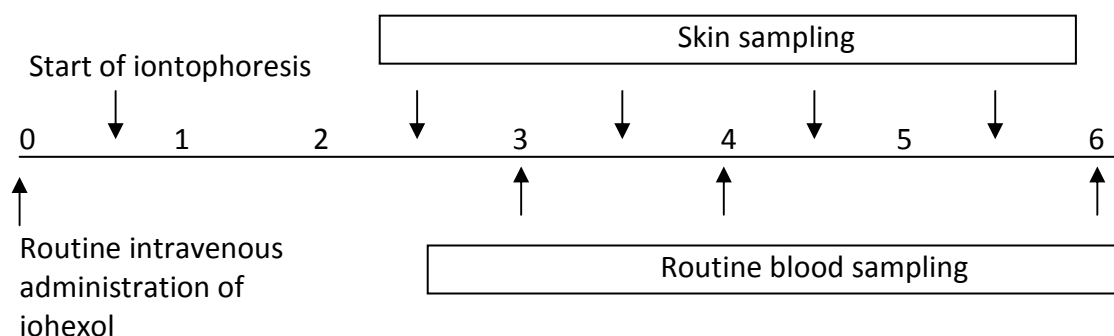
9) During the study, the participant can mobilise but the researcher will accompany the participant throughout the study. As the study is performed on the non-dominant arm, the participant is able to use the other arm freely. So, the participant can, for example, go to the play room, read, and write. We will make sure the participant is kept entertained during the study and they can choose to watch their favourite cartoons and DVDs or read their favourite books.

10) A comfort-break is allowed at any time during the study. Unless the participant is already restricted from food/drink due to their routine hospital care, our study has no restrictions.

11) Participants may experience some mild tingling and heat sensation, especially at the start of iontophoresis. Redness may also appear at the site of iontophoresis but tends to disappear after a few days (figure 3). Upon positive consent from the participant and their parents, photographs of only the participant's arm will be taken before and after the study to show the effect of iontophoresis on the skin.

Redness/sensitisation may also occur as a result of the adhesive material of the patches.

12) If the participant is in discomfort, or decides to withdraw from the study at any time and for any reason, the study will be stopped immediately. The procedure will be undertaken in wards staffed by nurses with skills to act appropriately in the unlikely event that the participant feels unwell during the study.

13) Upon completion of the experiment, the participant will be asked to complete a short questionnaire, using the Wong-Baker faces pain scale, to evaluate the level of discomfort/tingling sensation they have experienced during the study. They will also be asked whether they prefer transdermal iontophoresis over blood sampling.

14) Feedback with the results obtained from the iontophoresis sampling technique will be provided to the participant and parents should they wish to find out the outcome of their individual participation. A summary of the main findings and/or published reports will also be provided upon request.
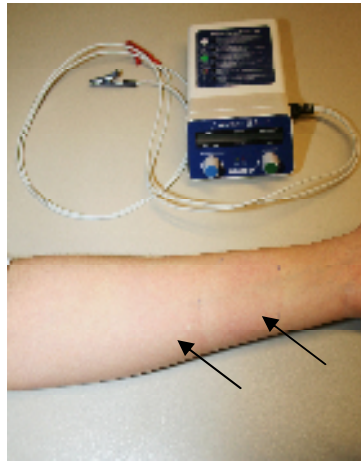
Figure 3. Example of redness occurring after iontophoresis

4. Data analysis

Data obtained from iohexol skin sampling, using iontophoresis, will be used to evaluate its association to that of the blood sampling technique. Regression analysis will be performed to assess the linearity of the data obtained. The slope of the regression line and iohexol pharmacokinetic parameters will be calculated from the skin sampling data. Subsequently, GFR values will be estimated from the pharmacokinetic data. Agreement of values obtained from the two sampling methods (skin and blood) will be assessed using the method of Bland and Altman [12].

5. Calculation of sample size:

Statistical input was obtained from Dr. Gavin Shaddick, a senior lecturer in statistics at the University of Bath.

The hypothesis supported by the *in vitro* studies, is that the slopes corresponding to the semi logarithmic plasma concentration versus time and the semi logarithmic iontophoretic flux versus time profiles are the same. If this hypothesis were proved to be true, then the slope obtained non-invasively could be used instead of that obtained via blood sampling for the assessment of kidney function.

The statistical calculations relate to the ability to detect a difference between two slopes; the first corresponding to the iohexol plasma concentration values and obtained using measurements at different sampling times, the second corresponding to the iohexol iontophoretic fluxes. The aim of the study is to determine whether these two slopes are the same, which translates in terms of statistical testing into accepting a null hypothesis of no difference between the two slopes. The interpretation of a power calculation in this case would be to find the smallest difference at which a true difference could be detected, the smaller this difference the more confidence that a true finding is not being overlooked because of a small sample size.

The results of the power calculations assume that the slopes are normally distributed and use a significance level of 5%. The difference is expressed in a percentage change of a *0.4 h^{-1} slope* which is representative of values found in the clinical setting (range 0.1-0.7 h^{-1}). The standard deviation is an estimate of the standard deviation of the differences between the two slopes. Results for a suitable range for both of these are presented, with the expected standard deviation being approximately 0.06.

Using a sample of 12 individuals, 80% power can be achieved with the ability to detect down to a 15% difference. However, it is expected that some participants will not complete the study, for example if they experience discomfort or restlessness through the 5-6 hours sampling process. Obtaining data from 10 individuals means that 80% power can be achieved in all but the most extreme estimate of standard deviation. A sample size of less than 10 sees power drop and only larger differences being detected. However, a difference of 20-25% between the slopes could be detected (depending on the standard deviation) even if half of the participants did not complete their participation (n=6). Differences between the slopes greater than 25% would be considered unacceptable for practical applications and the use of transdermal iontophoresis for this purpose would be no longer pursued. Thus, even when n=6, the main objective of this study, deciding on the feasibility of the technique, could be accomplished.

6. Funding

The salary costs for the researcher are paid by a grant from the Algerian government sponsoring her PhD studentship. Purchase of the iontophoresis device and consumables is covered by existing external grants. As this study takes place in parallel and for the same duration as the routine clinical GFR test, no patient expenses are anticipated.

Involvement of Trust staff (Drs. van't Hoff, Brock and Ms. Tulloh) is principally limited to advice, recruitment, consent and supervision. Dr van't Hoff has additional involvement as Principal investigator; this time is within his funded role as the Director of Clinical Research Facility.

7. References

[1] Schwartz, G.J. and Furth, S.L. *Glomerular filtration rate measurement and estimation in chronic kidney disease*. Pediatric Nephrology 22 (2007) 1839-1848.

[2] Wilks, Z.; Standing, J. and Van't Hoff, W. *Clinical guideline. Glomerular filtration rate measurement: Iohexol^{TM} method* [online]. London: Great Ormond Street Hospital.   Available   from: http://www.ich.ucl.ac.uk/clinical_information/clinical_guidelines/cpg_guideline_00 063/ [Accessed 24 January 2008].

[3] Leboulanger, B.; Guy, R.H. and Delgado-Charro, M.B. *Reverse iontophoresis for non-invasive transdermal monitoring*. Physiological Measurement 25 (2004) R35-R50.

[4] Sieg, A.; Guy, R.H. and Delgado-Charro, M.B. *Noninvasive glucose monitoring by reverse iontophoresis in vivo: application of the internal standard concept*. Clinical Chemistry 50 (2004) 1383-1390

[5] Sieg, A.; Guy, R.H. and Delgado-Charro, M.B. *Simultaneous extraction of urea and glucose by reverse iontophoresis in vivo*. Pharmaceutical Research 21 (2004) 1805-1815.

[6] Leboulanger, B.; Aubry, J.M.; Bondolfi, G.; Guy, R.H. and Delgado-Charro, M.B. *Lithium monitoring by reverse iontophoresis in vivo.* Clinical Chemistry 50 (2004) 2091-2100.

[7] Wascotte, V.; Rozet, E.; Salvaterra, A.; Hubert, P.; Jadoul, M.; Guy, R.H.; Préat, V. *Non-invasive diagnosis and monitoring of chronic kidney disease by reverse iontophoresis of urea in vivo*. European Journal of Pharmaceutics and Biopharmaceutics (2008), doi:10.1016/j.ejpb.2008.02.012 (in press)

[8] Nixon, S.; Sieg, A.; Delgado-Charro, M.B. and Guy, R.H. *Reverse iontophoresis of L-lactate: In vitro and in vivo studies.* Journal of Pharmaceutical Sciences 96 (2007) 3457-3465.

[9] Jeanneret, F. *Etude du liquide interstitiel cutané comme matrice alternative lors de suivi thérapeutique: couplage LC-MS pour l'analyse des acides aminés extraits par ionophorèse inverse in vitro et in vivo*. PhD Thesis (2004). University of Geneva. Geneva.

[10] Tierney, M.J.; Tamada, J.A.; Potts, R.O.; Jovanovic, L.; Garg, S. and Cygnus Research Team. *Clinical evaluation of the GlucoWatch® biographer: a continual, non-invasive glucose monitor for patients with diabetes.* Biosensors and Bioelectronics 16 (2001) 621-629.

[11] Leboulanger, B.; Fathi, M.; Guy, R.H. and Delgado-Charro, M.B. *Reverse iontophoresis as a noninvasive tool for lithium monitoring and pharmacokinetic profiling.* Pharmaceutical Research 21 (2004) 1214-1222.

[12] Bland, J.M.; Altman, D.G. *Statistical methods for assessing agreement between two methods of clinical measurement.* Lancet i (1986) 307-310.

Great Ormond Street **NHS**
Hospital for Children
NHS Trust

Great Ormond Street
London WC1N 3JH

Tel: 020 7405 9200

Parent/Guardian invitation letter: Can we monitor your child's kidney function without the need of blood samples?

Date

Dear …..

The doctors taking care of your child at Great Ormond Street Hospital have decided he/she needs to have their kidney function checked. They will do this by injecting a special dye called "iohexol". Then, they check your child's kidney function by taking two to three blood samples from them.

We are writing to inform you of some new and exciting project taking place at the hospital. It is about the possible use of an alternative non-invasive sampling method for measuring your child's kidney function. We would like to ask your permission to involve your child in this project to compare our technique, "iontophoresis", with the conventional blood sampling. Our proposed project will be carried out in the same ward and at the same time as the child's routine kidney test. Enclosed with this letter are two participant information sheets (one for you and one for your child). Please read them and if you and your child are happy to participate with us, please fill in the reply slip and return it in the pre-paid envelope.

Looking forward to hearing from you.

Yours Sincerely,

Dr. William Van't Hoff BSc, MD, FRCPCH.
Consultant Paediatric Nephrologist, Great Ormond Street Hospital for Children

Great Ormond Street **NHS**
Hospital for Children
NHS Trust

Great Ormond Street
London WC1N 3JH

Tel: 020 7405 9200

Can we monitor your child's kidney function without the need of

blood samples?

Reply Slip

Dear Dr. Van't Hoff,

My child and I have read the information sheets about your proposed study which is taking place at Great Ormond Street Hospital.

We would like to know more information ☐

(Please tick as appropriate)

We would like to participate ☐

Signed ………………………………………………… Date …………………………..

Name (BLOCK LETTERS) …………………………………………………………………...

Great Ormond Street **NHS**
Hospital for Children
NHS Trust

Great Ormond Street
London WC1N 3JH

Tel: 020 7405 9200

Can we monitor your child's kidney function without the need of blood samples?

Information sheet for the legal representative of the child

The doctors taking care of your child have decided he/she needs to have their kidney function checked. They will do this by injecting a special dye called "iohexol". Then, they check your child's kidney function by taking two to three blood samples from them. We are currently doing a project to try to find an alternative non-invasive technique which does not need blood sampling. It is called "iontophoresis" and it works via the skin. We would like to ask your permission to include your child in this project to compare our technique "iontophoresis" with the conventional blood sampling.

Before you decide, it is important for you to understand why the study is being done and what it will involve. Please take time to read the following information carefully and discuss it with others if you wish. Please ask us if there is anything that is not clear or if you would like more information. Take time to decide whether or not you wish your child to take part in this study.

1. Why is this project being done?

We are looking at an alternative sampling for the method for monitoring kidney function. This is because the current conventional method, i.e. blood sampling, has many disadvantages, particularly pain and discomfort to the patient; invasiveness, and risk of infection. These inconveniences are even worse in children

because of the sensitivity that many children have about blood sampling. In addition, the conventional blood sampling technique relies only on two to three samples. This may not be sufficient to precisely estimate how well your child's kidneys work.

We, therefore, propose in our study a non-invasive alternative technique to blood sampling that does not use needles. Our aim is to examine whether our proposed technique, iontophoresis, can at least estimate kidney function as accurately as blood sampling.

Iontophoresis involves the application of a very small electrical current across two parts of the skin already covered with two patches. The current passage facilitates the transport of iohexol (the dye used to monitor kidney function) from inside the body into the patches situated at the surface of the skin. By doing this, we can measure iohexol amounts in the patches at several intervals and an accurate but non-invasive estimation of kidney function could be made possible.

2. Why have you asked my child to help?

The doctors taking care of your child have decided he/she needs to have their kidney function checked as part of their routine hospital care. To do so, they will use the conventional blood sampling technique. We would like to examine whether our technique, iontophoresis, could prove to be an accurate, non-invasive alternative. We can only do this by comparing results obtained from the conventional blood sampling with those from our alternative technique.

3. Does my child have to take part?

No. Taking part in the study is entirely voluntary. We fully understand that people may be unable or unwilling to participate. If you do not want your child to take part, you do not have to give a reason. This will not affect your child's treatment in any way.

You and your child may withdraw at any time during the study. You can choose not to answer the questionnaire. Samples obtained from your child will be treated as a gift but you have the right to ask for them to be removed from the study at any time.

4. How will my child be involved?

Please let us know if your child suffers from any skin condition, such as eczema, or has irritated or damaged skin.

Our proposed project is planned to be carried out in parallel to the routine kidney test that is requested by your child's doctors.

Usually, the routine kidney test takes between 4 and 6 hours. Participation in our study is for around 6 to 6.5 hours and will take place in the same ward and at the same time as the routine kidney test of your child.

We require that no cosmetic products, such as creams, are applied to your child's arms during the 12 hours before the study's commencement.

The child's non-dominant arm is first cleansed with a routine alcohol wipe and then allowed to dry.

The iontophoresis system (figure 1) is composed of the current device (a sophisticated battery) and two electrode patches (a square dispersive pad and an oval gel-sponge patch). The battery is a small, light and portable machine. A strap-worn pouch, to carry the device, will be used to make your child's participation in this study more comfortable.

Figure 1. Example of an iontophoresis system

After hydration of the oval patch with 1.5 ml sterile water, the square pad and the hydrated oval patch are attached onto the arm of your child. The battery is then connected to the electrodes and set to deliver a small current.

In total, current is passed for 5 hours starting half an hour after your child receives their routine intravenous dose of iohexol, as part of their routine care.

Both patches are replaced with new ones after 2 and 4 hours of current passage. The oval patch is additionally replaced at 3 hours. So, a total of 7 patches are used. Each time we do a patch exchange, we stop the current briefly.

The used patches are then examined to give us information about iohexol collected by iontophoresis. We only look for specific compounds (i.e. iohexol and normal sugars and salts present in the body) and we will not look at anything else such as drugs.

During participation with us, your child can mobilise but the researcher will accompany your child throughout the study. As our study is performed on the non-dominant arm, your child is able to use the other arm freely. So your child can, for example, go to the play room, read, and write. We will make sure your child is kept entertained during the study and they can choose to watch their favourite cartoons and DVDs or read their favourite books.

Your child is allowed to go to the toilet at any time during the study.

Unless your child is already restricted from food/drink due to their routine hospital care, our study has no restrictions.

Once we finish the study, we will ask your child to answer a short questionnaire about the level of discomfort/ tingling sensation experienced during the study. They will also be asked whether they prefer iontophoresis over blood sampling.

Feedback with the results obtained from the study will be provided to you and your child should you wish to find out the outcome of your child's participation. A summary of the main findings and/or published reports will also be provided upon request.

If any step of the study is unclear to you, or if you have any questions please contact us for more information.

5. Will there be any effects on my child's routine treatment?

No, the study will not affect your child's routine treatment in any form.

6. Will there be any side effects?

Iontophoresis is considered a safe technique with several devices approved and available commercially. It is used in hospitals, including Great Ormond Street Hospital, for both adults and children.

The current device used in our project has a CE mark which means that it has passed all the safety tests needed. It also means that it is licensed for use in humans.

Your child may experience slight tingling and heat sensation (especially at the start of iontophoresis). Redness may also appear at the sites of iontophoresis (figure 2) but tends to disappear after a few days.

Redness/sensitisation may also occur as a result of the adhesive material of the patches.
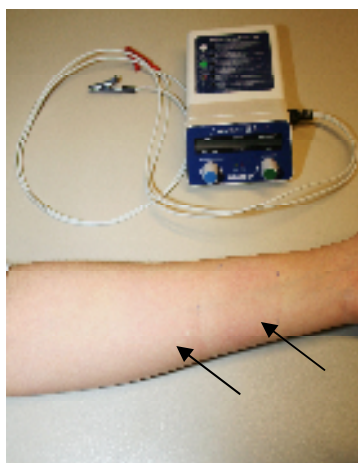
Figure 2. Example of redness occurring after iontophoresis.

If you or your child find any of the side effects uncomfortable or unacceptable, or decide to withdraw for any reason, the study will be stopped immediately.

Medical staff will also be present to take appropriate action in case your child feels unwell during the study.

7. What are the arrangements for compensation?

This project has been approved by Great Ormond Street Hospital for Children NHS Trust Research Ethics Committee. The committee believes that this project is fair and of minimal risk to your child. However, research can carry unexpected risks and we want you to be informed of your rights in the unlikely event that any harm should occur as a result of your child's participation.

This project is covered by the University of Bath insurance policy (NHE-05CA07-0013). This includes potential legal liability for harm to your child arising from the management and/or the design of the research. In addition, cover for compensation in the event of harm to your child, where no legal liability arises, can be claimed.

8. Will there be any benefits for taking part?

There is no immediate benefit to your child. If the results of this study are promising; then a potentially non-invasive alternative sampling technique for monitoring kidney function is on the horizon. This, in turn, could make an end to the traditional invasive blood sampling. This would benefit children in particular, as it will give an accurate estimation of kidney function without all the disadvantages associated with blood sampling.

9. Will anyone else be told about my child's participation in the study?

We will keep all of your child's information confidential. This means we will only tell those who have a need or right to know. With your positive consent, your child's family doctor will be informed of their participation.

10. Who will have access to my child's information?

All information collected during the study (data collection, processing, and storage) will be treated in strict confidence. No names, initials, or any type of information that could result in your child's identification will be mentioned in any reports of the study.

Throughout the study, we use a special code number instead of your child's name to make their participation in this study completely confidential.

All data information will be stored and analysed in computers secured with a password and only the research team involved in this study will have access to it.

Upon your positive consent, we will take some photographs of your child's arm before and after the study to show the effect of iontophoresis on the skin. The photographs will only include the arm.

11. Who do I speak to if I have further questions, worries, or complaints?

If you have any questions, comments, enquiries, or complaints about this project, please contact either Ms. Asma Djabri (A.Djabri@bath.ac.uk, 01225383900) or Dr. William Van't Hoff (VANTHW@gosh.nhs.uk, 02074059200 ext. 5583/5930).

If you have any unresolved issues, please contact the chairman of the Research Ethics Committee by post via the Research and Development Office, Institute of Child Health, 30 Guilford Street, London WC1N 3EH or, if urgent, by telephone on 020 7905 2620 and the Committee administration will put you in touch with him.

Thank you for your interest in this study- please ask us any questions

Great Ormond Street **NHS**
Hospital for Children
NHS Trust

Great Ormond Street
London WC1N 3JH

Tel: 020 7405 9200

Can we monitor your kidney function without the need of blood samples?

Information sheet for participants aged over 12 years

The doctors taking care of you have decided you need to have your kidney function checked. They will do this by injecting a special dye called "iohexol". Then, they check your kidney function by taking two to three blood samples from you. We are currently doing a project to try to find an alternative non-invasive technique which does not need blood sampling. It is called "iontophoresis" and it works via the skin. We would like to ask you and your parents for permission for you to participate in this project to compare our technique "iontophoresis" with the conventional blood sampling.

Take time to decide if you want to say YES or NO to this. Please read this information carefully. Don't worry if you don't understand it straight away. Your parents have also been told about this, and you can ask them to help you understand.

1. Why is this project being done?

We are looking at an alternative sampling method for monitoring kidney function. This is because the current conventional method, i.e. blood sampling, has many disadvantages and relies only on two to three blood samples which may not be sufficient to estimate precisely how well your kidneys work.

We, therefore, propose in our study a non-invasive alternative technique to blood sampling. Our aim is to examine whether our proposed technique, iontophoresis, can at least estimate kidney function as accurately as blood sampling.

Iontophoresis involves the application of a very small electrical current across two parts of the skin already covered with two patches. The current passage facilitates the transport of iohexol (the dye used to monitor kidney function) from inside the body into the patches situated at the surface of the skin. By doing this, we can measure iohexol amounts in the patches at several intervals and an accurate but less invasive estimation of kidney function could be made possible.

2. Why have you asked me to help?

The doctors taking care of you have decided you need to have your kidney function checked as part of your routine hospital care. To do so, they will use the conventional blood sampling technique. We would like to examine whether our technique, iontophoresis, could prove to be an accurate, non-invasive alternative. We can only do this by comparing results obtained from the conventional blood sampling technique with those from our alternative technique.

3. Do I have to take part?

No. Taking part in the study is entirely voluntary. We fully understand that people may be unable or unwilling to participate. If you do not want to take part, you do not have to give a reason. This will not affect your treatment in any way.

You and your parents may withdraw at any time during the study. You can choose not to answer the questionnaire. Samples obtained from you will be treated as a gift but you have the right to ask for them to be removed from the study at any time.

4. How will I be involved?

Please let us know if you suffer from any skin condition, such as eczema, or have irritated or damaged skin.

Our proposed project is planned to be carried out in parallel to the routine kidney test requested by your doctors.

Usually, the routine kidney test takes between 4 and 6 hours. Participation in our study is for around 6 to 6.5 hours and will take place in the same ward and at the same time as your routine kidney test.

We require that no cosmetic products, such as creams, are applied to your arms during the 12 hours before the study's commencement.

Our study will be done on one of your arms. We will choose the one that you use less often. We, first, cleanse it with an alcohol wipe and then leave it to dry.

The iontophoresis system (Picture 1) is composed of the current device (a sophisticated battery) and two electrode patches (a square dispersive pad and an oval gel-sponge patch). As you can see from the picture, the battery is very small and light and it can be carried in a pouch.

Picture 1. Example of an iontophoresis system

Firstly, we attach the square pad and the hydrated oval patch onto your arm. We will then connect the battery to these patches and set it to deliver a small current.

In total, current is passed for 5 hours starting half an hour after iohexol dose was administered to you as part of your routine treatment.

Both patches are replaced with new ones after 2 and 4 hours of current passage. The oval patch is also replaced at 3 hours. So, a total of 7 patches are used. Each time we do a patch exchange, we stop the current briefly.

Then, we examine these patches to give us information about iohexol. We only look for specific compounds (i.e. iohexol and normal sugars and salts present in the body) and we will not look at anything else such as drugs.

During participation with us, you can mobilise but the researcher will accompany you throughout the study. As our study is performed on the arm you use least, you are able to use the other arm freely. So you can, for example, go to the play room, read, and write. We will make sure you are kept entertained during the study and you can choose to watch your favourite cartoons and DVDs or read your favourite books.

You are allowed to go to the toilet at any time during your participation.

Unless you are already restricted from food/drink due to your routine hospital care, our study has no restrictions.

Once we finish the study, we will ask you to answer a short questionnaire about the levels of discomfort and tingling sensation you have experienced during the study. You will also be asked whether you prefer iontophoresis over blood sampling.

Results obtained from the study will be provided to you and your parents should you wish to find out the outcome of your participation.

If any step of the study is unclear to you or if you have any questions please talk to your parents and/or contact us for more information.

5. Will there be any effects on my routine treatment?

No, the study will not affect your treatment in any form.

6. Will there be any side effects?

Iontophoresis is considered a safe technique, with several devices used in hospitals, including Great Ormond Street Hospital, for both adults and children.

You may experience slight tingling and heat sensation (especially at the start of study). Redness may also appear on the skin sites below the patches (Picture 2)
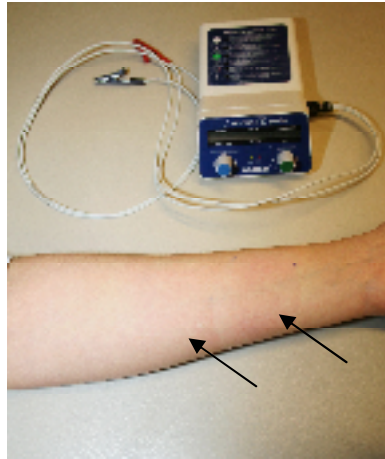
Picture 2. Example of redness occurring after iontophoresis.

but tends to disappear after a few days. Redness may also occur as a result of the adhesive material of the patches.

If you find any of the side effects uncomfortable or unacceptable, or decide to withdraw for no reason, the study will be stopped immediately.

Medical staff will also be present to take appropriate action in case you feel unwell during the study.

If you are worried about any of the side effects please talk to your parents or to us.

7. What are the arrangements for compensation?

This project has been approved by Great Ormond Street Hospital for Children NHS Trust Research Ethics Committee. The committee believes that this project is fair and of minimal risk to you. However, research can carry unexpected risks and we want you to be informed of your rights in the unlikely event that any harm should occur as a result of your participation.

This project is covered by the University of Bath insurance policy (NHE-05CA07-0013). This includes potential legal liability for harm to you arising from the management and/or the design of the research. In addition, cover for compensation in the event of harm, where no legal liability arises, can be claimed.

8. Will there be any benefits for taking part?

There is no immediate benefit to you. If the results of this study are promising; then a potentially non-invasive alternative method for monitoring kidney function is on the horizon. This could make an end to the traditional invasive blood sampling and could benefit children in particular, as it will give an accurate estimation of kidney function without all the disadvantages associated with blood sampling.

9. Will anyone else be told about my participation in the study?

We will keep all of your information confidential. This means we will only tell those who have a need or right to know. Your parents and family doctor will be informed of your participation.

10. Who will have access to my information?

As a patient, you have rights regarding medical information recorded about you.

All your personal information collected during the study (data collection, processing, and storage) will be treated in strict confidence. No names, initials, or any type of information that could result in your identification will be mentioned in any reports of the study.

Throughout the study, we use a special code number instead of your name to make your participation in this study completely confidential.

All data information will be stored and analysed in computers secured with a password and only the research team involved in this study will have access to it.

With your agreement, we will take some photographs of your arm before and after the study to show the effect of iontophoresis on the skin. The photographs will only include your arm.

11. Who do I speak to if I have further questions, worries, or complaints?

If you have any questions, comments, enquiries, or complaints about this project, please talk to your parents or contact either Ms. Asma Djabri

(A.Djabri@bath.ac.uk, 01225383900) or Dr. William Van't Hoff (VANTHW@gosh.nhs.uk, 02074059200 ext. 5583/5930).

Thank you for your interest in this study- please ask us any questions

Great Ormond Street NHS
Hospital for Children
NHS Trust

Great Ormond Street
London WC1N 3JH

Tel: 020 7405 9200

Can we monitor your kidney function without the need of blood samples?

Information sheet for children aged between 8 and 11 years

❖ Your doctors have decided they want to check your kidneys using a special dye called "iohexol". They do this by taking some blood samples from you. We are working all the time to improve this technique to see if we can better check your kidneys without the need of blood samples. Our alternative technique is called "iontophoresis". We ask you and your parents for permission for you to participate in this project.

❖ Take time to decide if you want to say YES or NO to this. Please read this information. Don't worry if you don't understand it straight away. Your parents have also been told about this, and you can ask them to help you understand.

1) Why are you doing this?

❖ We want to see if we can monitor your kidneys with our technique. If our technique gives good results, blood sampling could be replaced in the future.

2) Why have you asked me?

❖ We ask children who are going to have their kidneys tested to participate.

3) What will be different for you?

❖ If you agree, the project will be done during your routine kidney test that you are already booked in for. It will start half an hour after your routine test begins and will be carried out in the same ward.

❖ As part of your routine hospital care, your doctors will test your kidneys by administering the dye and then taking 2 to 3 blood samples from you. This usually takes between 4 and 6 hours.

❖ Your participation with us takes around 6 to 6.5 hours.

❖ In our project, we attach two sticky sponges on your skin. These sponges look like sticky band-aid (See picture 1).

Picture 1

❖ Then, we connect the sponges to a small battery which will deliver a small current to your skin. We then keep changing these sponges for 5 hours.

❖ We will use the arm you use least. This means that you can use the other arm freely to play, write…etc.

❖ You can also go to the play room with one of our project team. We will keep you entertained and you can watch your favourite DVDs and cartoons. We can also read you your favourite story book.

❖ You are allowed to go to the toilet at any time. Food and drink are allowed in our project unless you are already restricted by your other treatments.

4) Do I have to participate?

❖ No, it is completely up to you and your parents. Whether you say YES or NO, your present or future treatment will not be affected at all.

5) Is it dangerous?

❖ No, but you may feel slight tingling and sense some heat especially at the start of project. Redness may also appear on the skin below the sponges (Picture 2) but it usually disappears after a few days.
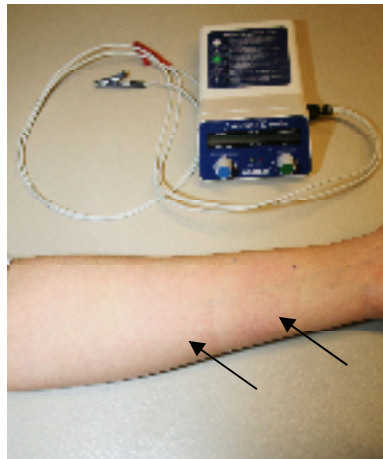
Picture 2

❖ But if you don't like something, we will stop straight away. At the end we will ask you some questions about how you felt during your participation with us.

6) Who can I speak to if I have any questions?

❖ We have given more information to your parents about what we are doing. If you have any questions, speak to your parents, or to the doctors or nurses in the ward.

Thank you for your interest in this study- please ask us any questions

Great Ormond Street **NHS**
Hospital for Children
NHS Trust

Great Ormond Street
London WC1N 3JH

Tel: 020 7405 9200

Can we monitor your kidney function without the need of blood samples?

Information sheet for children aged less than 8 years

❖ Your doctors want to check how good your kidneys are by using a special dye. They do this by taking some blood samples from you. We want to improve this method. Therefore, we ask you and your parents for permission to help us and participate in our mission.

❖ Your routine test usually takes between 4 and 6 hours. If you are happy to help us, we need your participation for 6 to 6.5 hours. We start our mission at the same time as your routine test.

❖ This picture shows how you can help:

❖ We will attach two sticky sponges on your skin. These sponges look like sticky band-aid.

❖ We connect these sponges to a small battery. We then keep changing the sponges for 5 hours.

❖ We will use the arm you use least. This means that you can use the other arm freely to play, write…etc.

❖ You can also go to the play room with one of our mission team (Asma, see her photo below). You can watch your favourite DVDs and cartoons. We can also read you your favourite story book.

❖ You can go to the toilet at any time. Food and drink are allowed unless you are already restricted by your other treatments.

❖ You may feel some tingling and heat under the sponges. But if you don't like it, we will stop everything at any time you want.

❖ At the end, we will ask you some questions about how you felt during your participation with us.

❖ We have given a lot more information to your mum and dad. So please ask them if you don't understand something.

Thank you for your interest in this study- please ask us any questions

Great Ormond Street **NHS**
Hospital for Children
NHS Trust

Great Ormond Street
London WC1N 3JH

Tel: 020 7405 9200

Can we monitor your child's kidney function without the need of blood samples?

Consent form for the legal representative of the child

The legal representative of the child should complete the whole of this sheet himself/herself: (Please circle one of the answers)

1. Have you read the Participant information sheet (legal representative)? (Please keep one)	YES/NO
2. Have you had a chance to discuss the study and had satisfactory answers to all of your questions?	YES/NO
3. Do you understand that you are free to withdraw your child from the study at any time, without having to give any reason, and without affecting any of their future medical care or legal rights?	YES/NO
4. Do you give permission for photographs of your child's arm to be taken during the study?	YES/NO
5. Do you give permission for the researcher to inform your child's GP of his/her participation in the study?	YES/NO
6. Do you give your permission for the research team involved in this study to have access to your child's anonymised clinical samples and data?	YES/NO

7. Have you had enough time to come to your decision?   YES/NO

8. Do you agree to your child taking part in the study?   YES/NO

LEGAL REPRESENTATIVE OF: ……………………………………………………………………………....

Participant identification code ………………………………………………………………………....

Signature ………………………………………….. Date …………………………………………………....

Name (BLOCK LETTERS)……………………………………………………………………………………....

INVESTIGATOR

I have explained the study to the above legal representative and he/she has indicated his/her willingness for his/her child to take part.

Signature ………………………………………….. Date …………………………………………………....

Name (BLOCK LETTERS)……………………………………………………………………………………....

Great Ormond Street **NHS**
Hospital for Children
NHS Trust

Great Ormond Street
London WC1N 3JH

Tel: 020 7405 9200

Can we monitor your kidney function without the need of blood samples?

Assent form for Participants

The participant should complete the whole of this sheet himself/herself. If the child is too young to read, this form should be read to the child by their legal representative and then completed by them on their behalf.

(Please circle one of the answers)

1. I have read (or had read to me) the participant information sheet (Please keep one)	YES	NO
2. The doctors and my parents have explained everything to me	YES	NO
3. I have had the opportunity to ask questions and I understand the answers	YES	NO
4. I understand what is being asked in this project	YES	NO
5. I know that I can stop participating in this study at any time	YES	NO
6. I am happy for photographs of my arm to be taken	YES	NO
7. I agree to my GP being informed of my participation in the study	YES	NO
8. I am happy to take part in the study	YES	NO

PARTICIPANT

Signature …………………………………………….. Date …………………………………………….......

Name (BLOCK LETTERS)…………………………………………………………………………………….

Participant identification code ……………………………………………………………………..

INVESTIGATOR

I have explained the study to the above participant and he/she has indicated his/her willingness to take part.

Signature …………………………………………….. Date ……………………………….........................

Name (BLOCK LETTERS)………………………………………………………………………….............

Great Ormond Street **NHS**
Hospital for Children
NHS Trust

Great Ormond Street
London WC1N 3JH

Tel: 020 7405 9200

Can we monitor your kidney function without the need of blood samples?

Questionnaire

Participant identification code:

1. Please circle one of the following faces which expresses the level of tingling sensation and discomfort felt in your skin during the study:

a) Square pad

| 0 | 1 | 2 | 3 | 4 | 5 |
| NO HURT | HURTS LITTLE BIT | HURTS LITTLE MORE | HURTS EVEN MORE | HURTS WHOLE LOT | HURTS WORST |

b) Oval patch

| 0 | 1 | 2 | 3 | 4 | 5 |
| NO HURT | HURTS LITTLE BIT | HURTS LITTLE MORE | HURTS EVEN MORE | HURTS WHOLE LOT | HURTS WORST |
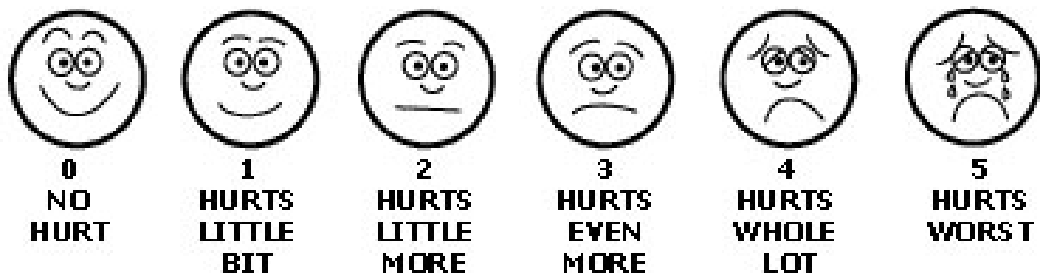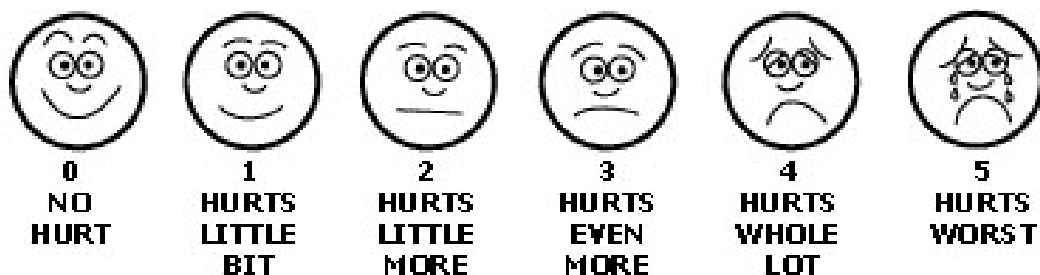
2. Which one do you prefer?

Skin sampling   OR   Blood sampling

Thank you for your participation!

Great Ormond Street NHS Hospital for Children

NHS Trust

Great Ormond Street
London WC1N 3JH

Tel: 020 7405 9200

Assessment of kidney function: Non-invasive transdermal Iontophoresis as an alternative to blood sampling in the iohexol GFR test

Date

Dear Dr.

We are trying to recruit paediatric volunteers for our investigation of the possible use of transdermal iontophoresis as a sampling technique for iohexol, a marker used to estimate the glomerular filtration rate. The study is carried out at Great Ormond Street Hospital for Children, London.

Our primary aim is to assess the feasibility of using transdermal iontophoresis, as an alternative approach to blood sampling of iohexol. Glomerular filtration rate estimated from both techniques will be compared to determine any correlation. If this study proves its validity, a potentially non-invasive method for the monitoring of kidney function could be possible.

Your patient: --- and his legal representative have agreed to participate in the study and I am writing to inform you of their participation.

Yours Sincerely,

Dr. William Van't Hoff BSc, MD, FRCPCH.
Consultant Paediatric Nephrologist
Great Ormond Street Hospital for Children

Great Ormond Street **NHS**
Hospital for Children
NHS Trust

Great Ormond Street
London WC1N 3JH

Tel: 020 7405 9200

Assessment of kidney function: Non-invasive transdermal iontophoresis as an alternative to blood sampling in the iohexol GFR test
Information sheet for the GP of the participant

We are trying to recruit paediatric volunteers for our investigation of the possible use of transdermal iontophoresis as a non-invasive alternative to blood sampling in the iohexol GFR test.

Transdermal iontophoresis involves the application of a small electrical current across the skin. This is used to facilitate the active transport of molecules present in the subdermal fluid from inside the body into the surface of the skin at levels much higher than those of their passive transport. The subdermal fluid is in direct communication with blood and can therefore serve as a good alternative sampling matrix.

We plan to recruit paediatric volunteers, to whom iohexol is going to be administered and sampled intravenously as part of their normal hospital care, and we intend to carry out transdermal iontophoresis in parallel to compare values obtained from both sampling procedures. Usually, the routine kidney function test takes between 4 and 6 hours.

Participation in the study is for around 6 to 6.5 hours and will take place in the same ward as the participant's routine GFR test.

The participant as well as the parent will be requested to inform us if the child suffers from any skin condition, such as eczema, or has irritated or damaged skin.

The study will be carried out using an approved (CE mark) current device, the
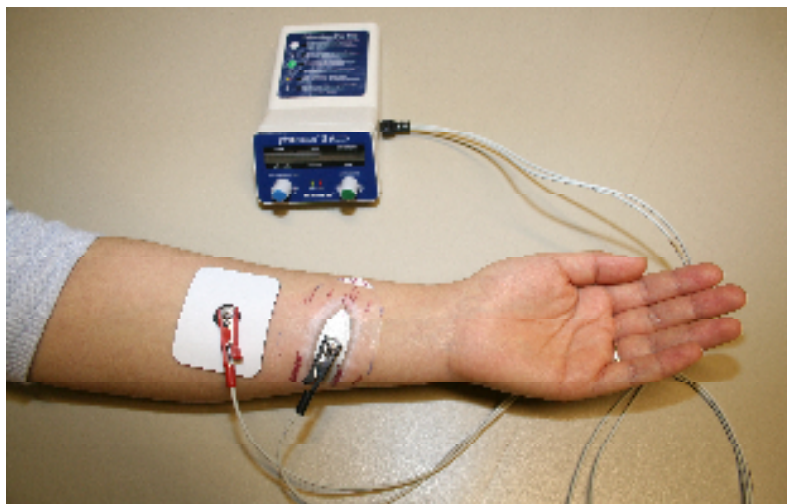
Figure 1. Example of an iontophoretic system: Phoresor® II auto device (power supply) connected to Iogel® small patches (IOMED, Salt Lake city, Utah, USA). Each pair of patches is composed of a karaya gel dispersive pad (the square pad) and a hydratable gel-sponge patch (the oval patch).

"Phoresor® II auto" (Model: PM850, Iomed, Salt Lake city, Utah, USA. Figure 1), already in the market for more than 10 years and used for iontophoresis in hospitals and health clinics for both adults and children.

The device has safety features which will automatically activate upon, for example, an increase in the resistance of the current circuit above a pre-set limit. The device is also fully controllable manually and the current could be stopped at any time should, for example, the volunteer decides to withdraw from the study for any reason.

The Phoresor® II device is a small, light and portable machine. A strap-worn pouch, to carry the device, will be used to make participation in this study more comfortable.

The device will be cleansed thoroughly with alcoholic wipes before and after each study.

The experimental protocol is summarized as follows:

1)   A minimum of 24 hours (for inpatients) or 2 weeks (for outpatients) is given to potential participants and their parents to read the participant information sheets and decide on whether they would like to take part in the study. They are encouraged to ask any questions and full explanation of all steps involved is

provided to them. Informed consent from the parent and child (as appropriate to age and understanding) will be taken.

2)   Upon participant and parent positive consent, a special code number instead of the participant's name is used throughout the study to make participation completely confidential. The consent form is the only document which includes both the participant name as well as the allocated code number. All consent forms will be stored in a locked cabinet and only the local collaborators will have access to it.

3)   During the 12 hours before the study's commencement, the participant is required not to apply any cosmetic products, such as creams, onto the arm used in the study.

4)   Iontophoresis is performed on the non-dominant arm of the participant. The arm is first cleansed with a routine alcohol wipe and then allowed to dry naturally.

5)   The iontophoresis system is composed of the Phoresor® II device and two electrode patches (a square dispersive pad and an oval gel-sponge patch). After hydration of the oval patch with 1.5 ml sterile water for injection, the square pad and the hydrated oval patch are affixed onto the arm of the participant. The Phoresor® II device is then connected to the electrodes and is set to precisely deliver 0.8 mA of constant direct current (~0.1 mA/cm^2).

6)   In total, current is passed for 5 hours starting 0.5 hours after the volunteer receives their routine intravenous dose of iohexol. Both patches are replaced with new ones after 2 and 4 hours of current passage. The oval patch is additionally replaced at 3 hours (see illustration below). So, a total of 7 patches are used. Each time we do a patch exchange, we stop the current briefly.

Figure 2. Example of redness occurring post-iontophoresis.

7)   During the study, the participant can mobilise but the researcher will accompany the participant throughout the study. As the study is performed on the non-dominant arm, the participant is able to use the other arm freely. So, the participant can, for example, go to the play room, read, and write. We will make sure the participant is kept entertained during the study and they can choose to watch their favourite cartoons and DVDs or read their favourite books.

8)   A comfort-break is allowed at any time during the study. Unless the participant is already restricted from food/drink due to their routine hospital care, our study has no restrictions.

9)   Participants may experience some mild tingling and heat sensation, especially at the start of iontophoresis. Redness may also appear at the site of iontophoresis but tends to disappear after a few days (figure 3). Upon positive consent from the participant and their parents, photographs of only the participant's arm will be taken before and after the study to show the effect of iontophoresis on the skin.

Redness/sensitisation may also occur as a result of the adhesive material of the patches.

10)   If the participant is in discomfort, or decides to withdraw from the study at any time and for any reason, the study will be stopped immediately. The procedure will be undertaken in wards staffed by nurses with skills to act appropriately in the unlikely event that the participant feels unwell during the study.

11)   Upon completion of the experiment, the participant will be asked to complete a short questionnaire, using the Wong-Baker faces pain scale, to evaluate the level of discomfort/tingling sensation they have experienced during the study. They will also be asked whether they prefer transdermal iontophoresis over blood sampling.

12)   Feedback with the results obtained from the iontophoresis sampling technique will be provided to the participant and parents should they wish to find out the outcome of their individual participation. A summary of the main findings and/or published reports will also be provided upon request.

Appendix 3.

Raw data

Chapter 2, in vitro study:

B.1 Fixed-subdermal concentration extraction

Iohexol passive diffusion fluxes (nmol/h), 2.44 mM subdermal concentration

	Time (h)					
Replicate	1	2	3	4	5	6
1	0.00	0.00	0.00	0.04	0.04	0.02
2	0.00	0.00	0.00	0.03	0.02	0.03
3	0.00	0.00	0.00	0.04	0.03	0.05
4	0.00	0.04	0.06	0.08	0.09	0.12
Average	0.00	0.01	0.01	0.05	0.05	0.06
SD	0.00	0.02	0.03	0.02	0.03	0.04

Iohexol iontophoretic fluxes (nmol/h), 2.44 mM subdermal concentration

	Time (h)					
Replicate	1	2	3	4	5	6
1	1.10	3.31	4.78	5.35	5.70	6.08
2	0.36	1.64	3.11	4.30	5.01	5.55
3	0.58	1.15	1.80	2.19	2.60	2.82
4	0.63	1.80	3.12	4.03	4.60	4.83
5	0.93	1.68	2.32	2.69	3.15	3.39
6	0.47	2.07	3.51	4.40	4.92	5.06
7	0.72	2.23	3.49	4.69	5.30	5.82
Average	0.69	1.98	3.16	3.95	4.47	4.79
SD	0.26	0.68	0.95	1.12	1.15	1.24

Iohexol iontophoretic fluxes (nmol/h), 1.22 mM subdermal concentration

Replicate	1	2	3	4	5	6
1	0.21	1.17	2.01	2.64	2.92	3.28
2	0.36	0.58	1.04	1.40	1.67	1.90
3	0.34	0.65	1.14	1.60	1.82	2.04
4	0.22	0.61	1.25	1.59	1.83	1.94
5	0.11	0.35	0.58	1.02	1.24	1.41
6	0.29	0.81	1.49	1.94	2.32	2.61
Average	0.26	0.69	1.25	1.70	1.97	2.20
SD	0.09	0.27	0.48	0.55	0.58	0.65

Iohexol iontophoretic fluxes (nmol/h), 0.61 mM subdermal concentration

	Time (h)					
Replicate	1	2	3	4	5	6
1	0.14	0.29	0.61	0.85	1.07	1.09
2	0.23	0.55	0.72	0.84	0.94	0.98
3	0.31	0.74	0.91	1.10	1.19	1.18
4	0.89	0.59	0.90	1.01	1.26	1.18
5	0.35	0.61	0.77	0.83	0.95	0.98
6	0.19	0.48	0.78	0.92	1.05	1.09
Average	0.35	0.54	0.78	0.92	1.07	1.08
SD	0.27	0.15	0.11	0.11	0.13	0.09

Iohexol iontophoretic fluxes (nmol/h), 0.31 mM subdermal concentration

	Time (h)					
Replicate	1	2	3	4	5	6
1	0.10	0.08	0.20	0.30	0.40	0.44
2	0.19	0.34	0.42	0.54	0.54	0.56
3	0.21	0.29	0.44	0.54	0.58	0.58
4	0.15	0.21	0.38	0.52	0.54	0.59
5	0.24	0.39	0.45	0.45	0.50	0.45
6	0.06	0.14	0.20	0.25	0.35	0.49
Average	0.16	0.24	0.35	0.43	0.49	0.52
SD	0.07	0.12	0.12	0.13	0.09	0.07

Iohexol iontophoretic fluxes (nmol/h), 0.15 mM subdermal concentration

	Time (h)					
Replicate	1	2	3	4	5	6
1	0.12	0.17	0.26	0.35	0.38	0.36
2	0.10	0.12	0.19	0.25	0.30	0.33
3	0.10	0.07	0.09	0.16	0.18	0.19
4	0.14	0.13	0.24	0.33	0.33	0.34
Average	0.12	0.12	0.19	0.27	0.30	0.31
SD	0.02	0.04	0.07	0.09	0.08	0.08

B.2 Effect of iontophoretic pre-treatment of the skin on iohexol transport

Iohexol iontophoretic fluxes (nmol/h), 2.44 mM subdermal concentration (with pre-treatment)

	Time (h)					
Replicate	1	2	3	4	5	6
1	1.30	3.62	4.31	4.94	5.28	5.12
2	1.03	2.94	4.05	4.73	5.12	5.12
3	1.31	4.85	6.41	6.86	7.31	7.29
4	0.74	3.36	4.95	5.66	6.12	5.94
5	1.27	3.36	4.32	5.09	5.55	5.36
6	0.95	3.60	4.86	5.37	6.26	6.05
7	1.91	4.93	5.65	5.96	6.21	6.21
8	2.41	6.21	7.07	7.41	7.07	7.26
9	1.87	4.04	5.15	5.75	5.66	5.66
10	1.66	3.51	4.15	4.42	4.53	4.65
11	0.76	3.02	4.10	5.07	5.13	5.44
12	0.67	2.54	3.88	4.44	4.82	4.39
Average	1.33	3.83	4.91	5.47	5.76	5.71
SD	0.54	1.03	1.01	0.92	0.86	0.91

Iohexol iontophoretic fluxes (nmol/h), 2.44 mM subdermal concentration (without pre-treatment)

	Time (h)					
Replicate	1	2	3	4	5	6
1	1.10	3.31	4.78	5.35	5.70	6.08
2	0.36	1.64	3.11	4.30	5.01	5.55
3	0.58	1.15	1.80	2.19	2.60	2.82
4	0.63	1.80	3.12	4.03	4.60	4.83
5	0.93	1.68	2.32	2.69	3.15	3.39
6	0.47	2.07	3.51	4.40	4.92	5.06
7	0.72	2.23	3.49	4.69	5.30	5.82
Average	0.69	1.98	3.16	3.95	4.47	4.79
SD	0.26	0.68	0.95	1.12	1.15	1.24

Iohexol passive fluxes (nmol/h), 2.44 mM subdermal concentration (with pre-treatment)

Replicate	Time (h)					
	1	2	3	4	5	6
1	0.07	0.09	0.18	0.24	0.23	0.25
2	0.07	0.12	0.15	0.15	0.17	0.21
3	0.09	0.06	0.12	0.13	0.16	0.19
4	0.11	0.17	0.21	0.27	0.24	0.26
5	0.10	0.17	0.21	0.28	0.29	0.26
Average	0.09	0.12	0.18	0.22	0.22	0.24
SD	0.02	0.05	0.04	0.07	0.05	0.04

Iohexol passive fluxes (nmol/h), 2.44 mM subdermal concentration (without pre-treatment)

Replicate	Time (h)					
	1	2	3	4	5	6
1	0.00	0.00	0.00	0.04	0.04	0.02
2	0.00	0.00	0.00	0.03	0.02	0.03
3	0.00	0.00	0.00	0.04	0.03	0.05
4	0.00	0.04	0.06	0.08	0.09	0.12
Average	0.00	0.01	0.01	0.05	0.05	0.06
SD	0.00	0.02	0.03	0.02	0.03	0.04

Acetaminophen iontophoretic fluxes (nmol/h), 7.5 mM subdermal concentration (without pre-treatment)

Replicate	Time (h)								
	1	2	3	4	5	6	7	8	9
1	7.42	19.70	23.79	22.95	26.05	26.04	27.22	27.01	27.32
2	7.55	20.99	25.78	35.51	33.97	33.84	34.77	33.36	34.46
3	7.34	15.76	21.76	26.84	23.55	24.98	26.50	25.34	25.25
4	7.10	12.49	15.52	17.17	18.39	19.88	20.33	20.64	20.99
5	2.80	10.18	16.49	19.14	20.78	20.67	24.03	23.38	24.26
6	2.98	8.88	13.72	16.35	16.88	19.15	19.81	21.50	18.35
Average	5.86	14.67	19.51	22.99	23.27	24.09	25.45	25.21	25.11
SD	2.31	5.00	4.92	7.27	6.22	5.54	5.50	4.64	5.58

Acetaminophen passive fluxes (nmol/h), 7.5 mM subdermal concentration (without pre-treatment)

Replicate	Time (h)								
	1	2	3	4	5	6	7	8	9
1	0.00	0.16	0.24	0.29	0.23	0.44	0.39	0.43	0.42
2	0.00	0.00	0.00	0.16	0.09	0.11	0.23	0.36	0.32
3	0.00	0.07	0.14	0.11	0.23	0.28	0.37	0.41	0.48
4	0.00	0.10	0.37	0.37	0.47	0.75	0.90	0.96	1.02
5	0.00	0.21	0.39	0.67	0.89	1.24	1.41	1.72	1.76
Average	0.00	0.11	0.23	0.32	0.38	0.56	0.66	0.77	0.80
SD	0.00	0.08	0.16	0.22	0.31	0.45	0.49	0.58	0.60

B.3 Pharmacokinetic simulations

1. Untreated skin, initial subdermal concentration 0.31 mM, pump flow rate 1.5 ml/h

Subdermal concentration (mM):

replicate						Time(h)						
	0.25	0.75	1.25	1.75	2.25	2.75	3.25	3.75	4.25	4.75	5.25	5.75
1	0.25	0.20	0.15	0.14	0.14	0.11	0.08	0.07	0.06	0.04	0.03	0.03
2	0.28	0.24	0.17	0.14	0.11	0.11	0.08	0.06	0.05	0.05	0.03	0.03
3	0.23	0.21	0.19	0.18	0.15	0.14	0.09	0.08	0.06	0.05	0.04	0.03
4	0.27	0.21	0.16	0.14	0.12	0.09	0.07	0.06	0.05	0.05	0.04	0.03
Average	0.26	0.21	0.17	0.15	0.13	0.11	0.08	0.07	0.06	0.05	0.04	0.03
SD	0.02	0.02	0.02	0.02	0.02	0.02	0.01	0.01	0.00	0.00	0.00	0.00

Iontophoretic fluxes (nmol/h):

replicate						Time(h)						
	0.50	1.00	1.50	2.00	2.50	3.00	3.50	4.00	4.50	5.00	5.50	6.00
1	0.05	0.12	0.16	0.35	0.53	0.45	0.33	0.33	0.24	0.18	0.15	0.14
2	0.22	0.30	0.31	0.26	0.46	0.52	0.40	0.30	0.29	0.26	0.19	0.14
3	0.08	0.12	0.12	0.20	0.40	0.59	0.40	0.32	0.27	0.25	0.19	0.15
4	0.15	0.19	0.16	0.31	0.31	0.47	0.42	0.37	0.30	0.19	0.18	0.14
Average	0.13	0.18	0.19	0.28	0.42	0.51	0.39	0.33	0.27	0.22	0.18	0.14
SD	0.07	0.08	0.08	0.06	0.09	0.06	0.04	0.03	0.03	0.04	0.02	0.01

2. Pre-treated skin, initial subdermal concentration 1.22 mM, pump flow rate 1 ml/h

Subdermal concentration (mM):

replicate	Time(h)											
	0.25	0.75	1.25	1.75	2.25	2.75	3.25	3.75	4.25	4.75	5.25	5.75
1	1.27	1.10	0.95	0.77	0.66	0.58	0.52	0.45	0.42	0.34	0.31	0.26
2	1.16	0.99	0.89	0.72	0.61	0.54	0.46	0.41	0.36	0.31	0.29	0.26
3	1.22	1.07	0.92	0.78	0.66	0.61	0.54	0.44	0.38	0.33	0.32	0.27
4	1.20	1.01	0.87	0.73	0.62	0.59	0.51	0.43	0.38	0.34	0.29	0.24
5	1.18	1.01	0.84	0.70	0.59	0.54	0.46	0.40	0.36	0.31	0.27	0.21
Average	1.21	1.04	0.89	0.74	0.63	0.57	0.50	0.43	0.38	0.33	0.29	0.25
SD	0.04	0.05	0.04	0.03	0.03	0.03	0.03	0.02	0.02	0.02	0.02	0.02

Iontophoretic fluxes (nmol/h):

replicate	Time(h)											
	0.50	1.00	1.50	2.00	2.50	3.00	3.50	4.00	4.50	5.00	5.50	6.00
1	0.43	3.14	3.95	3.40	2.98	2.67	2.39	2.09	1.96	1.63	1.47	1.25
2	1.66	3.96	3.80	3.10	3.34	3.02	2.56	2.35	2.07	1.77	1.69	1.53
3	1.90	4.98	5.16	4.43	3.83	3.64	3.00	2.57	2.22	1.86	1.94	1.54
4	1.52	4.23	4.32	3.77	3.29	3.23	2.76	2.32	2.13	1.84	1.65	1.48
5	0.26	2.38	4.73	4.09	2.87	2.67	2.34	2.09	1.93	1.56	1.39	1.10
Average	1.15	3.74	4.39	3.76	3.26	3.05	2.61	2.28	2.06	1.73	1.63	1.38
SD	0.75	1.00	0.56	0.53	0.37	0.41	0.27	0.20	0.12	0.13	0.21	0.20

3. Pre-treated skin, initial subdermal concentration 6.04 mM, pump flow rate 3 ml/h from 0 – 3 h then 1 ml/h from 3 -6 h

Subdermal concentration (mM):

replicate	Time (h)											
	0.25	0.75	1.25	1.75	2.25	2.75	3.25	3.75	4.25	4.75	5.25	5.75
1	5.30	3.30	2.25	1.63	1.00	0.69	0.53	0.48	0.41	0.36	0.31	0.28
2	4.89	3.33	2.20	1.50	0.97	0.64	0.48	0.44	0.36	0.33	0.30	0.27
3	5.03	3.24	2.20	1.43	0.99	0.67	0.44	0.38	0.34	0.29	0.27	0.21
4	5.16	3.55	2.24	1.54	1.05	0.72	0.59	0.48	0.42	0.36	0.33	0.24
5	4.86	3.19	2.22	1.47	0.98	0.65	0.46	0.41	0.35	0.31	0.28	0.25
Average	5.05	3.32	2.22	1.51	1.00	0.67	0.50	0.44	0.38	0.33	0.30	0.25
SD	0.19	0.14	0.02	0.07	0.03	0.03	0.06	0.05	0.03	0.03	0.03	0.03

Iontophoretic fluxes (nmol/h):

replicate	Time (h)											
	0.50	1.00	1.50	2.00	2.50	3.00	3.50	4.00	4.50	5.00	5.50	6.00
1	2.99	12.25	12.39	9.42	5.87	4.25	3.61	3.33	2.85	2.49	2.17	1.95
2	1.90	7.69	10.35	7.37	4.86	3.31	2.77	2.85	2.39	2.25	2.08	1.86
3	5.06	12.36	12.42	8.42	5.87	4.11	2.08	1.59	1.46	1.23	1.19	1.16
4	9.55	15.16	12.72	9.09	6.27	4.42	3.71	3.28	2.87	2.44	2.32	1.79
5	9.32	13.84	12.80	8.91	6.01	4.07	2.84	2.62	2.43	2.08	1.92	1.70
Average	5.77	12.26	12.14	8.64	5.78	4.03	3.00	2.73	2.40	2.10	1.94	1.69
SD	3.54	2.82	1.01	0.80	0.54	0.42	0.67	0.71	0.57	0.51	0.44	0.31

Chapter 2, in vivo study

1. Blood sampling data

Time of sampling (post-bolus injection) (h):

Patient 1	Patient 2	Patient 3	Patient 4
2.95	2.98	3.00	3.08
3.98	4.10	4.17	4.03

Iohexol blood concentration (µg/ml):

Patient 1	Patient 2	Patient 3	Patient 4
92.8	25.6	52.0	29.3
64.4	13.6	31.6	18.7

2. Skin sampling data

Time of sampling (post-bolus injection) (h):

Patient 1	Patient 2	Patient 3	Patient 4
2.75	2.57	2.63	2.57
3.80	3.65	3.67	3.62
4.88	4.73	4.73	4.67
6.00	5.87	5.80	5.72

Iohexol iontophoretic fluxes (µg/h): Current was 0.5 mA in all patients except patient 3 (0.3 mA)

Patient 1	Patient 2	Patient 3	Patient 4
0.59	0.31	0.27	0.39
0.62	0.35	0.42	0.47
0.52	0.24	0.25	0.25
0.44	0.12	0.20	0.22

Sodium iontophoretic fluxes (µg/h per 0.5 mA):

Patient 1	Patient 2	Patient 3	Patient 4
178.07	168.38	180.48	194.95
226.85	228.31	350.93	299.52
197.27	237.64	293.40	284.23
240.92	235.21	415.61	250.88

Potassium iontophoretic fluxes (µg/h per 0.5 mA):

Patient 1	Patient 2	Patient 3	Patient 4
109.96	72.46	78.40	86.47
118.27	96.35	103.64	104.78
114.28	91.56	93.89	110.72
126.93	91.44	150.28	99.18

Chapter 3, Ranitidine transdermal delivery study

3.1 Ranitidine delivery from aqueous solutions

3.1.1 Effect of donor vehicle

Ranitidine iontophoretic fluxes (µmol/h), 25 mM drug in water (pH 5.6)

Replicate	Time (h)					
	1	2	3	4	5	6
1	0.24	0.41	0.53	0.56	0.62	0.67
2	0.21	0.46	0.51	0.56	0.55	0.58
3	0.35	0.62	0.67	0.64	0.71	0.70
4	0.25	0.45	0.50	0.59	0.57	0.61
5	0.31	0.49	0.49	0.49	0.51	0.51
Average	0.28	0.49	0.54	0.57	0.59	0.61
SD	0.06	0.08	0.08	0.05	0.08	0.08

Ranitidine iontophoretic fluxes (µmol/h), 25 mM drug in 5 mM Tris (pH 7)

Replicate	Time (h)					
	1	2	3	4	5	6
1	0.13	0.37	0.49	0.58	0.66	0.71
2	0.11	0.42	0.52	0.69	0.78	0.80
3	0.15	0.43	0.57	0.69	1.10	0.86
4	0.22	0.53	0.60	0.68	0.75	0.80
5	0.25	0.50	0.58	0.66	0.73	0.71
Average	0.17	0.45	0.55	0.66	0.80	0.78
SD	0.06	0.06	0.04	0.05	0.17	0.06

3.1.2 Effect of current intensity

Ranitidine iontophoretic fluxes (µmol/h), 0.1 mA

Replicate	Time (h)					
	1	2	3	4	5	6
1	0.04	0.11	0.15	0.19	0.22	0.24
2	0.06	0.13	0.16	0.20	0.23	0.25
3	0.07	0.14	0.17	0.21	0.21	0.22
4	0.05	0.13	0.16	0.20	0.21	0.23
5	0.05	0.14	0.17	0.20	0.23	0.26
Average	0.05	0.13	0.16	0.20	0.22	0.24
SD	0.01	0.01	0.01	0.01	0.01	0.01

Ranitidine iontophoretic fluxes (µmol/h), 0.2 mA

Replicate	Time (h)					
	1	2	3	4	5	6
1	0.06	0.25	0.35	0.36	0.42	0.45
2	0.08	0.24	0.32	0.32	0.38	0.41
3	0.08	0.26	0.34	0.33	0.40	0.42
4	0.07	0.24	0.33	0.34	0.40	0.43
Average	0.07	0.25	0.33	0.34	0.40	0.43
SD	0.01	0.01	0.01	0.01	0.02	0.02

Ranitidine iontophoretic fluxes (µmol/h), 0.3 mA

Replicate	Time (h)					
	1	2	3	4	5	6
1	0.29	0.57	0.69	0.73	0.79	0.81
2	0.25	0.55	0.63	0.68	0.72	0.74
3	0.16	0.46	0.58	0.67	0.75	0.80
4	0.22	0.53	0.63	0.78	0.84	0.89
5	0.22	0.51	0.59	0.67	0.73	0.75
Average	0.23	0.52	0.62	0.71	0.77	0.80
SD	0.04	0.04	0.04	0.05	0.05	0.06

3.1.2 Effect of drug concentration

Ranitidine iontophoretic fluxes (µmol/h), 25 mM

Replicate	Time (h)					
	1	2	3	4	5	6
1	0.13	0.37	0.49	0.58	0.66	0.71
2	0.11	0.42	0.52	0.69	0.78	0.80
3	0.15	0.43	0.57	0.69	1.10	0.86
4	0.22	0.53	0.60	0.68	0.75	0.80
5	0.25	0.50	0.58	0.66	0.73	0.71
Average	0.17	0.45	0.55	0.66	0.80	0.78
SD	0.06	0.06	0.04	0.05	0.17	0.06

Ranitidine iontophoretic fluxes (µmol/h), 50 mM

Replicate	Time (h)					
	1	2	3	4	5	6
1	0.29	0.57	0.69	0.73	0.79	0.81
2	0.25	0.55	0.63	0.68	0.72	0.74
3	0.16	0.46	0.58	0.67	0.75	0.80
4	0.22	0.53	0.63	0.78	0.84	0.89
5	0.22	0.51	0.59	0.67	0.73	0.75
Average	0.23	0.52	0.62	0.71	0.77	0.80
SD	0.04	0.04	0.04	0.05	0.05	0.06

Ranitidine iontophoretic fluxes (µmol/h), 150 mM

Replicate	Time (h)					
	1	2	3	4	5	6
1	0.16	0.55	0.76	0.92	1.12	0.97
2	0.25	0.66	0.83	0.88	0.96	0.94
3	0.21	0.61	0.72	0.80	0.85	0.94
4	0.26	0.68	0.80	0.84	1.04	0.92
5	0.24	0.54	0.64	0.73	0.89	0.72
Average	0.23	0.61	0.75	0.83	0.97	0.90
SD	0.04	0.06	0.07	0.07	0.11	0.10

3.2 Ranitidine delivery from gel formulations

Passive diffusion fluxes (nmol/h)

0 % F-127 formulation

	Time (h)						
Replicate	2	4	6	8	10	22	24
1	0.02	0.05	0.15	0.33	0.56	1.17	1.28
2	0.03	0.04	0.10	0.20	0.33	0.97	1.62
3	0.02	0.04	0.06	0.09	0.15	0.50	0.82
Average	0.02	0.04	0.10	0.21	0.35	0.88	1.24
SD	0.00	0.00	0.04	0.12	0.20	0.34	0.40

20 % F-127 formulation

	Time (h)						
Replicate	2	4	6	8	10	22	24
1	0.05	0.17	0.30	0.38	0.54	0.85	1.04
2	0.01	0.03	0.07	0.14	0.22	0.48	0.67
3	0.07	0.20	0.27	0.32	0.45	0.75	0.87
Average	0.04	0.13	0.21	0.28	0.40	0.69	0.86
SD	0.03	0.09	0.12	0.13	0.16	0.19	0.18

30 % F-127 formulation

	Time (h)						
Replicate	2	4	6	8	10	22	24
1	0.0254	0.042	0.068	0.083	0.099	0.196	0.266
2	0.0146	0.051	0.071	0.142	0.140	0.434	0.727
3	0.0306	0.133	0.232	0.218	0.268	0.598	0.832
Average	0.024	0.076	0.124	0.148	0.169	0.409	0.608
SD	0.008	0.050	0.094	0.067	0.088	0.202	0.301

Iontophoretic fluxes (µmol/h)

0 % F-127 formulation

Replicate	Time (h)					
	1	2	3	4	5	6
1	0.16	0.55	0.76	0.92	1.12	0.97
2	0.25	0.66	0.83	0.88	0.96	0.94
3	0.21	0.61	0.72	0.80	0.85	0.94
4	0.26	0.68	0.80	0.84	1.04	0.92
5	0.24	0.54	0.64	0.73	0.89	0.72
Average	0.23	0.61	0.75	0.83	0.97	0.90
SD	0.04	0.06	0.07	0.07	0.11	0.10

20 % F-127 formulation

Replicate	Time (h)					
	1	2	3	4	5	6
1	0.31	0.68	0.81	0.80	0.83	1.08
2	0.28	0.73	0.72	0.90	0.70	1.02
3	0.22	0.64	0.65	0.88	0.86	0.89
4	0.28	0.63	0.72	0.75	0.83	0.91
5	0.15	0.50	0.61	0.70	0.77	0.85
Average	0.25	0.64	0.70	0.81	0.80	0.95
SD	0.07	0.08	0.08	0.09	0.06	0.10

30 % F-127 formulation

Replicate	Time (h)					
	1	2	3	4	5	6
1	0.13	0.55	0.73	0.72	0.78	0.75
2	0.23	0.60	0.69	0.68	0.70	0.72
3	0.15	0.40	0.79	0.65	0.76	0.81
4	0.13	0.53	0.66	0.71	0.78	0.83
5	0.15	0.44	0.48	0.54	0.59	0.66
Average	0.16	0.50	0.67	0.66	0.72	0.75
SD	0.04	0.08	0.12	0.07	0.08	0.07

Chapter 4, Midazolam transdermal delivery study

3.1 pH effect

Midazolam iontophoretic fluxes (nmol/h), pH 3

Replicate	Time (h)					
	1	2	3	4	5	6
1	0.03	1.14	2.20	8.63	8.89	8.97
2	0.02	0.28	1.03	3.91	3.76	3.64
3	0.06	0.41	0.59	3.37	3.41	3.10
4	0.08	0.75	3.19	8.46	8.72	8.21
Average	0.05	0.64	1.75	6.09	6.19	5.98
SD	0.03	0.38	1.18	2.84	3.02	3.04

Midazolam iontophoretic fluxes (nmol/h), pH 3.5

Replicate	Time (h)					
	1	2	3	4	5	6
1	0.04	1.09	5.07	10.60	11.03	7.42
2	0.04	1.25	9.67	12.47	12.63	9.66
3	0.25	2.44	4.86	6.05	6.80	14.06
Average	0.11	1.59	6.54	9.70	10.15	10.38
SD	0.12	0.74	2.72	3.30	3.02	3.38

Midazolam iontophoretic fluxes (nmol/h), pH 4

Replicate	Time (h)					
	1	2	3	4	5	6
1	1.82	2.21	7.94	10.61	11.53	11.77
2	0.80	5.33	11.63	12.88	13.17	16.04
3	0.09	2.85	8.81	9.32	9.43	10.05
4	0.94	3.53	7.62	13.96	14.46	12.37
Average	0.91	3.48	9.00	11.69	12.15	12.55
SD	0.71	1.34	1.82	2.11	2.17	2.52

Midazolam iontophoretic fluxes (nmol/h), pH 4.5

Replicate	Time (h)					
	1	2	3	4	5	6
1	4.70	12.47	14.82	19.95	20.87	21.15
2	2.63	8.37	12.07	15.28	14.91	15.02
3	2.43	8.50	17.81	18.24	20.67	19.84
4	2.36	18.34	13.91	15.75	14.69	14.92
Average	3.03	11.92	14.65	17.31	17.79	17.73
SD	1.12	4.69	2.40	2.19	3.45	3.23

3.2 Current effect

Midazolam iontophoretic fluxes (nmol/h), 0.1 mA

Replicate	Time (h)					
	1	2	3	4	5	6
1	1.12	1.28	1.68	2.01	2.19	3.10
2	0.19	0.40	0.40	0.81	1.18	1.91
3	0.27	0.27	0.54	0.91	1.28	2.07
Average	0.53	0.65	0.87	1.24	1.55	2.36
SD	0.52	0.55	0.70	0.66	0.55	0.64

Midazolam iontophoretic fluxes (nmol/h), 0.2 mA

Replicate	Time (h)					
	1	2	3	4	5	6
1	0.06	0.54	4.29	3.62	4.15	4.77
2	0.05	0.11	2.14	2.94	3.59	5.49
3	0.31	2.66	1.66	6.50	5.85	5.91
Average	0.14	1.10	2.70	4.36	4.53	5.39
SD	0.15	1.37	1.40	1.89	1.18	0.57

Midazolam iontophoretic fluxes (nmol/h), 0.36 mA

Replicate	Time (h)					
	1	2	3	4	5	6
1	0.04	1.09	5.07	10.60	11.03	7.42
2	0.04	1.25	9.67	12.47	12.63	9.66
3	0.25	2.44	4.86	6.05	6.80	14.06
Average	0.11	1.59	6.54	9.70	10.15	10.38
SD	0.12	0.74	2.72	3.30	3.02	3.38

3.3 Molar fraction effect

Midazolam iontophoretic fluxes (nmol/h), 1 mM midazolam, 37.8 mM sodium, pH 3.5

	Time (h)					
Replicate	1	2	3	4	5	6
1	0.27	0.41	1.48	2.11	2.84	3.48
2	0.25	0.43	1.04	1.95	2.47	2.92
3	0.16	0.32	0.67	1.50	2.43	2.72
Average	0.23	0.39	1.06	1.85	2.58	3.04
SD	0.06	0.06	0.41	0.32	0.23	0.39

Midazolam iontophoretic fluxes (nmol/h), 7.5 mM midazolam, 37.8 mM sodium, pH 3.5

	Time (h)					
Replicate	1	2	3	4	5	6
1	0.04	1.09	5.07	10.60	11.03	7.42
2	0.04	1.25	9.67	12.47	12.63	9.66
3	0.25	2.44	4.86	6.05	6.80	14.06
Average	0.11	1.59	6.54	9.70	10.15	10.38
SD	0.12	0.74	2.72	3.30	3.02	3.38

Midazolam iontophoretic fluxes (nmol/h), 15 mM midazolam, 37.8 mM sodium, pH 3.5

	Time (h)					
Replicate	1	2	3	4	5	6
1	2.10	6.42	16.68	20.19	24.17	27.33
2	3.50	12.82	19.55	22.06	26.03	28.70
3	2.91	7.64	32.15	36.42	32.69	32.66
4	0.49	8.95	17.07	16.24	16.88	20.82
5	1.47	3.57	7.53	14.34	22.46	21.84
6	3.01	10.57	19.21	22.60	26.83	25.29
7	11.55	27.85	22.16	25.89	27.82	25.58
8	7.56	12.14	13.67	18.17	17.69	18.44
9	8.40	8.22	8.05	12.02	14.60	13.82
Average	4.56	10.91	17.34	20.88	23.24	23.83
SD	3.73	6.97	7.48	7.26	5.90	5.71

Midazolam iontophoretic fluxes (nmol/h), 15.9 mM midazolam, pH 3.6

	Time (h)					
Replicate	1	2	3	4	5	6
1	12.05	60.15	64.02	76.57	75.75	60.67
2	1.87	52.40	51.97	50.27	50.23	49.10
3	65.27	74.70	72.84	80.19	85.59	90.41
4	50.14	57.12	45.50	50.53	49.11	47.27
5	3.38	21.26	38.84	48.66	56.98	63.56
Average	26.54	53.13	54.63	61.24	63.53	62.20
SD	29.20	19.67	13.78	15.71	16.31	17.28

Midazolam iontophoretic fluxes (nmol/h), 15 mM midazolam, 7.8 mM sodium, pH 3.5

	Time (h)					
Replicate	1	2	3	4	5	6
1	58.88	40.40	56.97	64.60	56.48	53.56
2	21.07	42.27	47.53	57.71	63.42	60.09
3	15.80	49.99	46.54	46.22	45.61	48.22
4	6.83	19.22	28.32	37.66	46.84	52.37
5	16.07	28.78	27.18	38.90	42.47	46.05
6	6.84	22.61	29.48	33.70	35.95	36.83
Average	20.92	33.88	39.34	46.46	48.46	49.52
SD	19.43	12.17	12.62	12.27	9.91	7.89

Midazolam iontophoretic fluxes (nmol/h), 15 mM midazolam, 97.8 mM sodium, pH 3.5

	Time (h)					
Replicate	1	2	3	4	5	6
1	2.82	5.68	7.59	10.71	12.83	12.84
2	2.51	5.10	8.22	10.41	12.36	13.54
3	1.80	5.70	11.56	11.31	12.10	13.56
4	3.42	9.37	13.17	16.90	20.48	20.46
5	2.19	2.60	2.11	2.22	2.84	3.26
Average	2.55	5.69	8.53	10.31	12.12	12.73
SD	0.62	2.42	4.27	5.24	6.25	6.14

3.4 Permeation across barrier compromised skin

Passive diffusion fluxes (nmol/h)

Intact skin

Replicate	Time (h)					
	2	4	6	8	10	21
1	0.000	0.022	0.035	0.058	0.049	0.043
2	0.000	0.015	0.019	0.047	0.049	0.038
3	0.000	0.015	0.031	0.039	0.051	0.051
Average	0.000	0.017	0.028	0.048	0.049	0.044
SD	0.000	0.004	0.008	0.010	0.001	0.007

Half compromised skin

Replicate	Time (h)					
	2	4	6	8	10	21
1	0.06	0.43	1.49	1.92	2.45	2.30
2	0.07	0.65	2.03	2.54	0.88	1.41
3	0.26	0.54	2.06	2.08	2.38	2.37
Average	0.13	0.54	1.86	2.18	1.90	2.03
SD	0.11	0.11	0.33	0.32	0.89	0.54

Fully compromised skin

Replicate	Time (h)					
	2	4	6	8	10	21
1	1.12	10.97	22.99	31.30	34.31	38.83
2	3.02	18.42	35.74	37.45	36.46	39.53
3	3.41	23.91	38.70	47.27	50.54	47.32
Average	2.52	17.77	32.48	38.67	40.44	41.89
SD	1.22	6.50	8.35	8.06	8.81	4.71

Iontophoretic fluxes (nmol/h)

Intact skin

Replicate	Time (h)					
	1	2	3	4	5	6
1	2.10	6.42	16.68	20.19	24.17	27.33
2	3.50	12.82	19.55	22.06	26.03	28.70
3	2.91	7.64	32.15	36.42	32.69	32.66
4	0.49	8.95	17.07	16.24	16.88	20.82
5	1.47	3.57	7.53	14.34	22.46	21.84
6	3.01	10.57	19.21	22.60	26.83	25.29
7	11.55	27.85	22.16	25.89	27.82	25.58
8	7.56	12.14	13.67	18.17	17.69	18.44
9	8.40	8.22	8.05	12.02	14.60	13.82
Average	4.56	10.91	17.34	20.88	23.24	23.83
SD	3.73	6.97	7.48	7.26	5.90	5.71

Half compromised skin

Replicate	Time (h)					
	1	2	3	4	5	6
1	4.65	10.79	18.99	26.27	31.45	35.61
2	2.90	5.51	6.25	9.54	13.03	16.87
3	0.49	2.69	6.30	9.96	12.30	17.14
4	1.50	5.10	24.21	45.21	50.64	47.35
5	0.23	1.96	5.50	9.66	15.52	18.67
Average	1.96	5.21	12.25	20.13	24.59	27.13
SD	1.83	3.47	8.74	15.75	16.53	13.76

Fully compromised skin

Replicate	Time (h)					
	1	2	3	4	5	6
1	16.77	69.57	93.08	110.15	127.87	126.77
2	4.82	25.69	48.38	46.82	82.22	75.28
3	19.87	68.21	115.35	133.40	154.77	174.56
4	16.78	91.90	140.84	151.39	159.83	172.12
5	0.84	9.18	21.90	35.11	47.14	57.49
6	1.15	33.67	58.89	102.91	113.23	106.29
7	4.49	45.31	60.25	81.18	124.39	139.21
8	13.24	69.90	80.70	112.59	158.24	174.23
Average	9.75	51.68	77.42	96.69	120.96	128.25
SD	7.73	27.75	38.32	40.23	39.84	45.67

Chapter 5, Phenobarbital transdermal delivery study

3.1 Permeation across intact skin

3.1.1. Passive diffusion fluxes (nmol/h)
Untreated skin

Replicate	Time (h)								
	1	2	3	4	5	18	20	22	24
1	0.09	0.33	0.56	0.71	0.92	1.66	2.83	3.46	3.80
2	0.00	0.03	0.19	0.42	0.70	2.68	5.24	6.02	7.22
3	0.00	0.03	0.21	0.56	1.02	3.72	6.99	7.87	8.50
Average	0.03	0.13	0.32	0.56	0.88	2.69	5.02	5.78	6.50
SD	0.05	0.17	0.21	0.15	0.16	1.03	2.09	2.22	2.43

Pre-hydrated skin

Replicate	Time (h)											
	1	2	3	4	5	6	7	8	9	20	22	24
1	0.13	1.42	3.29	5.16	6.98	7.72	8.74	7.99	10.40	9.75	11.11	15.30
2	0.11	0.90	2.42	3.62	4.83	5.91	6.61	6.62	7.83	8.39	10.35	7.45
3	0.09	1.00	2.39	3.85	4.44	6.46	5.70	8.00	8.03	7.92	8.34	11.99
4	0.06	0.63	2.01	3.08	4.78	6.22	4.86	6.92	6.40	6.71	8.45	10.21
Average	0.09	0.99	2.53	3.93	5.26	6.58	6.48	7.38	8.17	8.19	9.56	11.24
SD	0.03	0.32	0.54	0.88	1.16	0.79	1.67	0.72	1.66	1.26	1.39	3.29

Pre-treated skin

Replicate	Time (h)												
	1	2	3	4	5	6	7	8	9	10	20	22	24
1	3.67	9.79	16.30	18.64	20.98	15.98	18.65	18.98	19.65	19.09	19.30	23.04	23.47
2	0.26	1.88	5.12	6.82	8.12	9.57	9.84	12.44	9.09	10.98	12.03	15.92	12.82
3	0.37	2.69	7.52	10.75	11.07	13.63	13.80	14.19	15.39	15.00	16.50	20.95	21.81
4	3.37	2.86	5.96	6.69	8.39	8.98	9.77	9.75	10.36	9.92	11.05	14.84	11.95
Average	1.92	4.30	8.73	10.72	12.14	12.04	13.02	13.84	13.62	13.75	14.72	18.69	17.51
SD	1.85	3.68	5.15	5.61	6.04	3.34	4.21	3.89	4.85	4.18	3.87	3.94	5.97

3.1.2. Iontophoresis versus passive diffusion flux (nmol/h)

Iontophoresis:

Replicate	Time (h)				
	1	2	3	4	5
1	329.23	432.43	389.50	302.40	290.77
2	153.58	408.09	442.92	411.67	413.72
3	181.63	300.37	328.62	324.90	318.76
Average	221.48	380.30	387.01	346.33	341.08
SD	94.36	70.28	57.19	57.70	64.45

Passive:

Replicate	Time (h)								
	1	2	3	4	5	18	20	22	24
1	0.09	0.33	0.56	0.71	0.92	1.66	2.83	3.46	3.80
2	0.00	0.03	0.19	0.42	0.70	2.68	5.24	6.02	7.22
3	0.00	0.03	0.21	0.56	1.02	3.72	6.99	7.87	8.50
Average	0.03	0.13	0.32	0.56	0.88	2.69	5.02	5.78	6.50
SD	0.05	0.17	0.21	0.15	0.16	1.03	2.09	2.22	2.43

3.1.3. Anodal *versus* cathodal delivery

Cathodal flux (nmol/h)

Replicate	Time (h)				
	1	2	3	4	5
1	17.91	37.64	41.94	41.84	39.30
2	18.23	32.69	33.64	38.52	34.17
3	36.15	62.78	60.85	54.14	61.26
4	18.12	50.69	49.98	51.01	55.66
Average	22.60	45.95	46.60	46.38	47.60
SD	9.03	13.55	11.61	7.40	12.92

Anodal flux (nmol/h)

Replicate	Time (h)				
	1	2	3	4	5
1	0.97	3.25	7.53	10.85	14.08
2	0.20	1.88	5.89	7.99	10.62
3	0.44	3.49	8.20	12.91	14.19
4	0.21	2.24	5.14	8.43	10.49
Average	0.45	2.71	6.69	10.04	12.34
SD	0.36	0.78	1.42	2.29	2.07

Passive flux (nmol/h)

Replicate	Time (h)				
	1	2	3	4	5
1	0.14	2.01	3.99	3.26	8.03
2	1.41	4.75	7.11	7.50	10.22
3	0.28	0.79	0.83	1.21	2.19
4	1.20	2.25	1.54	2.52	3.22
5	0.69	1.49	4.40	5.19	3.59
6	0.50	1.38	1.76	3.99	4.08
Average	0.70	2.11	3.27	3.95	5.22
SD	0.51	1.39	2.36	2.20	3.16

3.1.4. Co-ion competition

Phenobarbital iontophoretic fluxes (nmol/h)

Experiment number 1 in Table 1

Replicate	Time (h)				
	1	2	3	4	5
1	329.23	432.43	389.50	302.40	290.77
2	153.58	408.09	442.92	411.67	413.72
3	181.63	300.37	328.62	324.90	318.76
Average	221.48	380.30	387.01	346.33	341.08
SD	94.36	70.28	57.19	57.70	64.45

Experiment number 2 in Table 1

Replicate	Time (h)				
	1	2	3	4	5
1	17.91	37.64	41.94	41.84	39.30
2	18.23	32.69	33.64	38.52	34.17
3	36.15	62.78	60.85	54.14	61.26
4	18.12	50.69	49.98	51.01	55.66
Average	22.60	45.95	46.60	46.38	47.60
SD	9.03	13.55	11.61	7.40	12.92

Experiment number 3 in Table 1

Replicate	Time (h)				
	1	2	3	4	5
1	71.16	202.06	207.73	151.21	138.11
2	36.70	154.98	166.85	201.07	174.45
3	67.19	169.79	213.92	147.12	156.39
4	99.40	253.40	226.53	210.83	164.93
5	34.90	110.75	156.94	151.52	114.77
6	166.07	226.74	195.18	157.09	216.89
Average	79.24	186.29	194.52	169.81	160.92
SD	48.85	51.67	27.40	28.34	34.65

Experiment number 4 in Table 1

Replicate	Time (h)				
	1	2	3	4	5
1	91.54	205.79	205.25	222.10	211.07
2	137.00	289.53	291.87	272.60	339.40
3	120.14	221.54	208.96	211.84	199.62
4	155.15	288.32	290.23	273.02	296.85
5	120.89	200.33	214.91	205.06	220.33
Average	124.94	241.10	242.24	236.92	253.45
SD	23.52	44.35	44.69	33.32	61.36

Experiment number 5 in Table 1

Replicate	Time (h)				
	1	2	3	4	5
1	116.99	259.15	278.34	271.73	289.84
2	161.42	318.32	296.86	305.53	317.71
3	89.43	231.45	238.81	264.20	248.22
4	203.67	334.16	313.89	344.12	293.83
5	115.12	333.75	352.35	351.08	351.28
Average	137.33	295.37	296.05	307.33	300.18
SD	45.23	47.18	42.07	40.00	37.96

3.2 Permeation across compromised skin

Passive diffusion fluxes (nmol/h)

Intact skin

Replicate	Time (h)								
	1	2	3	4	5	18	20	22	24
1	0.09	0.33	0.56	0.71	0.92	1.66	2.83	3.46	3.80
2	0.00	0.03	0.19	0.42	0.70	2.68	5.24	6.02	7.22
3	0.00	0.03	0.21	0.56	1.02	3.72	6.99	7.87	8.50
Average	0.03	0.13	0.32	0.56	0.88	2.69	5.02	5.78	6.50
SD	0.05	0.17	0.21	0.15	0.16	1.03	2.09	2.22	2.43

20 – 40 % compromised skin

Replicate	Time (h)											
	1	2	3	4	5	6	7	8	9	20.5	22	24
1	6.98	22.12	27.39	28.41	21.89	28.63	27.50	30.29	27.17	29.04	37.48	41.01
2	18.10	40.95	37.97	46.16	25.97	38.52	35.63	37.98	35.14	36.62	49.93	56.69
3	30.72	46.78	45.95	69.29	44.47	47.27	50.18	40.61	54.50	45.88	21.03	47.37
Average	18.60	36.62	37.10	47.95	30.77	38.14	37.77	36.29	38.94	37.18	36.15	48.36
SD	11.88	12.89	9.31	20.50	12.03	9.32	11.49	5.36	14.06	8.43	14.50	7.88

40 – 60 % compromised skin

Replicate	Time (h)											
	1	2	3	4	5	6	7	8	9	20.5	22	24
1	467.43	741.82	702.20	850.37	511.36	699.30	726.46	666.50	694.29	575.33	584.39	789.11
2	104.84	256.89	330.03	432.65	333.58	412.45	404.37	480.03	334.63	352.49	469.59	517.12
3	138.68	693.25	732.31	733.82	737.86	742.88	746.30	752.09	674.43	416.09	575.83	444.36
4(23-04: 4)	131.49	507.54	589.55	640.91	662.84	672.77	652.62	657.29	639.60	469.98	561.55	629.51
Average	210.61	549.88	588.52	664.44	561.41	631.85	632.44	638.98	585.74	453.47	547.84	595.02
SD	171.83	219.87	182.95	176.70	178.73	149.10	157.30	114.24	168.93	94.37	53.01	150.14

Fully compromised skin

Replicate	Time (h)											
	1	2	3	4	5	6	7	8	9	20.5	22	24
1	584.35	1324.49	1332	1340.32	1091.69	1219.41	1220.14	1320.41	1038.42	939.21	1043.97	1012.00
2	184.49	537.68	691.41	679.05	611.77	680.24	684.40	685.32	659.57	555.47	802.71	755.08
3	103.84	430.47	597.45	690.93	726.08	807.78	779.12	783.03	771.66	604.24	692.99	665.34
Average	290.90	764.21	873.62	903.43	809.85	902.48	894.56	929.59	823.22	699.64	846.56	810.81
SD	257.32	488.17	399.74	378.40	250.69	281.78	285.92	341.97	194.62	208.91	179.55	179.92

Iontophoretic fluxes (nmol/h)

Intact skin

Replicate	Time (h)									
	1	2	3	4	5	6	7	8	9	10
1	329.23	432.43	389.50	302.40	290.77	153.01	92.36	86.26	45.38	36.99
2	153.58	408.09	442.92	411.67	413.72	267.93	141.56	88.28	50.40	42.67
3	181.63	300.37	328.62	324.90	318.76	227.57	129.76	87.43	61.74	57.03
Average	221.48	380.30	387.01	346.33	341.08	216.17	121.23	87.32	52.51	45.56
SD	94.36	70.28	57.19	57.70	64.45	58.30	25.69	1.02	8.39	10.33

20 – 40 % compromised skin

Replicate	Time (h)									
	1	2	3	4	5	6	7	8	9	10
1	64.12	380.34	555.92	664.97	665.69	525.23	423.90	366.73	325.96	316.29
2	137.31	548.40	675.18	682.23	689.06	455.78	358.04	303.94	271.41	266.74
3	273.17	520.32	549.33	544.17	523.20	340.02	195.70	149.46	132.19	130.49
4	60.11	556.79	555.92	503.71	507.20	327.16	226.57	230.09	258.79	261.76
Average	133.68	501.46	584.09	598.77	596.29	412.05	301.05	262.56	247.09	243.82
SD	99.54	82.24	60.81	88.25	94.34	95.07	107.99	93.82	81.96	79.46

40 – 60 % compromised skin

Replicate	Time (h)									
	1	2	3	4	5	6	7	8	9	10
1	106.41	513.84	648.26	705.41	730.49	574.62	443.35	401.20	391.70	382.41
2	584.44	1119.11	1445.81	1332.95	992.71	705.92	599.34	567.21	553.50	576.47
3	117.90	441.24	537.86	588.19	595.07	433.88	358.11	322.34	298.10	302.04
4	190.32	1082.37	1074.28	1056.38	1134.40	952.55	894.39	919.09	886.80	954.41
5	450.70	1169.83	1209.60	1287.32	1242.54	1101.48	1069.31	1002.15	1021.42	953.53
Average	289.95	865.28	983.16	994.05	939.04	753.69	672.90	642.40	630.30	633.77
SD	215.51	356.24	382.12	336.44	271.56	272.55	301.41	305.06	313.03	308.85

Fully compromised skin

Replicate	Time (h)									
	1	2	3	4	5	6	7	8	9	10
1	594.15	1115.49	1126.96	1142.98	1194.50	909.07	887.01	890.39	879.49	868.90
2	765.03	1495.29	1503.73	1512.55	1571.35	1252.03	1178.31	1144.90	1155.26	1195.77
3	178.69	579.89	793.09	877.60	934.51	790.42	710.93	652.29	669.88	706.67
Average	512.62	1063.56	1141.26	1177.71	1233.45	983.84	925.42	895.86	901.55	923.78
SD	301.55	459.91	355.54	318.89	320.20	239.72	236.04	246.35	243.44	249.13